Université de Montréal

Rôles physiologiques du transporteur vésiculaire du glutamate VGLUT2 dans les neurones dopaminergiques

par
Guillaume Fortin

Département de pharmacologie
Faculté de Médecine

Thèse présentée à la Faculté de Médecine
en vue de l'obtention du grade de Philosophiae Doctor (Ph. D.)
en pharmacologie
option neuropharmacologie

Avril 2015

Université de Montréal
Faculté des études supérieures et postdoctorales

Cette thèse intitulée:

Rôles physiologiques du transporteur vésiculaire du glutamate VGLUT2 dans les neurones dopaminergiques

Présenté par :
Guillaume Fortin

a été évaluée par un jury composé des personnes suivantes :

Anne-Noël Samaha, président-rapporteur
Louis-Éric Trudeau, directeur de recherche
Nicole Leclerc, membre du jury
Martin Lévesque, examinateur externe
Pierre-Paul Rompré, représentant du doyen de la FES

Résumé

Des travaux récents démontrent que certains neurones dopaminergiques du mésencéphale ont la capacité de libérer du glutamate en plus de la dopamine (DA). Ce phénomène de « co-transmission » requiert l'expression du transporteur vésiculaire du glutamate de type 2 (VGLUT2) dans les neurones dopaminergiques. Certaines observations montrent que l'expression de VGLUT2 dans les neurones dopaminergiques survient tôt durant leur développement et est essentiellement limitée aux neurones de l'aire tegmentaire ventrale (VTA). De plus, cette libération de glutamate se retrouve principalement au niveau des terminaisons de ces neurones dans le striatum ventral, mais pas dans le striatum dorsal. Ces données suggèrent d'une part un rôle développemental possible du glutamate dans les neurones dopaminergiques, et d'autre part, que les signaux dérivés des neurones cibles puissent réguler le double phénotype des neurones dopaminergiques menant ainsi à une plasticité phénotypique. Par ailleurs, il est toujours inconnu si cette libération de glutamate se fait à partir des terminaisons qui relâchent la DA ou à partir de terminaisons axonales distinctes. De plus, le rôle physiologique de ce surprenant phénomène de co-transmission reste également inconnu. Ainsi, dans cette étude, nous avons d'abord démontré *in vitro* et *in vivo* que l'expression de VGLUT2 est nécessaire pour la survie et la croissance d'une sous-population de neurones dopaminergiques. En utilisant une lignée de souris ayant une délétion génique spécifique de VGLUT2 dans les neurones dopaminergiques, nous avons observé une diminution du nombre de terminaisons dopaminergiques et glutamatergiques dans le striatum, une baisse de libération de DA dans le striatum ventral, une diminution de la coordination motrice ainsi qu'une diminution de l'activité locomotrice induite par les drogues d'abus. D'autre part, nous avons démontré *in vitro* et *in vivo* que les neurones dopaminergiques au double phénotype établissent des terminaisons distinctes afin de relâcher le glutamate et la DA. De plus, nous démontrons que ce phénomène de ségrégation des sites de libération semble être induit par une interaction avec les neurones du striatum ventral. Ces travaux démontrent le rôle physiologique déterminant de la co-transmission DA-glutamate pour l'homéostasie du système DAergique et dévoile une caractéristique fondamentale de l'établissement des terminaisons axonales de ces neurones. Ces travaux permettent ainsi de mieux comprendre les rôles physiologiques de la co-libération de glutamate par les neurones du système

nerveux central et présentent une nouvelle perspective sur les dysfonctions potentielles de ces neurones dans les maladies du cerveau.

Mots-clés : dopamine, glutamate, co-transmission, vglut2, survie, croissance, hétérogénéité, ségrégation, striatum

Abstract

A subset of midbrain dopamine (DA) neurons has been shown to express the type 2 vesicular glutamate transporter (VGLUT2) supporting their capacity for glutamate co-release from some of their axon terminals. However, the physiological significance of this phenomenon is presently unknown. VGLUT2 expression by DA neurons occurs early during their development and is mainly found in DA neurons localized to the ventral tegmental area (VTA). Glutamate release by DA neurons can be detected at terminals contacting ventral but not dorsal striatal neurons. Together, these findings suggest the possibility glutamate co-release by DA neurons plays a developmental role and that target-derived signals regulate the neurotransmitter phenotype of DA neurons. Whether glutamate can be released from the same terminals that release DA or from a special subset of axon terminals is undetermined. Moreover, the physiological role of glutamate release by DA neurons is essentially unknown. Using a conditional gene knock-out approach to selectively disrupt the Vglut2 gene in mouse DA neurons, we obtained *in vitro* and *in vivo* evidence demonstrating reduced growth and survival of mesencephalic DA neurons, associated with a decrease in the density of DA innervation in the nucleus accumbens, reduced activity-dependent DA release, decreased motor coordination and impaired locomotor activation induced by drugs of abuse. In this study we also provide *in vitro* and *in vivo* data supporting the hypothesis that DA and glutamate-releasing terminals are mostly segregated and that striatal neurons regulate the co-phenotype of midbrain DA neurons and the segregation of release sites. These findings provide strong evidence for a functional role of the glutamatergic cophenotype in the development of mesencephalic DA neurons, unveils a fundamental feature of dual neurotransmission and plasticity of the DA system and open new perspectives into the pathophysiology of brain diseases implicatingthe DA system.

Keywords : dopamine, glutamate, co-release, vglut2, survival, growth, heterogeneity, segregation, striatum

Table des matières

Liste des figures

Liste des abréviations

5-HT:	Sérotonine
6-OHDA:	6-hydroxydopamine
AMPA :	Amino-3-hydroxy-5-méthyl-4-isoxazolepropionate
AMPc :	Adénosine monophosphate cyclique
ARNm :	Acide ribonucléique messager
ATP :	Adénosine triphosphate
VTA :	Aire tegmentale ventrale
CLi :	Central linear nucleus
DA:	Dopamine
DAergique :	Dopaminergique
DAG :	Diacylglicérol
DAT :	Transporteur de la dopamine
GIRKs	Canaux potassiques à rectification entrante activés par les protéines G
GLU:	Glutamate
GABA :	Acide-γ-aminobutyrique
IFN:	Interfascicular nucleus
IP3:	Inositol triphosphate
L-DOPA :	3,4-dihydroxyphenylalanine
LRRK2:	Parkin, leucine-rich repeat kinase 2
mGluRs :	Récepteurs métabotropes du glutamate
MPTP :	1-methyl-4-phenyl-1,2,3,6-tetrahydropyridine
nAcb :	Noyau accumbens
NMDA :	N-méthyl-D-aspartate
PBP :	Parabrachial pigmented area
PCP :	Phencyclidine
PFR:	Parafasciculus retroflexus area
PKA :	cAMP-dependent protein kinase
PKC :	Protéine kinase C
PLT:	Potentialisation à long terme
PINK1 :	PTEN induced putative kinase 1
PLC :	Phospholipase C
PN :	Paranigral nucleus
RLi :	Rostral linear nucleus
RRF :	Retrorubral field,
RT-PCR :	Reverse transcriptase polymerase chain reaction
SN :	Substance noire
SNc :	Substance noire compacte
SNr :	Substance noire reticulée
SNC :	Système nerveux central

TH : Tyrosine hydroxylase
VAChT : Transporteur vésiculaire de l'acétylcholine
VGLUT : Transporteur vésiculaire du glutamate
VMAT2 : Transporteur vésiculaire des monoamines de type 2
VTT : Ventral tegmental tail

À mes parents,

Remerciements

J'aimerais remercier famille et amis, mentors et collègues, qui m'ont permis de franchir avec succès le fil d'arrivée du marathon qu'est le doctorat. Sans votre support, je n'aurais pu y arriver.

Je veux d'abord remercier mes parents, mes sœurs adorées ainsi que mon frère qui ont toujours cru en moi et m'ont supporté dans les moments les plus durs. Ensuite, je veux remercier mes amis: Mathieu, Luigi, Louis-Alexandre, Arthur, Nicolas et Myriam.

Je veux également remercier particulièrement mon directeur de recherche Louis-Éric Trudeau pour sa passion contagieuse pour la recherche et son support inébranlable à mon égard. Un grand merci à Marie-Josée Bourque, la meilleure et la plus talentueuse des agentes de recherche que l'on peut avoir.

Un merci particulier à mes collègues du passé et du présent: Alfredo Mendez qui a été un véritable mentor pour moi, Christian Kortleven, Dominic Thibault, Clélia Florence, Minas Al-Bagdhadi, Anne-Marie Claveau, Fabien Loustalot, Noémie Bérubé-Carrière, Mustapha Riad, Vincent Migneron, Gregory Dal Bo, Caroline Fasano, Phillipe Martel, Damiana Leo, Gonzalo Sanchez, Consiglia Pacelli, Aurore Voisin, Rafael Varaschin, Nicolas Giguère et Sara Saneei.

Je veux également remercier mes collaborateurs suédois, avec qui j'ai eu la chance de travailler durant un séjour à Uppsala : Asa, Klass, Carolina, Karin, Johan, Chetan, Lena, Emma, Martin, Emelie, Malin, Emma, Kasia, Henrik B. Et un énorme merci à mes collaborateurs d'ici : Salah El Mestikawy, feu Laurent Descarries, avec qui j'ai eu le privilège d'interagir, et Abbas Sadikot. Je veux remercier aussi les collègues du département : le laboratoire Samaha et le laboratoire Girouard. Un grand merci à Diane Vallerand. Merci également à Graciela Pineyro, Pierre-Paul Rompré et René Cardinal.

Finalement, un merci tout particulier à Nataliya, ma plus grande fan, pour sa présence et son support.

"The true delight is in the finding out rather than in the knowing."

Isaac Asimov

Avant-propos

À la fin du 19è siècle, deux grandes théories sur la structure et l'organisation du système nerveux central s'affrontaient. La première théorie, appelée réticulariste, stipulait que les neurones formaient un réseau connecté par des ponts membranaires entre elles et n'agissaient pas ainsi indépendamment les uns des autres. À l'inverse, la deuxième théorie, appelée cellulaire, décrivait plutôt les neurones comme étant indépendants et les considéraient comme des entités uniques. Au début du 20è siècle, la deuxième théorie fût appuyée par de nombreuses données anatomiques et approuvée par la communauté scientifique. Néanmoins, cette théorie impliquait inévitablement que les neurones étaient en mesure de communiquer entre eux par un mécanisme qui était alors inconnu.

Encore une fois, deux grandes théories se sont affrontées afin d'expliquer ce mécanisme. La première théorie proposée par John Carew Eccles proposait que les neurones communiquent entre eux par l'intermédiaire de signaux électriques. La deuxième théorie avait comme hypothèse que la neurotransmission s'effectue par l'intermédiaire de messagers chimiques, tel que proposé par T.R. Elliott. Les expériences réalisées de 1920 à 1940 par Otto Loewi et Sir Henry Hallett Dale, co-récipiendaires du prix Nobel de Médecine, ont ainsi permis de démontrer que la neurotransmission s'effectuait principalement par le biais de messagers chimiques. En effet, leurs travaux innovateurs ont démontré la libération d'acétylcholine et de noradrénaline dans les divisions sympathiques et parasympathiques du système nerveux végétatif.

C'est suite à ces intéressantes découvertes que Sir Henry Hallett Dale formula son réputé principe selon lequel un neurone devrait raisonnablement libérer le même neurotransmetteur à toutes ses terminaisons axonales, qu'elles soient centrales ou périphériques.

Des dizaines d'années suivant l'énoncé de ce principe, d'étonnants travaux ont démontré que certains de ces neurones étaient également en mesure de libérer d'autres molécules chimiques : soit des neuropeptides et/ou des acides aminés. C'est ainsi qu'apparu pour la première fois le principe de co-libération neuronale : c'est-à-dire la possibilité de libération de deux messagers chimiques distincts par un même neurone. C'est ainsi que John Eccles suggéra une interprétation différente de ce principe en énonça que toutes les branches axonales libèrent le

ou les mêmes messagers chimiques. Puis aux débuts des années 1990, Nicoll et Malenka interpréta encore une fois ce fameux énoncé en stipulant que les neurones étaient en mesure de libérer qu'un seul type de neurotransmetteur.

Pourtant, c'est à cette époque qu'il a été démontré pour la première fois le phénomène de co-libération de neurotransmetteurs dits 'classiques'. Tout d'abord, les travaux de Sandler et Smith en 1991 dévoilaient l'existence de relâche de glutamate et de GABA par les mêmes neurones. Ensuite, les travaux de Johnson et collègues publiées en 1994 révélaient la possibilité de relâche de glutamate et de sérotonine par certains neurones. Enfin, les travaux de David Sulzer et collègues en 1998 démontraient pour la première fois la possibilité de relâche de glutamate et dopamine par les mêmes neurones.

Depuis, de nombreux autres laboratoires ont entrepris la tâche de démontrer et comprendre les implications de ce concept de co-libération de neurotransmetteurs 'classiques' dans le système nerveux central. Ces récentes découvertes ont eu pour conséquence de bouleverser et complexifier la classification neuronale moderne; en rendant du même coup le célèbre principe de Dale, datant de plus de 80 ans, désuet.

Bien que cette nouvelle réalité d'hétérogénéité neuronale soit présentement acceptée par l'étendue de la communauté scientifique, les rôles physiologiques et physiopathologiques de ce surprenant phénomène restent cependant méconnus à ce jour.

Chapitre 1 : Introduction

1. Système dopaminergique

1. 1 Introduction

La découverte des neurotransmetteurs et en particulier la découverte de la dopamine, a été un sans aucun doute un des points tournants de la neuroscience moderne. En effet, à ce jour, il a été démontré que la dopamine régule de nombreux comportements cruciaux tels que la motricité, la motivation, la cognition, l'humeur, et semble être impliqué dans plusieurs troubles neurologiques et psychiatriques tels que la maladie de Parkinson, la schizophrénie, le trouble de l'attention et la dépendance aux drogues d'abus, pour ne nommer que les principaux.

La recherche sur le système dopaminergique a été très dynamique ces dernières années comme peut témoigner le prochain tableau relatant une recherche dans pubmed sur le nombre d'articles publiés par année sur la dopamine :

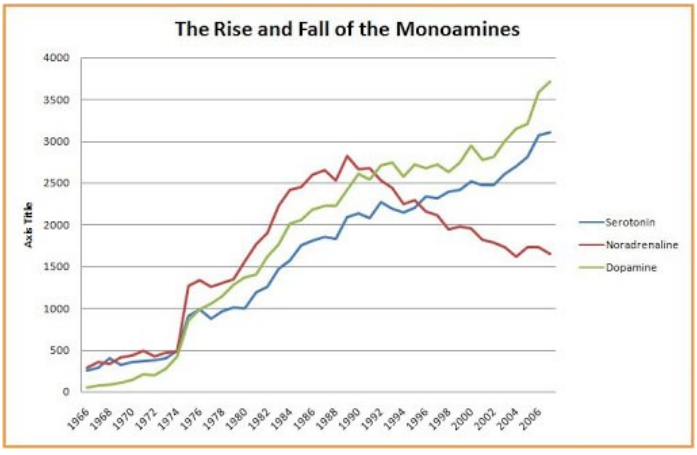

Figure 1. Nombres d'articles trouvés sur pubmed en utilisant comme mot-clé chacune des monoamines en fonction de la date de publication.

Source : http://blogs.discovermagazine.com/neuroskeptic/2008/12/05/alas-poor-noradrenaline/#.U-QP0Pl5OSo

1. 2 Découverte

Bien que la dopamine ait été synthétisée pour la première fois en 1910 par George Barger et James Ewens, les premières observations de la présence biologique de la dopamine chez le mammifère ont été effectuées par le Dr Arvid Carlsson (voir Figure 2). Né en 1923 à Uppsala, en Suède, il a débuté sa carrière de recherche dans le laboratoire du Dr Parkurst A. Shore en étudiant les effets de la réserpine sur la capacité de la sérotonine à s'introduire dans les plaquettes sanguines *in vitro*. Le Dr Carlsson développa à cette époque un modèle *in vitro* permettant de démontrer l'efficacité de la réserpine à bloquer le transport de la sérotonine dans les plaquettes. Par la suite, le Dr Carlsson a continué à travailler sur les effets neuropharmacologiques de la réserpine dans différents systèmes avec l'aide du Dr Hillarp et du Dr Brodie.

Figure 2. Photo du Dr Arvid Carlsson (Roe, 1999)

C'est en 1958 que le Dr Arvid Carlsson démontra pour la première fois la présence de la dopamine chez le lapin (Carlsson et al., 1958). Par le fait même, il a été le premier a démontré que la dopamine n'était finalement pas un simple précurseur de la noradrénaline, une hypothèse majoritairement acceptée à l'époque, mais un neurotransmetteur bien distinct. Ces travaux innovateurs sur la découverte des neurotransmetteurs et de la dopamine lui ont permis d'être colauréat du Prix Nobel de Médecine en 2000, en compagnie des Drs Éric Kandel et Paul Greengard.

Des étudiants du Dr Carlsson, les Drs Bertler et Rosengen ont par la suite étudié la distribution anatomique de la dopamine et ce dans différentes espèces. Ils ont ainsi démontré l'existence de la dopamine chez le cochon, la vache, le mouton, le chat, le rat et ce, principalement dans le système des ganglions de la base dans le cerveau, au niveau du caudé putamen (Bertler and Rosengren, 1959). Durant la même année, d'autres chercheurs ont réussi à démontrer la présence de dopamine chez l'humain (Sano et al., 1959).

1.3 Biochimie de la dopamine

La dopamine est dérivée de l'acide aminé tyrosine. La L-tyrosine est d'abord transformée en 3,4-dihydroxyphenylalanine (L-DOPA) par l'enzyme tyrosine hydroxylase (TH). Ensuite, la L-DOPA est décarboxylée par l'enzyme L-DOPA décarboxylase (également appelée décarboxylase des acide aminés aromatiques) afin de produire la dopamine.

La L-DOPA a été synthétisée pour la première fois en 1911 par Casimir Funk (Funk, 1911). Deux années, plus tard, le laboratoire Roche a réussi à isoler la L-DOPA à partir de fèves (Guggenheim., 1913). L'enzyme DOPA décarboxylase a été découverte par un groupe allemand en 1938 (Holtz et al., 1938). Près d'un an plus tard, il a été proposé que la L-DOPA et la dopamine soient des métabolites intermédiaires de la biosynthèse des catécholamines, de l'épinéphrine et de la norépinephrine (Holtz et al., 1939; Blaschko et al., 1942). La TH, l'enzyme limitante de la synthèse de la dopamine, a par la suite été découverte en 1964 (Nagatsu et al., 1964).

1.4. Transporteurs et récepteurs

1.4.1 Transporteurs

Les neurones dopaminergiques expriment deux différents transporteurs : le transporteur membranaire de recapture de la dopamine (DAT) et le transporteur vésiculaire des monoamines de type 2 (VMAT2).

Le transporteur DAT a comme rôle de transporter la dopamine du milieu extracellulaire vers le milieu intracellulaire du neurone dopaminergique. En effet, le transporteur DAT est principalement localisé au niveau de la membrane cellulaire des neurones dopaminergiques (Pickel et al., 1996). La caractérisation neurochimique et comportementale de la souris DAT-KO a démontré le rôle important du DAT dans la régulation de l'homéostasie dopaminergique (Giros et al., 1996; Gainetdinov and Caron, 2003). L'expression du DAT est spécifique et unique aux neurones dopaminergiques, ce qui permet à l'expression de cette protéine d'être un excellent marqueur de cette population de neurones.

Le transporteur VMAT2 fait partie d'une famille de transporteurs des monoamines. Elle est exprimée au niveau de la membrane des vésicules synaptiques et permet de transporter les monoamines du cytosol vers l'intérieur des vésicules synaptiques. Le transporteur VMAT2 est en mesure d'effectuer le transport de la sérotonine, dopamine, norépinephrine et de l'histamine (Erickson and Eiden, 1993; Eiden et al., 2004). Sa présence dans un neurone permet ainsi le stockage vésiculaire et la relâche de ces neurotransmetteurs par exocytose.

1.4.2 Récepteurs

L'effet physiologique de la neurotransmission dopaminergique est principalement médié par cinq différents types de récepteurs couplé aux protéines G qui sont catégorisés en deux grandes familles : famille D1 et famille D2. La description de ces différents sous-types de récepteurs dopaminergiques a été effectuée pour la première fois en 1978 grâce à des études biochimiques et de radioliaison (Spano and Trabucchi, 1978; Spano et al., 1978). Une année plus

tard, les familles D1 et D2 ont été classifiées selon l'effet activateur ou inhibiteur de leur activation sur l'adénylate cyclase, l'enzyme responsable de la conversion de l'ATP en AMP cyclique (Kebabian and Calne, 1979). On retrouve les récepteurs D1 et D5 dans la famille D1 et les récepteurs D2, D3, D4 dans la famille D2.

1.5 Voies de signalisation

La signalisation de la dopamine la mieux caractérisée s'effectue par l'activation de voies intracellulaires contrôlant la production de l'adénosine monophosphate cyclique (AMPc) et l'activation de la protéine kinase A (PKA) suite à la liaison de la dopamine sur les récepteurs D1 ou D2. La classe de récepteurs D1 est généralement couplée aux sous-unités $G\alpha_{s/olf}$ des protéines G hétérotrimériques et augmente la production du second messager chimique AMPc et l'activation de la PKA. À l'opposé, l'activation de la classe de récepteurs D2, couplé aux sous-unités $G\alpha_{i/o}$ régule négativement la production d'AMPc induisant ainsi une diminution de l'activité de la PKA (Enjalbert and Bockaert, 1983; Kebabian and Greengard, 1971).

Dans certaines conditions, tel que dans le contexte de formation d'hétéromères entre les récepteurs D1 et D2 (George et al., 2014), il semblerait que certains récepteurs dopaminergiques puissent se coupler à la sous-unité $G\alpha_q$ afin de réguler la phospholipase C (PLC), menant à la production d'inositol triphosphate (IP_3) et de diacylglycérol (DAG). Cette production entrainerait une augmentation de la mobilisation de calcium intracellulaire (Felder et al., 1989; Sahu et al., 2009). Outre ces voies de signalisations couplées aux protéines G, les récepteurs dopaminergiques interagissent aussi avec d'autres effecteurs tels certains canaux ioniques, récepteurs ionotrope ou protéines kinases telles que Akt (Beaulieu et al., 2009). A titre d'exemple, l'activation des récepteurs de la famille D2 inhibe la fonction des canaux calciques de type L et N et facilite l'ouverture de canaux potassiques à rectification entrante(GIRK) (Yan et al., 1997; Kuzhikandathil et al., 1998; Lavine et al., 2002).

1.6. Anatomie

1.6.1 Nomenclature

L'observation et la caractérisation des régions du cerveau contenant des dopaminergiques ont été effectuées suite à la découverte de la dopamine et de ses enzymes de synthèse dans les années 1960. Ce sont dans un premier lieu les Drs Carlsson, Dr Falck et Dr Hillarp qui, grâce à la méthode d'histofluorescence en utilisant le formaldéhyde, ont été en mesure de décrire la distribution des neurones dopaminergiques (Carlsson et al., 1962). Ce n'est que deux ans plus tard que le Dr Dahlström et le Dr Fuxe publièrent la première caractérisation de la distribution des noyaux noradrénergiques et sérotoninergiques. Ils ont ainsi désigné 12 groupes de noyaux (désigné A1 à A12) (Dahlström and Fuxe, 1964). Huit autres groupes (A13 à A17, C1 à C3) ont été rajouté par la suite (Hökfelt et al., 1984). La méthode de l'histofluorescence à l'aide de la vapeur de formaldéhyde a été la première méthode suffisamment sensible permettant de visualiser un neurotransmetteur *in situ*. Cette méthode a ainsi été utilisée pendant vingt ans dans le domaine de la recherche sur les catécholamines jusqu'à l'apparition de la méthode immunohistochimique moderne au début des années 1980.

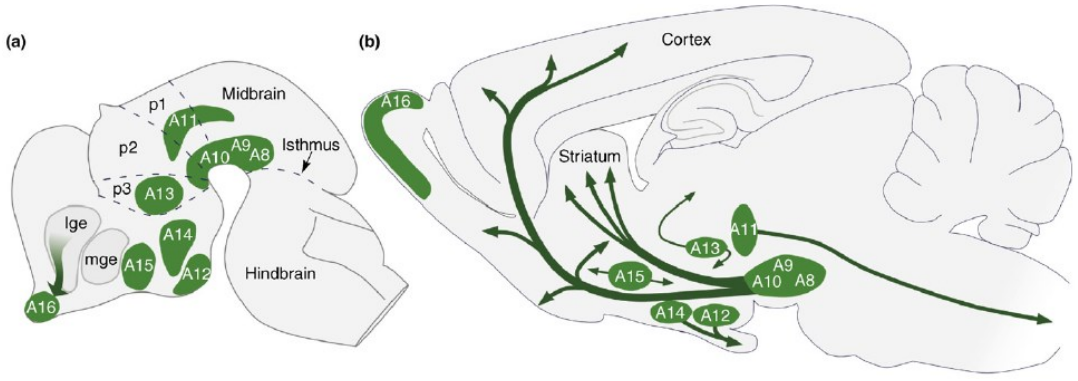

Figure 3. Distribution des noyaux catécholaminergiques et de leurs projections (flèches) chez le rongeur chez l'embryon (a) et dans le cerveau adulte (b) (Björklund and Dunnett, 2007).

Aujourd'hui, cette nomenclature est toujours utilisée afin de distinguer les différents noyaux dopaminergiques chez les différentes espèces animales.

1.6.2 Mésencéphale

Les neurones dopaminergiques sont situés dans neuf différents noyaux chez le mammifère (A8 à A16), distribués entre le mésencéphale et le bulbe olfactif (voir Figure 3).

Les neurones dopaminergiques sont en grande majorité situés dans le mésencéphale, plus précisément dans le noyau A9 (substance noire, SN) et dans le noyau A10 (aire tegmentale ventrale, VTA) et en plus faible quantité dans le noyau A8 (retrorubral field, RRF). La densité des neurones dopaminergiques et la complexité de leurs projections sont différentes selon les différentes espèces. Par exemple, le nombre de neurones dopaminergiques chez la souris est approximativement entre 20 000 et 30 000. Chez le rat, on compte plutôt entre 40 000 et 50 000 neurones. De plus, la moitié de ces neurones se situent dans la SN chez ces rongeurs. Chez les mammifères avec un système nerveux plus avancé, on compte entre 160 000 et 320 000 neurones dopaminergiques chez le singe et entre 400 000 et 700 000 neurones dopaminergiques chez l'humain. Près de 70% de la population totale de ces neurones se retrouve dans la substance noire (German and Manaye, 1993; Nelson et al., 1996; Emborg et al., 1998; Chu et al., 2002).

La SN est divisée en deux parties distinctes : substance noire pars reticulata (SNr) et substance noire pars compacta (SNc). La SNc est majoritairement composée de neurones dopaminergiques mais également de neurones GABAergiques et glutamatergiques. La SNr est une structure principalement composée de neurones GABAergiques, mais qui inclus également une grande densité de dendrites des neurones dopaminergiques.

Le VTA est divisé en plusieurs sous-structures selon différentes nomenclatures. On y retrouve le noyau paranigral (PN), l'aire parabrachiale pigmentée (PBP), l'aire parafasciculée retroflexus (PFR), la queue de l'aire tegmentale ventrale (VTT), le noyau interfasciculaire (IFN), le noyau rostral linéaire (RLi) et le noyau central linéaire (CLi). Le VTA est lui aussi composé de neurones dopaminergiques, GABAergiques et glutamatergiques.

1.6.3 Projections dopaminergiques du mésencéphale

Les projections dopaminergiques mésencéphaliques se divisent en 3 grandes familles : la voie mésotriée, la voie mésolimbique et la voie mésocorticale (voir Figure 4). La voie mésotriée est composée de neurones du VTA et de la SN projetant au niveau du striatum dorsal. La voie mésolimbique est composée de neurones du VTA, de la SN et du RRF projetant au striatun ventral, à l'amygdale, au septum, au tubercule olfactif et également à l'hippocampe (Dal Bo et al. non publié). Finalement, on retrouve les projections mésocorticales qui sont composés de neurones du VTA, de la SN et du RRF projetant au cortex cingulaire, préfrontal et périrhinal.

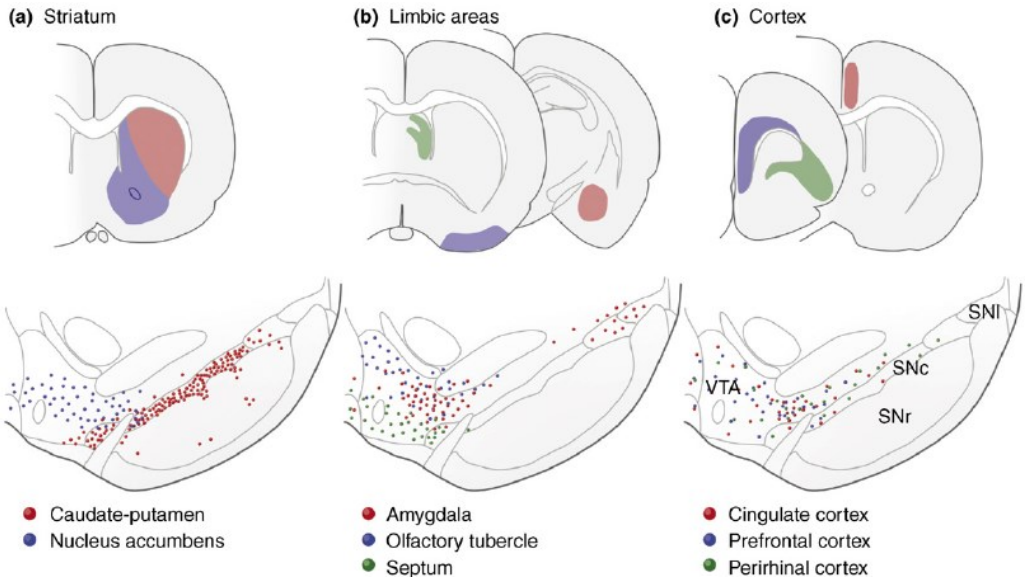

Figure 4. Localisation des neurones dopaminergiques du VTA (bleu), de la SN (rouge) et du RRF (vert) ainsi que leurs lieux de projection chez le rat (Björklund and Dunnett, 2007).

1.6.4 Striatum

Les neurones dopaminergiques de la SN et du VTA innervent ainsi le striatum. Le striatum est divisé en deux parties distinctes bien qu'aucunes frontières anatomiques précise ne les divisent. On retrouve le noyau accumbens, aussi appelé stiatum ventral, ainsi que le noyau caudé putamen, aussi appelé striatum dorsal ou néostriatum.

Le noyau accumbens peut être divisé lui aussi en deux parties dictinctes : le cœur et la coquille. La coquille peut être aussi divisée en 4 parties distinctes : vertex, cone, intermédiaire et ventrolateral. Le noyau caudé putamen peut quant à lui être divisé en 4 parties distinctes : ventral médian, ventral latéral, dorsal médian, dorsal latéral.

1.7 Développement

Les voies dopaminergiques s'établissent en plusieurs phases. Les cellules progénitrices neuronales sont d'abord différenciées en progéniteurs dopaminergiques. Puis ces neurones se différencient en neurones dopaminergiques immatures afin de se transformer finalement en neurones dopaminergiques matures (Ferri et al., 2007). Plusieurs facteurs de transcriptions sont impliqués durant chacune de ces phases afin d'assurer une migration, une différenciation et une croissance adéquates. Pitx3, Otx2, Wnt1, Dkk1, Lmx1a et Lmx1b semblent des facteurs de transcription cruciaux pour la différenciation des neurones dopaminergiques (Acampora et al., 1995; Deng et al., 2011; Prakash et al., 2006; Ribeiro et al., 2011; Yan et al., 2011). La migration et l'innervation des neurones dopaminergiques nécessitent en partie l'expression de DCC et Ebf1 (Yin et al., 2009; Xu et al., 2010). Finalement, l'expression de TH, VMAT2 et de DAT est régulée durant le développement de ces neurones par certains facteurs de transcription dont Nurr1 (Castillo et al., 1998; Wallén et al., 1999; Smits et al., 2003).

La migration des neurones dopaminergiques du mésencéphale ainsi que la croissance des axones s'effectuent vers le 13^{e} jour embryonnaire chez le rat (E13). Ces fibres axonales réussissent à atteindre le striatum vers E14 et le cortex vers E16. L'innervation de ces régions se complète environ une semaine après la naissance (Hegarty et al., 2013).

1.8 Hétérogénéité des neurones dopaminergiques

Bien que les neurones dopaminergiques mésencéphaliques soient situés à l'intérieur de trois structures distinctes et projettent également au niveau de trois voies distinctes, ces neurones ont par le passé toujours été considérés comme une population cellulaire plutôt homogène par rapport à leurs caractéristiques fonctionnelles et anatomiques. Néanmoins, depuis près de 20 ans, de nombreux travaux démontrent une réalité bien différente. Le tableau suivant résume certaines de ces différences :

Subtype	Cell body position	Gene expression for maintenance	Axonal projection	Synaptic inputs	*In vitro* physiology	*In vivo* physiology
Mesostriatal	SN	*PITX3*	Dorsal striatum (DS)	CX (M1, M2, S1), DS (patch compartment), STN, PPN etc.		Tonic and burst firing
Mesostriatal subclass 1	Rostromedial SN		Posterior dorsomedial striatum (pDMS)		Low frequency HCN channels, D2 autoreceptor response	K-ATP channel-mediated bursting
Mesostriatal subclass 2	SN dorsal tier (calbindin positive)		DS		Low frequency HCN channels, D2 autoreceptor response	Oscillatory bursting
Mesolimbic	VTA		Ventral striatum (VS)	CX (LO), VS (patch), LH, dorsal raphe, etc.		Tonic and burst firing
Mesolimbic subclass 1	Rostrolateral VTA		Lateral shell of NAc		Low frequency, HCN channels, D2 autoreceptor response	
Mesolimbic subclass 2	Posteromedial VTA	*OTX2*	Medial shell and core of NAc, and basolateral amygdala		High frequency, absent HCN channels, D2 autoreceptor response	
Mesocortical	VTA		PFC			?
	Posteromedial VTA	*OTX2*	Pre- and infralimbic CX		High frequency, absent HCN channels and absent D2 autoreceptor	

Figure 5. Hétérogénéité des propriétés des neurones dopaminergiques (Roeper, 2013).

L'organisation structurale des neurones dopaminergiques de la SN et du VTA peut également être divisée en deux parties distinctes selon leur localisation et leurs lieux de projections distincts : le tiers dorsal et le tiers ventral.

Les neurones du tiers dorsal sont une population de neurones très hétérogène au niveau de leur composition, de leur localisation ainsi que dans leurs lieux de projections. Ils sont ainsi composés essentiellement des neurones ventraux du VTA et de la SN ainsi que des neurones du RRF. Ces neurones projettent au striatum ventral, aux aires corticales et limbiques ainsi qu'en plus faible densité au striatum dorsal. Ces cellules du tiers dorsal sont majoritairement rondes, expriment un faible niveau de DAT et expriment en majorité la calrétinine, une protéine liant le calcium et impliquée dans la signalisation liée au calcium. Les neurones du tiers ventral sont majoritairement composés des neurones de la partie ventrale de la SN et du VTA. Ils innervent pratiquement exclusivement la partie dorsale du striatum. La morphologie de ces neurones est plutôt allongée, angulaire et dense. Ils expriment fortement DAT et GIRK2, un canal ionique à rectification entrante activé par les protéines G.

Da façon étonnante, certains neurones dopaminergiques mésencéphaliques ne semblent pas exprimer l'enzyme TH. En effet, des travaux ont démontré une baisse de l'expression de TH selon l'âge dans les neurones DAT (Lynd-Balta and Haber, 1994; Emborg et al., 1998; Prensa and Parent, 2001; ; McCormack et al., 2004; Thompson et al., 2005; Björklund and Dunnett, 2007). D'autres observations récentes ont démontré la présence de trois différentes classes de neurones dopaminergiques selon l'expression hétérogène de TH, DAT et VMAT2 dans le PBP, RLi et IF (Li et al., 2013). Il semblerait également que les neurones dopaminergiques de la SN aient une arborisation beaucoup plus dense et complexe que celle des neurones du VTA (Prensa and Parent, 2001; Parent and Parent, 2006; Bolam and Pissadaki, 2012).

1.9 Rôles et maladies associées

Le réseau très complexe du système dopaminergique régule de nombreux processus neurophysiologiques cruciaux chez l'humain. En effet, la dopamine est impliquée entre autres dans la thermorégulation, la faim et la soif, la motricité, la motivation, le traitement des émotions, la mémoire, l'attention, la vision et l'olfaction.

Considérant que les neurones dopaminergiques régulent ainsi de nombreuses fonctions importantes du corps humain, il n'est pas surprenant de noter que ceux-ci sont également impliqués dans plusieurs maladies qui ont pour conséquence de perturber ces fonctions vitales. Ainsi, le système dopaminergique est impliqué dans la maladie de Parkinson, la schizophrénie, la toxicomanie et également la dépression.

1.9.1 Maladie de Parkinson

La maladie de Parkinson est une maladie neurodégénérative de nature progressive. Elle est caractérisée par une mort importante des neurones dopaminergiques de la SNpc et en plus faible proportion dans le VTA. Cette neurodégénérescence induit un débalancement du circuit des ganglions de la base qui est responsable du contrôle du mouvement. Ainsi, apparaissent chez les patients atteints de la maladie de nombreux symptômes moteurs tels que l'akinésie (lenteur à l'initiation du mouvement), la bradykinésie (lenteur à l'exécution du mouvement), des tremblements au repos ainsi que de l'hypertonie plastique.

La cause de la maladie reste cependant inconnue. Néanmoins, des études ont identifié une cause génétique dans approximativement 10% des cas (Bekris et al., 2010). Les formes idiopathiques seraient vraisemblablement dues à des facteurs environnementaux, à des mutations spontanées ainsi qu'au vieillissement. Dans les forment familiales de la maladie, des travaux récents ont identifié la présence de mutations de plusieurs gènes incluant DJ-1, Parkin, leucine-rich repeat kinase 2 (LRRK2), et PTEN induced putative kinase 1 (PINK1); des gènes dont les produits sont tous associés directement ou indirectement à la fonction mitochondrie (Kitada et al., 1998; Bonifati et al., 2003; Valente et al., 2004), suggérant du fait même l'implication d'une dysfonction mitochondriale dans la maladie.

Il existe plusieurs modèles animaux murins de la maladie de Parkinson, incluant les modèles neurotoxiques et les modèles génétiques. La validation des modèles génétiques, incluant des souris chez lesquels les gènes DJ-1, LRRK2, PINK1 ou Parkin ont été invalidés, s'est avérée difficile jusqu'à maintenant. En effet, malgré le fait que ces modèles se concentrent directement sur les gènes retrouvés dans le formes familiales de la maladie, ils ne présentent pas de

neurodégénérescence des neurones dopaminergiques du mésencéphale ni de symptômes moteurs apparentés à la maladie de Parkinson (Sanchez et al., 2014; Le et al., 2014).

D'autre part, des modèles animaux murins ont été développés basés sur l'injection de neurotoxines. Parmi ceux-ci, on retrouve tout d'abord le modèle d'injection intra-cérébrale de 6-hydroxy-dopamine (6-OHDA) chez le rat adulte. Ensuite, il existe le modèle d'injection de intrapéritonéale de 1-methyl-4-phenyl-1,2,3,6-tetrahydropyridine (MPTP) chez la souris. Ces deux différents modèles provoquent la mort spécifique des neurones dopaminergiques du mésencéphale. Il existe également d'autres modèles d'animaux inductibles de la maladie de Parkinson par des neurotoxines ou des pesticides (voir revue de littérature Blandini and Armentero, 2012).

1.9.2 Schizophrénie

La schizophrénie est un trouble psychiatrique qui se caractérise par la perte partielle de la réalité. Les symptômes ressentis chez les patients sont des hallucinations et des altérations cognitives, une pensée désordonnée, un discours incohérent ainsi qu'un retrait social. Au cours des dernières décennies, plusieurs chercheurs ont proposé qu'un débalancement des systèmes glutamatergiques et dopaminergiques serait en cause dans cette maladie.

C'est d'abord l'observation des propriétés antipsychotiques de la chlorpromazine qui fût à la base du développement de l'hypothèse dopaminergique de la schizophrénie (Carlsson and Lindqvist, 1963). La capacité de la chlorpromazine à agir comme un antagoniste des récepteurs D2 a conduit à l'hypothèse d'une hyperactivité dopaminergique dans la schizophrénie (Seeman et al., 1976). Cette hypothèse est encore aujourd'hui la plus soutenue par la communauté scientifique. Néanmoins, l'observation de symptômes de type psychotiques chez les humains suite à la prise de phencyclidine (PCP) ou de kétamine, des antagonistes non compétitifs des récepteurs N-méthyl-D-aspartate (NMDA) du glutamate, a mené à l'hypothèse d'une hypofonction glutamatergique dans la schizophrénie.

1.9.3 Drogue d'abus

La consommation de drogues d'abus modifie des processus cognitifs importants tels que la perception, les émotions et la motivation et peut mener à une dépendance envers ces substances. Ces substances ont également de nombreux effets comportementaux incluant une activation psychomotrice, une diminution du temps de réaction, une perte d'appétit, une augmentation de l'anxiété et des troubles du sommeil.

L'implication du système dopaminergique dans les effets physiologiques induits par les drogues d'abus est bien documentée (Di Chiara et al., 1992). En effet, les psychostimulants augmentent la neurotransmission dopaminergique par divers mécanismes. La plupart des psychostimulants tels que la cocaïne et l'amphétamine bloquent le transporteur DAT des neurones dopaminergiques, ce qui entraine une augmentation des concentrations de DA extracellulaire. L'amphétamine agit également comme une base faible qui dissipe le gradient de protons des vésicules synaptiques dans les neurones dopaminergiques, interférant ainsi avec la capacité de VMAT2 de charger les vésicules en DA. Finalement, l'amphétamine permettrait également d'inverser la direction du transport de DA via DAT, induisant ainsi une sécrétion non-vésiculaire de DA dans le milieu extracellulaire (Rothman and Baumann, 2003; Heal et al., 2013). Les manifestations comportementales des drogues d'abus ainsi que les mécanismes impliqués dans la toxicomanie impliquent d'avantage les projections dopaminergiques vers le striatum ventral que vers le striatum dorsal (Koob and Volkow, 2010).

2. Système glutamatergique

Le glutamate est considéré comme le neurotransmetteur excitateur du système nerveux central. En effet, ses propriétés excitatrices sont connues et décrites depuis le début des années 1950. Ce n'est cependant que quelques années plus tard que le glutamate a été décrit comme le neurotransmetteur excitateur principal du système nerveux central des vertébrés (Hayashi et al., 1952; Curtis and Watkins et al., 1960). Le glutamate est clairement un des neurotransmetteurs les plus importants pour le fonctionnement du système nerveux central. Ce neurotransmetteur est

un dérivé de l'α-kétoglutarate et est un précurseur de la glutamine. Néanmoins, le glutamate peut également être synthétisé dans les terminaisons synaptiques à partir de la glutamine via la glutaminase, en prenant avantage du recyclage de la glutamine par les cellules gliales avoisinantes.

2.1 Récepteurs

Il a été démontré que le glutamate agit sur deux grandes familles de récepteurs, soit les récepteurs ionotropes et métabotropes. Les récepteurs ionotropes sont des canaux ioniques cationiques dont l'ouverture est contrôlée par la liaison du glutamate. On compte trois types de récepteurs à l'intérieur de cette famille : NMDA, acide 2a-amino-3-hydroxy-5-methyl-4-isoxazolepropionic (AMPA) et kaïnate (Hollmann et al., 1989; Hollmann and Heinemann, 1994). La neurotransmission glutamatergique est généralement caractérisée par une réponse post-synaptique rapide expliquée par le cours délai d'activation de ces récepteurs suite à la libération du glutamate à la synapse.

Les récepteurs métabotropes (mGluR) sont quant à eux des récepteurs à sept passages transmembranaires qui sont généralement couplés aux protéines G hétérotrimériques et qui sont responsables de réponses post-synaptiques lentes ou autres phénomènes de plasticité. Il existe huit de ces récepteurs classés en trois groupes distincts : mGlur1 (mGlur1 et mGlur5), mGlur2 (mGlur2 et mGlur3) et mGlur3 (mGlur4, mGlur6, mGlur7, mGlur8). Selon les familles, ces récepteurs peuvent se situer soit sur les terminaisons axonales, soit sur le compartiment somatodendritique (Lujan et al., 1996; Luján et al., 1997; Shigemoto et al., 1997).

2.2 Transporteurs vésiculaires

Avant d'être relâché dans le milieu extracellulaire pour se lier aux récepteurs glutamatergiques, le glutamate doit tout d'abord être chargé à l'intérieur de ces vésicules grâce à

un transporteur vésiculaire (El Mestikawy et al., 2011). Ces VGLUTs sont caractérisés comme des anti-porteurs et utilisent donc un gradient électrochimique de protons afin d'incorporer le glutamate dans la vésicule (voir Figure 6). Il existe trois isoformes de VGLUT : VGLUT1, VGLUT2 et VGLUT3 (Bellocchio et al., 2000; Fremeau, 2001, 2002; Takamori et al., 2000).

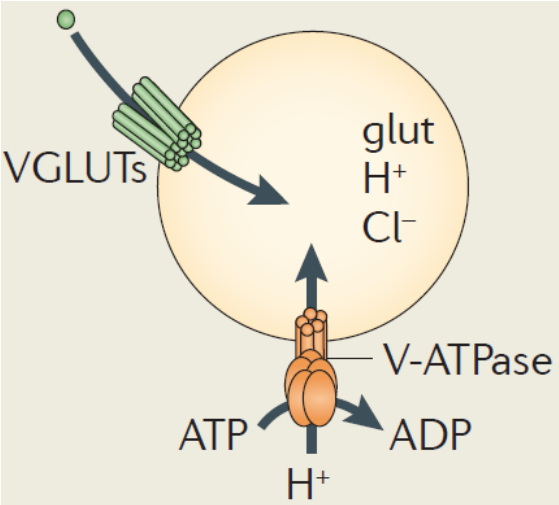

Figure 6. Mécanisme du transporteur vésiculaire de glutamate (El Mestikawy et al., 2011).

2.3 Localisation

L'expression d'acide ribonucléique messager (ARNm) des transporteurs vésiculaires dans les neurones est très hétérogène dans le cerveau. Alors que l'ARNm de VGLUT1 se retrouve principalement dans le cortex ainsi que dans l'hippocampe, l'ARNm de VGLUT2 se retrouve surtout dans les structures sous-corticales incluant le thalamus et le tronc cérébral. Le patron d'expression de l'ARNm de VGLUT1 et de VGLUT2 est ainsi très complémentaire dans le cerveau. L'ARNm de VGLUT3, très faiblement exprimé dans le cerveau, se retrouve dans une sous-population de neurones du raphé, du striatum, du cortex et de l'hippocampe.

L'expression des différentes VGLUTs est régulée durant le développement. En effet, l'expression de VGLUT1 est faible en bas âge et forte plus tard dans le développement. Inversement, l'expression de VGLUT2 est forte en bas âge et diminue avec le temps. L'expression de l'ARNm de VGLUT3 est stable tout au long du développement.

2.4 Rôles et maladies associées

Le glutamate est bien connu pour jouer un rôle prédominant dans les fonctions cérébrales d'apprentissage et de mémorisation. En effet, ce neurotransmetteur est crucial dans le phénomène de potentialisation à long terme (PLT) qui se caractérise par une augmentation durable de l'efficacité synaptique. Cependant, le glutamate peut également influencer d'autres fonctions neurobiologiques cruciales.

2.4.1 Survie et neurodégénérescence

Le glutamate semble jouer un rôle important dans la différenciation neuronale et la migration neuronale dû à son effet sur l'entrée d'ions calciques (Hack and Balázs, 1994; Yano et al., 1998). Le blocage des récepteurs NMDA durant la période prénatale semble induire l'apoptose de certaines populations neuronales (Ikonomidou et al., 1999). Il a également été démontré que l'activation du récepteur NMDA augmente la croissance des neurones dopaminergiques (Schmitz et al., 2009).

D'autres travaux ont démontré que le glutamate peut avoir un rôle trophique ou neurotoxique selon la localisation et l'activité des récepteurs NMDA (voir revue Hardingham and Bading, 2010). Par exemple, l'action du glutamate peut être neurotoxique selon l'effet agoniste sur les récepteurs AMPA ou la famille des mGLUR1. Il semble que l'entrée excessive d'ions calciques contribue à la mort cellulaire induite par le glutamate (Meldrum and Garthwaite, 1990; Beal et al., 1992). Un agoniste agissant sur les récepteurs mGluR1 et mGluR5 injecté dans l'hippocampe a été démontré pour induire une activité épileptique et une neurodégénérescence

des neurones avoisinants. L'activation de ces récepteurs semblent également contribuer à la mort cellulaire induite par une ischémie cérébrale (Mukhin et al., 1996; Sacaan and Schoepp, 1992).

2.4.2 Maladies

Le rôle ambivalent du glutamate dans le SNC fait de ce neurotransmetteur une cible potentielle pour plusieurs maladies. Ceci inclut l'épilepsie, l'amnésie, les accidents vasculaires cérébraux, l'anxiété, la schizophrénie et la sclérose latérale amyotrophique.

Des travaux ont démontré par exemple que des antagonistes des récepteurs NMDA et AMPA sont de puissants anticonvulsivants dans différents modèles d'épilepsie. Des antagonistes des récepteurs métabotropes de la famille mGluR1 et mGluR3 semblent également être des cibles pour le traitement de l'épilepsie (Meldrum and Garthwaite, 1990; Chapman et al., 1991). La neurodégénérescence des neurones moteurs dans la sclérose latérale amyotrophique semble impliquée les transporteurs glutamatergiques et une augmentation de l'activité des récepteurs AMPA (Lacomblez et al., 1996; Leigh and Meldrum, 1996). Ainsi, des médicaments tels que le riluzole, capable de bloquer les effets synaptiques du glutamateont été développées pour le traitement de cette maladie (Lacomblez et al., 1996; Leigh and Meldrum, 1996). L'hypothèse hypoglutamatergique de la schizophrénie, basée sur une fonction diminuée du récepteur NMDA, suggère également que le système glutamatergique est une cible potentielle thérapeutique dans le traitement des psychoses chez les patients. En effet, la potentialisation du récepteur NMDA semble diminuer les symptômes chez les patients (Goff and Wine, 1997). Il a été proposé que les effets thérapeutiques de médicaments comme l'haloperidol et la clozapine, qui visent principalement le système dopaminergique, nécessiterait en partie l'activation du récepteur NMDA (Banerjee et al., 1995).

3. Co-libération

3.1 Découverte

Plusieurs années après l'énoncé du fameux principe de Dale stipulant qu'un neurone libère le même neurotransmetteur à partir de toutes ses terminaisons axonales, plusieurs travaux ont démontré que les neurones du SNC sont en mesure de libérer d'autres messagers chimiques. En effet, des premières observations ont d'abord démontré la co-libération de peptides. Par la suite, plusieurs groupes de recherche ont démontré la capacité de certains neurones à libérer deux ou parfois trois neurotransmetteurs classiques.

Au début des années 1970, des études ont démontrés la co-libération d'adénosine triphosphate (ATP) et d'acétylcholine à la jonction neuromusculaire et la co-libération d'ATP et de norépinéphrine dans le système nerveux autonome (Nakanishi and Takeda, 1972, 1973; Silinsky et al., 1975). Durant la même époque, des études ont par la suite observé la co-libération d'acétylcholine et de norépinéphrine par des neurones post-ganglionnaires du système nerveux sympathique (Patterson and Chun, 1974; Furshpan et al., 1976).

Quelques années plus tard, l'observation de la co-libération de GABA et de glycine fût observée au niveau de la moelle épinière (Jonas et al., 1998). Une étude a par la suite démontré la co-libération de ces deux acides aminés à partir des mêmes vésicules synaptiques. De plus, cette étude suggéra que ce double phénotype semblait être plastique durant le développement (Nabekura et al., 2004).

3.2 Co-libération de glutamate

Bien que la co-libération de peptides ou d'acides aminés soit proposée depuis des dizaines d'années, le phénomène de co-transmission de neurotransmetteurs classiques est une hypothèse

relativement récente. En effet, la caractérisation et le clonage des transporteurs vésiculaires du glutamate au début des années 2000 ont permis à la communauté scientifique d'identifier de nombreuses populations neuronales du cerveau possédant la capacité de co-libérer le glutamate.

3.2.1 GABA-glutamate

Malgré qu'une étude suggéra pour la première fois en 1991 l'existence du glutamate et du GABA à l'intérieur d'une sous-population de terminaisons de l'hippocampe (Sandler and Smith, 1991), il a fallu attendre près de dix ans plus tard afin d'avoir les premières preuves fonctionnelles de la co-libération de ces deux neurotransmetteurs. En effet, une première étude démontra une neurotransmission simultanée de glutamate et de GABA dans l'hippocampe à l'aide de l'électrophysiologie (Gutiérrez et al., 2000). Cette observation surprenante de la co-libération de neurotransmetteurs excitateurs et inhibiteurs fût par la suite confirmée par la caractérisation des différentes isoformes des VGLUTs dans le cerveau. En effet, l'expression de VGLUT1 et de l'enzyme de synthèse du GABA (glutamate décarboxylase 2 ou GAD65) a été observée dans une population de neurones de la rétine (Kao et al., 2004). Puis, VGLUT1, VGLUT2 et VGLUT3 ont également été observés dans des terminaisons GABAergiques du cortex et de l'hippocampe (Boulland et al., 2004, 2009; Herzog et al., 2004; Gillespie et al., 2005; Soussi et al., 2010; Zander et al., 2010). Le rôle physiologique de la co-transmission glutamatergique par des neurones GABAergiques est présentement inconnu. Néanmoins, des études ont proposées que l'expression de ce co-phénotype serait nécessaire pour le développement et la maturation des synapses du système auditif (Gillespie et al., 2005; Noh et al., 2010).

3.2.2 Acétylcholine-glutamate

Deux études publiées la même année suivant la caractérisation de VGLUT3 ont démontré pour la première fois la capacité des neurones cholinergiques de libérer le glutamate comme

neurotransmetteur. En effet, la présence d'ARNm de VGLUT3 dans les interneurones cholinergiques du striatum dorsal et ventral a été observée (Gras et al., 2002; Schafer et al., 2002). Puis, une étude démontra la présence d'ARNm de VGLUT1 et de VGLUT2 dans les motoneurones (Herzog et al., 2004). En utilisant un système de micro-cultures, une autre étude observa la libération de glutamate par des neurones cholinergiques isolés du prosencéphale basal (Huh et al., 2008). Finalement, grâce à la technique d'optogénétique, une autre étude confirma la co-libération de glutamate par les neurones cholinergiques (Ren et al., 2011). Cependant, il semble que l'expression de la protéine des différentes isoformes des VGLUTs ne colocalisent pas avec l'expression protéique des différents marqueurs des terminaisons cholinergiques, suggérant du fait même la capacité de certains neurones cholinergiques à établir des sites de relâches distincts pour l'acétylcholine et le glutamate (Kraus et al., 2004; Nishimaru et al., 2005).

Le rôle physiologique de ce double phénotype est présentement peu connu. Il a été proposé que la libération de glutamate soit cruciale pour l'action synaptique rapide aux neurones cibles (Ren et al., 2011). Finalement, il a été proposé que la présence de VGLUT3 dans les vésicules synaptiques exprimant le transporteur vésiculaire de l'acétylcholine (VAChT) augmente l'accumulation d'acétylcholine à l'intérieur de la vésicule via un processus appelé synergie vésiculaire (Gras et al., 2008).

3.3.3 Sérotonine-glutamate

La co-libération de glutamate a également été observée chez les neurones monoaminergiques. À l'aide d'un système de microculture, il a été démontré que les neurones sérotoninergiques sont en mesure de libérer le glutamate à certaines de leurs synapses (Johnson, 1994). Puis, l'ARNm de VGLUT3 et l'expression de la protéine furent pour la première fois observés dans les neurones sérotoninergiques *in vitro* et *in vivo* (Fremeau et al., 2002; Gras et al., 2002). La libération fonctionnelle du glutamate par les neurones sérotoninergiques a par la suite été validée *in vivo* par optogénétique (Varga et al., 2009). Il semblerait que la majorité des varicosités axonales des neurones sérotoninergiques exprimant VGLUT3 *in vitro* soit également

immunopositive pour la sérotonine (Voisin et al. en rédaction). Néanmoins, *in vivo*, des observations proposent plutôt que les terminaisons glutamatergiques et sérotoninergiques se retrouvent plutôt à des sites distincts (Schafer et al., 2002; Tsudzuki and Tsujita, 2004; Martin-Ibanez et al., 2006).

La signification physiologique de la co-libération du glutamate dans les neurones sérotoninergiques est peu étudiée. Une seule étude suggère que l'expression de VGLUT3 dans les neurones sérotoninergiques soit impliquée dans la synergie vésiculaire de la sérotonine et serait en mesure de jouer un rôle important dans le contrôle de l'anxiété (Amilhon et al., 2010) .

4. Co-libération dopamine-glutamate

4.1 Découverte

Il existe cependant une autre population de neurones monoaminergiques possédant la capacité de libérer le glutamate. En effet, une première étude en 1998 suggéra que les neurones Dopaminergiques sont en mesure de co-libérer le glutamate en plus de la dopamine à l'aide d'enregistrements électrophysiologiques effectués sur des neurones dopaminergiques en micro-cultures dopaminergiques (Sulzer et al., 1998). Par la suite, une étude confirma le phénotype glutamatergique d'une sous-population de neurones dopaminergiques par la démonstration de la présence d'ARNm de VGLUT2 et de la protéine du transporteur *in vitro* dans des neurones dopaminergiques en micro-culture dopaminergiques (Dal Bo et al., 2004). Puis, des travaux mesurant la libération de glutamate dans le striatum ventral après stimulation extracellulaire des projections axonales dopaminergiques ont appuyé l'hypothèse du double phénotype des neurones dopaminergiques (Chuhma et al., 2004; Lavin et al., 2005). En utilisant la technique de Reverse transcriptase polymerase chain reaction (RT-PCR) sur cellule unique, une autre étude confirma également l'expression de l'ARNm de VGLUT2 dans les neurones dopaminergiques (Mendez et al., 2008). Finalement, des travaux récents ont démontré la libération de glutamate des neurones dopaminergiques *in vivo* par optogénétique (Stuber et al., 2010; Tecuapetla et al., 2010).

4.2 Hétérogénéité

Bien que l'expression du co-phénotype dans les neurones dopaminergiques soit bien documentée, elle semble différée selon les espèces. Il a été suggéré que chez les rongeurs, l'expression de VGLUT2 dans les neurones dopaminergiques soit différente chez le rat et la souris. En effet, la proportion de neurones dopaminergiques exprimant l'ARNm de VGLUT2 *in vivo* a été rapportée comme étant très faible chez le rat adulte (Dal Bo et al., 2008; Bérubé-Carrière et al., 2009; Yamaguchi et al., 2011), alors qu'elle semble être plus élevée chez la souris adulte (Mendez et al., 2008). La sensibilité différentielle des techniques de détection utilisées dans ces études (hybridation *in situ* vs RT-PCR sur cellule unique) pourrait cependant expliquer ces différences.

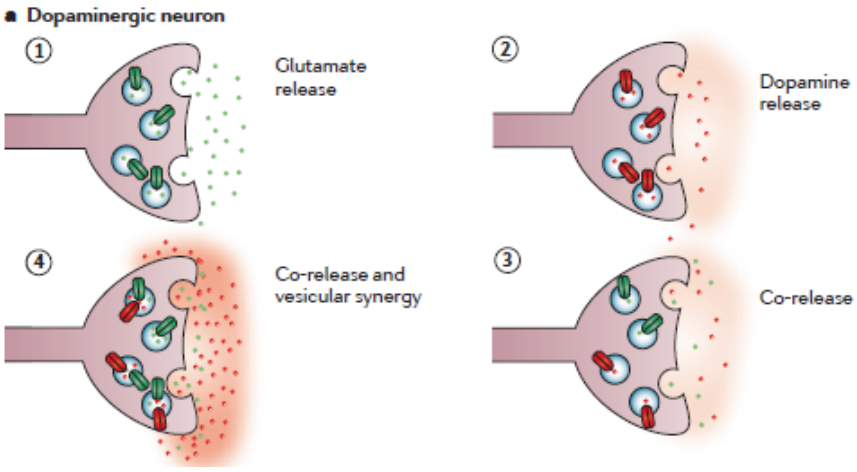

Figure 7. Hétérogénéité des terminaisons dopaminergiques libérant la dopamine et le glutamate (El Mestikawy et al., 2011).

Malgré le fait que l'ARNm de VGLUT2 soit exprimée dans une sous-population de neurones dopaminergiques du mésencéphale *in vivo*, l'expression de la protéine est rarement

observée dans les terminaisons dopaminergiques. Alors que 30% des terminaisons dopaminergiques striatales (immunopositive pour la TH) expriment VGLUT2 chez le rat de 15 jours (Dal Bo et al., 2008), presque qu'aucune varicosité axonale dopaminergiques exprimant VGLUT2 n'a été observée dans le striatum chez le rat adulte (Yamaguchi et al., 2007; Dal Bo et al., 2008; Bérubé-Carrière et al., 2009; Forlano and Woolley, 2010). Une explication à ce paradoxe pourrait être une ségrégation presque complète des terminaisons dopaminergiques libérant le glutamate et la dopamine (voir Figure 7), un phénomène qui pourrait varier durant le développement. Il n'y a cependant aucune donnée démontrant ceci directement.

4.3 Rôles physiologiques

La signification physiologique du co-phénotype DA/glutamate des neurones dopaminergiques est présentement méconnue. Néanmoins, plusieurs hypothèses ont été proposées afin d'expliquer le rôle fonctionnel de VGLUT2 dans ces neurones dopaminergiques. L'expression de VGLUT2 pourrait théoriquement augmenter l'entrée de DA dans les vésicules synaptiques par le processus de synergie vésiculaire (Hnasko et al., 2010). Des études proposent par ailleurs que le co-phénotype soit crucial pour le développement d'une sous-population de neurones dopaminergiques. En effet, plusieurs travaux ont démontré que le co-phénotype est régulé durant le développement (Bérubé-Carrière et al., 2009; Dal Bo et al., 2008; Mendez et al., 2008). De plus, le contact avec des neurones GABAergique semble réguler ce double phénotype (Mendez et al., 2008). Il a également été proposé que l'activation des récepteurs NMDA et AMPA aux cônes axonaux dopaminergiques régule la croissance axonale (Schmitz et al., 2009). Finalement une étude a proposé que l'expression de VGLUT2 soit importante pour la neuroprotection des neurones dopaminergiques face à des neurotoxines (Dal Bo et al., 2008). Finalement, des études comportementales ont proposé que l'expression de VGLUT2 favorise la motivation de consommation des drogues d'abus et module les comportements moteurs induits par ces drogues d'abus (Birgner et al., 2010; Hnasko et al., 2010; Alsiö et al., 2011).

5. Hypothèses

Depuis la caractérisation des transporteurs vésiculaires du glutamate, des dizaines de travaux ont rapporté la présence de ces transporteurs chez d'autres populations de neurones libérant des neurotransmetteurs classiques. Néanmoins, peu d'études ont analysé la signification physiologique de ce phénomène et la plasticité phénotypique de ces neurones. Ainsi, la signification physiologique de la co-transmission par une sous-population de neurones dopaminergiques, l'hétérogénéité des sites de libération ainsi que les signaux régulant ce double phénotype sont présentement inconnus.

Considérant des études récentes suggérant un rôle développemental du co-phénotype des neurones dopaminergiques; la première hypothèse est que l'expression de VGLUT2 est nécessaire pour A) la survie et B) la croissance d'une sous-population de neurones dopaminergiques. Afin de répondre à cette hypothèse, nous avons utilisé une souris transgénique ayant une délétion spécifique de VGLUT2 dans les neurones dopaminergiques. Nous avons ensuite évalué *in vitro* et *in vivo* l'effet de cette délétion génique sur la survie et la croissance des neurones dopaminergiques. Des analyses du nombre de terminaisons dopaminergiques et des niveaux de DA libérés dans striatum ont ensuite été examinées. Finalement, afin de mieux caractériser les impacts fonctionnels, la coordination motrice et l'activité locomotrice induite par des drogues d'abus ont également été étudiées chez ces souris transgéniques.

Considérant d'une part, certaines études démontrant l'absence de co-localisation de VGLUT2 avec la TH, le marqueur habituel des terminaisons dopaminergiques *in vivo*, et d'autre part dopaminergiques la régulation de l'expression de VGLUT2 par le contact avec des neurones GABAergiques, la deuxième hypothèse est que A) les neurones dopaminergiques établissent des sites de libération distincts pour la DA et le glutamate et que B) la ségrégation des terminaisons et l'expression du double phénotype sont régulés par le contact avec les neurones cibles. Afin de répondre à cette hypothèse, nous avons utilisé une souris transgénique ayant une délétion spécifique de VGLUT2 dans les neurones dopaminergiques ainsi qu'une souris transgénique

infectée par un gène rapporteur spécifiquement dans les neurones dopaminergiques. Nous avons analysé *in vitro* et *in vivo* l'hétérogénéité des terminaisons et la régulation du double phénotype en présence ou en absence des neurones striataux.

Chapitre 2: Résultats

Article 1

Glutamate co-release promotes growth and survival of midbrain dopamine neurons

Abbreviated title: Glutamate co-release promotes growth

Guillaume M. Fortin [1], Marie-Josée Bourque [1], Jose Alfredo Mendez [1], Damiana Leo [1], Karin Nordenankar [6], Carolina Birgner [6], Emma Arvidsson [6], Vladimir V. Rymar [5], Noémie Bérubé-Carrière [2], Anne-Marie Claveau[1], Laurent Descarries [2,3,4], Abbas F. Sadikot [5], Åsa Wallén-Mackenzie [6] and Louis-Éric Trudeau [1,4]

Departments of [1] Pharmacology, [2] Pathology and Cell Biology, [3] Physiology, and
[4] Groupe de Recherche sur le Système Nerveux Central, Faculty of Medicine,
Université de Montréal, Montréal, QC, Canada H3C 3J7;
[5] Montreal Neurological Institute, Department of Neurology and Neurosurgery,
McGill University, Montreal, QC, Canada H3A 2B4,
[6] Unit of Developmental Genetics, Department of Neuroscience, Uppsala University,
S-751 24 Uppsala, Sweden

Corresponding author: Louis-Eric Trudeau, Ph.D., Department of pharmacology, Faculty of Medicine, Université de Montréal, C.P. 6128, Succursale Centre-Ville, Montréal, Québec, H3C 3J7

Publié dans *The Journal of Neuroscience*, 2012, 32:17477-17491

Contribution des auteurs

Guillaume M. Fortin : Il a réalisé les expériences (Fig 1 à 7 et Fig 9) d'immunocytochimie, d'immunohistochimie, de RT-PCR sur cellule unique a ainsi que la quantification d'imagerie. Il a analysé les données des Fig. 8,10 et 11. Il a participé à l'élaboration des hypothèses. Il a réalisé tous les graphiques et figures ainsi que l'écriture du manuscrit.

Marie-Josée Bourque : Elle a préparé toutes les cultures cellulaires, à la collection de cellules uniques pour les expériences de RT-PCR, réalisé des immunocytochimies et la quantification d'imagerie. Elle a participé aux Figures 1 à 4.

Alfredo J. Mendez : Il a mis en place la technique de RT-PCR sur cellule unique. Il a également contribué à la génération des animaux cKO. Il a réalisé des expériences d'immunocytochimie et de RT-PCR. Il a contribué aux Fig. 1 à 2.

Damiana Leo : Elle a réalisé les expériences de voltammétrie (Fig.8).

Karin Nordenankar : Elle a réalisé les expériences de comportement (Fig.10 et 11).

Carolina Birgner : Elle a réalisé les expériences de comportement (Fig.10 et 11).

Emma Arvisson : Elle a réalisé les expériences de comportement (Fig.10 et 11).

Vladimir V. Rymar : Il a réalisé les expériences de compte stéréologique (Fig.6).

Noémie-Bérubé-Carrière : Elle a réalisé les expériences d'immunohistochimie en collaboration avec Guillaume M. Fortin (Fig.5).

Anne-Marie Claveau : Elle a réalisé les expériences d'immunocytochimie en collaboration avec Guillaume M. Fortin (Fig.3).

Laurent Descarries : Il a participé à l'écriture du manuscrit et à l'élaboration des hypothèses.

Abbas F. Sadikot : Il a participé à l'écriture du manuscrit.

Åsa Wallén-Mackenzie : Elle a participé à l'écriture du manuscrit.

Louis-Éric Trudeau : Il a réalisé les expériences d'électrophysiologie (Fig.2), participé à l'écriture du manuscrit et à l'élaboration des hypothèses.

Acknowledgments

This work was funded by grants to L.-E.T from the Canadian Institutes of Health Research (CIHR, MOP-106556), the Parkinson Society of Canada and Brain Canada Foundation (Krembil Foundation), and partially supported by CIHR grants MOP-3544 and MOP-106562 to L.D. L.-É.T. and L.D. also benefit from an infrastructure grant of the Fonds de la recherché en santé du Québec (FRSQ) to the GRSNC (Groupe de Recherche sur le Système Nerveux Central). G.F. received a graduate scholarship from the Parkinson Society of Canada and N.B.-C. was recipient of a doctoral studentship from FRSQ. D.L. was supported by a postdoctoral fellowship from the Department of Foreign Affairs and International Trade of Canada, and by a postdoctoral fellowship from the FRSQ. Research in Å.W.-M.'s laboratory was supported by the Swedish Research Council, the Swedish Brain Foundation, the Åhlén and Wiberg Foundations, the National Board of Health and Welfare, and Uppsala University, Sweden. The Swedish Foundation for International Cooperation in Research and Higher Education (STINT) also provided support for collaboration between L.-É.T.'s and Å.W.-M.'s laboratories. A.B.S. was funded by operating grants from the CIHR and NSERC.

Abstract

Recent studies have proposed that glutamate co-release by mesostriatal dopamine (DA) neurons regulates behavioral activation by psychostimulants. How and when glutamate release by DA neurons might play this role remains unclear. Considering evidence for early expression of the type 2 vesicular glutamate transporter (VGLUT2) in mesencephalic DA neurons, we hypothesized that this cophenotype is particularly important during development. Using a conditional gene knockout (cKO) approach to selectively disrupt the *Vglut2* gene in mouse DA neurons, we obtained *in vitro* and *in vivo* evidence for reduced growth and survival of mesencephalic DA neurons, associated with a decrease in the density of DA innervation in the nucleus accumbens, reduced activity-dependent DA release and impaired motor behavior. These findings provide strong evidence for a functional role of the glutamatergic cophenotype in the development of mesencephalic DA neurons, opening new perspectives into the pathophysiology of neurodegenerative disorders involving the mesostriatal DA system.

Introduction

Since their discovery (Bellocchio et al., 2000; Herzog et al., 2001; Takamori et al., 2000), the presence of one or the other of the three vesicular glutamate transporters (VGLUTs) has been demonstrated in many neuron populations of CNS and notably in dopamine (DA) neurons (El Mestikawy et al., 2011).

Patch-clamp recordings in single-neuron cultures initially demonstrated that mesencephalic DA neurons can establish glutamatergic synapses (Bourque and Trudeau, 2000). Mesencephalic DA neurons were then found to express vesicular glutamate transporter 2 (VGLUT2) mRNA (Dal Bo et al., 2004), and VGLUT2 mRNA and protein were visualized in subsets of these DA neurons and their axon terminals in both rats and mice (Kawano et al., 2006; Yamaguchi et al., 2007; Dal Bo et al., 2008; Descarries et al., 2008; Mendez et al., 2008; Bérubé-Carrière et al., 2009). *Vglut2* expression by mesencephalic DA neurons was shown to be regulated developmentally (Dal Bo et al., 2008; Mendez et al., 2008). Moreover, VGLUT2 immunoreactivity was reported to disappear from tyrosine hydroxylase (TH) positive terminals of adult rat striatum (Bérubé-Carrière et al., 2009b). While VGLUT2 allows DA neurons to release glutamate, it has been hypothesized that it may also facilitate the vesicular loading of DA (Hnasko et al., 2010), a concept called "vesicular synergy", first described for VGLUT3 in striatal cholinergic interneurons (Gras et al., 2008b).

Little information is currently available regarding the functional significance of glutamate co-release by DA neurons of the CNS, but specific deletion of the *Vglut2* gene in DA neurons of mice has been shown to decrease DA release in the nucleus accumbens (Hnasko et al., 2010) and alter psychostimulant-induced locomotor activation (Birgner et al., 2010; Hnasko et al., 2010) as well as cocaine self-administration (Alsiö et al., 2011). Whether such anomalies are due to loss of glutamate co-release and/or of vesicular synergy in the adult brain, or rather to a developmental perturbation, is presently unclear. The early expression of *Vglut*2 in developing brain (Herzog et al., 2001; Takamori et al., 2001) argues for a role of VGLUT2 during this period. Although not entirely conclusive, there is data to support an early expression of VGLUT2 by DA neurons (Dal Bo et al., 2008; Mendez et al., 2008). Evidence for regulation of DA neuron growth by glutamate

(Schmitz et al., 2009) and for enhanced expression of *Vglut*2 in surviving DA neurons following toxin-induced lesions (Dal Bo et al., 2008) also argues for a developmental and perhaps pro-survival role of VGLUT2 in DA neurons.

To test this hypothesis, we generated mice with a conditional deletion of the *Vglut2* gene in DA neurons (cKO) and examined the effects of this deletion on the survival and growth of mesencephalic DA neurons in culture. We also determined the number of mesencephalic DA neurons, the density of striatal DA innervation, the ultrastructural morphology of these axon terminals and their capacity for DA release in the cKO mice, and examined the motor activity of these mice.

Materials and methods

Animals

All procedures involving animals and their care were conducted in strict accordance with the *Guide to care and use of experimental animals* (2nd Ed.) of the Canadian Council on Animal Care as well as the Swedish regulation and European Union Legislation. The experimental protocols were approved by the animal ethics committees (CDEA) and the Université de Montréal and by the University of Uppsala animal ethics committee. Housing was at a constant temperature (21°C) and humidity (60%), under a fixed 12 hours light/dark cycle and free access to food and water.

TH-GFP mice. The characterization of VGluT2 expression in DA neurons during development was performed using the tyrosine hydroxylase green fluorescent protein (TH-GFP) transgenic mouse line *TH-EGFP/21–31*, which carries the enhanced GFP (EGFP) gene under the control of the TH promoter (Matsushita et al., 2002). The presence of GFP allowed identification and selection of DA neurons for single-cell RT-PCR experiments.

Conditional Vglut2 knockout mice. All other experiments were performed using conditional *Vglut2* knockout mice and control littermates. DAT-CRE transgenic mice (129/ Sv/J background) (Zhuang et al., 2005) were mated with *Vglut2 flox/flox* mice (129, C57Bl/6

background) (Tong et al., 2007) carrying the exon 2 surrounded by loxP sites. A breeding colony was maintained by mating DAT-CRE;*Vglut2*$^{flox/+}$ mice with *Vglut2*$^{flox/flox}$ mice. 25% of the offsprings from such mating were thus used as controls (i.e. DAT-CRE;*Vglut2*$^{flox/+}$ mice) and 25% lacked *Vglut2* in DA neurons (i.e. DAT-CRE;*Vglut2*$^{flox/flox}$ mice). Only male littermates of such mating were used as study subjects.

Tissue processing and cell culture

P0-P2 mice were cryoanesthetized and decapitated for tissue collection. For older mice, animals were anaesthetized with Halothane (Sigma-Aldrich, Oakville, ON, Canada) and decapitated. Freshly dissociated cells were prepared and obtained as previously described (Mendez et al., 2008). Primary cultures of mesencephalic DA neurons were also prepared according to previously described protocols (Fasano et al., 2008a). Mesencephalic cells were plated onto either microislands (microcultures) or monolayers (standard cultures) of astrocytes. The microculture system was used in order to isolate single neuron and perform recordings of autaptic synaptic responses. Mesencephalic microcultures were used for immunocytochemistry or electrophysiology experiments at 10 DIV. Cultures of FACS-purified mesencephalic DA neurons from TH-GFP mice were prepared as previously described (Mendez et al., 2008). TH immunostaining revealed that 86% of the neurons in such cultures were dopaminergic (total of 3 cultures analysed). Purified cultures were chronically treated (every three days) with 20 µM AP5 (Tocris, St-Louis, MO, USA), 10 µM CNQX (Sigma, St-Louis, MO, USA) or 40 µM LY 341945 (Ascent Scientific, New Jersey, USA) until 12 DIV.

Multiplex single-cell RT-PCR

Collection of freshly dissociated GFP-positive neurons was performed as previously described (Mendez et al., 2008). For the single-cell RT-PCR experiments performed with TH-GFP mice, the cDNA produced was used for a multiplex TH and *Vglut2* amplification. For the experiments performed on freshly dissociated cells from P0-P2 cKO mice, half of the cDNA was used to amplify TH. The other half was used to amplify the wild type or cKO *Vglut2* allele.

Primers were designed not to interact with other primers for multiplex PCR. Primers were synthetized by AlphaDNA (Montreal, QC, Canada). Nested PCRs were performed during the second round for TH, WT *Vglut2* and KO *Vglut2*. The identity of PCR products as confirmed by

sequencing. Primers for single-cell RT-PCR in experiments on TH-GFP mice were: TH 5'-gttctcaacctgctcttctcctt-3' and 5'-ggtagcaatttcctcctttgtgt-3'; TH nested (374 bp) 5'-gtacaaaaccctcctcactgtctc-3' and 5'-cttgtattggaaggcaatctctg-3'; WT *Vglut2* 5'-atctacagggtgctggagaagaa-3' and 5'-gatagtgctgttgttgaccatgt-3'; WT *Vglut2* nested (234 bp) 5'-atctacagggtgctggagaagaa-3′ and 5′-gatagtgctgttgttgaccatgt-3′. Primers used for single-cell RT-PCR in experiments on conditional knockout mice were: KO *Vglut2* 5′-aagaatggagtcggtaaaacaaag-3′ and 5′-gtgatgatatagccccagaagaac-3′; KO *Vglut2* nested (wild type allele: 417 bp; cKO allele: 165 bp) 5′-atccgtctttcatagccacaac-3′and 5′-tcagcatattgagggtagaggtg-3′. Primers used for genotyping conditional knockout mice were: DAT-Cre 5′-accagccagctatcaactcg-3′ and 5′-ttacattggtccagccacc-3′; lox-VGluT2: 5′-gtctactgtaagtgaagacac-3′ and 5′-ctttaggctttcatccttgag-3′.

Electrophysiology

Patch-clamp recordings were obtained from single dopamine neurons in microcultures using a Warner PC-505 patch-clamp amplifier (Warner Instruments Corp., Hamden, CT, USA) and PClamp 10 software (Axon Instruments, Union City, CA, USA). Borosilicate glass patch pipettes (3-6 MΩ, World Precision Instruments Inc., Sarasota, FL, USA) were filled with a potassium methylsulfate intrapipette solution consisting of (mM): $KMeSO_4$ 145, NaCl 10, EGTA 0.1, ATP (Mg salt) 2, GTP (Tris salt) 0.6, HEPES 10, phosphocreatine (Tris salt) 10, pH 7.35 and osmolarity 295-300 mOsm. Series resistance was compensated to approximately 75%. After recordings, the dopamine phenotype of patched neuron was confirmed by TH immunocytochemistry as described below.

Immunocytochemistry on cell cultures

Standard and micro cultures from cKO mice and standard FACS-purified cultures from TH-GFP mice were fixed with 4% paraformaldehyde (PFA), permeabilized, and nonspecific binding sites blocked. Primary anti-GFP (Ab290; Abcam, Cambridge, MA, USA) antibody was used at a 1:5000 dilution, in order to amplify and visualize the GFP signal of freshly dissociated cells on fixed coverslips after collection of cells. Images of GFP immunostaining were then acquired with a Hamamatsu Orca-II digital-cooled CCD camera, and a workstation using the ImagePro Plus imaging software suite.

To identify and analyse the density and the development of DA neurons, a rabbit anti-TH antibody (Ab132;Millipore, Etobicoke, ON, Canada) was used at a dilution of 1:1000 in combination with a mouse anti-VGLUT2 antibody (135611; Synaptic Systems, Goettingen, Germany), at a dilution of 1:2000. The same rabbit anti-TH antibody (1:1000) was also used in combination with a mouse anti-Tau1 antibody (MAB3420PS, Chemicon, Temecula, CA, USA) (1:1000) to visualize DA neuron axons. To study the segregation of dopaminergic and glutamatergic terminals established by DA neurons, a chicken anti-GFP (GFP-1020, Aves Labs, Tigard, OR, USA) was used at a dilution 1:1000 in combination with a rabbit anti-VGLUT2 (135 402; Synaptic Systems, Goettingen, Germany) at a dilution of 1:4000 and a mouse anti-TH (MAB318; Millipore, Etobicoke, ON, Canada) at a dilution of 1:3000 or a rat anti-DAT (MAB369; Millipore, Etobicoke, ON, Canada) at a dilution of 1:1000.

Immunohistochemistry

Male P70 mice were deeply anesthetised with sodium pentobarbital (80 mg/kg i.p.) and fixed by intra-cardiac perfusion of 150 ml of 4% PFA. The brain was removed, post-fixed by immersion for 24-48 h in the PFA solution at 4°C, and washed in phosphate-buffered saline (PBS: 0.9% NaCl in 50 mM PB, pH 7.4). Coronal and sagittal 50 um sections were cut using a VT1000S vibrating microtome (Leica Microsystems, Richmond Hill, ON, Canada). Coronal sections were permeabilized, nonspecific binding sites blocked and incubated overnight with a mouse anti-TH antibody (T1299; Sigma-Aldrich, St-Louis, MO, USA or MAB318; Millipore, Etobicoke, ON, Canada) (1:1000) or with a rat anti-DAT antibody (MAB369; Millipore, Etobicoke, ON, Canada) (1:1000) in combination with a rabbit anti-VGLUT2 antibody (135 402; Synaptic Systems, Goettingen, Germany) (1:2500); these were subsequently detected using mouse or rat Alexa-fluor 488 and rabbit Alexa-fluor 546-conjugated secondary antibodies (Invitrogen Canada, Burlington, ON, Canada) (1:200). For the evaluation of TH activity, coronal 150 µm sections were cut using a VT1000S vibrating microtome. Coronal sections were permeabilized, nonspecific binding sites blocked and incubated overnight with a mouse anti-TH antibody (MAB318; Millipore, Etobicoke, ON, Canada) (1:1000) in combination with a rabbit anti-phospho-(Ser40) TH antibody (cat.2971; Cell signalling, Danvers, MA, USA) (1:100); these were subsequently detected using mouse Alexa-fluor 488 and rabbit Alexa-fluor 546-conjugated secondary antibodies (Invitrogen Canada, Burlington, ON, Canada) (1:200). Sagittal sections were

preincubated for 1 h in a blocking solution containing 5% normal goat serum, 0.3% Triton X-100, and 0.5% gelatin in PBS and incubated overnight with anti-TH antibody (1:1,000) and then for 2 h in biotinylated goat anti-mouse (1:1000) (Jackson Immunoresearch-Cerlane, Burlington, ON, Canada) in blocking solution. After rinses in PBS (3 × 10 min), they were incubated for 1h in horseradish peroxidase (HRP)-conjugated streptavidin (1:1000) (Jackson Immunoresearch-Cederlane, Burlington, ON, Canada), washed in PBS, and incubated for 2–5 min in Tris-buffered saline (TBS) containing 3,3′-diaminobenzidine tetrahydrochloride (0.05% DAB) and hydrogen peroxide (0.02%). The reaction was stopped by several washes in TBS followed by PB, and the sections were mounted on microscope slides, dehydrated in ethanol, cleared in toluene, and coverslipped with DPX. They were examined and photographed with a Leitz Diaplan optical microscope coupled to a Spot RT color digital camera.

Image acquisition with confocal microscopy

All of the *in vitro* and *in vivo* imaging quantification analyses from cKO mice were performed on images captured using confocal microscopy. Images were acquired using an Olympus Fluoview FV1000 microscope (Olympus Canada, Markham, Ontario). Images acquired using 488 and 546 laser excitation were scanned sequentially in order to reduce non-specific bleed-through signal. For the quantification of soma diameter, TH surface and axon length, 10 cells per coverslip were randomly chosen and pictures acquired using a 40X water immersion objective. For the Sholl analysis, 10 cells per coverslip were randomly chosen and pictures acquired using a 20X water immersion objective. For quantification of terminals in adult nucleus accumbens shell, core or dorsal striatum, images were acquired using a 60X oil immersion objective. For image acquisition in the dorsal striatum, 5 random fields on each side were taken from the left and the right hemisphere in each section. For acquisition in the nucleus accumbens core, 5 fields were selected next (ventromedian to ventrolateral) to the anterior commissure from the left and the right hemisphere in each section. For acquisition in the nucleus accumbens shell, 5 fields were acquired from the cone, intermediate and ventrolateral subregions, from the left and the right hemisphere in each section.

Image quantification

All image quantification was performed using Image J (NIH) software. We first applied a background correction at the same level for every image analysed before quantification of any of the parameters described below. The Image J Sholl analysis plugin was used to quantify neurite complexity: images were first thresholded at the same level in both control and cKO groups. The Image J NeuronJ (Meijering et al., 2004) plugin was used to measure axon length. The soma diameter, average TH surface, Sholl analysis and axon length values were obtained by averaging the values from 10 different DA neurons for each coverslip analysed. At least 9 coverslips from 3 different cultures were used for all quantifications. The quantification of dopaminergic and glutamatergic terminals in striatal sections performed by averaging 5 images coming from 5 different sections for every structure analysed per animal. Images were thresholded at the same level for the control and cKO groups and quantification of terminals were performed by selecting objects with a surface area between 0.28 and 5.75 um^2, as previously described (Fasano et al., 2010). TH and VGLUT2 colocalization analysis on slices was performed by measuring the Pearson coefficient using the Image J Manders coefficient (Manders et al., 1993) plugin.

Unbiased stereological analysis

Unbiased estimates of the number of midbrain DA neurons were obtained using the optical fractionator method as previously described (van den Munckhof et al., 2003). The rostrocaudal extent of the midbrain was examined in TH-immunostained 40 µm- thick coronal serial sections from male P90 cKO and control mice, with the observer blind to genotype. TH-immunoreactive neurons were counted in every fourth section at 100X magnification using a 60x60 μm^2 counting frame. Sections counted corresponded to levels -2.54, -2.80, -3.08, -3.40, -3.64, -3.88, -4.16 mm (240 µm interval), with respect to Bregma (Paxinos and Franklin, 2008). A 10 µm optical dissector was used with 2 µm guard zones, and counting sites were located at 150 µm intervals after a random start. Mesencephalic DA nuclei, including VTA, substantia nigra pars compacta (SNc), substantia nigra pars reticulata (SNr) and retrorubral field (RRF) were examined. Stereological estimates of the total number of TH-immunoreactive neurons within each nucleus were obtained.

Fast scan cyclic voltammetry

One month-old male mice were anesthetized with halothane (Sigma-Aldrich, Oakville, ON, Canada), decapitated, and the brain was quickly removed. Coronal slice (300 μm) containing the striatum were cut with a VT1000S vibrating microtome (Leica Canada) in ice-cold artificial cerebrospinal fluid (aCSF, mM:125 NaCl, 26 $NaHCO_3$, 2.5 KCl, 2.4 $CaCl_2$, 1.3 $MgSO_4$, 0.3 KH_2PO_4 and 10 D-Glucose saturated with 95/5% O_2/CO_2). After 1 h of recovery at room temperature, slices were put in a recording chamber and perfused with aCSF at 1ml/min (32°C ± 0.5). Experimental recording started 20 min after transfer to the slice chamber. Carbon-fibre electrodes (5 μm) were prepared as described previously (Kawagoe et al., 1993). The electrode tips were placed ~ 100 nm below the slice surface and the potential was linearly scanned from −400 mV to +1000 mV at 300 V/s every 100 ms using an Axopatch 200B amplifier (Axon Instruments, Union City, CA, USA). Single (400 μA, 1 ms), and train (10 Hz, 20 pulses) pulses were computer generated and delivered by a S-900 stimulator (Dagan Corporation, Minneapolis, MN, USA) through a bipolar electrode (Plastics One, Roanoke, VA, USA) placed on the surface of the slice. Slices were stimulated every 2 min. The DA oxidation current was converted to DA concentration after calibration of the electrode with DA (1 μM).

Animal housing for behavioral studies

Three to five month-old male mice were housed in standard macrolon cages (59x38x20 cm) with aspen wood bedding (Scanbur AB Sollentuna, Sweden) and a wooden house. The temperature was 21-22°C, the humidity 45-55 % and a 12-h light/12-h dark cycle was used, lights on at 7h00. The animals had free excess to water and food (R36, Labfor, Lactamin, Vadstena, Sweden). In all experiments, littermates were used to ensure that group differences were only dependent on genotype. The experimenter/observer was blind to the genotype of the mice throughout the study. Behavioral tests were performed on 12 male cKO animals and 7 male control mice. The animals were tested between 8:00 a.m. and 18:00 p.m.

Rotarod

The accelerating rotarod task was used to assess motor coordination and balance. The apparatus consisted of five rotating rods separated by walls and elevated 30 cm from the ground. The mouse was placed facing forward on the rod and the speed of rotation was gradually increased from 0 rpm to 45 rpm in one minute. The mouse had to continuously walk forward to

stay on the cylinder. The rotations were counted and the trial was stopped upon falling from the rod. Duration, speed and number of rotations were compared. Three trials per day were performed and averaged.

Forced swim test

The forced swim test was used to assess depressive behavior (Porsolt et al. 1977). The mice were subjected to two trials where they were placed in a Plexiglas cylinder filled with 30 cm deep water (25°C). Each animal was videotaped for 6 min and thereafter scored using AniTracker software for the time spent swimming and latency to first become still.

Spontaneous and psychostimulant-induced motor activity in a novel environment

To evaluate spontaneous motor behavior in a novel environment, the mice were placed in cages designed for activity monitoring (Locobox, Kungsbacka Reglerteknik AB, Sweden) containing a plastic box (55 x 55 x 22 cm) inside a ventilated and illuminated (10 lux) cabinet for 40 min. Mice were then administered saline and three different doses of amphetamine (0.75 mg/kg, 1.5 mg/kg and 3.0 mg/kg of amphetamine, respectively) through i.p. injection in a randomized order with a minimum of one week between doses. Motor behavior was monitored for 90 min following injection. Preceding all injections, animals were allowed to acclimatize to the environment and basal motor activity was recorded. The mice were returned to their home cages directly after activity monitoring.

Five weeks after the amphetamine study was finished, the mice were analysed for cocaine-induced response in the same activity-monitoring setup as for amphetamine-induced response. In this study, the same mice were used, except one cKO male mouse that had died. First, the mice were injected i.p. with saline and activity was recorded. After a one week rest, they were treated with 10 mg/kg cocaine and activity was recorded again.

Statistics

Data are represented throughout as mean ± SEM. Statistically significant differences were analysed using Student's *t* test, one-way repeated measures ANOVA, two-way ANOVA or the Mann-Whitney Rank Sum test, as appropriate. One animal was considered as an outlier (>2 SD) and was rejected from the final analysis of the stereological counting experiment.

Results

Early developmental expression of *Vglut2* in DA neurons

In order to substantiate previous findings showing that *Vglut2* is expressed early in developing DA neurons (Dal Bo et al., 2004; Dal Bo et al., 2008), we profiled DA neurons, using single-cell reverse transcriptase polymerase chain reaction (RT-PCR), to detect the presence of *Vglut2* mRNA, as well as mRNA for the DA neuron marker TH, at different pre- (E14, E16, E18) and postnatal (P1, P14, P35, P70) time points. Neurons were freshly-dissociated from the ventral mesencephalon of TH-GFP transgenic mice expressing the green fluorescent protein (GFP) gene under control of the TH promoter. Only GFP expressing neurons were collected (Fig. 1*A*, 1*B*).

The proportion of TH positive neurons expressing *Vglut2* mRNA (Fig. 1*C*) was 7% (1/15) at E14, 47% at E16 (9/19), 33% (9/27) at E18, 22% (8/37) at P0-P2, 14% (4/28) at P14, 30% (10/33) at P35 and 47% (7/15) at P70 (Fig. 1*D*). To extend these data, obtained from whole ventral mesencephalon, we also examined separately substantia nigra (SN) and ventral tegmental area (VTA) DA neurons obtained from P0-P2 and P70 mice (Fig. 1*E*). The proportion of TH/*Vglut2* neurons was almost threefold higher in the VTA (P0-P2: 36%, 5/14; P70: 78%, 14/18) than in the SN (P0-P2: 13%, 3/23; P70: 25%, 2/8). mRNA for the DA transporter (DAT), another marker of DA neurons, was detected in a majority of DA neurons at both pre- (83% at E16) and post-natal (89% at P35) ages (Fig. 1*F,* 1*G*). Together, these results indicate that *Vglut2* is expressed early in developing VTA and SN DA neurons, in keeping with a role early in development.

Absence of *Vglut*2 mRNA, VGLUT2 protein and glutamate release in DA neurons from cKO mice

We used a conditional gene KO approach to selectively disrupt the *Vglut2* gene in DAT-expressing DA neurons (Fig.2). The cKO mice were generated by crossing DAT-Cre mice with *Vglut2* floxed mice (see Methods). The effectiveness of the strategy was evaluated by single-cell RT-PCR on freshly dissociated cells from the mesencephalon of P0-P2 pups. We found that in cKO pups, all TH positive DA neurons expressed the *Vglut2* KO allele, but not the *Vglut2* WT

allele (Fig. 2*A-B*). Likewise, every TH positive DA neuron collected from control littermates expressed the WT *Vglut2* allele (Fig. 2*A-B*). We also found a small contingent of TH negative neurons collected from cKO tissue that expressed the *Vglut2* KO allele (Fig. 2*B*), thus suggesting that the DAT promoter was active temporarily during development in a subset of mesencephalic glutamatergic neurons.

To further confirm the success and selectivity of the conditional KO strategy, we examined VGLUT2 protein expression in single neuron cultures prepared from the ventral mesencephalon of cKO mice and control littermates (Fig. 2*C-D*). Mesencephalic DA neurons cultured on microislands can form autapses and express high levels of VGLUT2 protein (Dal Bo et al., 2004; Mendez et al., 2008), thus allowing the recording of robust autaptic currents mediated by glutamate. Confirming previous findings (Dal Bo et al., 2004; Mendez et al., 2008), we found that the majority of isolated TH positive DA neurons in control cultures were immunopositive for VGLUT2 (32/42) (Fig. 2*C-D*). We also found 5 control TH negative neurons expressing VGLUT2, consistent with the presence of glutamatergic neurons in the ventral mesencephalon (Yamaguchi et al., 2007; Dobi et al., 2010). In cultures prepared from cKO mice, there were no DA neurons positive for VGLUT2 (0/51) (Fig. 2*C-D*). In cKO cultures, we also found 12 TH negative neurons positive for VGLUT2, thus demonstrating that the KO was selective for DA neurons and did not lead to loss of *Vglut2* in all mesencephalic glutamate neurons.

Patch-clamp recordings of autaptic synaptic currents from isolated DA neurons were used to evaluate whether *Vglut2* gene deletion leads to the predicted loss of the capacity for glutamate release by DA neurons. In keeping with previous findings (Bourque and Trudeau, 2000)), autaptic glutamate- mediated excitatory postsynaptic currents (EPSCs) were detected in 7 out of 13 isolated TH positive neurons in control cultures (Fig. 2*E*). In contrast, no EPSCs were observed in 18 isolated TH positive DA neurons recorded from cKO cultures (Fig. 2*E*). Post-recording immunocytochemistry confirmed that EPSCs were recorded in DA neurons containing VGLUT2, while this protein was undetectable in DA neurons from cKO cultures (Fig. 2*F*). Together, these results confirm the selective and complete deletion of the *Vglut2* gene from DA

neurons and show that this manipulation abrogates the ability of DA neurons to release glutamate.

Deletion of *Vglut2* causes DA neuron loss in culture

To evaluate the possibility of a developmental role of VGLUT2 in DA neurons and to test the hypothesis of a contribution of glutamate cotransmission to cell survival, we first counted the number and proportion of DA neurons in primary mesencephalic cultures prepared from WT and cKO P0-P2 mice (Fig. 3*A*). In similar cultures prepared, this time from TH-GFP mice, we observed that 38% (8/21) of TH+ cells contained VGLUT2 mRNA at 1 day *in vitro* (DIV), by using single-cell RT-PCR. Immunocytochemistry experiments revealed that the number of TH positive neurons normalized to the total population of neurons present on each coverslip was significantly decreased in the cKO cultures compared to WT at all time-points examined: 1 DIV: 23% (77.1±6.0% of control); 5 DIV: 29% (71.2±6.3% of control, and 14 DIV: 36% (64.3±5.1% of control). The average data, normalized to the control group of each experiment, is shown in Fig. 3*B*. There was no significant difference in the survival of DA neurons in cKO cultures from 1 to 14 DIV (Fig. 3*B*).

NMDA receptors contribute to the survival of dopamine neurons in purified dopamine neurons culture

Considering that glutamate release from DA neurons has been shown to activate ionotropic AMPA/kainate and NMDA receptors (Tecuapetla et al., 2010; Stuber et al., 2010) and that NMDA receptors are also present on the growth cone of developing DA neurons (Schmitz et al., 2009), we next evaluated which class of glutamate receptors contributes to survival. Purified DA neuron cultures were prepared by automated cell sorting from P0-P2 TH-GFP mice in order to exclude indirect drug effects through an action on non-DA neurons. DA neurons were treated chronically for 12 days with either AMPA/kainate (CNQX), NMDA (AP5) or mGluR (LY 341495) receptor antagonists. The number of TH positive neurons was significantly decreased in AP5-treated cultures (87.38 ±4.38% of control, P=0.02) (Fig. 3*C*). However, no difference was observed in cultures treated with CNQX or LY 341495 (Fig. 3*C*). If glutamate release in

developing DA neuron growth cones leads to a pro-survival autocrine-like activation of NMDA receptors (Schmitz et al., 2009), we reasoned that blocking these receptors at an early stage of development should have a greater effect on survival than at a later stage. To test this hypothesis, we treated purified DA neuron cultures with AP5 from 0 to 7 DIV or from 7 to 14 DIV. We observed decreased survival of TH+ neurons treated with AP5 between 0-7 DIV (82.54 ±3.64% of control, P=0.0006), but no difference when treated from 7-14 DIV (115.1 ±8.99% of control, P=0.14) (Fig. 3*D*).

Deletion of *Vglut2* impairs dopamine neurons growth *in vitro*

In keeping with a developmental role, it has recently been proposed that glutamate regulates axonal growth in cultured DA neurons (Schmitz et al., 2009). To test the hypothesis that glutamate release by DA neurons contributes to the growth of these cells, we examined DA neurons in culture after 1 DIV to quantify soma size, neurite complexity and axonal length (Fig. 4A, 4B). The soma diameter of TH positive neurons was found to be modestly (6.2%) but significantly reduced in cultures prepared from cKO mice in comparison to control (93.8±1.6% of control, P=0.03) (Fig. 4*C*). We also examined the total surface of TH immunoreactive neurites to provide a global index of cell size, including axons and dendrites. This surface was 17.9% smaller in cKO cultures (82.1±4.4% of control, P=0.001) compared to control DA neurons (Fig. 4*D*). Sholl analysis was also used to evaluate branching complexity. The number of intersections crossing analysis circles was significantly smaller (P=0.05) in cKO than in control DA neurons (Fig. 4*E*), reflecting reduced complexity. Axon growth rate was finally quantified by measuring the length of the longest neurite, confirmed in initial experiments to be immunopositive for Tau1 (Fig. 4*F*). We observed that at 1 DIV, axon length was 15.7% shorter in cKO DA neurons (84,3±4.0% of control, P=0.005) than in control DA neurons (Fig. 4*G*). Together, these results show that loss of VGLUT2 and the capacity for glutamate release impairs the morphological development of DA neurons.

Deletion of Vglut2 compromises the development of the mesostriatal dopamine system *in vivo*

To determine whether the growth impairment observed *in vitro* would result in some disorganization of the meso-striatal DA projection, we examined sagittal brain sections from adult cKO and control mice after TH immunolabeling with the immunoperoxidase-diaminobenzidine technique. No overt changes in the configuration of the median forebrain bundle DA pathway were observed (Fig.5).

The reduced number of TH positive neurons observed as soon as 1DIV in mesencephalic cultures prepared from cKO mice suggests the possibility that *in vivo* as well, independently of cell culture, there is a reduced number of DA neurons. Therefore, we next used unbiased stereological counting to quantify the number of DA neurons in mesencephalic brain sections prepared from both control and cKO P90 mice. The total number of TH positive neurons was found to be decreased by 19.7% in cKO tissue compared to control littermate tissue (control=12185±413, cKO=9784±302, P=0.0006). Analysis of different mensencephalic sub-structures revealed that the number of TH positive neurons was reduced by 24.4% in the VTA (control=4362±189, cKO=3297±185, P=0.002) and by 19.4% in the SN pars compacta (SNc) (control=5522±209, cKO=4450±170, P=0.002) (Fig. 6*A*). However, no differences were observed in either the SN pars reticulata (SNr) or the retro-rubral field (RRF) (Fig. 6*A*).

To determine whether the abnormal development of mesencephalic dopamine neurons in VGLUT2 deficient mice was associated with a defect in dopaminergic and/or glutamatergic innervation of the striatum, we used TH/VGLUT2 double immunohistochemistry coupled to confocal microscopy to quantify the relative number of TH, VGLUT2 and TH/VGLUT2 axon varicosities in the nucleus accumbens and neostriatum of cKO versus control P70 mice. A significant 33.3% decrease in the number of TH positive punctae was measured in the nucleus accumbens shell of the cKO mice (66.7±6.7% of control, P=0.006) (Fig. 6*B*,*D*). Although this did not reach statistical significance (P=0.08), a similar tendency was found in the nucleus accumbens core. Likewise, we observed a 33.6% and 38.2% decrease in the number of VGLUT2-positive axon-like varicosities in the accumbens shell (67.4±6.3% of control, P=0.004) and core (61.8±8.7% of control, P=0.005), respectively (Fig. 6*C*,*E*). However, in the neostriatum, there were no significant differences in the number of either TH or VGLUT2 punctae (Fig. 6*B-E*).

Interestingly, in these double labeling experiments, we did not detect any significant colocalization of TH and VGLUT2 (Fig. 6F,H*)* or DAT and VGLUT2 (Fig. 6*G)* in axon varicosities of the ventral or dorsal striatum of WT mice. The percentage of TH+ terminals colocalizing with VGLUT2+ terminals by confocal microscopy were relatively low in these WT animals, with a value ranging from 2 to 4 % in the different striatal sub-compartments (data not shown). Compatible with the possibility that much of this low level of co-localisation was actually false positive signal due the dense packing of terminals in the striatum, there was no significant difference in the extent of correlation between the two between cKO and WT tissue, as revealed by determination of the Pearson coefficient (Fig. 6H).

The demonstration of striatal glutamate release by DA neurons in adult mice by optogenetic approaches (Tecuapetla et al., 2010; Stuber et al., 2010) combined with the present results showing there is no apparent colocalization of TH or DAT and VGLUT2 in axon terminals *in vivo* could be interpreted as suggesting the existence of segregation of glutamatergic and dopaminergic terminals established by DA neurons. To evaluate this hypothesis, we used FACS-purified DA neurons in low density standard cultures prepared from TH-GFP mice and used immunocytochemistry to examine the phenotype of axonal varicosities and axonal branches emanating from confirmed, isolated DA neurons. First, we profiled such purified 7 DIV DA neurons by single-cell RT-PCR (Fig. 7*A*). We found that 95% of the GFP positive neurons collected contained TH mRNA and that 53 % of the GFP/TH positive neurons also contained VGLUT2 mRNA (Fig. 7*B*). We performed triple imunolabelling for GFP, TH and VGLUT2 on such cultures and found that 75% of isolated GFP positive neurons were immunolabeled by TH; moreover, 40% of these GFP/TH immuno-positive neurons were also immuno-positive for VGLUT2 (Fig. 7*C-D*). VGLUT2-positive axonal varicosities were found to co-express GFP and TH in the majority of isolated DA neurons examined. However, in some cases, VGLUT2 immunoreactivity was found in a strong GFP immunolabled axonal branch with very weak TH immunolabeling (Fig. 7*E*). A triple immunolabeling experiment to localize GFP, DAT and VGLUT2 revealed similar findings, with VGLUT2-positive terminals usually showing strong GFP and DAT immunolabeling (Fig. 7*F*), with occasional branches showing strong GFP signal but low DAT immunolabeling (Fig. 7*G*). Together, these results suggest that *in vitro*, DA neurons can establish at least two types of glutamatergic terminals which are either strongly or weakly immunopositive for dopaminergic markers.

Reduced dopamine release in the nucleus accumbens of cKO mice

The reduced density of DA innervation in the nucleus accumbens suggested that DA release might also be decreased in this part of the striatum in cKO mice. Cyclic voltammetry was therefore used to measure electrically-evoked DA release in striatal brain slices prepared from male P30 cKO mice and their littermate controls. We compared the nucleus accumbens shell, where the most robust reduction in terminals was detected, and the neostriatum, which showed no significant change in number of axon terminals. Single pulse stimulation (400 μA, 1 ms) was used to evaluate basal release, while short, physiologically-relevant action potential trains (10 Hz, 20 pulses) were used to more closely examine DA release under more demanding conditions, where D2 autoreceptors and DAT function regulate DA overflow. We found a 36.8% decrease in the amplitude of DA overflow evoked by single pulses in the nucleus accumbens shell (control=5.7±0.4nA, cKO=3.6±0.4 nA, P=0.005) (Fig. 8*A*). In neostriatum, there were no significant differences between the two genotypes under these conditions (Fig. 8*D*). This observation confirmed previous findings (Hnasko et al., 2010). The kinetics of DA overflow (rise time and decay time) remained unchanged (Fig. 8*B-F*). Using action potential trains, we observed a 37.8% decrease in the maximal amount of DA overflow in the nucleus accumbens shell of cKO mice (control=8.2±0.8nA, cKO=5.1±0.7nA, P=0.03) (Fig. 8*G*). Here again, no significant differences were observed in the neostriatum (Fig. 8*J*) or in the rise time or decay time of DA overflow in either region (Fig. 8*H-L*). Finally, the ratio of train-evoked versus single pulse-evoked DA overflow was also unchanged in both regions (Fig. 8*M-N*).

The reduced number of TH-positive terminals and of DA release observed in the nucleus accumbens of cKO mice could also suggest a perturbation in TH activity and/or TH expression. We performed a double-labelling experiment in mesencephalic brain sections using a TH antibody as well as a phospho-TH antibody. Quantification of the level of immunoreactivity allowed us to obtain an index of total TH as well as relative TH activity. First, we found that total TH immunoreactivity per neuron in the VTA and SNc was not different. Second, we found a decrease in the phospho-TH/TH ratio per DA neuron in the VTA (Fig. 9), but not in the SNc, of

cKO mice. This later observation is compatible with a partial contribution of reduced TH activity to the reduction in DA release.

cKO mice exhibit motor deficits

The reduced DA neuron number and growth in conditional *Vglut2* cKO mice raised the possibility of perturbations of DA dependent behaviors in these mice, as suggested by recent studies (Birgner et al., 2010; Hnasko et al., 2010; Alsiö et al., 2011). We examined three to five month-old male *Vglut2* cKO mice and first monitored spontaneous motor activity in a novel environment. In this setting, cKO mice displayed a significant decrease of 30% in horizontal activity (total horizontal beam breaks) (P=0.03) compared to littermate controls (Fig. 10*A*). Locomotion (sequences of > 2 beam breaks in one direction) also showed a tendency toward a reduction, but this did not reach statistical significance (P=0.11) (Fig. 10*B*). Rearing activity was not different between genotypes (Fig. 10*C*).

Neurotoxin-induced loss of DA neurons is known to decrease performance on the accelerating rotarod task (Rozas et al., 1998), a measure of crude motor activity and coordination. We thus examined the performance of cKO mice in this paradigm. Control and cKO mice were put on the spinning rotarod for three one min trials on two consecutive days. Compared to control, the *Vglut2* cKO mice scored less for distance (Fig. 10*D*) on day 1 (control=0.52±0.08m, cKO=0.31±0.07m, P=0.018), on speed (Fig. 10*E*) for both days (day 1: control=19.9±1.5rpm, cKO=15.4±1.4rpm, P=0.016; day 2: control=202±2.1rpm, cKO=15.0±1.5rpm, P=0.047), and on the latency to fall (Fig. 10*F*) for both days (day 1: control=22.2±2.2s, cKO=15.6±2.0s, P=0.014; day2: control=22.7±3.2s, cKO=15.1±2.3s, P=0.042).

The cKO mice and their controls were also evaluated on the forced swim test, an index of behavioral despair. The latency to the first immobilization and the total time immobile were recorded on two consecutive trials. There was no apparent difference between genotypes in the total time spent immobile (Fig. 10*G*). However, in the first trial, the cKO mice showed a significant decrease in the latency to first immobilization (control=135.4±44.2s, cKO=23.0±12.8s, P=0.043) (Fig. 10*H*).

Finally, confirming earlier results (Birgner et al., 2010; Hnasko et al., 2010), the cKO mice displayed a blunted locomotor response when challenged with amphetamine (Fig. 11*A*-*F*) or cocaine (Fig. 11*G*-*L*).

Discussion

This study suggests an important role of the glutamatergic cophenotype for the developmental regulation of the central DA system. Selective deletion of the Vglut2 gene in these neurons reduced their survival, soma size, neuritic complexity and axonal length in culture, and entailed a reduction of their number in both the VTA and the SNc *in vivo*, accompanied with a selective decrease of the density of DA innervation and of DA release in the nucleus accumbens. The cKO mice also displayed motor deficits, an altered motor response to psychostimulants, and signs of behavioural despair. Altogether, these findings provide an explanation for the reduced sensitivity of such cKO mice to psychostimulants.

Early expression of *Vglut2* in DA neurons

In the present study, single-cell RT-PCR evidence was obtained for expression of *Vglut2* mRNA by a high proportion of mesencephalic DA neurons during the late embryonic period, followed by a decrease during the postnatal period, but a return to a relatively high proportion in the adult (close to 50% at P70). The lower proportion (15%) previously reported in P45 mice (Mendez et al., 2008) may have been due to the fact that in this earlier study, midline DA neuron cell groups, in which VGLUT2 and TH coexistence is the most frequent (Kawano et al., 2006; Yamaguchi et al., 2011), were not examined. Although the proportion of DA neurons expressing *Vglut2* mRNA was higher in the VTA than SN, in young and adult mice, a subset of SN DA neurons did express *Vglut2*, in agreement with our previous report. It is important to consider that the relatively high proportion of DA neurons containing VGLUT2 mRNA at some developmental stages does not necessarily imply that these neurons contain abundant levels of such mRNA or protein. It has recently been reported that double phenotype DA neurons express only low copy number of VGLUT2 mRNA compared to TH (Yamaguchi et al., 2011).

Role for VGLUT2 in the survival and growth of mesencephalic DA neurons

In the present study, an unbiased stereological counting method revealed a decrease of TH positive neurons in both VTA and SNc of cKO mice. Because the level of TH immuno-reactivity per neuron was found to be unchanged in either of these structures in cKO animals, the reduced

number of TH positive neurons found in these mice is unlikely to be due to reduced detection of TH-positive neurons. There were also significant reductions in the number of neurons in cKO mesencephalic DA neurons cultures. Considering that cKO mice exhibited a 20% decrease in the total number of mesencephalic TH+ neurons, the 23% decrease in the number of TH+ neurons in 1DIV mesencephalic cKO cultures is likely due to the prior loss of DA neurons *in vivo* before the time of plating. Moreover, we provide pharmacological evidence suggesting that NMDA receptors contribute to the survival of these neurons *in vitro.* Activation of glutamate receptors may result in excitotoxicity (Choi et al., 1987), but glutamate receptor stimulation may also be neuroprotective under specific conditions (Vernon et al., 2005). One hypothesis is that glutamate release by developing DA neurons could have autocrine neurotrophic effects mediated by NMDA receptors. The recent demonstration that activation of presynaptic NMDA receptors on growth cones of DA axons facilitates neuritogenesis (Schmitz et al., 2009) combined with the results of the present study showing that early (0-7 DIV) but not late (7-14 DIV) NMDA receptor blockade reduces survival, speaks in favor of such a model. Compatible with our model, a recent study reported attenuated phasic DA release in the nucleus accumbens following reward delivery in mice with a conditional knockout of NR1 in DA neurons (Parker et al. 2010). Glutamate could also act through other targets such as astrocytes (Hartmann et al., 2001; Ho et al., 1995; Lin et al., 1993).

We also provide evidence for a role of the glutamatergic cophenotype in DA neuron growth. Indeed, the maturation of DA neurons cultured from *Vglut2* cKO mice was significantly impaired, as indicated by decreased soma size, neurite complexity and axon length. Acute application of glutamate has already been shown to increase the rate of DA neuron axon growth (Schmitz et al., 2009). *In vivo*, there could be multiple sources of glutamate to regulate the growth of DA axons, but our results *in vitro* suggest that glutamate release by DA neurons themselves plays a significant role. An alternate explanation of the reduced survival and growth of DA neurons in cKO mice is that this could be due to loss of vesicular synergy between VMAT2 and VGLUT2, resulting in reduced vesicular packaging and release of DA (Hnasko et al., 2010). However, this would require that DA plays a prosurvival role in DA neurons, which is not compatible with previous work (Fasano et al., 2008b).

Impaired developmental regulation of the DA system in *Vglut2* cKO mice

Although the respective contribution of impaired survival and reduced proliferation could not be determined in the present study, we report a decrease of 25% and 20% in number of DA neurons in the VTA and SNc, respectively, in cKO mice. We also found a decrease in the ratio of phospho- to total TH, an index of the relative state of phosphorylation of TH and of TH activity, in VTA DA neurons. This later observation stands in contrast to findings reported in another study (Hnasko et al., 2010). The 30% decrease in density of DA innervation, associated with a 40% decrease in the amount of electrically evoked DA release in the nucleus accumbens of the cKO mice, was consistent with the DA cell loss in the VTA. Reduced TH activity could also have contributed in part to the observed decrease in DA release. A comparable decrease in DA release has been previously reported in the nucleus accumbens of such cKO mice (Hnasko et al., 2010). In the absence of differences in the kinetics of DA overflow or in the ratio of train-evoked versus single pulse-evoked DA overflow in cKO mice, major changes in DA reuptake, vesicle mobilization and/or DA autoreceptor feedback regulation seem unlikely (Benoit-Marand et al., 2001).

Loss of vesicular synergy between VMAT2 and VGLUT2, resulting in reduced vesicular packaging and release of DA (Hnasko et al., 2010), could represent an alternate explanation for the decreased release of DA in the nucleus accumbens of cKO mice. The almost complete absence of colocalization of TH and VGLUT2 in dual labeling immunofluorescence and in immuno-electron microscopy experiments (Bérubé-Carrière et al., 2012) does not provide strong support for the vesicular synergy hypothesis; however, these findings highlight an intriguing biological phenomenon. Our *in vitro* results revealing the existence of DAergic axonal branches with very weak TH or DAT immunoreactivity raise the hypothesis that VGLUT2-positive terminals established by DA neurons in the striatum *in vivo* express only low levels of TH, thus making them difficult to detect using standard immunohistochemical techniques. It is important to highlight the fact that immunolabelling approaches simply cannot distinguish between complete lack of expression and low, sub-detection, levels of proteins in specific cellular compartments.

Why the reduced number of SNc DA neurons did not lead to significant reductions in the number of axon varicosities and DA release in the neostriatum of *Vglut2* cKO mice remains to be

explained. Compensatory sprouting may have occurred, as seen in Parkinson's disease or in response to partial 6-OHDA lesions (Rosenblad et al., 1997; Lee et al., 2008). An alternate possibility is that the SNc neurons that were lost in the *Vglut2* cKO mice are part of the small contingent of SNc neurons that preferentially innervate the nucleus accumbens (Lynd-Balta and Haber, 1994; Prensa and Parent, 2001). It may also be that the stimuli used to trigger DA release in the present experiments did not sufficiently challenge DA pools in nigro-striatal terminals. Compatible with this possibility, evidence has been provided recently for reduced DA release in the dorsolateral striatum of *Vglut2* cKO in response to potassium depolarization (Alsiö et al., 2011).

As for the 35% decrease in the number of VGLUT2 positive axon terminals in the nucleus accumbens shell and core, it could account for the recent finding of a tendency towards a decrease in potassium-evoked glutamate release in the nucleus accumbens core of another conditional *Vglut2* cKO mice (Birgner et al., 2010). This reduced number of VGLUT2 positive axon terminals might reflect the absence of glutamatergic terminals established by DA neurons projecting to the nucleus accumbens, or represent an indirect effect.

Evidence for a role of the glutamate cophenotype in motor function

The behavioral profile of two different lines of conditional *Vglut2* cKO mice has been recently examined in two studies; interestingly, both of these groups reported reduced behavioral activation in response to amphetamine and cocaine (Birgner et al., 2010; Hnasko et al., 2010). The present report confirms these results, but also provides evidence supporting motor impairment in the cKO mice, (Hnasko et al., 2010) including reduced performance in the rotarod task. A similar deficit in the rotarod test was not found in the other reports (Birgner et al., 2010; Hnasko et al., 2010). The reason for this discrepancy is unclear, but sex differences could be involved because only males were used in the present work, while both males and females were used in the other studies (Birgner et al., 2010; Hnasko et al., 2010). As no changes were observed in DA release (but see Alsiö et al., 2011) and in the density of dopaminergic terminals in the neostriatum, reduced performance in the rotarod task could be due to reduced somatodendritic DA release in the SNc (Andersson et al., 2006), resulting from the decreased number of DA

neurons in this nucleus. Reduced somatodendritic DA release could also contribute to the impaired response to psychostimulants in these cKO mice. A contribution of reduced striatal glutamatergic drive to these behavioral impairments is also likely. Our finding of reduced performance in the forced swim test could reflect depressive behavior or behavioral despair in the cKO mice, due to perturbed interactions between DA and 5-HT neurons (Wong et al., 1995). An alternate explanation might be altered motivation, consistent with a role of the glutamatergic cophenotype of DA neurons in reward and motivated behaviors, as suggested by recent work demonstrating altered self-administration of high-sucrose food and cocaine in *Vglut2* cKO mice (Alsiö et al., 2011).

In summary, the present report suggests an important role for the glutamatergic cophenotype of DA neurons in the development and the regulation of the mesostriatal dopaminergic system. Considering the involvement of this system in a number of serious diseases such as Parkinson's, schizophrenia and drug dependence, it opens new perspectives into the underlying pathophysiological processes of such disorders.

References

Alsiö J, Nordenankar K, Arvidsson E, Birgner C, Mahmoudi S, Halbout B, Smith C, Fortin GM, Olson L, Descarries L, Trudeau L-É, Kullander K, Lévesque D, Wallén-Mackenzie Å (2011) Enhanced sucrose and cocaine self-administration and cue-induced drug seeking after loss of VGLUT2 in midbrain dopamine neurons in mice. J Neurosci 31:12593–12603.

Andersson DR, Nissbrandt H, Bergquist F (2006) Partial depletion of dopamine in substantia nigra impairs motor performance without altering striatal dopamine neurotransmission. Eur J Neurosci 24:617–624.

Beaudet A, Sotelo C (1981) Synaptic remodeling of serotonin axon terminals in rat agranular cerebellum. Brain Res 206:305–329.

Bellocchio EE, Reimer RJ, Fremeau RT, Edwards RH (2000) Uptake of glutamate into synaptic vesicles by an inorganic phosphate transporter. Science 289:957–960.

Benoit-Marand M, Borrelli E, Gonon F (2001) Inhibition of dopamine release via presynaptic D2 receptors: time course and functional characteristics in vivo. J Neurosci 21:9134–9141.

Bérubé-Carrière N, Riad M, Dal Bo G, Lévesque D, Trudeau L-É, Descarries L (2009) The dual dopamine-glutamate phenotype of growing mesencephalic neurons regresses in mature rat brain. J Comp Neurol 517:873–891.

Bérubé-Carrière N, Guay G, Fortin GM, Kullander K, Olson L, Wallén-Mackenzie Å, Trudeau L-É, Descarries L (2012) Ultrastructural characterization of the mesostriatal dopamine innervation in mice, including two mouse lines of conditional Vglut2 knockout in dopamine neurons. Eur J Neurosci 35:527-538

Birgner C, Nordenankar K, Lundblad M, Mendez JA, Smith C, le Grevès M, Galter D, Olson L, Fredriksson A, Trudeau L-E, Kullander K, Wallén-Mackenzie Å (2010) VGLUT2 in dopamine

neurons is required for psychostimulant-induced behavioral activation. Proc Natl Acad Sci U S A 107:389–394.

Bourque M-J, Trudeau L-E (2000) GDNF enhances the synaptic efficacy of dopaminergic neurons in culture. Eur J Neurosci 12:3172–3180.

Carter RJ, Lione LA, Humby T, Mangiarini L, Mahal A, Bates GP, Dunnett SB, Morton AJ (1999) Characterization of progressive motor deficits in mice transgenic for the human Huntington's disease mutation. J Neurosci 19:3248–3257.

Choi D, Maulucci-Gedde M, Kriegstein A (1987) Glutamate neurotoxicity in cortical cell culture. J Neurosci 7:357 –368.

Dal Bo G, St-Gelais F, Danik M, Williams S, Cotton M, Trudeau L-É (2004) Dopamine neurons in culture express VGLUT2 explaining their capacity to release glutamate at synapses in addition to dopamine. J Neurochem 1398–1405.

Dal Bo G, Bérubé-Carrière N, Mendez JA, Leo D, Riad M, Descarries L, Lévesque D, Trudeau L-É (2008) Enhanced glutamatergic phenotype of mesencephalic dopamine neurons after neonatal 6-hydroxydopamine lesion. Neuroscience 156:59–70.

Descarries L, Bérubé-Carrière N, Riad M, Dal Bo G, Mendez JA, Trudeau L-É (2008) Glutamate in dopamine neurons: Synaptic versus diffuse transmission. Brain Res Rev 58:290–302.

Dobi A, Margolis EB, Wang H-L, Harvey BK, Morales M (2010) Glutamatergic and nonglutamatergic neurons of the ventral tegmental area establish local synaptic contacts with dopaminergic and nondopaminergic neurons. J Neurosci 30:218–229.

Drouin J (2003) Pitx3 is required for motor activity and for survival of a subset of midbrain dopaminergic neurons. Development 130:2535–2542.

El Mestikawy S, Wallén-Mackenzie Å, Fortin GM, Descarries L, Trudeau L-É (2011) From glutamate co-release to vesicular synergy: vesicular glutamate transporters. Nat Rev Neurosci 12:204–216.

Fasano C, Poirier A, DesGroseillers L, Trudeau L-E (2008a) Chronic activation of the D2 dopamine autoreceptor inhibits synaptogenesis in mesencephalic dopaminergic neurons in vitro. Eur J Neurosci 28:1480–1490.

Fasano C, Thibault D, Trudeau L-É (2008b) Culture of postnatal mesencephalic dopamine neurons on an astrocyte monolayer. Curr Protoc Neurosci 44:3.21.1–3.21.19.

Fasano C, Kortleven C, Trudeau L-É (2010) Chronic activation of the D2 autoreceptor inhibits both glutamate and dopamine synapse formation and alters the intrinsic properties of mesencephalic dopamine neurons in vitro. Eur J Neurosci 32:1433–1441.

Gras C, Amilhon B, Lepicard EM, Poirel O, Vinatier J, Herbin M, Dumas S, Tzavara ET, Wade MR, Nomikos GG, Hanoun N, Saurini F, Kemel M-L, Gasnier B, Giros B, El Mestikawy S (2008) The vesicular glutamate transporter VGLUT3 synergizes striatal acetylcholine tone. Nat Neurosci 11:292–300.

Hartmann M, Heumann R, Lessmann V (2001) Synaptic secretion of BDNF after high-frequency stimulation of glutamatergic synapses. EMBO J 20:5887–5897.

Herzog E, Bellenchi GC, Gras C, Bernard V, Ravassard P, Bedet C, Gasnier B, Giros B, El Mestikawy S (2001) The existence of a second vesicular glutamate transporter specifies subpopulations of glutamatergic neurons. J Neurosci 21:RC181.

Hnasko TS, Chuhma N, Zhang H, Goh GY, Sulzer D, Palmiter RD, Rayport S, Edwards RH (2010) Vesicular glutamate transport promotes dopamine storage and glutamate corelease in vivo. Neuron 65:643–656.

Ho A, Gore AC, Weickert CS, Blum M (1995) Glutamate regulation of GDNF gene expression in the striatum and primary striatal astrocytes. NeuroReport 6:1454–1458.

Kawagoe KT, Zimmerman JB, Wightman RM (1993) Principles of voltammetry and microelectrode surface states. J Neurosci Methods 48:225–240.

Kawano M, Kawasaki A, Sakata-Haga H, Fukui Y, Kawano H, Nogami H, Hisano S (2006) Particular subpopulations of midbrain and hypothalamic dopamine neurons express vesicular glutamate transporter 2 in the rat brain. J Comp Neurol 498:581–592.

Lee J, Zhu W-M, Stanic D, Finkelstein DI, Horne MH, Henderson J, Lawrence AJ, O'Connor L, Tomas D, Drago J, Horne MK (2008) Sprouting of dopamine terminals and altered dopamine release and uptake in Parkinsonian dyskinaesia. Brain 131:1574 –1587.

Lin L, Doherty D, Lile J, Bektesh S, Collins F (1993) GDNF: a glial cell line-derived neurotrophic factor for midbrain dopaminergic neurons. Science 260:1130–1132.

Lynd-Balta E, Haber SN (1994) The organization of midbrain projections to the striatum in the primate: sensorimotor-related striatum versus ventral striatum. Neuroscience 59:625–640.

Manders EMM, Verbeek FJ, Aten JA (1993) Measurement of co-localisation of objects in dual-colour confocal images. J Microsc 169:375–382.

Matsushita N, Okada H, Yasoshima Y, Takahashi K, Kiuchi K, Kobayashi K (2002) Dynamics of tyrosine hydroxylase promoter activity during midbrain dopaminergic neuron development. J Neurochem 82:295–304.

Meijering E, Jacob M, Sarria J-CF, Steiner P, Hirling H, Unser M (2004) Design and validation of a tool for neurite tracing and analysis in fluorescence microscopy images. Cytometry 58A:167–176.

Mendez JA, Bourque M-J, Dal Bo G, Bourdeau ML, Danik M, Williams S, Lacaille J-C, Trudeau L-É (2008) Developmental and target-dependent regulation of vesicular glutamate transporter expression by dopamine neurons. J Neurosci 28:6309–6318.

Parker JG, Zweifel LS, Clark JJ, Evans SB, Phillips PE, Palmiter RD (2010) Absence of NMDA receptors in dopamine neurons attenuates dopamine release but not conditioned approach during Pavlovian conditioning. PNAS 30:13491-6

Paxinos G, Franklin KBJ (2008) The Mouse Brain in Stereotaxic Coordinates, Compact Third Edition: The coronal plates and diagrams. Academic Press. San Diego.

Prensa L, Parent A (2001) The nigrostriatal pathway in the rat: a single-axon study of the relationship between dorsal and ventral tier nigral neurons and the striosome/matrix striatal compartments. J Neurosci 21:7247–7260.

Porsolt RD, Le Pichon M, Jalfre M (1977) Depression: a new model sensitive to antidepressants treatments. Nature 21: 730-732.

Rosenblad C, Martinez-Serrano A, Björklund A (1997) Intrastriatal glial cell line-derived neurotrophic factor promotes sprouting of spared nigrostriatal dopaminergic afferents and induces recovery of function in a rat model of Parkinson's disease. Neuroscience 82:129–137.

Rozas G, López-Martín E, Guerra MJ, Labandeira-García JL (1998) The overall rod performance test in the MPTP-treated-mouse model of Parkinsonism. J Neurosci Methods 83:165–175.

Schmitz Y, Luccarelli J, Kim M, Wang M, Sulzer D (2009) Glutamate controls growth rate and branching of dopaminergic axons. J Neurosci 29:11973–11981.

Stuber GD, Hnasko TS, Britt JP, Edwards RH, Bonci A (2010) Dopaminergic terminals in the nucleus accumbens but not the dorsal striatum corelease glutamate. J Neurosci 30:8229–8233.

Sulzer D, Joyce MP, Lin L, Geldwert D, Haber SN, Hattori T, Rayport S (1998) Dopamine neurons make glutamatergic synapses in vitro. J Neurosci 18:4588–4602.

Takamori S, Rhee JS, Rosenmund C, Jahn R (2000) Identification of a vesicular glutamate transporter that defines a glutamatergic phenotype in neurons. Nature 407:189–194.

Takamori S, Rhee JS, Rosenmund C, Jahn R (2001) Identification of differentiation-associated brain-specific phosphate transporter as a second vesicular glutamate transporter (VGLUT2). J Neurosci 21:RC182.

Tecuapetla F, Patel JC, Xenias H, English D, Tadros I, Shah F, Berlin J, Deisseroth K, Rice ME, Tepper JM, Koos T (2010) Glutamatergic signaling by mesolimbic dopamine neurons in the nucleus accumbens. J Neurosci 30:7105–7110.

Tong Q, Ye C, McCrimmon RJ, Dhillon H, Choi B, Kramer MD, Yu J, Yang Z, Christiansen LM, Lee CE, Choi CS, Zigman JM, Shulman GI, Sherwin RS, Elmquist JK, Lowell BB (2007) Synaptic glutamate release by ventromedial hypothalamic neurons is part of the neurocircuitry that prevents hypoglycemia. Cell Metabolism 5:383–393.

van den Munckhof P, Luk KC, Ste-Marie L, Montgomery J, Blanchet PJ, Sadikot AF, Drouin J (2003) Pitx3 is required for motor activity and for survival of a subset of midbrain dopaminergic neurons. Development 130:2535–2542.

Vernon AC, Palmer S, Datla KP, Zbarsky V, Croucher MJ, Dexter DT (2005) Neuroprotective effects of metabotropic glutamate receptor ligands in a 6-hydroxydopamine rodent model of Parkinson's disease. Eur J Neurosci 22:1799–1806.

Wong PT-H, Feng H, Teo WL (1995) Interaction of the dopaminergic and serotonergic systems in the rat striatum: effects of selective antagonists and uptake inhibitors. Neurosci Res 23:115–119.

Yamaguchi T, Sheen W, Morales M (2007) Glutamatergic neurons are present in the rat ventral tegmental area. Eur J Neurosci 25:106–118.

Yamaguchi T, Wang H-L, Li X, Ng TH, Morales M (2011) Mesocorticolimbic glutamatergic pathway. J Neurosci 31:8476 –8490.

Zhuang X, Masson J, Gingrich JA, Rayport S, Hen R (2005) Targeted gene expression in dopamine and serotonin neurons of the mouse brain. J Neurosci Methods 143:27–32.

Figure legends

Figure 1. Dopamine neurons express *Vglut2* early in development.

A

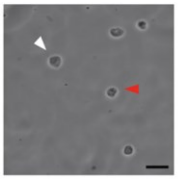

B

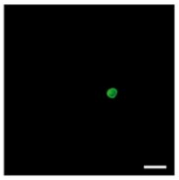

C

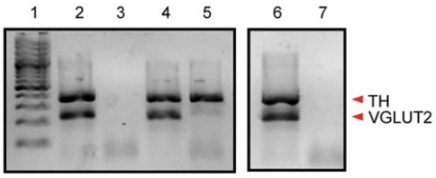

D

TH-GFP mice	% TH+ cells expressing VGLUT2
E14	7% (1/15)
E16	47% (9/19)
E18	33% (9/27)
P0-P2	22% (8/37)
P14	14% (4/28)
P35	30% (10/33)
P70	47% (7/15)

E

Age	Structure	% TH+ cells expressing VGLUT2
P0-P2	SN	13% (3/23)
	VTA	36% (5/14)
P70	SN	25% (2/8)
	VTA	78% (14/18)

F

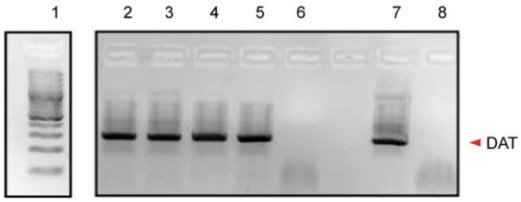

G

TH-GFP mice	% TH+ VGLUT2+ cells expressing DAT
E16	83% (5/6)
P35	89% (8/9)

A Phase-contrast and (***B***) epifluorescence view of a 40X field containing 5 dissociated cells obtained from the mesencephalon of an E18 TH-GFP mouse embryo. Only the GFP+ cells (red arrows) were individually collected for RT-PCR. Scale: bar = 25µm. ***C*** Single-cell RT-PCR from freshly dissociated E16 TH-GFP cells. In this example (wells 2-5), 2 of the 3 TH positive neurons collected expressed VGLUT2 mRNA. Well 1, DNA ladder. Well 6, whole mesencephalon RNA. Well 7, water control. ***D*** Table summarizing the results of single-cell RT-PCR experiments carried out with mice aged E14 to P70. ***E*** Table summarizing the results of single-cell RT-PCR experiments comparing the ventral tegmental area (VTA) and substantia nigra (SN) of a P0-P2 and P70 mice. ***F-G*** DAT mRNA is expressed in most double phenotype neurons. ***F*** Results of a single-cell RT-PCR experiment preformed with freshly dissociated P35 TH-GFP cells. In this example (wells 2-6), 4 of the 5 double phenotype neurons (TH and VGLUT2 positive neurons) collected expressed DAT mRNA. Well 1, DNA ladder. Well 7, whole mesencephalon RNA. Well 8, water control. ***G*** Table summarizing the results of single-cell RT-PCR experiments carried out with mice aged E16 and P35.

Figure 2. Absence of VGLUT2 prevents glutamate release from cultured dopamine neurons obtained from conditional KO mice.

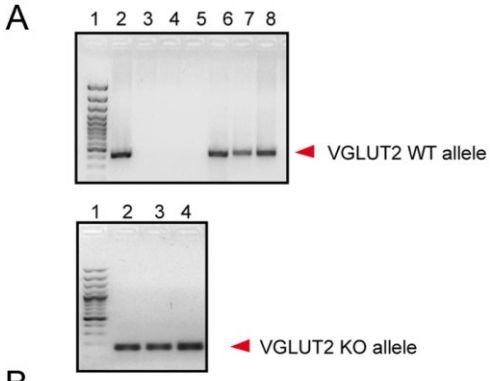

B

Phenotype	Ctrl	cKO
TH+ / VGLUT2 WT allele	7	0
TH+ / VGLUT2 KO allele	0	11
TH- / VGLUT2 WT allele	3	2
TH- / VGLUT2 KO allele	0	3

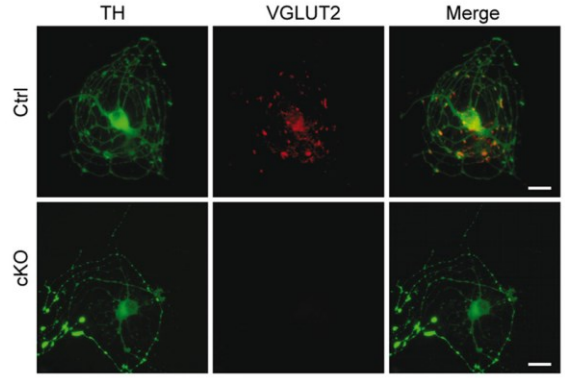

D

Phenotype	Ctrl	cKO
TH+ / VGLUT2+	32	0
TH+ / VGLUT2-	10	51
TH- / VGLUT2+	5	12

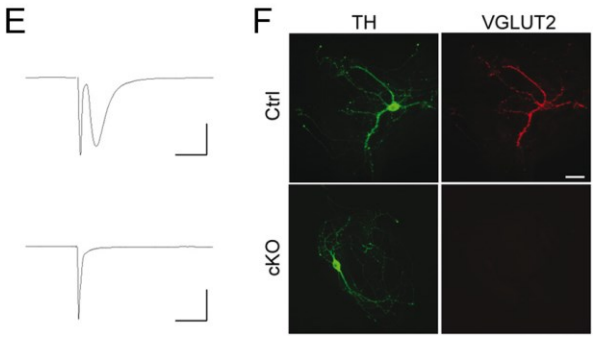

A Gel image showing a single-cell RT-PCR experiment performed with freshly dissociated cells from the mesencephalon of P0-P2 control and cKO mice. TH and *Vglut2* allele mRNA were amplified. Note that the size of the *Vglut2* wild type allele was 417 bp, whereas the KO allele was 165 bp. Upper gel: TH- (wells 2-5) or TH+ (wells 6-8), freshly dissociated cells from the mesencephalon of P0-P2 control pups were tested to detect *Vglut2*; 3 of the 3 DA neurons expressed the wild-type *Vglut2* allele. Well 1: DNA ladder. Lower gel: TH- (well 2) or TH+ (wells 3-4) freshly dissociated cells from the mesencephalon of P1 cKO pups were tested to detect *Vglut2*; 2 of the 2 DA neurons expressed the KO *Vglut2* allele. Well 1: DNA ladder. ***B*** Summary data showing that the wild-type *Vglut2* allele was detected in all mesencephalic DA neurons collected from control mice, and the KO allele was detected in all TH positive DA neurons collected from cKO mice. ***C*** Immunofluorescence images of a TH and VGLUT2 immunolabeling experiment performed in single-neuron microcultures. VGLUT2 was undetectable in cultured DA neurons from cKO mice. Scale bar: 25 μm. ***D*** Summary data of the immunolabeling experiments shown in (***C***). ***E*** Upper trace: patch-clamp recording showing a sodium current followed by a large glutamate-mediated EPSC recorded in a control DA neuron. Lower trace: EPSCs were undetectable in DA neurons recorded from cKO cultures. Calibration: 5 nA, 10 ms. ***F*** Post-recording TH/VGLUT2 immunocytochemistry confirmed the absence of VGLUT2 protein from cKO DA neurons. Scale bar = 20 μm.

Figure 3. Loss of VGLUT2 reduces the survival of dopamine neurons in culture.

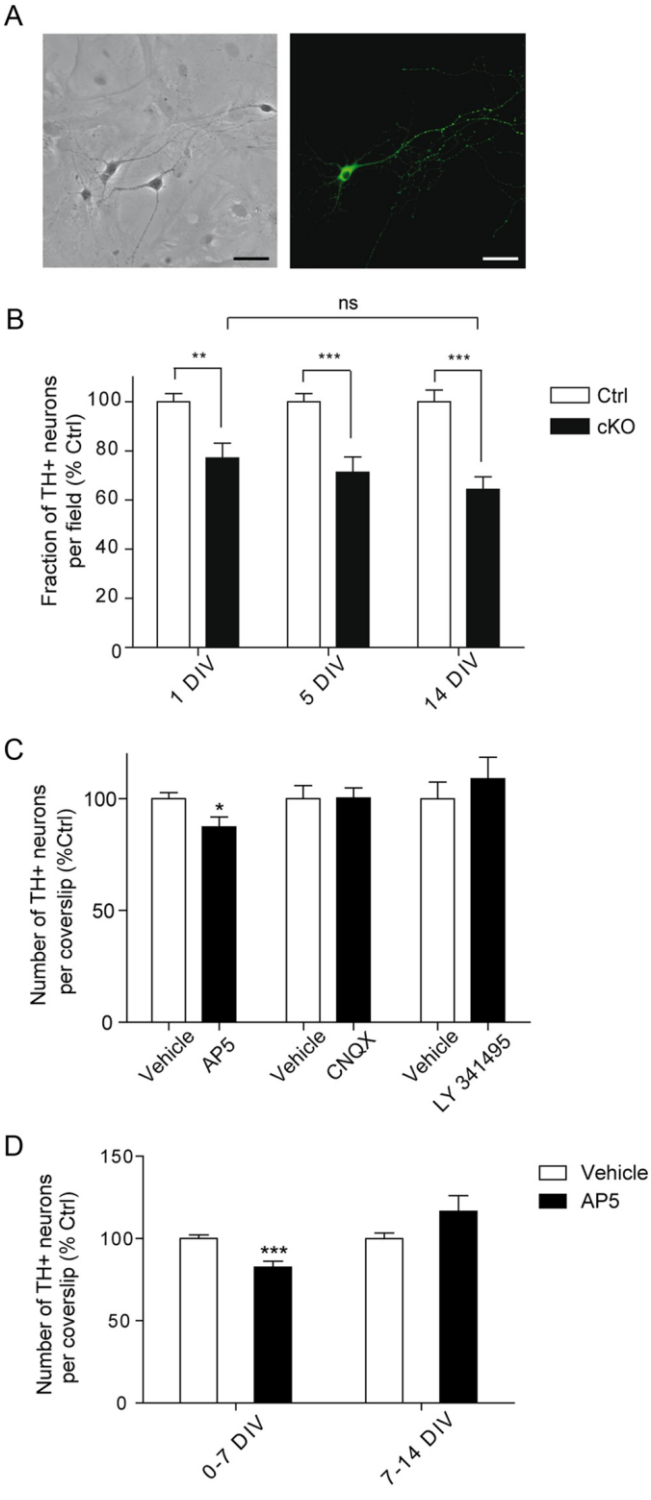

A Phase contrast (left) and immunofluorescence (right) micrographs prepared from control mesencephalic neurons after 5 days *in vitro* (DIV). One of the neurons is TH positive (green). Scale bar: 40 µm. ***B*** *In vitro* counts of TH positive mesencephalic neurons at 1, 5 and 14 DIV. The TH positive neuron counts are normalized to the total number of neurons per field. Compared to control cultures, there was a significant decrease in the proportion of TH positive neurons per coverslip in cKO cultures at 1DIV (**$P < 0.01$; Student's t test, n=9), 5DIV (***$P < 0.001$; Student's t test, n=8) and 14DIV (***$P < 0.001$; Student's t test, n=8). n represents the number of coverslips analysed in 3 different cultures. ***C*** *In vitro* counts of TH positive DA neurons after 12 DIV. DA neurons were FACS-purified from the mesencephalon of P0-P2 TH-GFP mice. Compared to control (water), there was a significant decrease in the number of TH positive neurons per coverslip in cultures treated chronically with 20µM AP5 (*$P < 0.05$; Student's t test, n=15). Compared to control (DMSO), there was no difference in the number of TH positive neurons per coverslip in cultures treated chronically with 10µM CNQX (n=9) or with 40 µM LY 341495 (n=11). ***D*** *In vitro* counts of TH positive DA neurons from FACS-purified DA neurons cultures treated chronically with 20µM AP5 from either 0 to 7 DIV or from 7 to 14 DIV. (***$P < 0.001$; Student's t test, n=14). n represents the number of coverslips analysed in at least 3 different cultures.

Figure 4. Deletion of *Vglut2* impairs dopamine neuron development.

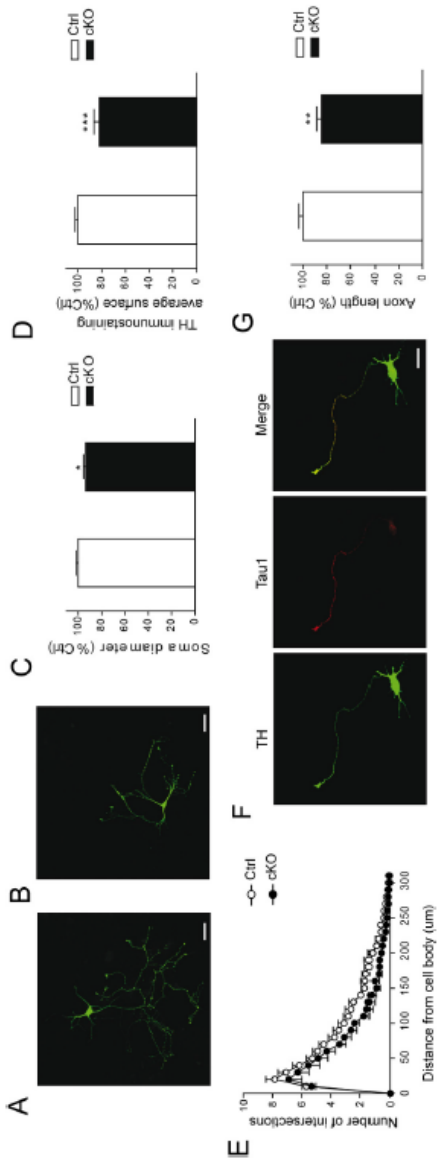

A Cultured mesencephalic DA neurons from control (***A***) or cKO P0-P2 mice (***B***) were identified by TH immunostaining (green) prior to quantitative image analysis. Scale bar: 40 µm. ***C*** cKO DA neurons are significant smaller in soma diameter (*$P < 0.05$; Student's *t* test, *n*=9 for both genotypes). ***D*** cKO DA neurons also have a smaller TH positive surface area, reflecting reduced neurite development (***$P < 0.001$; Student's *t* test, *n*=21 for control, *n*=20 for cKO). ***E*** Average results from a Scholl analysis of neurite complexity. cKO DA neurons show reduced neurite

complexity (*$P < 0.05$; two-Way ANOVA (genotype by distance), n=9 for both genotypes, no interaction). ***F*** Micrographs from a control DA neuron at 1DIV. Axon length (green) was evaluated by measuring the length of the longest neurite where an axonal growth cone was apparent. This longuest neurite was also generally Tau1-immunopositive (red). Scale bar: 25 µm. ***G*** Bar graph showing that axon length was significantly shorter in cKO DA neurons (**$P < 0.01$; Student's t test, n=21 for control, n=20 for cKO). n represents the number of coverslips per genotype analysed in a minimum of 3 different cultures; 10 neurons were analysed in each coverslip.

Figure 5. The general organization of dopaminergic projections is normal in cKO mice.

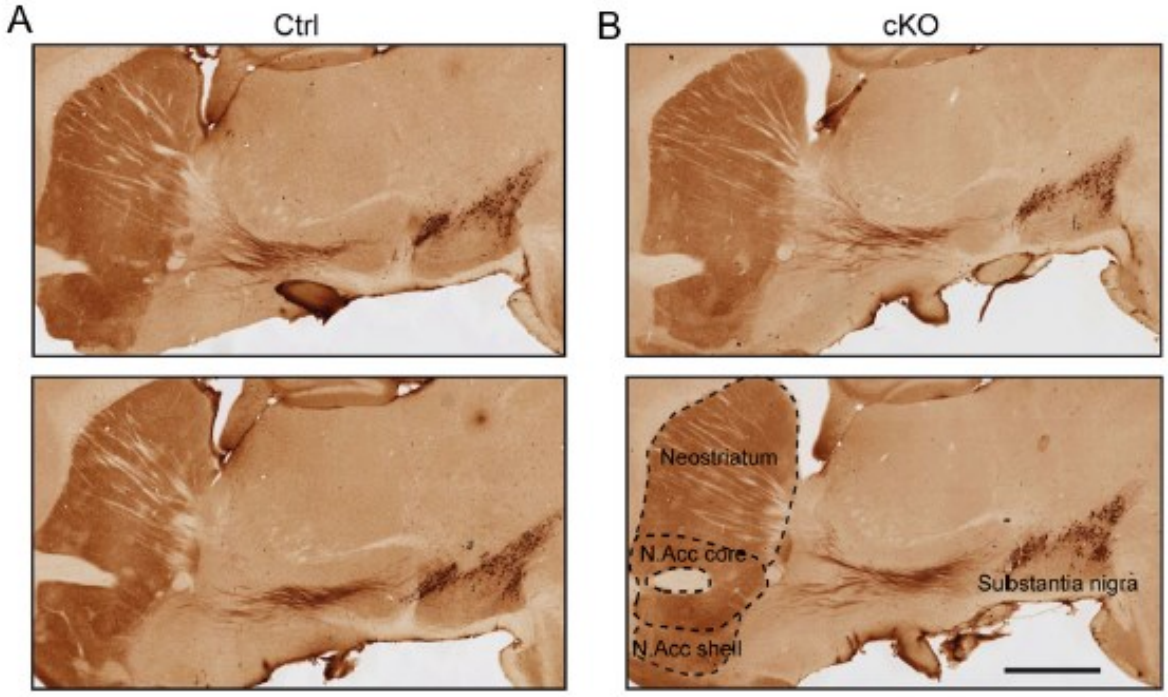

Micrographs showing TH immunostaining in 50µm sagittal brain sections prepared from either (***A***) control or (***B***) cKO P70 mice. Scale bar =1 mm

Figure 6. Reduced number of mensencephalic dopamine neurons and decreased density of dopaminergic and glutamatergic innervation in the nucleus accumbens of conditional *Vglut2* KO mice.

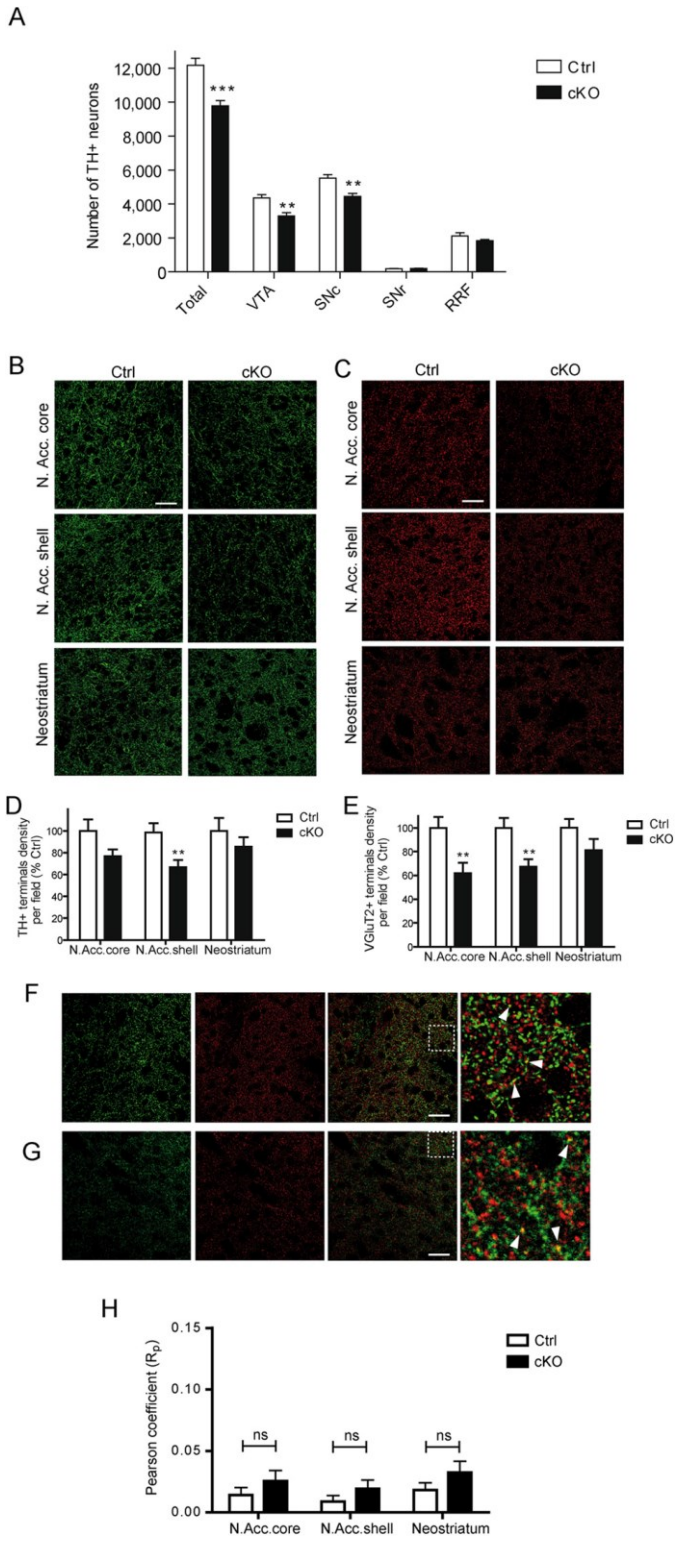

A Extrapolation of the total number of TH positive neurons in adult cKO and littermate control P90 mice by unbiased stereological counting. Compared to littermate control mice (Ctrl), there was a smaller number of TH positive neurons in the VTA (***P* < 0.01; Student's *t* test, *n*=6 for control, *n*=7 for cKO), SNc (***P* < 0.01; Student's *t* test, *n*=6 for control, *n*=7 for cKO) and whole SN (****P* < 0.001; Student's *t* test, *n*=6 for control, *n*=7 for cKO) of cKO mice (KO). *n* represents the number of animals. VTA, ventral tegmental area; RRF, retrorubral field; SNc, substantia nigra pars compacta; SNr, substantia nigra pars reticulata. Confocal images of (***B***) TH (green) and (***C***) VGLUT2 (red) immunoreactivity examined in the nucleus accumbens core, shell and neostriatum of control and P70 cKO mice. Scale bar: 40 µm. ***D*** Summary data showing the existence of a significant reduction in the number of TH positive varicosities in the nucleus accumbens shell of cKO mice (***P* < 0.01; Student's *t* test; *n*=24 for control, *n*=20 for cKO), but not in the nucleus accumbens core nor the neostriatum. ***E*** Summary data showing the existence of a significant reduction in the number of VGLUT2-positive varicosities in the nucleus accumbens shell (***P* < 0.01; Student's *t* test; *n*=24 for control; *n*=20 for cKO) and core (***P* < 0.01; Student's *t* test; *n*=24 for control; *n*=20 for cKO), but not in the neostriatum of cKO mice. ***F*** Colocalization of TH (green) and VGLUT2 (red) immunoreactivity was examined in the nucleus accumbens shell of cKO mice. In the merged images on the right, note that there is minimal colocalization (yellow). The area delineated by the white square is shown at higher magnification at the extreme right. Scale bar: 40 µm. ***G*** Colocalization of DAT (green) and VGLUT2 (red) immunoreactivity was also examined in the nucleus accumbens shell of P70 C57/BL6J mice. In the merged images on the right, note that there is here again minimal colocalization (yellow) between DAT and VGLUT2 (**F**). The area delineated by the white square is shown at higher magnification at the extreme right. Scale bar: 40 µm ***H*** Pearson coefficient of TH and VGLUT2 immunoreactivity colocalization was not different between the genotypes (*n*=24 for control; *n*=20 for cKO). *n* represents the number of 50 µm slices analysed in a total of 5 control and 4 cKO P70 mice.

Figure 7. Colocalization of DAergic markers with VGLUT2 in isolated DAergic neurons *in vitro.*

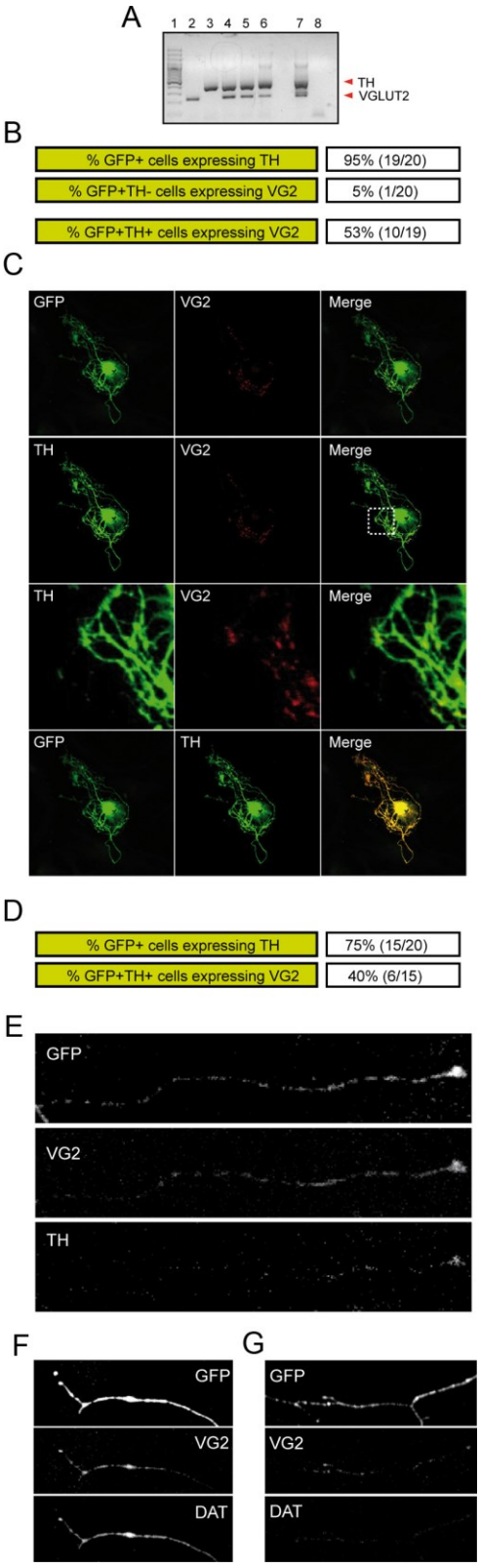

A Single-cell RT-PCR from 7DIV standard FACS-purified cultured DA neurons. In this example (wells 2-6), 4 of the 5 GFP positive neurons collected expressed TH mRNA. Well 1, DNA ladder. Well 7, whole mesencephalon RNA. Well 8, water control. ***B*** Table summarizing the results of single-cell RT-PCR experiments carried out with a standard 7 DIV FACS-purified culture. ***C*** Immunofluorescence images illustrating the results of a GFP/TH/VGLUT2 triple-immunolabeling experiment performed in a isolated DA neuron from a standard 7 DIV FACS-purified culture. ***D*** Summary data of the immunolabeling experiments shown in ***C***. ***E*** Immunofluorescence images illustrating a field from an isolated DA neuron with weak TH signal a an otherwise GFP and VGLUT2 positive axonal branch. ***F-G*** Immunofluorescence images illustrating the results of a strong (***F***) or weak (***G***) DAT immunoreactivity in a GFP and VGLUT2 positive axonal branch originating from an isolated DA neuron.

Figure 8. The magnitude but not the kinetics of dopamine release is decreased in the nucleus accumbens shell of conditional *Vglut2* KO mice.

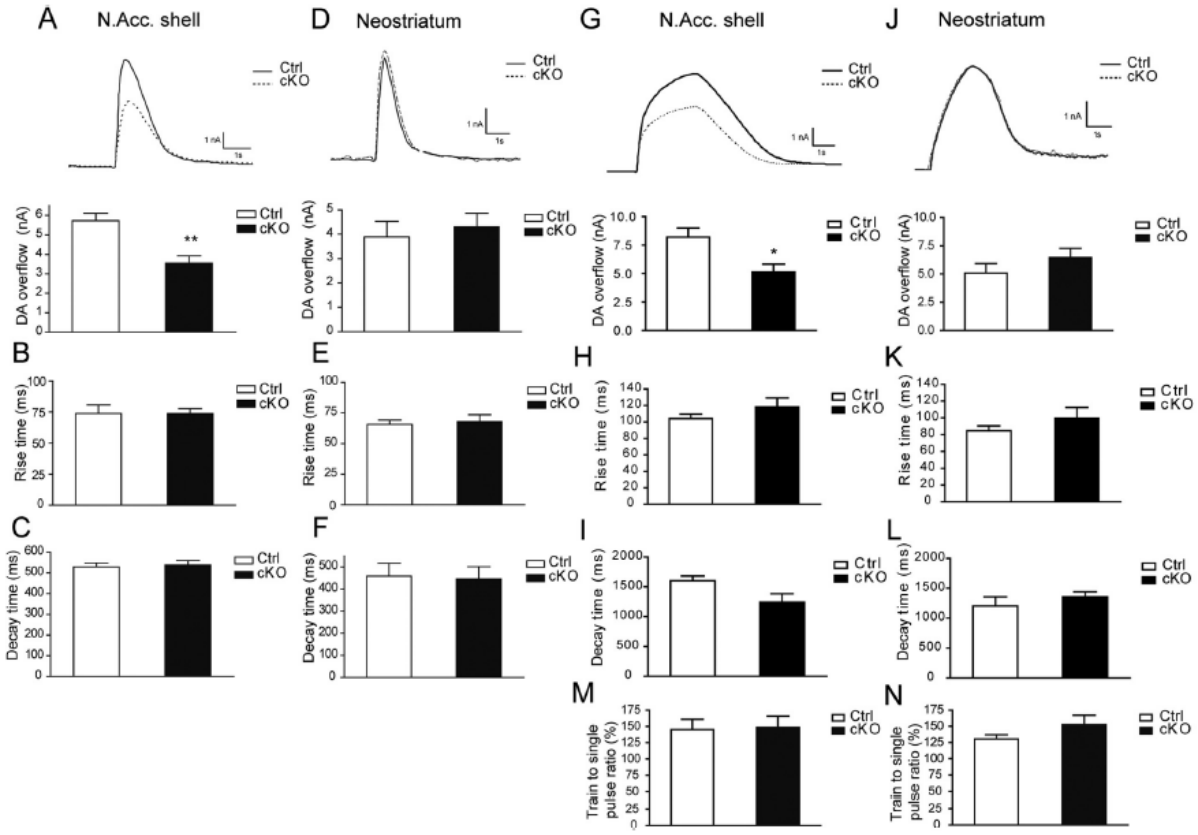

A-C Fast cyclic voltammetry recordings showing a decrease in single pulse-evoked DA overflow in the nucleus accumbens shell of a P30 cKO mice (**$P < 0.01$; Mann-Whitney Rank Sum test; n=5 for control; n=7 for cKO). The bar graphs illustrate average results and show that while the peak amplitude of DA overflow was reduced, the rise time and decay time of the response were not altered. ***D-F*** In the neostriatum, the amplitude and kinetics of single pulse-evoked DA overflow were not different between genotypes (n=6 for control; n=6 for cKO). ***G*** Train stimulation (20 pulses, 10 Hz) was also used to evoke DA overflow. DA overflow evoked in this way was reduced (upper graph) in the nucleus accumbens shell of cKO mice (*$P < 0.05$; Mann-Whitney Rank Sum test; n=5 for control; n=7 for cKO). Rise (***H***) and decay (***I***) time of the response remained unchanged in this region. Train-evoked DA overflow (***J***), the rise (***K***) and decay (***L***) time of the response were unchanged in the neostriatum (n=6 for control; n=6 for cKO). The ratio of train-evoked to single pulse-evoked DA overflow, an index of vesicle mobilization and autoreceptor control of DA release was not changed in the nucleus accumbens shell (***M***) or in the neostriatum (***N***). n represents the total number of slices recorded in 3 control and 3 cKO P30 mice.

Figure 9. The ratio of Phospho-TH/TH but not total TH is reduced in the VTA of cKO mice.

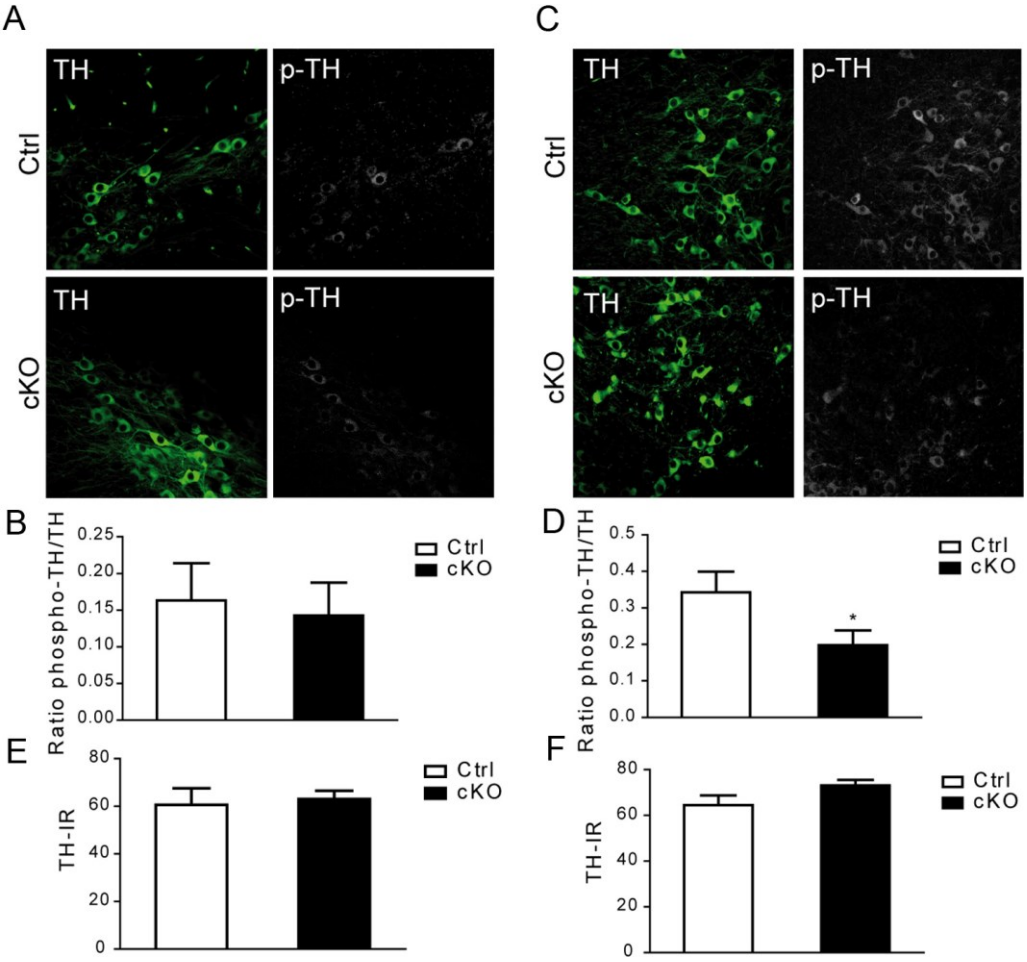

A,C Immunofluorescence images illustrating a TH/Ser(40)-Ph-TH double-immunolabeling experiment performed in the SN (***A***) or VTA (***C***) of CTRL and cKO P35 mice. ***B,D*** The p-TH/TH ratio per TH+ neuron was reduced in the VTA (***D)*** (*P*= 0.047; Mann-Whitney Rank Sum test; *n*=12 for control; *n*=13 for cKO) but not in the SN (***B***) (*P*= 0.74; Mann-Whitney Rank Sum test; *n*=10 for control; *n*=11 for cKO) of cKO mice. ***E,F*** There was no difference in total TH immunoreactivity per DAergic neuron in neither the SN (***E***) (*P*= 0.74; Mann-Whitney Rank Sum test; *n*=10 for control; *n*=11 for cKO) nor the VTA (***F***) (*P*= 0.089; Mann-Whitney Rank Sum test; *n*=12 for control; *n*=13 for cKO) of cKO mice . *n* represents the number of slices analysed on 3 animals of each genotype.

Figure 10. Impaired motor behavior and depression-like behavior in conditional *Vglut2* KO mice.

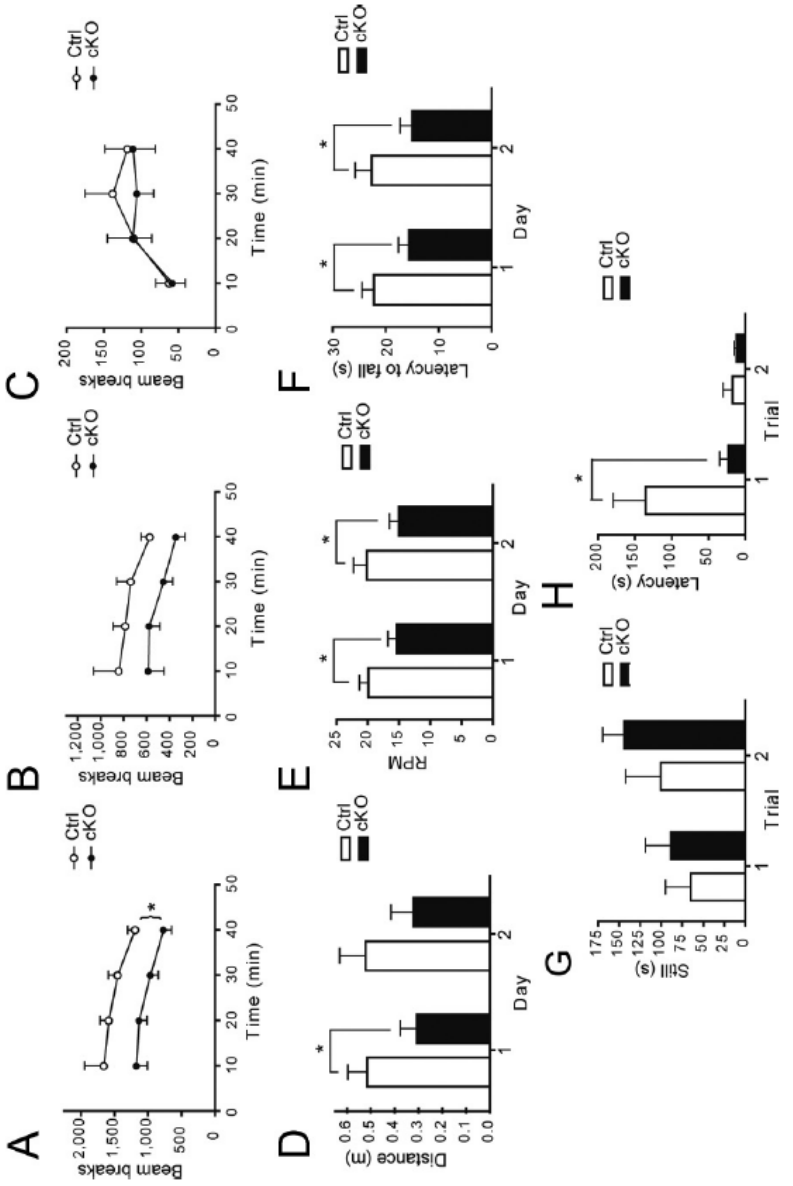

A-C Locomotor activity in a novel environment. cKO mice show decreased horizontal activity (***A***) (*$P < 0.05$; two-way ANOVA test; n=7 for control; n=12 for cKO) but (***B***) no difference in locomotion ($P = 0.11$; two-way ANOVA test; n=7 for control; n=12 for cKO) or rearing activity (***C***) compared to control mice. D-F cKO mice show impaired performance in the rotarod test, administered on two consecutive days. There is a significant decrease in distance for day 1, (***D***) speed (revolutions per minute; RPM) for days 1 and 2, (***E***) and in latency to fall for days 1 and 2 (***F***) for cKO mice (each value is the mean for three trials per animal per day, (*$P < 0.05$; Mann-Whitney rank rum test; n=7 for control; n=12 for cKO). ***G-H*** Forced-swim test paradigm. There is no effect of genotype for the total time spent immobilized (***G***) for both trials. cKO mice show a decreased latency to become immobile (***H***) for the first but not the second trial (*$P < 0.05$; Mann-Whitney rank sum test; n=6 for control; n=9 for cKO).

Figure 11. Blunted locomotor response to amphetamine and cocaine.

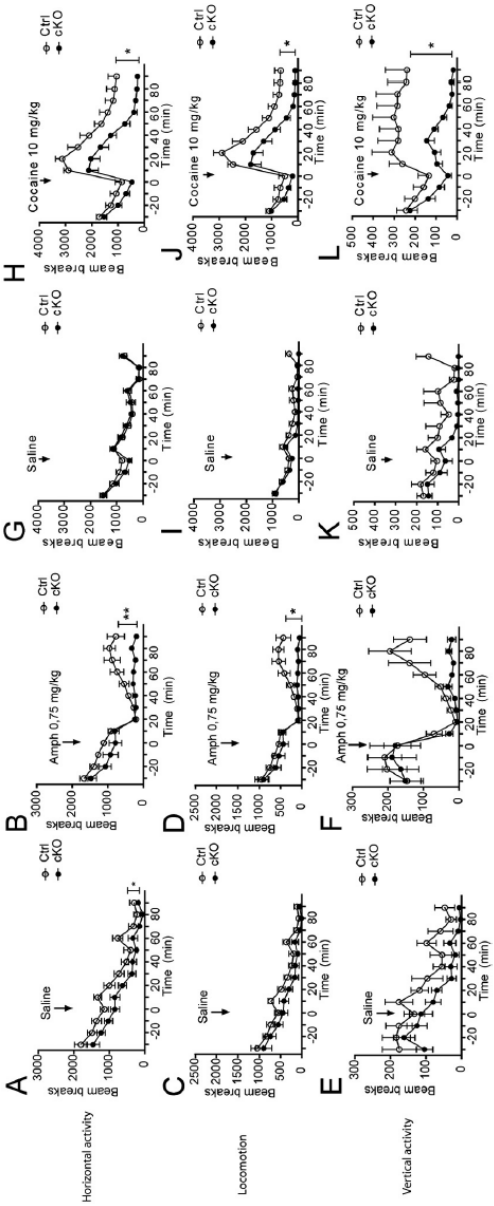

cKO mice displayed a decreased horizontal activity (***A-B***), locomotion (***C-D***) but not difference in vertical activity (***E-F***) when challenged by 0.75 mg/kg amphetamine (**P* < 0.05; ***P* < 0.01; two-way ANOVA test; *n*=7 for control; *n*=12 for cKO). cKO mice also displayed decreased horizontal activity (***G-H***), locomotion (***I-J***) and in vertical activity (***K-L***) when challenged by 10 mg/kg cocaine (**P* < 0.05;two-way ANOVA test; *n*=7 for control; *n*=12 for cKO). *n* represents the number of 3-5 months old control or cKO mice.

Article 2

Dopamine and glutamate co-transmission is segregated in distinct pools of axonal terminals *in vivo* and is regulated by striatal neurons

Guillaume M. Fortin [1], Marie-Josée Bourque [1], Sara Saneei [1], Consiglia Pacelli [1], Rafael Koerich Varaschin [1], Nicolas Giguère [1], Marion Brill [1], Sherdeep Singh [2], Paul W. Wiseman [2] and Louis-Éric Trudeau [1,3]

Department of [1] Pharmacology, [3] Groupe de Recherche sur le Système Nerveux Central, Faculty of Medicine, Université de Montréal, Montréal, QC, Canada H3C 3J7;

[2] McGill University, Department of Chemistry,

Montreal, QC, Canada H3A 0B8,

Corresponding author: Louis-Eric Trudeau, Ph.D.
Department of pharmacology, Faculty of Medicine
Université de Montréal
C.P. 6128, Succursale Centre-Ville
Montréal, Québec, H3C 3J7

En soumission pour *The Journal of Neuroscience*

Contribution des auteurs

Guillaume M. Fortin : Il a réalisé les expériences d'immunocytochimie, d'immunohistochimie, de RT-PCR, l'élaboration de technique et des expériences de RT-qPCR sur cellule unique a ainsi que la quantification d'imagerie. Il a analysé les données de toutes les figures. Il a réalisé tous les graphiques et figures ainsi que l'écriture du manuscrit.

Sara Saneei : Elle a participé à l'élaboration de la technique et aux expériences de RT-qPCR sur cellule unique. Elle a participé à la Fig.

Consiglia Pacelli : Elle a réalisée des expériences de RT-qPCR sur cellule unique. Elle a participé à la Fig.

Rafael Koerich Varaschin : Il a réalisé les injections virales par stéréotaxie chez les souris.

Nicolas Giguère : Il a réalisé les injections virales par stéréotaxie chez les souris.

Marion Brill : Elle a réalisé les expériences d'électrophysiologie. Elle a contribué à la Figure

Sherdeep Singh : Il a réalisé les expériences de SpIDA. Il a contribué à la Fig.

Paul W. Wiseman : Il a participé à l'écriture du manuscrit.

Louis-Éric Trudeau : Il a participé à l'élaboration des hypothèses et à l'écriture du manuscrit.

Abstract

A subset of midbrain DA neurons has been shown to express the type 2 vesicular glutamate transporter, supporting their capacity for glutamate release from some of their axon terminals. Glutamate release is found mainly by DA neurons of the VTA and can be detected at terminals contacting ventral but not dorsal striatal neurons, suggesting the possibility that target-derived signals regulate the neurotransmitter phenotype of DA neurons. Whether glutamate can be released from the same terminals that release DA or from a special subset of axon terminals is undetermined. Here we provide *in vitro* and *in vivo* data supporting the hypothesis that the DA and glutamate-releasing terminals are mostly segregated and that striatal neurons regulate the co-phenotype of midbrain DA neurons and the segregation of release sites. Our work unveils a fundamental feature of dual neurotransmission and plasticity of the DA system.

Introduction

Growing evidence has demonstrated the presence of vesicular glutamate transporters (VGLUT) in chemically diverse neuronal populations in the brain, conferring to those neurons the ability to functionally co-release glutamate as a second transmitter (El Mestikawy et al., 2011). Based on electrophysiological evidence in cultured neurons, it was first proposed that dopamine (DA) neurons establish glutamatergic synapses (Sulzer et al., 1998; Bourque and Trudeau, 2000). The presence of VGLUT2 mRNA and protein in DA neurons was subsequently demonstrated (Bérubé-Carrière et al., 2009; Dal Bo et al., 2004; Kawano et al., 2006), followed by *in vivo* confirmation of functional glutamate release by DA neurons using optogenetics (Stuber et al., 2010; Tecuapetla et al. 2010).

The physiological significance of this dual neurotransmission in DA neurons has been recently highlighted in a number of studies, suggesting a crucial role of glutamate co-release in the homeostasis of the DA system. Expression of VGLUT2 in DA neurons was proposed to regulate DA release (Fortin et al., 2012; Hnasko et al., 2010) and psychostimulant-induced locomotor activity and behaviour (Alsiö et al., 2011; Birgner et al., 2010; Fortin et al., 2012; Hnasko et al., 2010) and have a developmental role (Fortin et al., 2012; Mendez et al., 2008).

Although the characterization and understanding of the functional significance of this dual neurotransmitter phenotype have made progress in recent years, little is known about the fundamental structural features of DA/glutamate neurotransmission. For example, whether DA neurons establish distinct sets of glutamatergic and DAergic axonal terminals is unclear. Partial colocalization of DA- and glutamate-containing terminals was previously demonstrated using an isolated DA neuron culture system (Sulzer et al., 1998; Dal Bo et al., 2004), a conclusion also supported by a study of the localization of VGLUT1 after its overexpression in cultured DA neurons (Onoa et al., 2010). In relative contradiction, *ex vivo* studies have reported very low

colocalization of tyrosine hydroxylase (TH), a characteristic DA neuron marker and VGLUT2 in DAergic striatal axonal varicosities (Bérubé-Carrière et al., 2009, 2012; Dal Bo et al., 2008; Forlano and Woolley, 2010; Fortin et al., 2012; Moss et al., 2011). A possible explanation of this discrepancy between *in vitro* and *ex vivo* data is that DA and glutamate release sites are mostly segregated *in vivo*, a process that may be regulated by target-derived signals. A recent *in vitro* study showing regulation of the DA/glutamate dual phenotype by contact with mesencephalic GABA neurons argues in favor of this possibility (Mendez et al., 2008). Contact with striatal neurons could therefore potentially be a key signal regulating the segregation of release sites in DA neurons.

To test this hypothesis, we first performed coefficient correlation analysis and spatial intensity distribution analysis (SpIDA) in wildtype and conditional VGLUT2 knockout mice to examine quantitatively the colocalization of DAergic (TH) and glutamatergic (VGLUT2) markers in striatal axonal varicosities. Our results suggest a complete absence of colocalization. Labelling of small subsets of DAergic axonal arborizations using viral-mediated overexpression of a reporter protein allowed us to demonstrate the presence of distinct, specialized DAergic and glutamatergic axonal varicosities along the same axonal branch in the ventral striatum. Furthermore, by using FACS-purified DA neuron cultures and co-culture with ventral or dorsal striatal neurons from TH-GFP mice, we observed that the segregation is induced by contact with ventral striatal neurons. Finally, by using single-cell multiplex RT-PCR, single-cell qPCR, and immunocytochemistry, we further document that the DA/glutamate co-phenotype is regulated by the presence of ventral striatal neurons.

Materials and methods

Animals

Experimental protocols were approved by the animal ethics committees (CDEA) at the Université de Montréal. Housing was at a constant temperature (21ºC) and humidity (60%), under a fixed 12 hours light/dark cycle, with free access to food and water.

TH-GFP mice. The characterization of VGluT2 expression in DA neurons during development was performed using the tyrosine hydroxylase green fluorescent protein (TH-GFP) transgenic mouse line *TH-EGFP/21–31*, which carries the enhanced GFP (EGFP) gene under the control of the TH promoter (Matsushita et al., 2002). The presence of GFP allowed identification and selection of DA neurons for single-cell RT-PCR experiments.

DAT-CRE mice. The analysis of segregation of glutamatergic and dopaminergic terminals was performed using DAT-CRE transgenic mice (129/ Sv/J background) (Zhuang et al., 2005).

Conditional Vglut2 knockout mice. All other experiments were performed using conditional *Vglut2* knockout (cKO) mice and control littermates. DAT-CRE transgenic mice (129/ Sv/J background) (Zhuang et al., 2005) were mated with *Vglut2 flox/flox* mice (129, C57Bl/6 background) (Tong et al., 2007) carrying the exon 2 surrounded by loxP sites. A breeding colony was maintained by mating DAT-CRE;*Vglut2*$^{flox/+}$ mice with *Vglut2*$^{flox/flox}$ mice. 25% of the offsprings from such mating were thus used as controls (i.e. DAT-CRE;*Vglut2*$^{flox/+}$ mice) and 25% lacked *Vglut2* in DA neurons (i.e. DAT-CRE;*Vglut2*$^{flox/flox}$ mice). Only male littermates of such mating were used as study subjects.

Tissue processing and cell culture

P0-P2 mice were cryoanesthetized and decapitated for tissue collection. For older mice, animals were anaesthetized with Halothane (Sigma-Aldrich, Oakville, ON, Canada) and decapitated. Freshly dissociated cells were prepared and obtained as previously described (Mendez et al., 2008). Primary cultures of mesencephalic DA neurons were also prepared according to previously described protocols (Fasano et al., 2008). Mesencephalic cells were plated onto monolayers of astrocytes. Cultures at a density of 5000 cells/ml of mesencephalic DA neurons purified from TH-GFP mice by fluorescence-activated cell sorting (FACS) were prepared as previously described (Mendez et al., 2008). For experiments with mixed mesencephalic/striatal cultures, ventral or dorsal striatal neurons at a density of 200 000 cells/ml were plated together with FACS-purified DA neurons.

Virus injection

Two-month old DAT-Cre positive mice were anesthetized with isoflurane (AErraneTM) and fixed on a stereotaxic frame (Stoelting, Wood Dale, IL, USA). Fur on top of the head was trimmed and the surgical area disinfected with iodine alcohol. Throughout the entire procedure, artificial tears (Equate^{TM}) were applied to the eyes and a heat pad was placed under the animal and kept at 37 ºC. Next, 0.05 ml of bupivacaine (Marcaine^{TM}) was subcutaneously injected at the surgical site, an incision of about 1 cm made with a scalpel blade and the cranium exposed. Using a dental burr, two holes of approximately 1 mm diameter were drilled above the VTA (AP: - 3.3 mm, ML: ± 0.4 mm, Franklin and Paxinos, 2008). Next, a blunt 34 G needle coupled to a water-filled polyethylene tube and a Hamilton syringe (Reno, NV, USA) was loaded with 0.9 % NaCl saline containing 1 x 10^{11} viral genome particles of AAV2-EF1α-DIO-ChETA-eYFP (UNC virus core, NC, USA), allowing expression of YFP-tagged ionic channel, used here as a reporter to label axon terminals since this protein is well known to be efficiently targeted to axon terminal

membranes (Jego et al., 2013; Yizhar et al., 2011). A small air bubble (~ 0.1 µL) was kept at the interface between water and virus solution. The needle was then slowly inserted in the VTA (DV: - 4.7 mm) and 0.4 µL of virus solution was injected at a rate of 0.1 µL per min using a syringe pump (Harvard Apparatus, Holliston, MA, USA). The needle was then withdrawn 0.2 mm and the injection repeated. After the second injection, the needle was left in place for 10 min to allow virus diffusion. Successful injections were confirmed by the movement of the air bubble in the polyethylene tube. After injection, the needle was slowly withdrawn and the procedure repeated in the contralateral side. Once bilateral injections were completed, the scalp skin was sutured and a subcutaneous injection of the anti-inflammatory drug carprofen (Rimadyl^{TM}, 4.4 mg/kg) was given. Animals were allowed to recover in their home cage and closely monitored for 24h. A second dose of carprofen was given if deemed necessary. Virus expression was optimal after three weeks of injection, at which time the brain was collected for immunohistochemistry.

Genotyping

Primers used for genotyping conditional knockout mice were: DAT-Cre 5′-accagccagctatcaactcg-3′ and 5′-ttacattggtccagccacc-3′; lox-VGluT2: 5′-gtctactgtaagtgaagacac-3′ and 5′-ctttaggctttcatccttgag-3′.

Multiplex single-cell nested RT-PCR

Collection of freshly dissociated GFP-positive neurons and reverse transcription reaction were performed as previously described (Mendez et al., 2008). Half of the cDNA produced was

used for a multiplex TH and *Vglut2* mRNA amplification. The other half was used to amplify DAT and VMAT2 mRNA. A first round of 25 cycles and a second round of 28 cycles were performed. Primers were designed not to interact with other primers for multiplex PCR. Primers were synthetized by AlphaDNA (Montreal, QC, Canada). Nested PCRs were performed during the second round of multiplex single-cell RT-PCR for TH, *Vglut2*, *DAT* and *VMAT2*. The identity of PCR products was confirmed by sequencing. Primers for single-cell RT-PCR in experiments on TH-GFP mice were: TH 5'-gttctcaacctgctcttctcctt-3' and 5'-ggtagcaatttcctcctttgtgt-3'; TH nested (374 bp) 5'-gtacaaaaccctcctcactgtctc-3' and 5'-cttgtattggaaggcaatctctg-3'; *Vglut2* 5'-ggggaaagaggggataaagaa-3' and 5'-gtggctttctccttgataactttg -3'; *Vglut2* nested (234 bp) 5'-atctacagggtgctggagaagaa -3' and 5'-gatagtgctgttgttgaccatgt-3'; DAT 5'-ttcactgtcatcctcatctctttc-3' and 5'- gaagctcgtcagggagttaatg -3'; DAT nested (292 bp) 5'- gtattttgagcgtggtgtgct -3' and 5'-gatccacacagatgcctcac-3'; VMAT2 5'-ctgagcgatctggtgctg-3' and 5'-gcagagggaccgatagcata-3'; VMAT2 nested (421 bp) 5'- gctgatcctgttcatcgtgtt -3' and 5'- gccaattctgttggttagaagtc -3';

Single-cell nested RT-qPCR

Collection of freshly dissociated GFP-positive neurons and reverse transcription reaction were performed as previously described (Mendez et al., 2008). A first outer round of 15 cycles was performed for TH and 20 cycles for VGLUT2 using 3 µl of cDNA in a final volume of 25 µl. Then, a quantitative real-time fluorescence polymerase chain reaction (qPCR) inner round was performed on 3 µl of the first round amplification for VGLUT2 and TH and on 3 ul of cDNA for GAPDH using PerfeCTa® SYBR® Green FastMix with an Illumina Eco qPCR machine. The specificity and identity of qPCR products were confirmed by analysis of melt curve and by regular RT-PCR using qPCR primers. The two steps protocol was optimized from a diluted 1:2 pool of 5 cells in order to obtain a final qPCR efficiency between 90% and 110%.

Nested primers used for qPCR were the following: VGLUT2 up: 5' gtggatttgctatctctggtttc 3' and VGLUT2 lw: 5' cccgtttcttcatccagttc 3'; TH up 5' cagttctcccaggacatt 3' and TH lw 5' acgggtcaaacttcacag 3'. qPCR primers used were VGLUT2 up: 5' tggtttgccctatcattgttg 3' and VGLUT2 lw: 5' gccattcttcacgggactt 3'; TH up 5' tggccttccgtgtgttt 3' and TH lw 5' aatgtcctgggagaactgg 3' ; GAPDH up: 5' ggagaaacctgccaagtatga 3' and GAPDH lw: 5' tgaagtcgcaggagacaacc 3'.

Outer round for TH gene: a) 95 ^{0}C 1 min b) 95 ^{0}C 30 sec c) 57 ^{0}C 40 sec d) 72 ^{0}C 40 sec (14 cycles) e) 72 ^{0}C 1 min . Outer round for VGLUT2 gene: a) 95 ^{0}C 1 min b) 95 ^{0}C 30 sec c) 57 ^{0}C 40 sec d) 72 ^{0}C 40 sec (19 cycles) e) 72 ^{0}C 1 min. qPCR protocol using Eco Real-Time PCR system from Illumina was: a) 95 ^{0}C 10 min b) 95 ^{0}C 30 sec c) 57 ^{0}C 40 sec d) 72 ^{0}C 40 sec (42 cycles) e) denaturation protocol.

Immunocytochemistry on cell cultures

Cultures were fixed with 4% paraformaldehyde (PFA), permeabilized and nonspecific binding sites blocked. To study the segregation of dopaminergic and glutamatergic terminals established by DA neurons, a chicken anti-GFP (GFP-1020; Aves Laboratories) was used at a dilution 1:1000, a rabbit anti-VGLUT2 (135 402; Synaptic Systems) at a dilution of 1:2000, a mouse anti-TH (MAB318; Millipore) at a dilution of 1:1000 or a rat anti-DAT (MAB369; Millipore) at a dilution of 1:1000. A rabbit anti-SV2a (119 002; Synaptic System) at a dilution of 1:1000 was also used to identify releases sites.

Immunohistochemistry

Control and VGLUT2 cKO male mice of 135 days were deeply anesthetized with halothane and fixed by intracardiac perfusion of 100 ml of 4% PFA. The brain was removed, postfixed by immersion for 24–48 h in PFA at 4°C and washed in PBS (0.9% NaCl in 50 mM PB, pH 7.4). Coronal 50 μm sections were cut using a VT1000S vibrating microtome (Leica Microsystems). Coronal sections were permeabilized, nonspecific binding sites blocked and incubated overnight with a mouse anti-TH antibody (T1299; Sigma-Aldrich or MAB318; Millipore, 1:1000), a rat anti-DAT antibody (MAB369; Millipore, 1:1000), a rabbit anti-VGLUT2 antibody (135 402; Synaptic Systems, 1:2000) or with a chicken anti-GFP (GFP-1020; Aves Laboratories, 1:10000). Primary antibodies were subsequently detected using a mouse or chicken Alexa Fluor 488-conjugated secondary antibody, a rabbit Alexa Fluor 546-conjugated secondary antibody or a mouse Alexa Fluor 647-conjugated secondary antibody (Invitrogen, 1:200).

Image acquisition with confocal microscopy

All of the *in vitro* and *ex vivo* imaging quantification analyses were performed on images captured using confocal microscopy. Images acquired using 488, 543 and 633 nm laser excitation were scanned sequentially to reduce nonspecific bleed-through signal. For the quantification of *in vitro* colocalization, 10 fields per coverslip were randomly chosen and pictures acquired using a 40× water-immersion objective.

For quantification of colocalization in adult nucleus accumbens shell, core, or dorsal striatum from control and cKO animals, images were acquired using a 60× oil-immersion objective. For image acquisition in the dorsal striatum, 4 random fields on each side were taken from the left and the right hemisphere in each section. For acquisition in the nucleus accumbens

core, two fields were selected next (ventromedial to ventrolateral) to the anterior commissure from the left and the right hemisphere in each section. For acquisition in the nucleus accumbens shell, three fields were acquired from the cone, intermediate and ventrolateral subregions, from the left and the right hemisphere in each section. Three animals of each genotype were analyzed.

For quantification of colocalization in adult nucleus accumbens shell or dorsal striatum from DAT-Cre viral injected mice, images were acquired using a 60× oil-immersion objective. For image acquisition, each field was acquired as an image stack with 2μm z-axis interval (between 8-14 images). Stacks were obtained from both the left and the right hemisphere in each section. For acquisition in the nucleus accumbens shell, two fields were selected from the cone and intermediate regions from the left and the right hemisphere in each section. For acquisition in the dorsal striatum, two fields were acquired from both hemispheres. Three animals were used for the analysis.

Image quantification

Image quantification was performed using ImageJ (National Institutes of Health) software. We first applied a background correction at the same level for every image analyzed before quantification of any of the parameters described below. For quantification of colocalization in virus-infected DAT-Cre mice, a threshold was also applied to all images. Colocalization analysis *in vitro* and *ex vivo* was performed by measuring the Pearson coefficient using the ImageJ Manders coefficient (Manders et al., 1993) plug-in.

The quantification of *ex vivo* colocalization in striatal sections were performed by averaging values obtained from all the fields acquired from each section for the control and cKO animals or by averaging values obtained from all the image stacks acquired in each section of the

virus-infected DAT-Cre mice. Images were thresholded at the same level for the control and cKO groups.

SpIDA analysis

The SQUAASH (segmentation and quantification of subcellular shapes) method was used to automatically segment regions of interest (ROIs) in confocal image sets. An advantage of this object based segmentation methods is that it is less sensitive to background fluorescence and imaging noise as compared to pixel based segmentation approaches. SQUAASH performs deconvolution and segmentation simultaneously yielding improved results because the two tasks naturally regularize each other. The SQUAASH technique also corrects for the microscopic intensity spread due to diffraction and background noise, yielding optimally de-convolved segmented images. SQUAASH image segmentation was performed using a multi-threaded software plug-in of Fiji (http://fiji.cs/), an open-source image processing software package. First, background subtraction was performed over the entire confocal image (1024x1024 pixels) to correct for uneven background noise using the rolling-ball algorithm. A window size of 100x100 pixels was used to make sure that the object size was smaller than the window size. To reduce the diffraction blur, the relevant imaging parameters of the confocal microscope (numerical aperture, refraction index, pinhole size, lateral and axial pixel size) were input to the software to calculate the point spread function using Gaussian approximations. A minimum intensity threshold of 0.05 and a regularization weight of 0.10 were used to remove very dim and very small objects which constitute background noise. After segmenting the images, manual inspection was carried out to make sure that all the relevant objects were successfully detected and outlined. Reconstruction of image datasets was achieved by mapping the coordinates of segmented images and the corresponding experimental confocal images using a custom written Matlab Script.

The simulated image datasets were generated using a custom written Matlab script for two independent species populations (simulating two confocal detection channels). The simulations were performed considering homogeneous spatially intermixed populations of independent monomers and hetero-oligomers. The fluorescent particle density, N, (particles per beam focal area (BA)) and the quantal brightness, ε, (intensity units per pixel dwell time, iu) were the main input parameters. Random distribution of N1, N2 and N12 (corresponding to particle densities of green -monomers, red-monomers and hetero-oligomers) were generated using a Poisson distribution of particles in space across a matrix and more than one particle was allowed to occupy the same matrix element. The two image channel matrices were then summed to generate a single-image matrix containing the two mixed populations. The inherent detector shot noise was modeled by applying a Gaussian noise function. The final image was obtained by convolution with a Gaussian function of user set e^{-2} radius, which simulated confocal imaging with a transverse electromagnetic wave laser beam of radius w_0. The simulated image sets were then analyzed via 2-Color SpIDA. A Matlab script was used to calculate fluorescence intensity distribution histograms for 2-Color SpIDA analysis.

Statistics

Data are represented throughout as mean ± SEM. Statistically significant differences were analyzed using Student's t test, one-way repeated-measures ANOVA, or a Fisher's exact test, as appropriate.

Results

Absence of colocalization of striatal DA and glutamate markers *in vivo*

In previous reports evaluating the co-localization of VGLUT2 with dopaminergic terminals in striatal substructures, TH immunohistochemistry was used as the primary marker (Bérubé-Carrière et al., 2012; Forlano and Woolley, 2010; Fortin et al., 2012; Moss et al., 2011), leaving open the possibility that VGLUT2 is found in TH-negative axon terminals expressing other dopaminergic markers such as the DA transporter (DAT). To test this hypothesis we used confocal microscopy to examine and quantify the colocalization of VGLUT2 with TH or DAT immunoreactivity in brain sections including the nucleus accumbens core, shell or dorsal striatum of control mice. Although a very small number of axonal-like varicosities occasionally appeared to be co-labelled, there was in general a very low level of colocalization of TH (**Fig.1a**) or DAT (**Fig.1a**) with VGLUT2. However, TH and DAT were strongly colocalized (**Fig.1c**) (Pearson coefficient=0.622, 9 slices analysed in 3 different Ctrl mice). There was no difference in the Pearson coefficient correlation between TH/VGLUT2 and DAT/VGLUT2 in all striatal subcompartments (**Fig.1d)**.

The negative value of the Pearson coefficient in TH/VGLUT2 or DAT/VGLUT2 double-labelling experiments suggests a random localization of DA and glutamate markers in the striatum *in vivo*. In favour of this possibility, we found no significant difference in the Pearson coefficient of TH and VGLUT2 immunoreactivity in the striatum of control (**Fig. 1g**) and cKO (**Fig. 1f**) mice in which the VGLUT2 gene was selectively disrupted in DA neurons (**Fig.1g)**. Similarly, an analysis of the colocalization of varicosities expressing DAT and VGLUT2 failed to detect any significant differences in the extent of correlation between the two signals in control (**Fig.1h)** and cKO (**Fig.1i)** mice (**Fig.1j)**.

Although the finding of an unchanged level of colocalization in VGLUT2 cKO mice strongly argues in favour of the possibility that the few colocalizing structures were labelled because of false-positive signal, our results still do not completely exclude a small level of true colocalization. To further evaluate whether such low colocalization is the result of a random distribution of the two signals in different structures and imaging quantification limitations, we employed the 2-color SpIDA (Spatial Intensity Distribution Analysis) technique which is an extension of the previously developed single color SpIDA technique (Godin et al. 2011). The method is based on a two-channel histogram comparison of pixel intensity values mapped from two detection channels within spatial regions of interest (ROI) selected from confocal image frames. The shape of a contour plot of the-2D intensity histogram gives qualitative information regarding the degree of spatial colocalization between two different color species detected in the dual channel imaging. Applying2-color SpIDA on representative experimental confocal images did not detect any significant spatial colocalization between VGLUT2 (green channel) and TH (red channel) (**Fig. 2a-b**) as only a small percentage (less than 0.5%) of the populations overlapped as 'yellow' pixels. To further increase the sensitivity of the SpIDA method, the population of pixels from the overlapped regions was increased by segmentation of specific regions of interest (ROIs).

The SQUAASH method was used to automatically segment the ROIs. The technique first detects and delineates the objects represented in the image and then quantifies their overlap. Additionally, simple intensity thresholding was used to eliminate dim image areas containing significant background noise. The pixel-intensity values were then normalized between 0 and 1 and stored as 64-bit Java double variables. The segmentation produced a binary mask image with the same dimensions as the input image segmented into ROIs of interest (**Fig.2c-g**).

For SpIDA analysis, new image datasets were constructed by performing pixel to pixel mapping of the segmented binary mask image to the corresponding background corrected original confocal images. This step allowed us to analyze the original intensity values only for pixels in ROIs of interest. Points cloud plots showing the 2D fluorescence intensity histograms were made from the spatial distribution of intensities by binning values from two separate channels of a merged image into common bins and creating a matrix of frequencies. A set of 4 experimental images from different regions was used to make the intensity histograms. The binning grid points were constructed by picking the minimum and maximum intensity values from the datasets of two imaging channels. The intensity values from the two channels were normalized to make the datasets comparable. An appropriate bin size was used to build the intensity histograms; a high value of the bin size effectively reduces the 'structural resolution' by binning significantly different values into common bins. Substantial improvement in the co-localization results was observed by performing the analysis on the segmented ROIs (**Fig.2h-i**). The shape of 2D fluorescence intensity distribution histogram followed a bivariate normal Gaussian distribution with an almost circular symmetry which indicates statistically random overlap of the populations.

To compare the experimental results with the expected scenarios for full, partial and no colocalization in dual-channel images, computer-simulated datasets of multiple images were generated with a range of distributions of set densities, N1, N2 and N12 (corresponding to particle densities of green -monomers , red-monomers and heterooligomers) and quantal brightness values, ε_{green} and ε_{red}. The interaction fraction between the various kinds of particles was varied by changing the ratio of monomeric-units. **Fig.2j-k** represents a typical simulated

image. A more detailed explanation on the simulations is provided in the methods section. The SpIDA analysis of the simulated images shows that the shape of the contour plot of the 2D intensity histogram provides detailed information on population overlap, encoded in the slope of the major axis of the elliptical contour plot (**Fig.2o-s**). As the relative ratios of populations change in the mixture of oligomers, the orientation/slope of the contour-plot changes in concert. A qualitative comparison of the 2D intensity histograms generated from the experimental dual-channel confocal images with that obtained from the simulated image datasets (**Fig.2m-n**) revealed that the best shape match is found with the curves having circular symmetry, which is the case when two variables X and Y are each normally distributed and independent. This corresponds to the case of no or very weak colocalization in the simulated images when the population of hetero-oligomers is less than 20% in the mixture of monomers and of oligomers. The distribution of intensities follows a Gaussian distribution that results from it being stochastic. The Pearson's correlation coefficient of 0.18, calculated only using the pixel intensity values from overlapped-yellow regions, also suggests that there is negligible correlation and hence very weak colocalization between VGLUT2 and TH-immunopositive varicosities.

Together, these observations suggest that the glutamate releases sites established by DA neurons in the striatum are segregated and distinct from axonal varicosities that contain characteristic DA markers.

DA neurons establish distinct releases sites for DA and glutamate

Although a subset of VTA DA neurons are now well-known to contain VGLUT2 mRNA (Birgner et al., 2010; Dal Bo et al. 2004; Fortin et al., 2012; Mendez et al., 2008; Yamaguchi et al., 2011) and to release glutamate at axonal varicosities in the striatum (Stuber et al., 2010; Tecuapetla et al., 2010), the lack of colocalization of DA markers and VGLUT2 as shown in the

present study suggests the existence of two distinct sets of neurotransmitter releases sites established by DA neurons.

To more directly test this hypothesis, we used a viral-mediated (AAV2-EF1α-DIO-ChETA-eYFP) reporter protein overexpression strategy in DAT-Cre mice to selectively label the striatal axonal arborization of a small subset of VTA DA neurons, irrespective of its neurotransmitter phenotype. We hypothesized that if DA neurons are able to establish segregated release sites for DA and glutamate, then it should be possible to detect eYFP-labelled axonal varicosities that are VGLUT2-positive but TH-negative. After validation that only a small number of VTA DA neurons were infected (**Fig.3a**), we examined in detail the localization of TH or VGLUT2 only in fields where a high proportion of eYFP-positive fibres were present either in the nucleus accumbens shell (**Fig.3b**) or dorsal (**Fig.3c**) striatum. In the ventral striatum, as expected, we observed frequent colocalization (white arrows) of GFP and TH signals (**Fig.3b upper**). However, only a minority of GFP-positive terminals contained VGLUT2 immunoreactivity (**Fig.3b lower**). In the dorsal striatum, we again observed a strong colocalization between GFP and TH (**Fig.3c upper**) but essentially no colocalization of GFP and VGLUT2 (**Fig.3c lower**). A small number of closely juxtaposed GFP and VGLUT2 varicosities were observed and likely represented sites of false colocalization (**Fig.3c lower, red arrow**). A quantitative analysis of this colocalization revealed that the extent of colocalization between GFP and TH was higher (***$p<0.001$; Student's t test, $n = 12$) in the dorsal than in the dorsal striatum (**Fig.3d**). However, although globally low, the extent of the colocalization between GFP and VGLUT2 was significantly higher (**$p<0.01$; Student's t test, $n = 12$) in the ventral than in the dorsal striatum (**Fig.3e**).

To evaluate if the segregation of TH-positive and VGLUT2-positive axonal varicositiesoccurred in different axonal branches or along the same axonal branch, we further

analysed the localization of TH and GFP in a small subset of isolated GFP+ fibres (**Fig.3f-i**). In most cases, we observed co-expression of TH and VGLUT2 at closely located sites along the same GFP positive fibre, but in distinct domains (**Fig.3f,h**). Some of the varicosities contained high levels of TH signal (**Fig.3g**), while others had had only very low levels (**Fig.3i**), which would have made them difficult to detect in a standard double-labelling experiment.

Considering the existence of such terminals with only very low levels of TH, we next took advantage of an *in vitro* DA neuron culture system to examine in more detail the possibility of segregated neurotransmitter releases sites, as proposed by other studies (Dal Bo et al., 2004; Onoa et al., 2010). We reasoned that it should be easier to resolve the presence of terminals with low TH levels in cultured neurons with less complex tri-dimensional morphology. By using FACs-purified DA neurons cultured from TH-GFP mice, we examined the co-expression of GFP, TH and VGLUT2 along isolated dopaminergic axonal segments with multiple varicosities (**Fig.4a-c**). In this model, it was indeed easier to detect axonal varicosities labelled for both TH and VGLUT2; some of these contained high levels of TH signal (**Fig.4a**), while others contained only low levels of TH (**Fig.4b**). In a subset of axonal segments, segregation was more apparent, with strings of GFP-positive varicosities containing VGLUT2 but either very low or undetectable levels of TH (**Fig.4c**). Finally, confirming that most TH-positive axonal varicosities are actual neurotransmitter release sites, we found that most of them contained the ubiquitous synaptic vesicle protein SV2A (synaptic vesicle glycoprotein 2A) (**Fig.4d**). All of the VGLUT2-positive varicosities observed contained SV2A (**Fig.4e**) and most GFP-positive varicosities were also SV2A-immunoreactive (**Fig.4f**). Together these results provide further support for the hypothesis of partial segregation of DA and glutamate releases sites along the same dopaminergic axonal branches.

The presence of ventral striatal neurons induces segregation of dopamine and glutamate releases sites

The ability to easily detect axonal varicosities containing both TH and VGLUT2 in cultured DA neurons stands in contrast to the great difficulty to detect such co-expression *in vivo*. Although the improved signal to noise ratio *in vitro* could facilitate identification of terminals containing low amounts of TH, another possibility is that segregation of neurotransmitter release sites is regulated *in vivo* by contact with target cells. To test this hypothesis, we examined cultures containing FACS-purified DA neurons grown either alone, or together with either ventral or dorsal striatal neurons. Strikingly, while TH and VGLUT2 were often colocalized in axonal varicosities in cultures containing DA neurons alone (**Fig.5a**) or together with dorsal striatal neurons (**Fig.5b**), the two signals were only rarely found in the same varicosities in cultures containing ventral striatal neurons (**Fig.5c**). A quantification of the extent of the colocalization revealed a significantly lower colocalization of TH and VGLUT2 in cultures containing ventral striatal neurons compared to pure DA neuron cultures (*$p<0.05$; ***$p<0.001$; One-way ANOVA) or co-cultures (*$p<0.05$; One-way ANOVA) with dorsal striatal neurons (**Fig.5d**). Although not significant ($p=0.05$; One-way ANOVA), there was also a trend toward reduced colocalization of TH and VGLUT2 in dorsal striatum co-cultures compared to pure DA neuron cultures (**Fig.5d**). Co-culture with striatal neurons did not cause any global change in the intensity of TH-immunoreactivity (**Fig.5e, f**), in the average size of the axonal arborisation of DA neurons (**Fig.5g**) or in the survival of DA neurons (**Fig.5h**).

Together, these observations suggest that the contact with striatal target neurons induces segregation of the DA and glutamate releases sites established by DA neurons.

The presence of ventral striatal neurons regulates the dual phenotype of DA neurons

In addition to regulating release site segregation, it is possible that interaction of DA neurons with striatal neurons also regulates the expression of neurotransmitter-related genes in these neurons, perhaps contributing to a shift in neurotransmitter phenotype. To test this hypothesis, we profiled DA neurons for the expression of DA and glutamate markers *in vitro* and *in vivo* by single-cell multiplex RT-PCR and single-cell RT-qPCR. We examined the expression of mRNA encoding TH, DAT, the vesicular monoamine transporter 2 (VMAT2) and VGLUT2.

We first examined mesencephalic DA neurons from TH-GFP mice (**Fig.6a**), maintained *in vitro* for 14 days and used single-cell multiplex RT-PCR (**Fig.6b-c**). The majority (76%) of the TH-positive/VGLUT2-negative neurons (i.e. "pure" DAergic neurons) expressed both DAT and VMAT2 mRNA (**Fig.6d**). This proportion was lower (59%) for TH-positive/VGLUT2-positive neurons ("dual-phenotype" neurons). A total of 83% of pure DA neurons expressed either DAT/VMAT2 or VMAT2 alone, in comparison to 66% of the dual phenotype neurons. Finally, 90% of pure DA neurons and 76% of dual phenotype neurons expressed either DAT or VMAT2. We also observed a small population (18%) of GFP+ neurons that was TH-negative/VGLUT2-positive, suggesting the possibility that *in vitro*, a population of neurons that were DAergic at some stage in their development (and thus still containing GFP) became purely glutamatergic at a later stage, perhaps due to downregulation of DA neuron markers.

A similar experiment was also performed on DA neurons freshly isolated from the mesencephalon of adult P70 TH-GFP mice (**Fig.6e**). While 63% of pure DA neurons expressed DAT/VMAT2 mRNA, none of the dual phenotype DA neurons did so. In addition, 92% of pure DA neurons and 50% of dual phenotype neurons expressed at least DAT or VMAT2 mRNA (**Fig.6d**). Although dual phenotype neurons were less abundant *in vivo* than *in vitro*, these

findings also argue in favour of a down-regulation of the DA phenotype in dual phenotype neurons.

We next evaluated if the presence of striatal neurons regulates the glutamatergic or the DAergic phenotype of GFP-positive neurons isolated from TH-GFP mice. We observed that the proportion of TH-positive neurons expressing VGLUT2 remained the same in the presence of ventral or dorsal striatal neurons (**Fig.6f**). The proportion of TH-positive neurons expressing DAT also remained unchanged (**Fig.6g**). Interestingly, the proportion of TH-positive neurons expressing VMAT2 decreased (*$p<0.05$; Proportion test) selectively in the presence of ventral striatal neurons (**Fig.6h**). This finding argues in favour of the hypothesis of a downregulation of the DA release machinery under conditions that favour neurotransmitter release site segregation in DA neurons. Single-cell RT-qPCR was also used to compare the level of TH and VGLUT2 mRNA in individual DA neurons under these same conditions (**Fig.7a-b**). GAPDH mRNA was amplified as a control (**Fig.7c**). Across the whole population of neurons examined, we found no significant difference in the average level of expression of TH in the three conditions (**Fig.7d**). There was also no global change in the level of expression of TH or VGLUT2 when comparing selectively dual-phenotype DA neurons, although a tendency toward an increase in VGLUT2 levels was observed (**Fig.7e-f**). A quantification of VGLUT2 immunoreactivity in the three experimental conditions revealed a significant increase (*$p<0.05$; One-way ANOVA) in the density of VGLUT2-immunoreactive axonal-like varicosities in DA neurons grown in contact with ventral striatal neurons (**Fig.7h-i**). Together these findings argue that contact with ventral striatal target cells induces a complex switch in the neurotransmitter phenotype of DA neurons, including increased release site segregation and altered balance of expression of glutamatergic markers.

Discussion

This study provides direct support for the concept that DA neurons establish distinct release sites for DA and glutamate. First, we failed to detect significant correlation between markers of DA and glutamate terminals in the striatum *in vivo* in mice by using confocal microscopy and spatial intensity distribution analysis. Using viral-delivered, cell-specific expression of a reporter protein in mensencephalic DA neurons, we observed for the first time the differential localization of TH and VGLUT2 axonal varicosities, at closely juxtaposed domains along individual GFP-positive fibers in the ventral striatum. Our *in vitro* work further suggests that interaction of DA neurons with ventral striatal neurons is a key factor inducing the

segregation of DA and glutamate terminals and shifting the relative expression of DAergic and glutamatergic genes, as revealed by single-cell RT-PCR and single RT-qPCR.

Distinct DA and glutamate release sites

Although previous studies have demonstrated expression of VGLUT2 mRNA and protein in DA neurons both *in vitro* and *in vivo* (Dal Bo et al., 2004; Fortin et al., 2012; Li et al., 2013; Mendez et al., 2008), release of glutamate by DA neurons both *in vitro* and *in vivo* (Bourque and Trudeau, 2000; Stuber et al., 2010; Tecuapetla et al., 2010) and co-localization of VGLUT2 and TH in cultured DA neurons (Dal Bo et al., 2004; Fortin et al., 2012), no convincing co-localization of glutamate and DA release sites has been observed *in vivo* (Bérubé-Carrière et al., 2009, 2012; Fortin et al., 2012; Moss et al., 2011). Our data are consistent with these findings by demonstrating the lack of co-localization of striatal DA and glutamate markers. Furthermore, our results obtained using viral labelling of sparse populations of DA neurons argue in favour of the hypothesis that DA neurons establish distinct neurotransmitter release for DA and glutamate sites along the same axonal branch, with glutamate release site often containing little if any TH or DAT immunoreactivity. Such a possibility could explain the decreased percentage of eYFP-positive fibres expressing TH and the increased percentage of eYFP-positive fibres expressing VGLUT2 in the ventral striatum compared to the dorsal striatum that we observed. Our results showing low or no TH in axonal fibres emanating from DA neurons is compatible with recent findings showing little if any TH immunoreactivity in axonal varicosities established in the lateral habenula by a subset of VTA DA neurons in the mouse (Stamatakis et al., 2013). Considering that using single-cell RT-PCR, we observed a small proportion of GFP/VGLUT2/DAT-positive neurons *in vitro* that were TH-negative, it is possible that some of

the infected GFP-positive fibres we observed in the striatum *in vivo* came from dual phenotype neurons not expressing TH. However, we failed to detect the existence of similar neurons in single-cell RT-PCR experiments performed with *in vivo* material. Our observation that VGLUT2-immunopositive and TH-immunopositive varicosities were closely juxtaposed along individual GFP-positive fibres also argues that these terminals originated from a neuron expressing TH in at least a subset of its axonal arborization. Further experiments using viral vectors to more extensively trace the axonal arborization of individual DA neurons could contribute to a better understanding of the axonal complexity and chemical identity of DA neurons. The segregation of DA and glutamate release sites we report here stands in contrast to the situation of noradrenergic neurons of the C1 subgroup, which appear to express TH and VGLUT2 in most of their axon terminals in the dorsal motor nucleus of the vagal nerve (DePuy et al., 2013).

The low percentage of GFP positive fibres (2-3%) expressing VGLUT2 in the dorsal striatum in the present study probably reflects false positive co-localization due to the limited spatial resolution of confocal microscopy and to the quantification technique used since we failed to detect any colocalization with the SpIDA analysis. This conclusion is congruent with previous work demonstrating that the DA neurons that express VGLUT2 are mainly found in the VTA along the midline in rodents (Kawano et al., 2006; Yamaguchi et al., 2011), with only a small subset of SN DA neurons containing VGLUT2 mRNA (Fortin et al., 2012; Yamaguchi et al., 2013). Perhaps more surprisingly, in our viral labelling experiments, we found that in both the ventral and dorsal striatum, a large subset of GFP-positive fibres emanating from DA neurons and innervating the striatum was immuno-negative for TH. What transmitter is released from such TH-negative /VGLUT2-negative axonal varicosities is presently undetermined, but considering recent work demonstrating GABA release by DA neurons, a GABAergic phenotype could be considered (Stamatakis et al., 2013; Tritsch et al., 2012, 2014).

Our data showing considerable co-localization of TH and VGLUT2 immunoreactivity in FACS-purified DA neurons is compatible with previous reports (Dal Bo et al., 2004; Fortin et al., 2012). It is possible that the more favourable signal to noise ratio of immunocytochemical experiments in cultured neurons compared to *in vivo* enhanced our ability to detect the localization of VGLUT2 in axonal varicosities that contain only low levels of TH. However, our data demonstrating that ventral striatal neurons induce the segregation of releases sites by DA neurons provides a likely explanation of the discrepancy between *in vitro* and *in vivo* data (Bérubé-Carrière et al., 2012; Moss et al., 2011). Further work will be required to identify the mechanism underlying the ability of striatal neurons to induce such a segregation of releases sites. Considering previous studies showing that the glutamatergic cophenotype of neurons is developmentally regulated (Fortin et al., 2012; Gutierrez et al., 2003; Mendez et al., 2008) and that contact with GABA neurons can negatively regulate the glutamate co-phenotype of DA neurons *in vitro* (Mendez et al., 2008), a likely possibility is that interaction of developing DA neurons with GABAergic medium spiny neurons of the ventral striatum plays a key role. Further experiments will need to evaluate that possibility and to also examine a possible role of striatal cholinergic neurons

Heterogeneity of DA neurons

Mesencephalic DA neurons have been shown throughout the years to be highly heterogeneous in their neurochemical and anatomical properties. For example, the expression of DAT, D2 autoreceptors and GIRK2 potassium channels has been shown to be lower in VTA than in SN DA neurons (Björklund and Dunnett, 2007; Blanchard et al., 1994; Thompson et al., 2005). Even within these regions, DA neurons appear heterogeneous, as suggested by a recent report

highlighting the heterogeneity of DA neuron marker expression in rat VTA (Li et al., 2013). In the present work, by profiling DA neurons *in vitro* and *in vivo*, we observed single phenotype (TH only) and dual phenotype (TH and VGLUT2) neurons of four sub-types: a) DAT/VMAT2-positive, b) DAT-positive, c) VMAT2-positive, and d) lacking both DAT and VMAT2. Our data demonstrate that dual phenotype neurons express DAT or VMAT2 mRNA less often compared to single phenotype DA neurons *in vitro* and *in vivo*, confirming earlier observations (Li et al., 2013). Together, these findings suggest that mesencephalic neurons specialized for glutamate release often express a partial DA neuron phenotype. However, the level of expression of TH amongst single phenotype and dual phenotype neurons appears similar, as shown by single-cell qPCR. Finally, we found a subpopulation of GFP-positive neurons expressing DAT and VMAT2, but without TH, suggesting a possible down-regulation of TH *in vitro* in some neurons. Since the glutamatergic co-phenotype has recently been demonstrated to change across development and to promote the growth and possibly the survival of DA neurons (Fortin et al., 2012; Mendez et al., 2008), further studies will be required to profile the different populations of mesencephalic neurons at different developmental stages *in vivo*.

Evidence for phenotypic plasticity

An increasing amount of data has shown that neurons expressing a mixed neurotransmitter phenotype can show developmental and plastic changes in their chemical identity. For example, firing activity and calcium influx have been shown to modulate the neurotransmitter phenotype of sympathetic, spinal cord and hippocampal neurons (Borodinsky et al., 2004; Gutiérrez et al., 2002; Gutierrez et al., 2003; Spitzer et al., 2004; Walicke and Patterson, 1981). The DA/glutamate co-phenotype has also been shown to be regulated during development, through interaction with GABA neurons and following toxin-induced lesions

(Bérubé-Carrière et al., 2009; Dal Bo et al., 2008; Fortin et al., 2012; Mendez et al., 2008). Our data further add to this body of knowledge by showing that the DA/glutamate co-phenotype is regulated in part through interactions with ventral striatal neurons. We observed that contrarily to mesencephalic cultures, in which VGLUT2 and TH were often co-localized at axonal varicosities, in mesencephalic/ventral striatal co-cultures, the two proteins were almost exclusively segregated, as they appear to be *in vivo* in the striatum. Together with our finding of an increased density of VGLUT2-immunoreactive varicosities and a reduced proportion of DA neurons expressing VMAT2 in such co-cultures, our findings suggest the novel model that interaction with ventral striatal neurons promotes the establishment of glutamate release sites by double-phenotype DA neurons, reduces the potential for DA packaging and induces the segregation of TH and VGLUT2 protein along the axonal domain of these neurons. In addition to other factors such as a reduced density of DA axon terminals in the ventral compared to dorsal striatum (Bolam and Pissadaki, 2012; Prensa and Parent, 2001), the reduced expression of VMAT2 that we observed in dual-phenotype DA neurons could perhaps contribute to the reduced levels of evoked-DA release previously observed in the ventral vs dorsal striatum of rodents (Avelar et al., 2013; Zhang et al., 2009). The molecular mechanisms involved in TH/VGLUT2 protein segregation remain to be defined, but our finding of an unchanged level of TH mRNA in DA neurons in mesencephalic/striatal co-cultures suggests that a global down-regulation of the expression of the TH gene is not involved. Although we haven't detected an overall decrease of TH immunoreactivity in these experiments, a redistribution of the TH protein could however be induced by interaction with ventral striatal neurons. Interestingly, the TH protein has previously been proposed to be partly membrane-bound (Cartier et al., 2010; Fahn et al., 1969; Halskau et al., 2009), making more plausible an eventual mechanism of protein retention or exclusion. Our qPCR results also fail to support the possibility of a global up-regulation of the VGLUT2 gene,

although we found a tendency towards an increase in VGLUT2 mRNA expression in DA neurons in co-cultures with ventral striatal neurons.

Conclusion

In summary, the present report presents a new perspective on the neurochemical identity of dual-phenotype DA neurons, suggesting the existence of a mostly segregated set of axonal terminals capable of releasing DA or glutamate, a configuration that appears to be instructed by interaction with ventral striatal neurons. Considering the crucial role of the glutamatergic co-phenotype of DA neurons in the development and regulation of the mesotelencephalic DA system and the involvement of this system in a number of important diseases such as schizophrenia and drug dependence, these findings open new perspectives into the underlying pathophysiological processes of such disorders.

Legends of figures

Figure 1. Absence of colocalization of TH or DAT with VGLUT2 in striatal areas from control and VGLUT2 cKO mice.

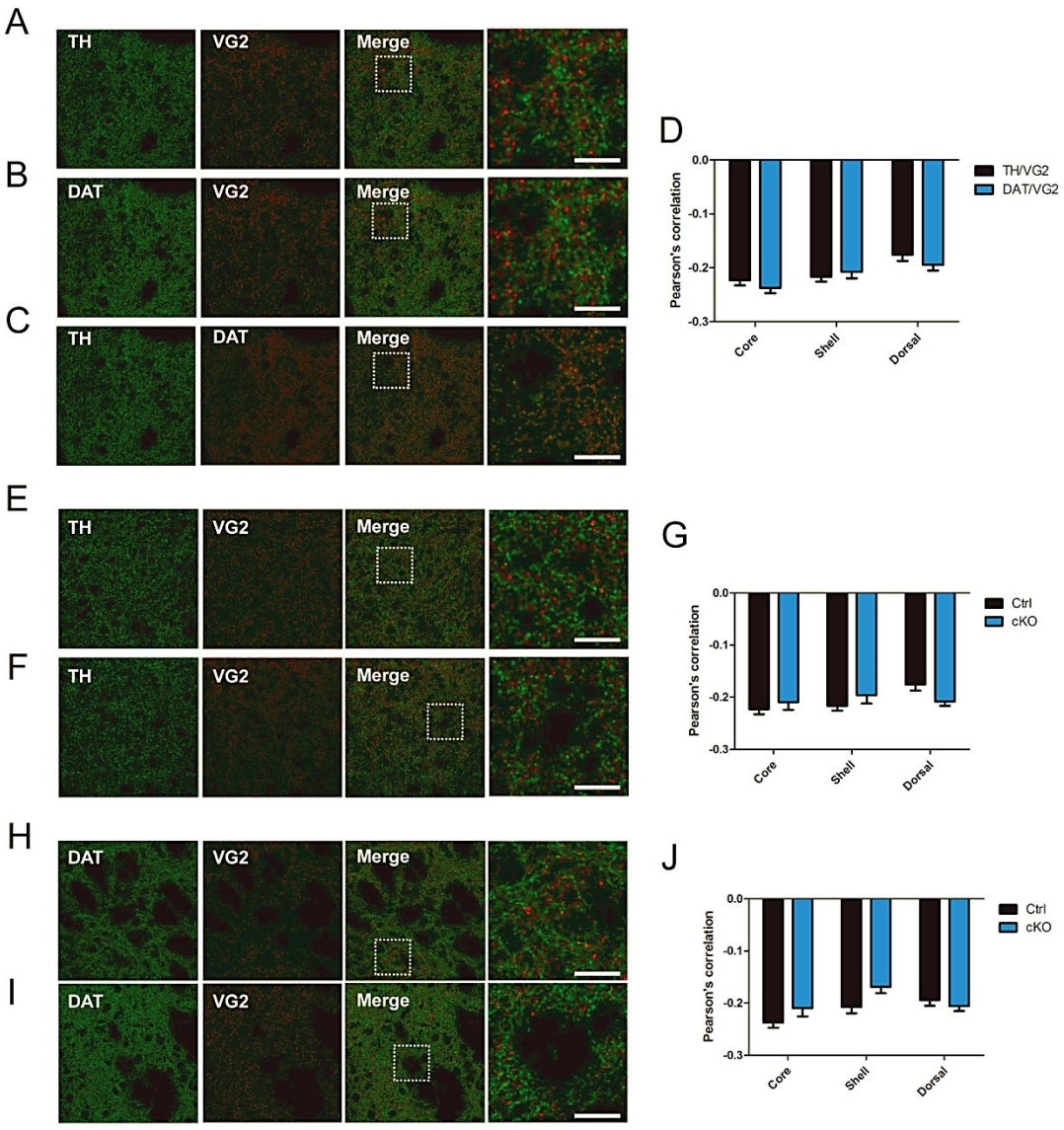

A-B Micrographs showing the localization of TH and VGLUT2 (**A**), DAT and VGLUT2 (**B**) and TH and DAT (**C**) immunoreactivity in the nucleus accumbens core of control mice. **D** Quantification of the localization of these markers in the different sub-regions of the striatum revealed a lack of significant colocalization, as revealed by a negative Pearson correlation coefficient. There was no difference in the colocalization of TH/VGLUT2 and DAT/VGLUT2 in control mice (two-way ANOVA test, n=13 for each dual labelling). **E-F** Micrographs showing the localization of TH and VGLUT2 immunoreactivity in the nucleus accumbens shell of control mice (**D**) or VGLUT2 cKO mice (**E**). **G** Quantification of the localization of these markers in the different sub-regions of the striatum shows a lack of significant colocalization, as revealed by a negative Pearson correlation coefficient. There was no difference between control and cKO mice(two-way ANOVA test, n=13 for each genotype). **H-I** Micrographs showing the localization of DAT and VGLUT2 immunoreactivity in the dorsal striatum of control mice (**H**) or VGLUT2 cKO mice (**I**). **J** Quantification of the localization of these markers in the different sub-regions of the striatum shows a lack of significant colocalization between DAT with VGLUT2, as revealed by a negative Pearson correlation coefficient. There was no difference in the colocalization of these two signals between control and VGLUT2 cKO mice (two-way ANOVA test, n=13 for each genotype). Scale bar =20 μm

Figure 2. Segmentation and Colocalization analysis of TH and VGLUT2 in striatal substructures from control animals.

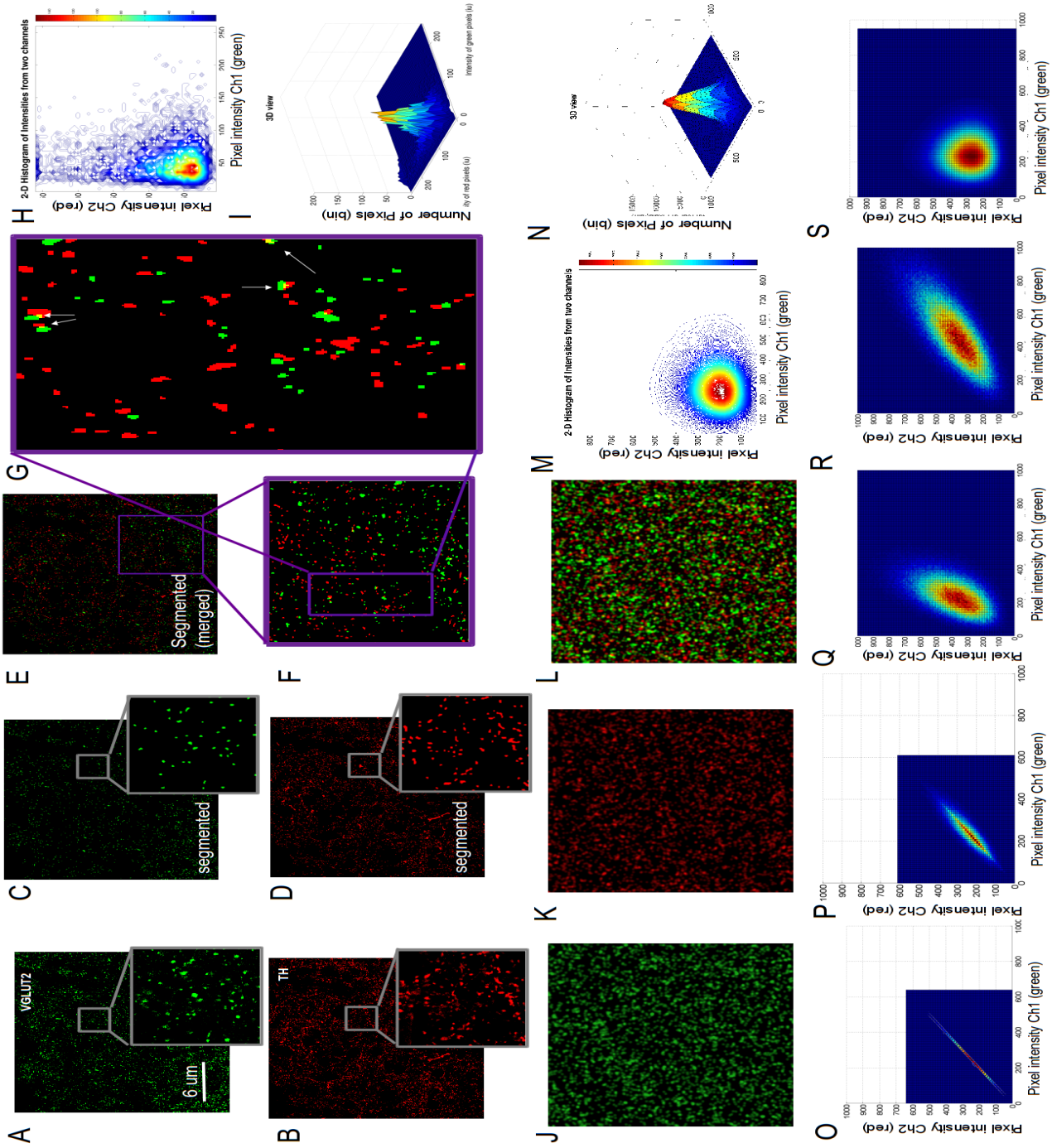

A-B Original dual-color confocal images of neuron showing VGLUT2-expressing axonal varicosities in green and TH-expressing axonal varicosities in red; scale bar, 6 μm. The image contrast was enhanced in both panels for visualization purposes. **C-D** Segmented images obtained by applying the SQUASSH segmentation method. **E** Composite image as a result of overlaying images C and D. **F-G** Close-up of the region highlighted by the purple square in E and F. **H-I** shows the contour plot and the 3D view of the 2D intensity histograms of a bivariate Gaussian distribution. The SpIDA analysis was performed on all the mixed-yellow pixels from a set of 4 experimental images. **J-K** Typical simulated image datasets representing a dual-color confocal image. Panel J corresponds to the green fluorescent channel and Panel K to red fluorescent channel. Panel L is the overlap of images A and B. The image shows three independent and intermixed populations of two monomers and one hetero-dimer, with N1 = 0.9 particle/BA, N2=0.9 particle/BA and N12=0.1 particles/BA and ε_{green} = 20 iu and ε_{red} = 25 iu. The simulations were done considering Poisson distribution of particles. The image size is 1024 x 1024 pixels, with an e^{-2} radius of the Gaussian convolution function set to 10 pixels. **M-N** The 2D intensity histogram of the simulated images (J, K) representing a case of perfectly independent population distribution of species with less than 10% colocalization. The contour plots of 2D intensity histograms of experimental and simulated images looks very similar indicating that there is no colocalization between VGLUT2 and TH. **O-P** are contour plots showing bivariate Gaussian distribution of pixel intensities from two independent channels (red and green) of the simulated datasets of three intermixed populations of two monomers and one hetero-oligomer. These plots were generated for qualitative comparison of the shapes of the contour-plots. Different plots correspond to different values of N (particles/BA) and ε (quantal brightness). N1 and ε_{green} corresponds to the green fluorescent particles (monomers) which are visible in channel 1. N2 and ε_{red} corresponds to the red fluorescent particles (monomers) visible

in channel 2. N12 are hetero-oligomers which are visible in both channels. The simulated datasets were generated with a total population density of 1 particle/BA. An arbitrary fixed set of the monomer quantal brightness values was used for all the simulations, $\varepsilon_{green} = 25$, and $\varepsilon_{red} = 20$. O, P corresponds to simulated images which were generated without adding the Gaussian noise, whereas the 2D contour plots from Q to S correspond to images which are simulated with the noise. O was generated with N1 = 0 particle/BA, N2=0 particle/BA and N12=1 particles/BA. P corresponds to N1 = 0.1 particle/BA, N2=0.1 particle/BA, N12=0.9. **Q-S** corresponds to a population of monomers and hetero-oligomers with a variable ratio of the monomeric-units in the hetero-oligomer. Q represents a population mixture of two monomers and a hetero-tetramer (Nmer red:green = 3:1) with N1 = 0.5 particle/BA, N2=0.5 particle/BA, N12=0.5, ε1 = 20 iu and ε2 = 25 iu. R represents a hetero-pentamer (Nmer red:green = 2:3) and corresponds to N1 = 0.2 particle/BA, N2=0.2 particle/BA, N12=0.8. S represents a hetero-pentamer (Nmer red:green = 3:2) and corresponds to N1 = 0.9 particle/BA, N2=0.9 particle/BA, N12=0.1. As ρ (correlation coefficient) increases toward 1, the ellipse becomes more tightly concentrated around y = x and when ρ approaches 0 the contours become circles. The tilt/slope of the major axis (along the x=y direction) of the contour plots gives information about the ratio of colocalized monomeric-units of the hetero-oligomers.

Figure 3. DA neurons established distinct set of neurotransmitters releases sites in the ventral striatum.

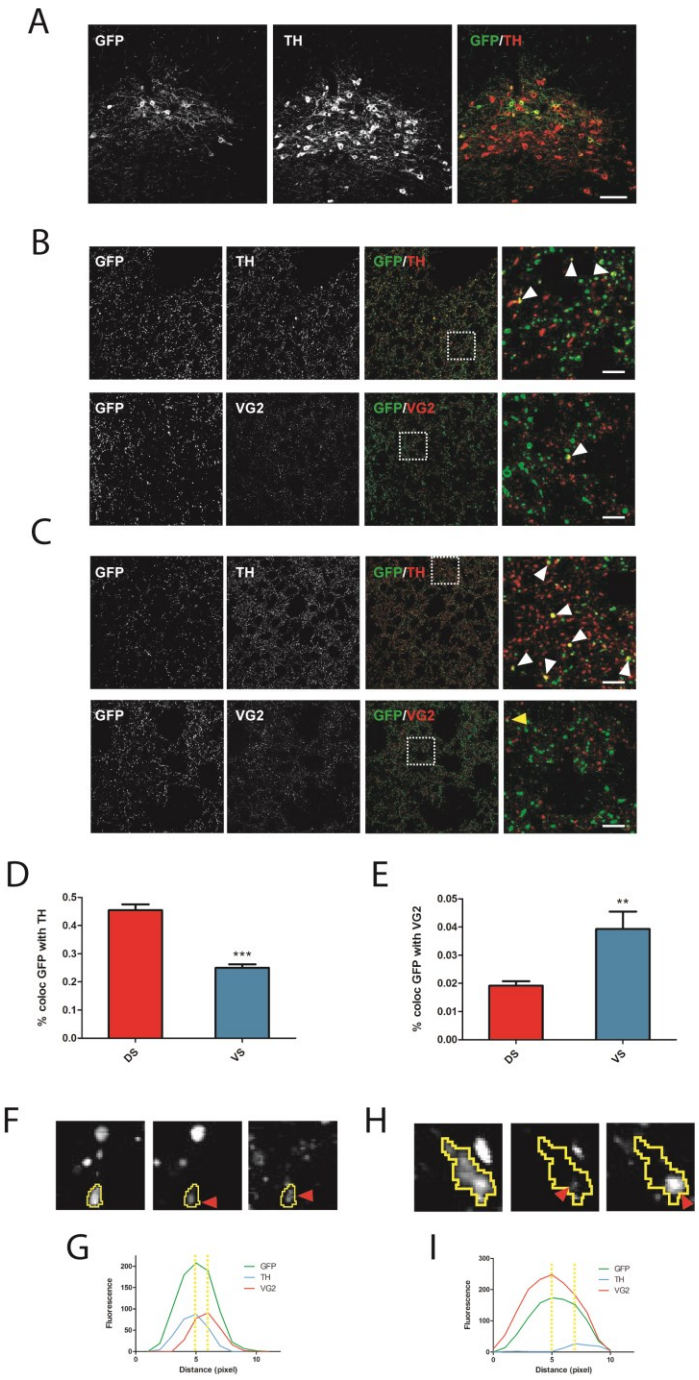

A Micrographs representing GFP and TH immunoreactivity of ventral tegmental area (VTA) DA neurons of DAT-CRE mice infected with a floxed GFP reporter virus. A subset of DA neurons was successfully infected. Scale bar =40 µm **B-C** Micrographs representing the localization of TH (top part) or VGLUT2 (bottom part) in GFP-positive infected axonal varicosities in the

ventral (**B**) or dorsal (**C**) striatum. White arrows represent areas of apparent colocalization. Scale bar =5 µm **D-E** Analysis of the percentage of GFP infected axonal varicosities colocalizing with TH (**D**) or VGLUT2 (**E**) in the dorsal and ventral striatum. There was decreased colocalization with TH (**E**), but increased colocalization with VG2 in the ventral striatum (**D**), compared to dorsal striatum. **F, H** Micrographs showing isolated GFP-positive fibers in the ventral striatum with segregated glutamate and DA releases sites along the same axonal fibre. eYFP (left), TH (middle) and VGLUT2 (right) immunoreactivity are shown in sequence. Red arrowheads show the center of distinct varicosities along the same infected fibre. **G, I** Fluorescence intensity profile plots of the isolated GFP-positive axonal varicosities identified by the arrowheads. The dotted yellow lines represent the distance at which the peak intensity of each signal was detected. The varicosity profiled in **G** contained equivalent levels of TH and VGLUT2 immunoreactivity. The varicosity profiled in **I** contained only a very low level of TH immunoreactivity (**$p<0.01$; ***$p<0.001$; Student's t test, n = 12).

Figure 4. Partial segregation of DA and glutamate axonal varicosities in cultured DA neurons.

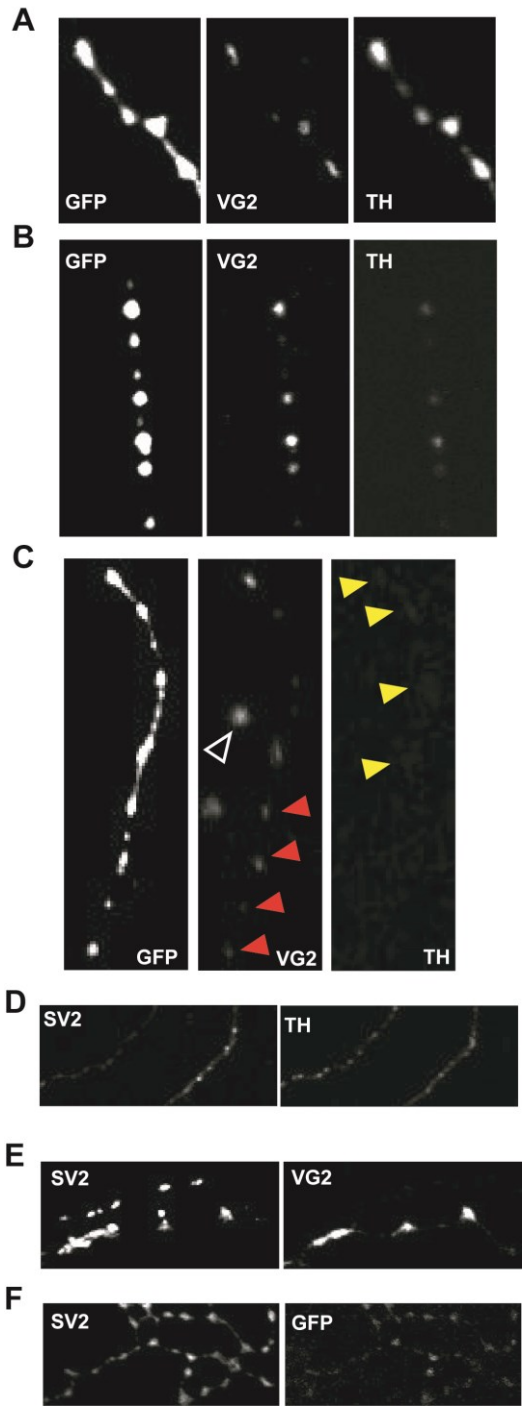

A-B Micrographs showing colocalization and TH and VGLUT2 with GFP in FACS-purified DA neurons in culture. The relative level of TH and VGLUT2 immunoreactivity often differed between individual GFP positive axonal fibres, as shown in **A** (TH>VGLUT2) and **B**

(VGLUT2>TH). **C** Segregation of VGLUT2 and TH along the same GFP-positive axonal fibre. The red triangles show GFP-positive/VGLUT2-positive/TH-negative varicosities, while the yellow triangles show GFP-positive/VGLUT2-positive varicosities with very low levels of TH signal. **D** Micrographs showing high colocalization of SV2A and TH immunoreactivity in axonal fibres of FACS-purified DA neurons. **E-F** Micrographs showing high colocalization of SV2A and VGLUT2 (**E**) or GFP immunoreactivity (**F**). Scale bar =5 μm

Figure 5. Presence of ventral striatal neurons induces segregation of glutamate releases sites.

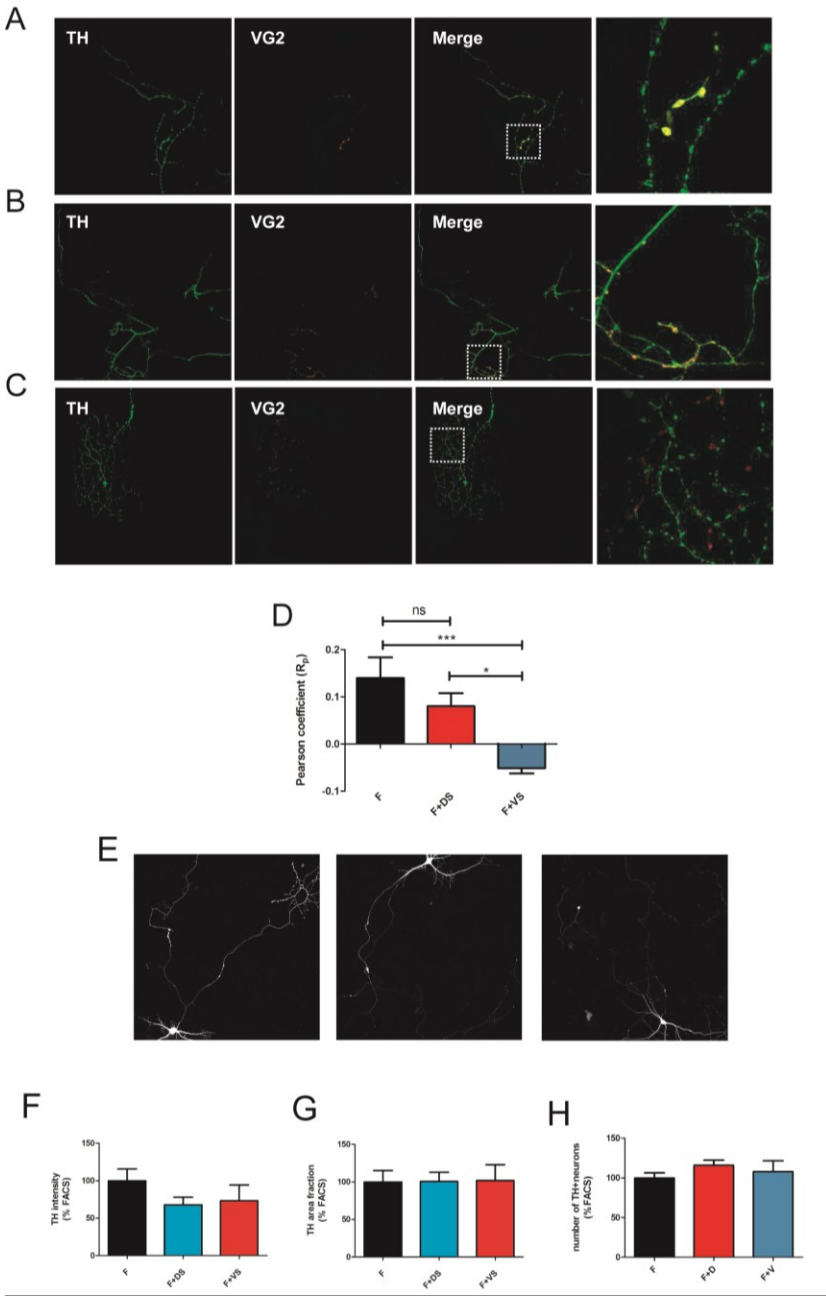

A-C Micrographs showing the colocalization of TH and VGLUT2 immunoreactivity in axonal varicosities established by FACS-purified DA neurons cultured alone (**A**) or together with dorsal (**B**) or ventral striatal neurons (**C**). Scale bar =5 µm. **D** While TH and VGLUT2

immunoreactivity were colocalized in a subset of axonal varicosities in DA neurons cultured alone or with dorsal striatal neurons, there was a complete absence of colocalization between TH and VGLUT2 in the presence of ventral striatal neurons. **E** Micrographs showing TH immunoreactivity in DA neurons cultured alone (left) or together with dorsal (center) or ventral (right) striatal neurons. Scale bar =40 μm **. F** There was no significant difference in the intensity of TH immunoreactivity between the three types of cultures. There were also no differences in the surface of TH immunoreactivity (**G**) or in the number (**H**) of DA neurons. (*$p<0.05$; ***$p<0.001$; One-way ANOVA, Tukey post-test, n= 9 or 10 coverslips, 3 different cultures).

Figure 6. Heterogeneity of DA neuron populations and regulation of VMAT2 mRNA by contact with ventral striatum neurons.

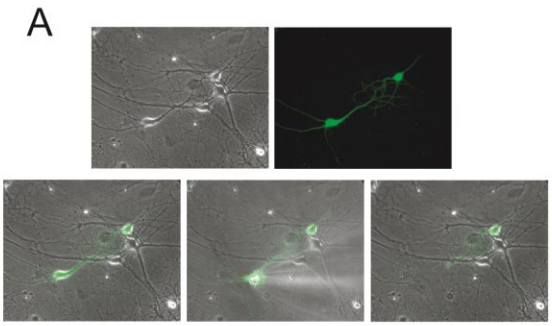

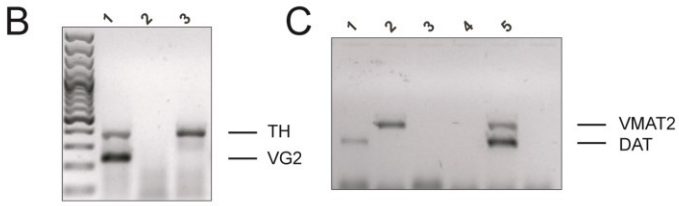

D

GFP+ cells	DAT+VMAT2+	DAT-VMAT2-	Only DAT+	Only VMAT2+
TH+VG2+	(17/29) 59%	(7/29) 24%	(3/29) 10%	(2/29) 7%
TH+VG2-	(23/30) 76%	(3/30) 10%	(2/30) 7%	(2/30) 7%
TH-VG2+	(2/11) 18%	(9/11) 82%	(0/11) 0%	(0/11) 0%

E

GFP+ cells	DAT+VMAT2+	DAT-VMAT2-	Only DAT+	Only VMAT2+
TH+VG2+	(0/4) 0%	(2/4) 50%	(2/4) 50%	(0/4) 0%
TH+VG2-	(15/24) 63%	(2/24) 8%	(7/24) 29%	(0/24) 7%
TH-VG2+	(0/2) 0%	(2/2) 100%	(0/2) 0%	(0/2) 0%

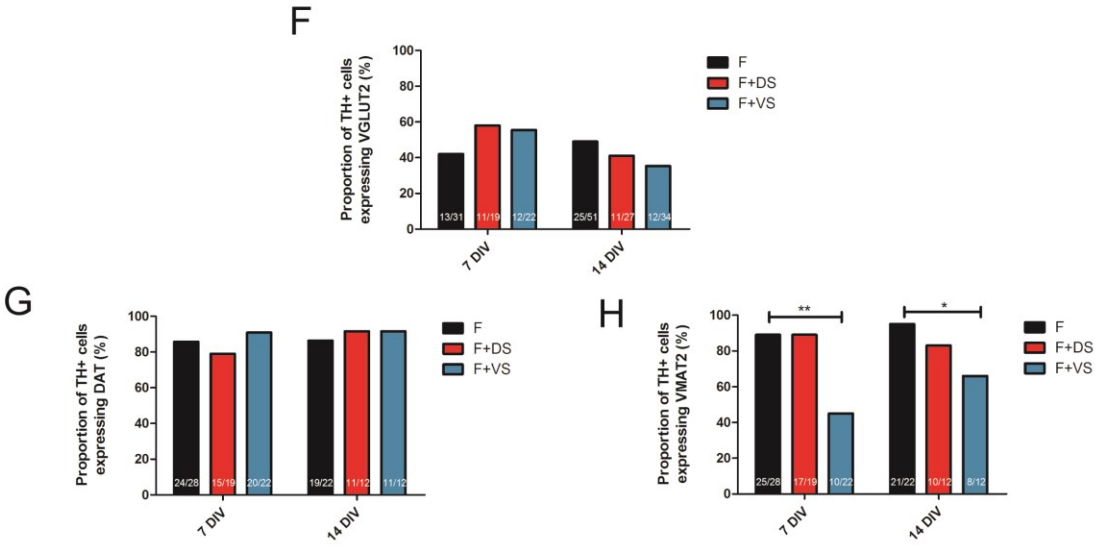

A. Micrographs representing phase contrast or endogenous eGFP fluorescence of mesencephalic cultures before and after collection of individual TH-GFP neurons with a glass pipette. **B-C** 1.5% agarose gel image representing multiplex single-cell RT-PCR detection of TH and VGLUT2

mRNA (**B**) or DAT and VMAT2 mRNA (**C**) from single GFP-positive DA neurons. **D-E.** Summary data of the different populations of DA neurons collected after 14 days *in vitro* (**D**) or acutely from P70 TH-GFP mice (**E**). **F-H** Analysis of the proportion of TH-positive neurons expressing VGLUT2 (**F**), DAT (**G**) or VMAT2 (**H**) mRNA after 7 or 14 days *in vitro* (DIV) from FACS-purified DA neurons grown alone or in co-culture with dorsal or ventral striatal neurons. Compared to FACS-purified DA neurons grown alone, there was a significant decrease in the proportion of TH-positive neurons expressing VMAT2 mRNA in the presence of ventral striatal neurons (*$p<0.05$; Proportion test). The numbers inside the columns represent the number of positive neurons over the total number of neurons collected and analyzed in at least 3 different cultures.

Figure 7. The presence of striatal neurons does not change the level of expression of TH or VGLUT2 in individual DA neurons.

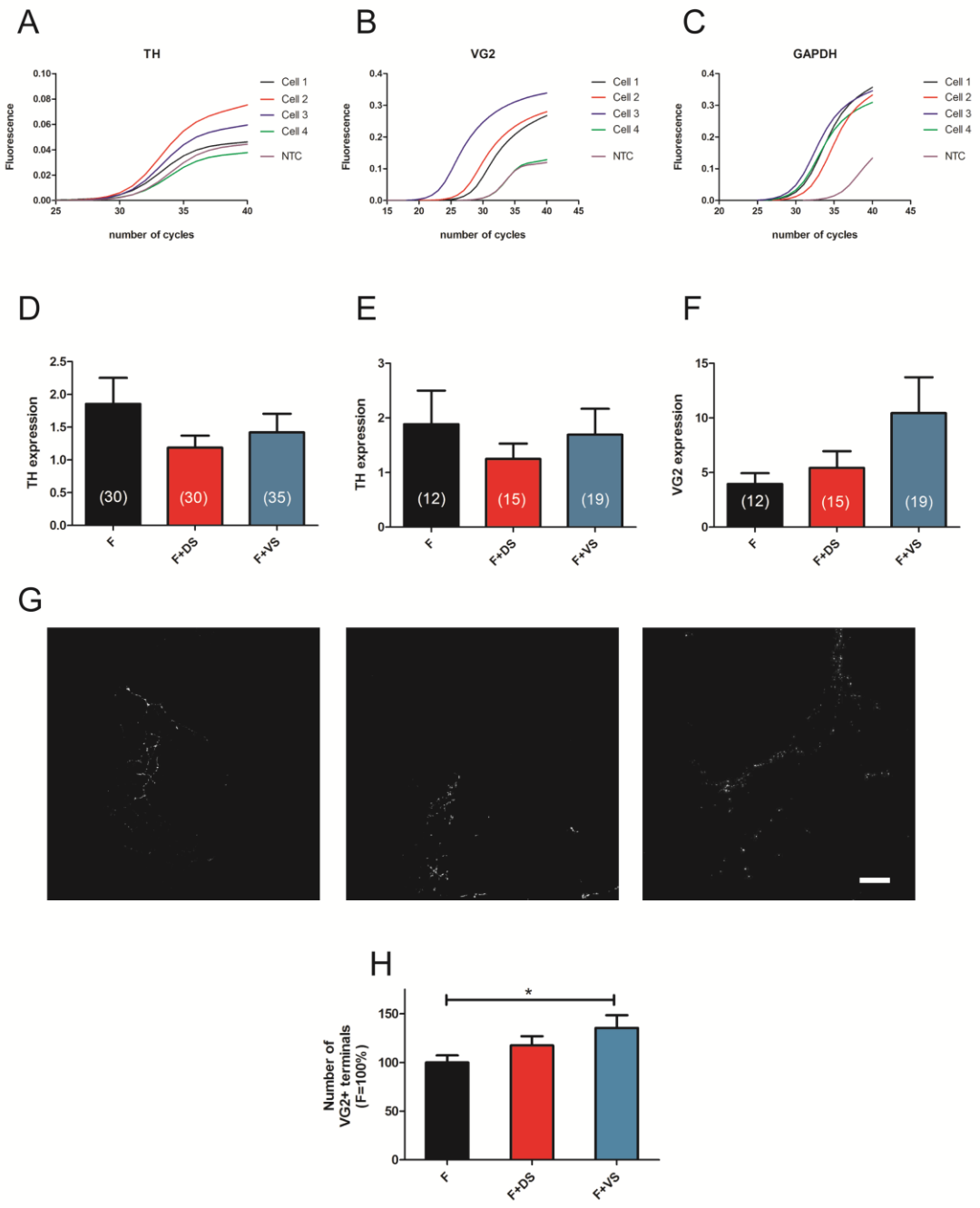

A-C Examples of amplification plot analysis from single neurons for TH (**A**), VGLUT2 (**B**) or GAPDH (**C**) mRNA. **D** Summary data showing the relative level of TH mRNA measured by qPCR from individual FACS-purified DA neurons collected after 14 DIV, either grown alone or in co-culture with striatal neurons. There were no significant differences between the groups. **E-F**

Summary data showing the relative level of TH and VGLUT2 mRNA measured by qPCR from individual dual-phenotype (TH/VGLUT2) FACS-purified DA neurons collected after 14 DIV, either grown alone or in co-culture with striatal neurons. There were no significant differences between the groups. The numbers in brackets represent the number of neurons collected and analyzed in at least 3 different cultures. **G** Micrographs showing VGLUT2 immunoreactivity in FACS-purified DA neurons grown either alone (left) or in co-culture with dorsal (center) or ventral (right) striatal neurons. **H** There was a significant increase in the number of VGLUT2-immunoreactive axonal varicosities between FACS-purified DA neurons grown alone or in contact with ventral striatal neurons. (*$p<0.05$; One-way ANOVA, Tukey post-test, n= 14 to 17 coverslips, 4 different cultures). Scale bar =40 μm

Bibliography

Alsiö, J., Nordenankar, K., Arvidsson, E., Birgner, C., Mahmoudi, S., Halbout, B., Smith, C., Fortin, G.M., Olson, L., Descarries, L., et al. (2011). Enhanced sucrose and cocaine self-administration and cue-induced drug seeking after loss of VGLUT2 in midbrain dopamine neurons in mice. J. Neurosci. *31*, 12593–12603.

Avelar, A.J., Juliano, S.A., and Garris, P.A. (2013). Amphetamine augments vesicular dopamine release in the dorsal and ventral striatum through different mechanisms. J. Neurochem. *125*, 373–385.

Bérubé-Carrière, N., Riad, M., Dal Bo, G., Lévesque, D., Trudeau, L.-E., and Descarries, L. (2009). The dual dopamine-glutamate phenotype of growing mesencephalic neurons regresses in mature rat brain. J. Comp. Neurol. *517*, 873–891.

Bérubé-Carrière, N., Guay, G., Fortin, G.M., Kullander, K., Olson, L., Wallén-Mackenzie, Å., Trudeau, L.-E., and Descarries, L. (2012). Ultrastructural characterization of the mesostriatal dopamine innervation in mice, including two mouse lines of conditional VGLUT2 knockout in dopamine neurons. Eur. J. Neurosci. *35*, 527–538.

Birgner, C. (2010). VGLUT2 in dopamine neurons is required for psychostimulant-induced behavioral activation. Proc Natl Acad Sci USA *107*, 389–394.

Björklund, A., and Dunnett, S.B. (2007). Dopamine neuron systems in the brain: an update. Trends Neurosci. *30*, 194–202.

Blanchard, V., Raisman-Vozari, R., Vyas, S., Michel, P.P., Javoy-Agid, F., Uhl, G., and Agid, Y. (1994). Differential expression of tyrosine hydroxylase and membrane dopamine transporter genes in subpopulations of dopaminergic neurons of the rat mesencephalon. Brain Res. Mol. Brain Res. *22*, 29–38.

Dal Bo, G. (2004). Dopamine neurons in culture express VGLUT2 explaining their capacity to release glutamate at synapses in addition to dopamine. J Neurochem *88*, 1398–1405.

Dal Bo, G. (2008). Enhanced glutamatergic phenotype of mesencephalic dopamine neurons after neonatal 6-hydroxydopamine lesion. Neuroscience *156*, 59–70.

Dal Bo, G., St-Gelais, F., Danik, M., Williams, S., Cotton, M., and Trudeau, L.-E. (2004). Dopamine neurons in culture express VGLUT2 explaining their capacity to release glutamate at synapses in addition to dopamine. J. Neurochem. *88*, 1398–1405.

Bolam, J.P., and Pissadaki, E.K. (2012). Living on the edge with too many mouths to feed: why dopamine neurons die. Mov. Disord. *27*, 1478–1483.

Borodinsky, L.N., Root, C.M., Cronin, J.A., Sann, S.B., Gu, X., and Spitzer, N.C. (2004). Activity-dependent homeostatic specification of transmitter expression in embryonic neurons. Nature *429*, 523–530.

Bourque, M.J., and Trudeau, L.E. (2000). GDNF enhances the synaptic efficacy of dopaminergic neurons in culture. Eur J Neurosci *12*, 3172–3180.

Cartier, E.A., Parra, L.A., Baust, T.B., Quiroz, M., Salazar, G., Faundez, V., Egaña, L., and Torres, G.E. (2010). A biochemical and functional protein complex involving dopamine synthesis and transport into synaptic vesicles. J. Biol. Chem. *285*, 1957–1966.

DePuy, S.D., Stornetta, R.L., Bochorishvili, G., Deisseroth, K., Witten, I., Coates, M., and Guyenet, P.G. (2013). Glutamatergic neurotransmission between the C1 neurons and the parasympathetic preganglionic neurons of the dorsal motor nucleus of the vagus. J. Neurosci. *33*, 1486–1497.

El Mestikawy, S., Wallén-Mackenzie, A., Fortin, G.M., Descarries, L., and Trudeau, L.-E. (2011). From glutamate co-release to vesicular synergy: vesicular glutamate transporters. Nat. Rev. Neurosci. *12*, 204–216.

Fahn, S., Rodman, J.S., and Côté, L.J. (1969). Association of tyrosine hydroxylase with synaptic vesicles in bovine caudate nucleus. J. Neurochem. *16*, 1293–1300.

Fasano, C., Thibault, D., and Trudeau, L.-É. (2008). Culture of postnatal mesencephalic dopamine neurons on an astrocyte monolayer. Curr. Protoc. Neurosci. *44*, 3.21.1–3.21.19.

Forlano, P.M., and Woolley, C.S. (2010). Quantitative analysis of pre- and postsynaptic sex differences in the nucleus accumbens. J Comp Neurol *518*, 1330–1348.

Fortin, G.M., Bourque, M.-J., Mendez, J.A., Leo, D., Nordenankar, K., Birgner, C., Arvidsson, E., Rymar, V.V., Bérubé-Carrière, N., Claveau, A.-M., et al. (2012). Glutamate corelease promotes growth and survival of midbrain dopamine neurons. J. Neurosci. *32*, 17477–17491.

Gutierrez, R. (2003). Plasticity of the GABAergic phenotype of the "glutamatergic" granule cells of the rat dentate gyrus. J Neurosci *23*, 5594–5598.

Gutiérrez, R. (2002). Activity-dependent expression of simultaneous glutamatergic and GABAergic neurotransmission from the mossy fibers in vitro. J. Neurophysiol. *87*, 2562–2570.

Halskau, Ø., Ying, M., Baumann, A., Kleppe, R., Rodriguez-Larrea, D., Almås, B., Haavik, J., and Martinez, A. (2009). Three-way interaction between 14-3-3 proteins, the N-terminal region of tyrosine hydroxylase, and negatively charged membranes. J. Biol. Chem. *284*, 32758–32769.

Hnasko, T.S., Chuhma, N., Zhang, H., Goh, G.Y., Sulzer, D., Palmiter, R.D., Rayport, S., and Edwards, R.H. (2010). Vesicular glutamate transport promotes dopamine storage and glutamate corelease in vivo. Neuron *65*, 643–656.

Jego, S., Glasgow, S.D., Herrera, C.G., Ekstrand, M., Reed, S.J., Boyce, R., Friedman, J., Burdakov, D., and Adamantidis, A.R. (2013). Optogenetic identification of a rapid eye movement sleep modulatory circuit in the hypothalamus. Nat. Neurosci. *16*, 1637–1643.

Kawano, M. (2006). Particular subpopulations of midbrain and hypothalamic dopamine neurons express vesicular glutamate transporter 2 in the rat brain. J Comp Neurol *498*, 581–592.

Li, X., Qi, J., Yamaguchi, T., Wang, H.-L., and Morales, M. (2013). Heterogeneous composition of dopamine neurons of the rat A10 region: molecular evidence for diverse signaling properties. Brain Struct. Funct. *218*, 1159–1176.

Matsushita, N., Okada, H., Yasoshima, Y., Takahashi, K., Kiuchi, K., and Kobayashi, K. (2002). Dynamics of tyrosine hydroxylase promoter activity during midbrain dopaminergic neuron development. J. Neurochem. *82*, 295–304.

Mendez, J.A., Bourque, M.-J., Bo, G.D., Bourdeau, M.L., Danik, M., Williams, S., Lacaille, J.-C., and Trudeau, L.-E. (2008). Developmental and target-dependent regulation of vesicular glutamate transporter expression by dopamine neurons. J. Neurosci. *28*, 6309–6318.

Moss, J., Ungless, M.A., and Bolam, J.P. (2011). Dopaminergic axons in different divisions of the adult rat striatal complex do not express vesicular glutamate transporters. Eur. J. Neurosci. *33*, 1205–1211.

Onoa, B., Li, H., Gagnon-Bartsch, J.A., Elias, L.A.B., and Edwards, R.H. (2010). Vesicular monoamine and glutamate transporters select distinct synaptic vesicle recycling pathways. J. Neurosci. *30*, 7917–7927.

Prensa, L., and Parent, A. (2001). The Nigrostriatal Pathway in the Rat: A Single-Axon Study of the relationship between dorsal and ventral tier nigral neurons and the striosome/matrix striatal compartments. J. Neurosci. *21*, 7247–7260.

Spitzer, N.C., Root, C.M., and Borodinsky, L.N. (2004). Orchestrating neuronal differentiation: patterns of Ca2+ spikes specify transmitter choice. Trends Neurosci. *27*, 415–421.

Stamatakis, A.M., Jennings, J.H., Ung, R.L., Blair, G.A., Weinberg, R.J., Neve, R.L., Boyce, F., Mattis, J., Ramakrishnan, C., Deisseroth, K., et al. (2013). A unique population of ventral tegmental area neurons inhibits the lateral habenula to promote reward. Neuron *80*, 1039–1053.

Stuber, G.D., Hnasko, T.S., Britt, J.P., Edwards, R.H., and Bonci, A. (2010). Dopaminergic terminals in the nucleus accumbens but not the dorsal striatum corelease glutamate. J. Neurosci. *30*, 8229–8233.

Sulzer, D. (1998). Dopamine neurons make glutamatergic synapses in vitro. J Neurosci *18*, 4588–4602.

Tecuapetla, F., Patel, J.C., Xenias, H., English, D., Tadros, I., Shah, F., Berlin, J., Deisseroth, K., Rice, M.E., Tepper, J.M., et al. (2010). Glutamatergic signaling by mesolimbic dopamine neurons in the nucleus accumbens. J. Neurosci. *30*, 7105–7110.

Thompson, L., Barraud, P., Andersson, E., Kirik, D., and Björklund, A. (2005). Identification of dopaminergic neurons of nigral and ventral tegmental area subtypes in grafts of fetal ventral mesencephalon based on cell morphology, protein expression, and efferent projections. J. Neurosci. *25*, 6467–6477.

Tong, Q., Ye, C., McCrimmon, R.J., Dhillon, H., Choi, B., Kramer, M.D., Yu, J., Yang, Z., Christiansen, L.M., Lee, C.E., et al. (2007). Synaptic glutamate release by ventromedial hypothalamic neurons is part of the neurocircuitry that prevents hypoglycemia. Cell Metab. *5*, 383–393.

Tritsch, N.X., Ding, J.B., and Sabatini, B.L. (2012). Dopaminergic neurons inhibit striatal output through non-canonical release of GABA. Nature *490*, 262–266.

Tritsch, N.X., Oh, W.-J., Gu, C., and Sabatini, B.L. (2014). Midbrain dopamine neurons sustain inhibitory transmission using plasma membrane uptake of GABA, not synthesis. eLife *3*, e01936.

Walicke, P.A., and Patterson, P.H. (1981). On the role of cyclic nucleotides in the transmitter choice made by cultured sympathetic neurons. J. Neurosci. *1*, 333–342.

Yamaguchi, T., Wang, H.-L., Li, X., Ng, T.H., and Morales, M. (2011). Mesocorticolimbic glutamatergic pathway. J. Neurosci. *31*, 8476 –8490.

Yamaguchi, T., Wang, H.-L., and Morales, M. (2013). Glutamate neurons in the substantia nigra compacta and retrorubral field. Eur. J. Neurosci. *38*, 3602–3610.

Yizhar, O., Fenno, L.E., Davidson, T.J., Mogri, M., and Deisseroth, K. (2011). Optogenetics in neural systems. Neuron *71*, 9–34.

Zhang, T., Zhang, L., Liang, Y., Siapas, A.G., Zhou, F.-M., and Dani, J.A. (2009). Dopamine signaling differences in the nucleus accumbens and dorsal striatum exploited by nicotine. J. Neurosci. *29*, 4035–4043.

Zhuang, X., Masson, J., Gingrich, J.A., Rayport, S., and Hen, R. (2005). Targeted gene expression in dopamine and serotonin neurons of the mouse brain. J. Neurosci. Methods *143*, 27–32.

Article 3

From glutamate corelease to vesicular synergy: new perspectives on the functions of vesicular glutamate transporters

Salah El Mestikawy [1, 2, 3, 4], Åsa Wallén-Mackenzie [5], Guillaume M. Fortin [7],

Laurent Descarries [6] and Louis-Eric Trudeau [7]

[1] Institut National de la Santé et de la Recherche Médicale (INSERM), U952, Université Pierre et Marie Curie, 9 quai Saint Bernard, 75005 Paris, France.

[2] Centre National de la Recherche Scientifique (CNRS) UMR 7224, 9 quai Saint Bernard, 75005 Paris, France.

[3] Université Pierre et Marie Curie (UPMC) Paris 06, Pathophysiology of Central Nervous System Disorders, 9 quai Saint Bernard, 75005 Paris, France.

[4] Douglas Hospital Research Center, Department of Psychiatry, McGill University, 6875 boulevard LaSalle Verdun, QC, Canada, H4H 1R3.

[5] Department of Neuroscience, Unit of Developmental Genetics, Uppsala University, Box 593, S-751 24, Sweden.

[6] Departments of Pathology and Cell Biology and of Physiology, Groupe de Recherche sur le Système Nerveux Central, Faculty of Medicine, Université de Montréal, C.P. 6128, Succursale Centre-ville, Montréal, QC, Canada, H3C 3J7.

[7] Department of Pharmacology, Groupe de Recherche sur le Système Nerveux Central, Faculty of Medicine, Université de Montréal, C.P. 6128, Succursale Centre-ville, Montréal, QC, Canada, H3C 3J7.

Publié dans *Nature Reviews Neuroscience*, 2011, 12:204-216

Contribution des auteurs

Salah El Mestikawy : Il a contribué à l'écriture du manuscrit.

Åsa Wallén-Mackenzie : Il a contribué à l'écriture du manuscrit.

Guillaume M. Fortin : Il a contribué à l'écriture du manuscrit.

Laurent Descarries : Il a contribué à l'écriture du manuscrit.

Louis-Éric Trudeau : Il a contribué à l'écriture du manuscrit.

Abstract

Recent data indicate that "classical" neurotransmitters can also act as cotransmitters. This notion has been strengthened by the demonstration that three vesicular glutamate transporters (VGLUT1-3) are present in central monoamine, acetylcholine and GABA (γ-aminobutyric acid) neurons, in addition to primarily glutamatergic neurons. Intriguing questions are thus raised about the morphological and functional organization of neuronal systems endowed with such a dual signalling capacity. In addition to fast signalling via glutamate receptors, vesicular synergy, a process leading to enhanced packaging of the "primary" transmitter, is increasingly recognized as

a major property of the glutamatergic cophenotype. The behavioural relevance of this cophenotype is presently the focus of considerable interest.

Introduction

Almost 80 years after the formulation of the hypothesis epitomized as Dale's principle (**Box 1**), there are many reasons to think that the complexity of the chemical and anatomical organization of the mammalian nervous system is much greater than was previously imagined. It is becoming increasingly clear that most if not all neurons of the central and the peripheral nervous systems do not use a single chemical transmitter. Neuropeptides were long considered to be the second transmitter most frequently colocalized in monoamine, acetylcholine (ACh) or GABA (γ-aminobutyric acid) containing neurons of the CNS. However, there is mounting evidence that many neuronal populations in the brain and spinal cord —hitherto defined as using a single "classical" transmitter plus or minus a neuropeptide — in fact use more than a single non-peptide transmitter.

The recent identification of proton-dependent carrier molecules, which transport glutamate from the cytosol into synaptic vesicles and therefore allow for the exocytotic release of glutamate, has renewed interest in the concept of neurons using multiple transmitters. In addition to permitting the formal identification of primarily glutamatergic neurons, the expression of a vesicular glutamate transporter (VGLUT) suffices to assign a glutamatergic phenotype to neurons already known to use another transmitter. In this review, we provide a brief historical overview of the discovery and functions of VGLUTs, and then discuss the increasing evidence for the presence of VGLUTs in "non-glutamatergic" CNS neurons. We next consider cellular, physiological and behavioural implications of such a phenomenon, including glutamate corelease and enhanced packaging of the primary transmitter through a process called vesicular synergy.

Discovery of the vgluts

In 1994, Ni and colleagues isolated brain-specific Na^+-dependent inorganic phosphate cotransporter (BNPI), a "brain-specific" protein that exhibited weak similarities with Na^+-

dependent inorganic phosphate transporters [1]. It came as a surprise when six years later, two independent studies elegantly unravelled that BNPI was in fact a vesicular glutamate transporter [2, 3]. Indeed, the heterologous transfection of this protein sufficed to endow GABA (γ-aminobutyric acid) neurons with a glutamatergic phenotype [3]. BNPI was subsequently renamed type 1 vesicular glutamate transporter (VGLUT1), and shown to share all of the basic characteristics previously reported for glutamate accumulation by brain vesicles, including 1) millimolar affinity for glutamate; 2) inability to transport aspartate, glutamine or GABA; 3) dependence on the proton gradient; 4) dependence on the $\Delta\Psi$ component (vesicular transmembrane potential) of the pH gradient (not the ΔpH) and 5) biphasic chloride dependence (allosteric activation between 1 and 4 mM, inhibition above 10 mM) [4, 5].

Interestingly, VGLUT1 was found to be strongly expressed by a subpopulation of neurons in the cerebral cortex, hippocampus and cerebellar cortex (**Figure 1A**), with very little expression in subcortical regions; this suggested that in these regions, glutamate vesicular packaging is mediated by a second subtype of the transporter [6].

In 2000, another member of the Na^+-dependent inorganic phosphate transporters (named differentiation-associated Na^+ -dependent inorganic phosphate cotransporter (DNPI)) was discovered by Aihara et al. [7]. DNPI shared a high degree of homology with BNPI/VGLUT1 and was strongly enriched in subcortical regions [7, 8] (**Figure 1A**). In 2002, five research groups reported that DNPI was also a vesicular glutamate transporter and renamed it VGLUT2 [9-13]. Like VGLUT1, VGLUT2 translocates glutamate inside vesicles using an electrochemical proton gradient as driving force [11] and is distributed in excitatory axon terminals that form asymmetrical synapses [11, 14]. It was concluded from these early observations that VGLUTs are genuine markers of glutamatergic synapses. Moreover, the presence of a single type of VGLUT seemed to be sufficient to fill synaptic vesicles with glutamate [15].

In 2002, a third subtype (VGLUT3) was discovered, which shared all structural and functional characteristics of the other two VGLUTs [16-19]. Unlike *Vglut1* and *Vglut2* transcripts, which were widely expressed in cortical and subcortical regions, respectively, the distribution of *Vglut3* mRNA was restricted to neuronal populations not previously considered as primarily

glutamatergic: VGLUT3 was found in serotonin (5-hydroxytryptamine, 5-HT) neurons in raphe nuclei, acetylcholine (ACh) neurons in dorsal and ventral striatum, and subclasses of GABA interneurons (basket cells) in cerebral cortex and hippocampus [17, 18, 20, 21] (**Figure 1A**). In addition, VGLUT3 is present in subgroups of primarily glutamatergic neurons in the raphe, habenula, hypothalamus, olfactory tubercles and sensory inner hair cells of the cochlea [17, 20, 22-25].

Three main conclusions could be reached from this initial phase of discovery and characterization. First, three VGLUTs ensure the vesicular uptake of glutamate in CNS neurons and thus represent unambiguous biomarkers of glutamatergic transmission; second, VGLUT1 and VGLUT2 are found in neuronal populations already known to be glutamatergic; and third, VGLUT3, by contrast, is mostly found in neurons not initially identified as glutamatergic, indicating that in these cells glutamate may act as a cotransmitter. As will be described below, a broader examination of the distribution and functions of VGLUTs subsequently revealed that VGLUT1 and VGLUT2 can also be found in neurons not initially characterized as glutamatergic, thus raising the hypothesis that glutamate acts as a cotransmitter in many types of neurons. (See **Boxes 2 and 3** for a discussion of the role of VGLUTs as transporters of inorganic phosphate and chloride)**.**

Vgluts in "non-glutamatergic" neurons

Abundant cytochemical data demonstrates the coexistence of vesicular glutamate transporter in CNS neurons whose identity is defined by another "primary" neurotransmitter (**Table 1).** Thus far, each of the three VGLUTs has been demonstrated to be present in some cholinergic (ACh) or GABAergic (GABA) neurons of CNS, but only VGLUT2 in noradrenaline (NA), adrenaline (A) or dopamine (DA) neurons, and VGLUT3 in serotonin (5-HT) neurons (**Figure 1B**).

VGLUT2 in dopamine neurons

Soon after the identification of VGLUT2, early studies combining *in situ* hybridization and immunocytochemistry revealed the existence of *Vglut2* mRNA in noradrenergic neurons of the A1 and A2 groups of the rat medulla, and adrenergic neurons of the C1, C2, and C3 groups, raising the possibility that glutamate might act as a cotransmitter in catecholamine neurons [26, 27].

The first evidence that both *Vglut2* mRNA and VGLUT2 protein could be present in DA neurons came from a study combining single-cell RT-PCR with tyrosine hydroxylase (TH) and VGLUT2 immunocytochemistry on isolated mesencephalic DA neurons from postnatal rat in microculture [28]. A subsequent single-cell RT-PCR study showed *Vglut2* mRNA to be present in mesencephalic DA neurons of both newborn (P0) and P45 mice, with a much higher yield at P0 [29], suggesting developmental regulation of *Vglut2* expression. Subsequent analyses revealed that *Vglut2* mRNA is expressed in tyrosin hydroxylase (TH)-expressing subpopulations of hypothalamic and ventral tegmental area DA neurons, whereas those in the substantia nigra show barely detectable levels of *Vglut2* mRNA [30,31, 32]. A dynamic regulation of *Vglut2* expression in these neurons has also been observed in a study which examined *Vglut2* and TH mRNA expression in the ventral mesencephalon of rats treated with 6-hydroxydopamine (6-OHDA) [33]. The abundance of *Vglut2* mRNA was increased in surviving DA neurons of these rats, suggesting an induction of *Vglut2* expression under pathological conditions or a negative regulation by DA [34]. Both in culture and *in vivo*, there are indications that *Vglut2* expression by mesencephalic DA neurons might be regulated through a contact-dependent interaction with GABA neurons and with other DA neurons [29]; In particular, contact with GABA neurons appears to act as a strong repressor of *Vglut2* expression in DA neurons and lesioning striatal GABA neurons, which project to DA neurons, leads to an increase in the proportion of DA neurons expressing *Vglut2*.

Recent immuno-electron microscopic studies in P15 rats showed that 28% of all TH immunopositive axon terminals in the nucleus accumbens, and 17% of those in neostriatum contain VGLUT2 [33]. Interestingly, such double-labeling was no longer found in adult rats (P90), which suggested an age-dependent regulation of VGLUT2 and TH coexpression [34, 35], although it is also possible that VGLUT2 and TH are segregated in different branches and/or axon terminals at later ages.

VGLUT3 in serotonin neurons

In most parts of adult rat or mouse dorsal and median raphe nuclei, the vast majority (~ 80%) of 5-HT neurons express *Vglut3* mRNA [18, 36], and VGLUT3 protein is present in the cell bodies and dendrites of these neurons [17, 22, 23, 37-40]. Although midbrain 5-HT neurons project widely and diffusely to most parts of forebrain (e.g., [41]), VGLUT3 has thus far only been detected in subsets of 5-HT axon terminals, notably in cerebral cortex [37, 38, 40] and hippocampus [18, 37, 40, 42]. Results from triple immunofluorescence confocal microscopy studies suggested that 5-HT/VGLUT3 positive terminals rarely contain the 5-HT reuptake **transporter** (SERT), in contrast to those which apparently lack VGLUT3 [3937]. 5-HT axon terminals of the olfactory bulb [40], amygdala [40], ventral tegmental area [43], supra-ependymal plexus [37], and intermediolateral cell column of the rat spinal cord [44] also show VGLUT3 immunoreactivity.

VGLUTs in acetylcholine neurons

Vglut1 and *Vglut2* mRNA are expressed in ACh (choline-acetyltransferase (ChAT) immunopositive) motoneurons of the rat spinal cord [45], but VGLUT1 and VGLUT2 protein seem to be absent from the motor endplates in skeletal muscles [45-47]. VGLUT1 protein is, however, present in ACh terminals innervating striated esophageal muscle [46], and VGLUT2 in non-cholinergic axons that originate from spinal motoneurons and contact Renshaw cells [45]. Renshaw cells are also contacted by cholinergic collaterals from spinal motoneurons, a pathway involved in feedback regulation of motor circuitry. The failure to detect VGLUT protein in all axon terminals established by motoneurons that otherwise express *Vglut1* or *Vglut2* transcripts has led to the suggestion that spinal motoneurons might give rise to separate sets of cholinergic and glutamatergic axon terminals, with the latter possibly involved in the regulation of motor functions [47] (but see [48] for conflicting results). VGLUT1 is also expressed in ACh axon terminals of the interpeduncular nucleus in mice, which may account for the corelease of glutamate and

ACh upon optogenetic stimulation of medial habenula neurons projecting to this nucleus [49].

In adult mouse and rat brain, *Vglut3* mRNA is expressed in ACh interneurons of dorsal and ventral striatum [17, 18], and some of the nucleus basalis ACh neurons projecting to the basolateral amygdala [50]. In ACh interneurons, VGLUT3 protein seems to be targeted to the soma and proximal dendrites [16, 51] , as well as to a majority, if not all, axon terminals [17, 18, 51]. The role of VGLUT3 in the somato-dendritic compartment of these neurons remains to be elucidated.

VGLUTs in GABA neurons

Neurons in several brain regions have been shown to express, seemingly paradoxically, both the inhibitory transmitter GABA and VGLUTs. For example, in cat retina, a subset of cone bipolar cells (and their terminals) contains VGLUT1 as well as GABA, its synthetic enzyme GAD_{65} and its vesicular transporter VIAAT [52]. There are also GABAergic axon terminals containing VGLUT1, VGLUT2 or VGLUT3 in developing and/or adult rat cerebral cortex and/or hippocampus [20, 38, 51, 53-56]. *Vglut2* is expressed by some GABA neurons in the ventral tegmental area [31], and *Vglut2* mRNA and VGLUT2 protein have respectively been detected in GABA neurons of the hypothalamic anteroventral periventricular nucleus and their terminals (in the rostral preoptic area) of female, adult rats [57]. During early post-natal development, *Vglut3* and VGLUT3 are respectively present in Purkinje cells and terminals around their cell body [58], as well as in neurons of the nucleus of the trapezoid body and their immature GABA/glycine synapses in the lateral superior olive (LSO) [59]. In adult rat brain, VGLUT3 is found in subpopulations of GABA neurons in CA1-CA3 of hippocampus [16], cholecystokinin-positive, GABAergic basket cells in cerebral cortex and hippocampus [21], and preprotachykinin B-producing GABAergic interneurons in neocortex [38].

The glutamatergic cophenotype

The growing evidence for the coexistence of VGLUTs in monoamine, ACh and GABA neurons raises fundamental issues regarding the structural and functional properties of neurons endowed with such a dual phenotype. A first and obvious question is whether glutamate is actually released by these neurons *in vivo*. Then, assuming it is, a second question is whether such glutamate release occurs at the same axon terminals that release the primary neurotransmitter (**Figure 2**). Thirdly, if both glutamate and the primary transmitter are released from the same terminals, are the vesicular transporters for both transmitters present in the same or in different synaptic vesicles (**Figure 2**)? Moreover, what are the mechanisms of VGLUT sorting and trafficking that are required to explain the fact that axon terminals can contain heterogeneous pools of synaptic vesicles with and without VGLUTs, as well as heterogeneous populations of axon terminals, with and without VGLUT-containing vesicles? Lastly, when a VGLUT is present in synaptic vesicles that also contain a vesicular transporter for another transmitter, does this have any impact on the vesicular loading of this transmitter? These questions are discussed below.

The glutamatergic cophenotype of DA neurons. Patch-clamp recordings of isolated rat mesencephalic DA neurons in microculture provided the first evidence that CNS DA neurons could form axon terminals capable of releasing glutamate [60, 61]. The short latency and rapid rise time of the recorded responses was strongly suggestive of synaptic contacts, even though in adult rats *in vivo*, these neurons release DA mainly from axon terminals that do not form morphologically-defined synaptic membrane specializations [62]. Interestingly, in the nucleus accumbens (nAcb) of P15 rats, all DA terminals doubly immunolabeled for TH and VGLUT2 were indeed found to make a synaptic junction, as opposed to those labeled for TH only [33, 34]. Recent studies in adult mice have provided unequivocal evidence for the release of glutamate by VTA DA neurons *in vivo* [63, 64]. These studies demonstrated that optogenetic activation of axon terminals originating from VTA DA neurons induced AMPA receptor-mediated glutamatergic fast synaptic responses in nAcb neurons. Furthermore, targeted deletion of *Vglut2* in the mesencephalic DA neurons completely abolished such light-dependent EPSCs [64].

The question arises as to whether such glutamate release from DA neurons occurs at the same axon terminals that release DA. Immunolabeling studies performed in cultured rat DA

neurons prior to the identification of VGLUTs showed that the vast majority of axon varicosities formed by DA neurons in single neuron microculture were double-labeled for TH and glutamate, suggesting that most terminals have the capacity to release both transmitters [60] (see also [62, 65] for early ultrastructural data suggesting that DA neurons establish two morphologically distinct subsets of axon terminals). Close examination of VGLUT2 immunoreactivity *in vitro* [28] and *in vivo* [66], however, suggests that DA neurons possess different subsets of axon terminals, perhaps as much as three: a first that contains only TH, a second, perhaps smaller, containing both TH and VGLUT2, and a third containing VGLUT2 but not TH (**Figure 2**). The possibility that TH might be absent from some axonal branches and/or axon terminals of DA neurons may come as a surprise in light of the fact that such biosynthetic enzymes are known to be mostly cytosolic. However, there is some evidence that TH may be membrane bound, even to synaptic vesicles, notably in the striatum [67], and may therefore be unevenly distributed among axon terminals. Indeed, isolated DA neurons in culture have a large number of VGLUT2 immunopositive, TH immunonegative varicosities, confirmed as axon terminals by the presence of synaptic vesicle 2-related protein (SV2) [28]. A recent study has suggested that VGLUT2 is only found in a small subset of TH- and VMAT2-containing axon terminals in cultured DA neurons [68]. The notion of a phenotypical heterogeneity among axon terminals of DA neurons might also explain why, in adult (as opposed to P15) rats, axon terminals dually labeled for TH and VGLUT2 are no longer observed in ventral or dorsal striatum[34]. This is even the case after a partial 6-hydroxydopamine lesioning of the mesencephalic DA neurons, a condition known to activate expression of *Vglut2* and increase the colocalization of TH and VGLUT2 in the DA axon terminals of postnatal rat [34]. These results now need to be re-evaluated by quantifying the colocalization of VGLUT2 with other dopaminergic markers such as DAT as well as VMAT2.

The glutamatergic cophenotype of 5-HT neurons. An early electrophysiological study demonstrated that isolated 5-HT neurons in culture can show fast AMPA receptor-mediated synaptic currents [69]. In a recent study, optogenetic stimulation of neuron axonal fibres arising from mouse raphe nuclei [42], triggered short-latency AMPA receptor-mediated synaptic responses in GABAergic interneurons in the hippocampus. Interestingly, in many neurons, the fast synaptic response was partially reduced by a 5-HT_3 ionotropic receptor antagonist (albeit at a relatively high dose) [42], suggesting that glutamate and 5-HT mediate synaptic excitation in the same time

frame. By contrast, optical stimulation evoked slow (rise time slower than 100 ms) postsynaptic-like responses in a subset of CA1 hippocampal pyramidal neurons, and these were reduced by a metabotropic 5-HT_{1A} receptor antagonist [42] (see also [69] for a similar and earlier finding in culture). A caveat of this study was that channelrhodopsin2 was not expressed in raphe neurons under the control of a 5-HT neuron-selective promoter, thus making it possible that VGLUT3-expressing non-5-HT neurons [23, 36, 38] were also optically stimulated. Nonetheless, these finding strongly suggest that 5-HT neurons can co-release glutamate and suggest the intriguing possibility that such co-release can lead to the encoding of parallel signals that operate along different time scales. Such, dual synaptic responses, with a fast, ionotropic component and a slower, metabotropic component have not yet been described in response to activation of DA or ACh neurons.

In isolated cultured postnatal rat 5-HT neurons, a majority of 5-HT immunoreactive axon varicosities contain VGLUT3, a substantial subset contains only 5-HT, and a small subset contains VGLUT3 but not 5-HT [16]. Similarly, in embryonic rat midbrain raphe cultures, some tryptophan hydroxylase (TPH) immunopositive varicosities are VGLUT3 immunopositive [18]. Axon terminals that are immunopositive for both VGLUT3 and 5-HT have also been reported in the ventral tegmental area and substantia nigra (pars compacta), [67],[70]; however the vast majority of 5-HT varicosities in these areas seem to be VGLUT3 immunonegative [67], suggesting segregation of the cotransmitters to different axonal branches (**Figure 2**). By contrast, in the limbic cortex, hippocampus and lateral septum, 30-50% of 5-HT immunoreactive terminals contain VGLUT3 and VMAT2, the rest being VGLUT3 immunonegative [37] (**Figure 2**). Taken together, these findings are consistent with axon terminal heterogeneity, as already suggested for DA neurons.

The glutamatergic cophenotype of ACh neurons. Cholinergic neurons of the medial septum in microculture can release glutamate from autaptic connections [71], in keeping with the previous demonstration of *Vglut1* or *Vglut2* expression in a subset of these neurons [72]. Interestingly, numerous neurons displayed mixed synaptic responses, with both AMPA receptor-mediated and nicotinic receptor-mediated components, which is suggestive of corelease of the two transmitters

[71]. Optogenetic stimulation of ACh neurons of the medial habenula projecting to the interpeduncular nucleus evoked fast, glutamate-mediated synaptic responses in neurons of this region[49]. Interestingly, stimulus trains at 20-50Hz evoked slow (15s rise time), nicotinic receptor-mediated postsynaptic inward current in target neurons[49]. This finding provides strong evidence for the hypothesis that glutamate corelease from cholinergic neurons mediates fast signals to target neurons, whereas release of ACh — presumably from non-synaptic axon terminals [73, 74] — mediates excitatory signals on a much slower time scale.

Glutamate release from striatal ACh interneurons has not yet been demonstrated. However, dual immunolabeling for both the vesicular ACh transporter (VAChT) and VGLUT3 has demonstrated that the vast majority of neostriatal ACh axon varicosities (terminals) do contain VGLUT3 [17]. Thus, in contrast to DA and 5-HT neurons, striatal ACh interneurons seem to show little if any segregation of their two vesicular transporters in distinct terminals (**Figure 2**).

The glutamatergic cophenotype of GABA neurons. Although a recent study provided strong evidence for *in vivo* release of GABA from glutamatergic hippocampal granule neurons [75], glutamate release by hippocampal GABA neurons remains to be demonstrated. Glutamate release from immature VGLUT3 positive GABA/glycine synapses has, however, been reported in the auditory system [59, 76]. The early developmental expression of *Vglut3* in some GABA neurons and the fact that VGLUT3 endows GABA/glycine synapses with the ability to release glutamate and to stimulate NMDA (N-methyl-D-aspartate) receptors [59, 76] suggests that glutamate release might have a role in the functional maturation of the GABAergic/glycinergic circuitry. Indeed, VGLUT3-mediated glutamate release in GABA/glycine neurons contributes to a refinement of the synaptic connections in the auditory system [76].

Sorting of VGLUTs

Cotransmission in the strictest sense implies that two neurotransmitters are released at the same time from a common pool of synaptic vesicles within one axon terminal. A few examples

of such corelease have already been documented, such as the release of glycine and GABA at synapses in the spinal cord [77]. Corelease of two transmitters from the same vesicle is quite difficult to demonstrate conclusively and would imply that (some) vesicles contain vesicular transporters for two different neurotransmitters. A number of recent studies have used synaptic vesicle immuno-purification (using paramagnetic beads coupled to vesicular transporter antibodies) to show that this can indeed occur (**Figure 2**). For example, VGLUT1 and VGLUT2 are coexpressed in the same vesicles in the hippocampus [78], VIAAT and VGLUT1 in cortical neurons [54], VAChT and VGLUT3 in striatal ACh interneurons [79], VAChT and VGLUT1 in the interpeduncular nucleus [49] and VMAT2 and VGLUT2 in striatal axon terminals [80]. Furthermore, VIAAT and VGLUT2 can be found on the same vesicle subset in vesicles purified from whole brain [56]. By contrast, in terminals of the dentate gyrus of rat hippocampus, VIAAT and VGLUT2 are coexpressed but localized to different subsets of vesicles, as observed by immuno-electron microscopy [53]. It is thus possible that transporter colocalization differs regionally. Whether it is also developmentally regulated is a question that remains to be explored.

How vesicular transporters are segregated in different populations of vesicles and axon terminals is an important area for future research. Neuronal synaptic proteins are thought to be synthesized in the membrane of the rough endoplasmic reticulum, followed by trafficking through the Golgi complex. Newly synthesized vesicular proteins such as VGLUTs can then be shipped to their proper location, mainly axon terminals, by trafficking either through constitutive or regulated secretory vesicles (see [81] and [82] for recent reviews). A specific synaptic vesicle trafficking motif has been identified in VMAT; however, corresponding sorting domains in VGLUTs have been more elusive [83]. Although direct data are presently lacking, it has been proposed that — similar to VMAT2 — VGLUT3 might be sorted to regulated secretory vesicles to reach both the somatodentritic and axonal compartments of neurons [81].

Most studies documenting the presence of VGLUTs and another vesicular transporter on the same vesicles used immuno-purification coupled to western blot analyzes. However, the lack of resolution of these biochemical methods does not allow a quantification of the percentage of colocalization or the identification of differences in expression between vesicles. Being able to answer such questions would increase our understanding of the nature and functions of

cotransmission. For example, axon terminals are known to contain two functionally distinct pools of vesicles, known as the reserve pool and the readily releasable pool [84]; could vesicles from these two pools be molecularly heterogeneous, with only one of two pools containing vesicles with two types of vesicular transporters? A better understanding of the sorting of VGLUTs and other vesicular carriers to various vesicular pools, as well as of the dynamics of vesicular protein content may come from the use in coming years of high-resolution microscopy techniques such as stimulated emission depletion (STED) microscopy and total internal reflection fluorescence (TIRF) microscopy [85].

Vesicular synergy

In addition to enabling the corelease of glutamate, there is increasing evidence that the presence of a VGLUT in axon terminals may have important functional consequences. For example, it may result in increased filling of synaptic vesicles with the primary transmitter, and hence increased release of this transmitter. This has been demonstrated for VGLUT3 in ACh and 5-HT neurons [37, 79], and has been suggested for VGLUT2 in DA neurons [80] and GABA neurons [56], but remains unexplored in other systems.

One study showed that in wild-type mice, VGLUT3 and VAChT were located in a common pool of vesicles and that vesicular co-accumulation of glutamate resulted in increased ACh filling of vesicles[79]. The functional significance of this was indicated by the hypo-cholinergic phenotype of *Vglut3* knockout mice (*Vglut3*$^{-/-}$) [79]. Basal as well cocaine-stimulated locomotor activity were also increased in these mice [79]. Such cooperation between two vesicular transporters was termed was termed vesicular synergy [37, 79] (**Box 4**).

Experiments in *Vglut3*$^{-/-}$ mice also demonstrated that vesicular synergy between VGLUT3 and VMAT2 occurs in 5-HT terminals of the hippocampus and prelimbic cortex [40]. Here, glutamate promoted the packaging of 5-HT in synaptic vesicles of VGLUT3 immunoreactive terminals [40]. Interestingly, the 5-HT terminals that also contained VGLUT3 were immunonegative for the 5-HT reuptake transporter SERT [40], suggesting that they might have the capacity to locally deliver a strong and prolonged 5-HT signal through both enhanced release (though vesicular synergy) and reduced reuptake (**Figure 2**). These results suggest that the

strength of 5-HT transmission might vary greatly, both regionally and temporally, according to the combination of vesicular and membrane transporters present in a given 5-HT terminal. It is noteworthy that *Vglut3*$^{-/-}$ mice also displayed increased anxiety-like behaviour [37], whereas other behaviours regulated by 5-HT transmission, such as aggression and depression-like responses, were unaltered [40], suggesting a specific role for glutamate in limbic areas and in anxiety-related behaviours.

Vesicular synergy between glutamate and other cotransmitters can be explained by the VGLUT-dependent acidification of the vesicular lumen [79, 80]. However, which one of the 3 substrates of VGLUTs (glutamate, chloride or Pi) is the actual buffering anion used to increase vesicular accumulation of 5-HT, ACh, DA or GABA is not yet clearly established (see **Boxes 2-3-4**).

A role for vgluts in reward?

Little is presently known regarding the behavioural roles of glutamate cotransmission or of VGLUT expression in monoamine and ACh neurons. An examination of the behavioural consequences of conditionally targeted *Vglut* deletion in these neurons is required to obtain initial insight into this important question. At the present time, this has only been achieved in DA neurons.

Based on the previously mentioned expression of *Vglut2* in DA neurons of the medial A10 area and the rostral linear nucleus [30], regions shown to project to the nAcb [86], as well as electrophysiological recordings showing glutamatergic transmission in mesoaccumbal slice preparations [87], it has been suggested that VGLUT2-mediated glutamate cotransmission might play a role in reward relevant pathways. A first evaluation of this question has been performed in mice in which *Vglut2* was specifically deleted in DA neurons (*Vglut2*$^{f/f;DAT\text{-}Cre}$). There are two *Vglut2*$^{f/f;DAT\text{-}Cre}$ lines, which differ both with regards to the floxed *Vglut2* allele and to the DAT-Cre line used [80, 88].

The first *Vglut2*$^{f/f;DAT\text{-}Cre}$ mice showed normal basal cognitive and locomotor functions [88]; in response to an acute challenge with low dose amphetamine (which triggers DA release), the conditional knockout mice showed reduced locomotor response compared to littermate controls. However, with increasing doses of amphetamine, they displayed increased locomotion and rearing [88]. In the other line of *Vglut2*$^{f/f;DAT\text{-}Cre}$ mice, cocaine (which blocks DA reuptake) induced a smaller increase in locomotion compared to controls [80]. As these studies administered different psychostimulants, a unified picture of how the absence of VGLUT2 influences psychostimulant-induced locomotion has not yet emerged.

Does VGLUT expression in DA neurons have a role in reward learning? A first attempt to address this question used a conditioned place preference (CPP) paradigm [80]. This study did not detect any differences between *Vglut2*$^{f/f;DAT\text{-}Cre}$ and control mice, which led the authors to suggest that at least some forms of reward and associative learning remain intact in the absence of VGLUT2. Further analyses are required to evaluate other aspects of the reward system; for example, drug self-administration paradigms could provide a measure of goal-directed responding and be utilized to discriminate between the reinforcing effects of a substance and the motivation to consume it. Thus, it is clear that more research is needed to address the possible role of VGLUT2-mediated cotransmission in the reward circuitry and in reward-related behaviour.

Concluding remarks

The time is now ripe to envisage new models of transmitter signalling in the CNS, taking into account that subpopulations of neurons use glutamate as a cotransmitter and/or as a synergistic enhancer of vesicular packaging and release. It may even be time to revisit the concept that neurons use a particular transmitter as "primary" and another as "secondary", especially if the cotransmitter phenotype varies during development or in response to physiological signals and injury. At the very least, four key issues still need to be tackled.

The first issue involves the fate and role of glutamate released from the axon terminals of DA, 5-HT, ACh or GABA neurons. Optogenetic studies have already demonstrated that glutamate released from such terminals can activate ionotropic glutamate receptors, but it remains

to be examined whether a majority of these terminals make direct contact with postsynaptic cells or exert their effect presynaptically through axonal ionotropic or metabotropic glutamate receptors. In addition, it is not known whether glutamate cotransmission has the potential to regulate synaptic transmission and mechanisms of synaptic plasticity such as long-term potentiation (LTP), and whether glutamate releasing terminals release only glutamate release as opposed to coreleasing the neuron's "primary" transmitter. With currently available techniques, corelease of two transmitters from the same vesicle can only be conclusively demonstrated by the presence of mixed miniature synaptic currents, mediated by ionotropic glutamate receptors, in addition to ionotropic receptors for ACh (nicotinic), 5-HT (5-HT_3), or GABA ($GABA_A$).

Even if corelease is difficult to prove, the demonstration of vesicular synergy between two transmitters — such as already shown for ACh and glutamate, 5-HT and glutamate and DA and glutamate — speaks in favour of the presence of two transporters in a common pool of vesicles. A second issue to be addressed, therefore, regards the physiological significance of such synergy. This will require experiments that enable discriminating the functional effects of a loss of glutamate release *per se*, versus a loss of vesicular synergy. The impact of vesicular synergy on quantum size also needs to be clarified, as the influx of cytoplasmic glutamate into synaptic vesicles may considerably increase vesicular storage of the coexistent transmitter, by as much as 300% in the case of striatal ACh [79]. Vesicular synergy operates in the physiological range of glutamate concentrations (between 0.1 and 10 mM, [79]), which implies that, in the presence of a VGLUT, the ACh or monoamine quantal size could vary markedly depending on the cytoplasmic concentration of glutamate. Continued research on this topic should determine whether and at which intracytoplasmic concentrations glutamate is able to regulate the amount of ACh, 5-HT or DA stored in synaptic vesicles. Experiments testing directly whether glutamate transport by the VGLUTs, as opposed to Cl^- or Pi transport (**Boxes 2 and 3**), is required for vesicular synergy are also needed to clarify the molecular mechanism leading to increased vesicular accumulation of 5-HT, ACh, DA or GABA.

Third, additional experiments are required to further document the morphological and functional heterogeneity of axon terminals in dual phenotype neurons expressing a VGLUT. If

VGLUTs are found in only a subset of axon terminals established by a given neuron, as seems to be the case for DA neurons[68], this requires a finely regulated sorting mechanism that has not yet been defined. Identification of such a mechanism will probably benefit from analyzing the proteome of axon terminals and the specific proteins that associate with VGLUTs.

Finally, considering the expression of VGLUT2 and VGLUT3 early in development [10, 11, 13, 16-18, 25, 51, 58], it will be important to investigate whether VGLUTs in DA, 5-HT or ACh neurons could have a developmental role, such as promoting neuronal survival or synapse formation. A detailed examination of the impact of conditional deletion of VGLUTs on neuronal survival and morphology should be a first step towards answering this question.

Knowledge emerging from studies of VGLUT-mediated cotransmission may also provide new insights into normal and pathological CNS function. At the organismic level, very little is known regarding the role of dual phenotype neurons and glutamate cotransmission in behaviour. Progress in this direction will undoubtedly continue to come from the study of constitutive and conditional knockout mice, which have already shown that the deletion of *Vgluts* in monoamine and ACh neurons leads to altered anxiety-related behaviours, sensitivity to psychostimulants and/or locomotion. The pathophysiological implications of glutamate cotransmission are also of great potential interest. Recent studies in DA neurons suggest that *Vglut* expression — and thus the transmitter phenotype of neurons — is highly plastic and can be altered in pathological contexts such as in response to brain lesions or to psychotropic medications [29, 33, 89-91]. Further studies are now required to evaluate whether and how up- or down-regulation of *Vgluts* in monoamine, ACh or GABA neurons might be pathogenic.

Box 1: Dale's principle

"Dale's principle" is commonly quoted as stating that "Neurons release only a single type of neurotransmitter at all of their synapses" [92, 93]. Notwithstanding the fact that we know today that this is not the case and that many if not most neurons use more than a single transmitter, it is important to set the record straight and acknowledge what sir Henry Hallet Dale (1875-1968), the famous Nobel laureate pharmacologist, actually said. In a lecture published in 1934, entitled "Pharmacology and nerve endings" [94], Dale wrote "*When we are dealing with two different endings of the same sensory neurone, the one peripheral and concerned with vaso-dilatation and the other at a central synapse, can we suppose that the discovery and identification of a chemical transmitter of axon reflex vasodilatation would furnish a hint as to the nature of the transmission process at a central synapse? The possibility has at least some value as a stimulus to further experiment.*" In reality, the statement was rather conservative and open-minded, and simply suggested that before considering a complicated hypothesis, one should start with the simplest one: that neurons perhaps release the same neurotransmitters from all of their axon terminals.

Box 2: VGLUTs and chloride transport

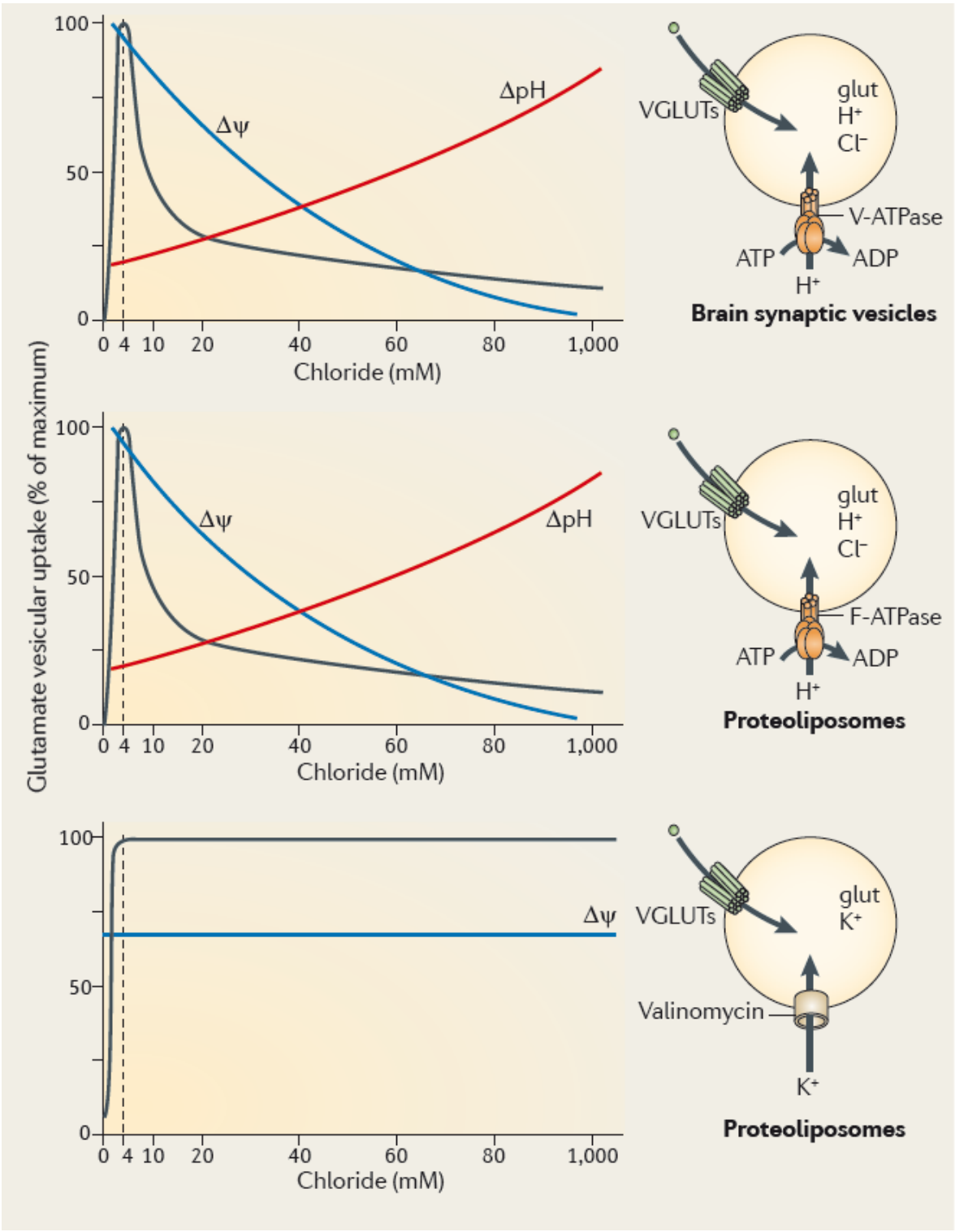

Chloride plays an intricate role in synaptic vesicle homeostasis and its implication in vesicle

acidification has long been known [95]. The impact of Cl^- on vesicular glutamate accumulation was first established with crude preparations of brain vesicles. Naito and Ueda reported that the permeant anion Cl^- sharply stimulated vesicular glutamate uptake at low concentrations, whereas it had an inhibitory effect at higher concentrations[5]. How Cl^- regulates glutamate uptake is not totally clear. In brain synaptic vesicles, the steep stimulation of vesicular glutamate accumulation at low vesicular Cl^- concentrations (below 4mM) has been proposed to be related to the presence of a positive allosteric regulatory binding site on the VGLUTs (with a highly cooperative Hill coefficient ≈3 [96, 97]). The inhibitory effect of high vesicular Cl^- levels on glutamate accumulation could be due to a buffering role. Specifically, VGLUT bioenergetics depends mostly on the component of the μH^+ (for review see [98]), and in the absence of an intravesicular buffering anion, the V-ATPase will generate a strong positive potential (blue line in the Figure and a small pH difference between the vesicular lumen and the cytoplasm (pH, red line in the Figure). A high luminal concentration of Cl^- will buffer H^+ ions (generating HCl), allowing V-ATPase to accumulate more protons inside the vesicle. Consequently, high chloride decreases and increases pH (see for example [99]). As is the main driving force for glutamate accumulation, high Cl^- concentrations would inhibit vesicular glutamate accumulation (see the Figure, left panels).

The role of Cl- in regulating glutamate accumulation raises the question of whether vesicles bear a Cl^- channel or transporter. The proteome of synaptic vesicles does not seem to include any Cl^- channels [100]. Two independent groups have reconstituted VGLUT1 or VGLUT2 in proteoliposomes containing the bacterial F-ATPase as an energy donor [99, 101]. They quite convincingly established that in this *in vitro* system, VGLUTs indeed behave as Cl^- channels [99, 101]. However, a recent study using liposomes containing exclusively VGLUT2 and valynomicin (used to generate a K^+ driving force) reported that VGLUT2 activity plateaued and did not decrease at high Cl^- concentrations [97], a finding that is incompatible with the hypothesis that VGLUT2 acts as a Cl^- channel. This conclusion was confirmed through the use of isotope tracing methods ([^{36}Cl] uptake) and Cl^- fluorescence probes (6-methoxy-N-(3-sulfopropyl)-quinolinum monohydrate) to directly measure Cl^- transport [97]. Thus, the data seem to indicate that VGLUTs do not function as chloride channels; the vesicular chloride channel therefore remains to be identified. Given these most recent data, a provocative and controversial suggestion emerges: perhaps ATP-dependent chloride transport (see [95]) could be driven by the V-ATPase itself. One

way to assess this new hypothesis would be to reconstitute highly purified V-ATPase in artificial liposomes and to assay them for [^{36}Cl] uptake. Indeed, when ATPases are absent (see the Figure, bottom panel), the remains stable and VGLUT activity is no longer inhibited by high chloride concentrations.

What is the relevance of these considerations for vesicular synergy (**Box 4**) and cotransmission? Concerning vesicular synergy, the buffering role of the anion could very well be played by chloride and/or glutamate. If this is the case, then chloride *per se* should be able to accelerate the vesicular accumulation of 5-HT, ACh, DA or GABA. However, recent evidence suggests that vesicular synergy is most probably operated by glutamate and not by chloride [79] Thus, as far as we can judge today, glutamate acts both as a neurotransmitter and as a buffering anion in subpopulations of 5-HT, ACh, DA and GABA terminals.

Box 3: VGLUTs and Pi transport

Studies in *Xenopus* oocytes transfected with mRNA encoding VGLUTs suggested that these proteins might also transport inorganic phosphate (Pi) [1, 7]. Pi uptake via VGLUTs was reinvestigated in 2006, when Juge *et al*., reconstituted proteoliposomes with purified VGLUT2 and bacterial F-ATPase (as energy source) [99]. They detected — in addition to a gradient was imposed to this simplified system. Surprisingly, the Pi transport in proteoliposomes was not affected by the presence of glutamate, VGLUT inhibitors (including Evans Blue), the chloride concentration or mutagenesis of aminoacids that are key to VGLUT2 function [99]. These results suggest either that the compact putative 3D structure of VGLUTs bear two independent transport machineries (one for glutamate and one for Pi) [99, 102], or that sodium-dependent Pi transport is not an intrinsic property of the VGLUTs.

In conclusion, of the three proposed functions of VGLUTs — glutamate transport, Cl- transport and Pi transport —, Pi transport is the least studied and the least firmly established. Additional experiments demonstrating that Na^+- dependent Pi uptake is an intrinsic property of VGLUTs are still awaited; reconstitution of VGLUTs alone in proteoliposomes may be required

(as described by [97]).

Box 4: Molecular mechanisms of vesicular synergy

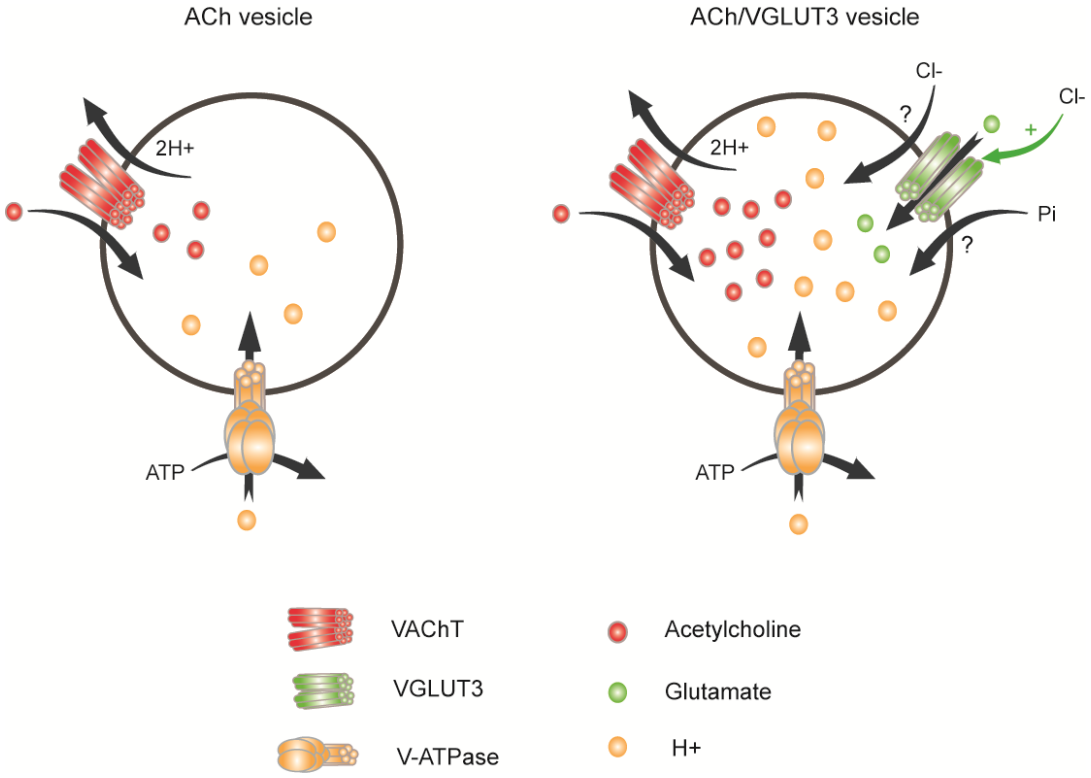

Neurotransmitter vesicular uptake is driven by an electrochemical gradient of protons (μH^+) across the membrane, which is established by the vacuolar type proton ATPase (V-ATPase, see the Figure) [103]. Vesicular packaging of cationic transmitters such as ACh and DA through the vesicular ACh transporter (VAChT, indicated in red in the Figure) and the vesicular monoamine transporter (VMAT2, not shown), respectively, largely depends on the pH gradient across the vesicular membrane (ΔpH). By contrast, vesicular glutamate transporter (VGLUT) function is largely driven by the vesicular transmembrane potential ($\Delta\Psi$) component of the proton gradient [98]. GABA and glycine accumulation by VIAAT depends on both ΔpH and $\Delta\Psi$ [98].

The kinetic properties of VMAT2 and VAChT are such that to accumulate one molecule of monoamine, 2 protons are extruded from the vesicle (see the Figure, left part). This has the consequence that VMAT2 and VAChT rapidly dissipate the ΔpH. Studies using the pH sensitive dye acridine orange have shown that glutamate and chloride acidify synaptic vesicles through

distinct and additive mechanisms [3, 80, 104]. It can thus be proposed that the presence of a VGLUT results in more acidified vesicles, and this enables VMAT2 and VAChT to accumulate higher amounts of their respective neurotransmitter in these vesicles [79]. Interestingly, despite its partial dependence on ΔpH, vesicular accumulation of GABA by VIAAT is also accelerated by glutamate [56]. The VGLUT-dependent increased vesicular accumulation of 5-HT, ACh, DA or GABA is known as vesicular synergy.

We suggest that vesicular synergy is fulfilled by glutamate itself. However, a possible role for other anions putatively transported by VGLUTs may be involved: Cl^- or Pi (See **Boxes 2 and 3**). In addition, low concentrations of Cl^- could have an indirect effect on vesicular synergy through its allosteric regulation of VGLUTs.

GLOSSARY

ASYMMETRICAL SYNAPSES: asymmetric synapses (or Gray type I synapses) contain predominantly round or spherical small synaptic vesicles and are characterized by a thickened postsynaptic density. These synapses are believed to be excitatory.

AUTAPSE: a synaptic contact established by a neuron onto its own dendrites or cell body.

CHOLINE-ACETYLTRANSFERASE (ChAT): the enzyme that catalyzes the synthesis of acetylcholine from Acetyl-CoA and choline. One isoform of *Chat* has been identified; it is a specific marker of cholinergic neurons.

CONDITIONED PLACE PREFERENCE TEST: a behavioral test commonly used with rodents, in which drug administration is paired with specific environmental cues. On the test day, the proportion of time spent in the chamber previously associated with the drug provides an estimate of the positive subjective properties of the drug, as well as of its addictive potential.

COTRANSMISSION: occurs when one, two or more neurotransmitters are present and released from the same terminals.

COTRANSMITTERS: refers to one, two or more neurotransmitters that are produced and released by a given neuron.

DOPAMINE TRANSPORTER (DAT): a plasma membrane protein from the family of Na^+/Cl^- -dependent transporters. It efficiently takes dopamine up from the extracellular space into neurons (affinity 10^{-7} M), using energy based on the Na^+ gradient generated by the Na^+/K^+ ATPase.

MASS CULTURES: term used to refer to primary neuron cultures that contain a large number of neurons.

MICROCULTURE: a primary culture system that allows single-neuron cultures by growing neurons on micro-droplets of growth substrate.

MINIATURE SYNAPTIC CURRENTS: synaptic currents which are due to the simultaneous activation of ionotropic receptors following the release of a quantum of neurotransmitter. A mixed miniature synaptic current is possible if two different types of neurotransmitters are present in a given synaptic vesicle and the corresponding receptors are present postsynaptically.

NON-SYNAPTIC AXON TERMINALS: axon terminals (varicosities) that display no morphologically identifiable synaptic membrane specialization (junctional complex). Also referred to as asynaptic terminals or free nerve endings.

OPTOGENETICS: use of genetically-encoded light-activated proteins (e.g. ion channels) to control functional parameters (e.g. membrane potential) of targeted neuronal populations.

RENSHAW CELLS (RC): these GABAergic interneurons are found in the ventral horn of the spinal cord. They form and receive excitatory recurrent collaterals from and send inhibitory synapses on spinal motoneurons.

STIMULATED EMISSION DEPLETION (STED) MICROSCOPY: a high resolution fluorescence microscopy technique that takes advantage of de-excitation of fluorescent dyes to partly overcomes the resolution limit imposed by diffraction.

TH-GFP TRANSGENIC MICE: a transgenic mouse line in which the expression of the fluorescent protein: enhanced Green Fluorescent Protein (EGFP) is driven in catecholaminergic neurons by the tyrosine hydroxylase promoter.

TOTAL INTERNAL REFLECTION FLUORESCENCE (TIRF) MICROSCOPY: a high resolution fluorescence microscopy technique that takes advantage of a laser-induced evanescent wave of fluorescence emission very close to the interface of two media that have different refractive indices.

TRYPTOPHAN HYDROXYLASE (TPH1, TPH2)**:** the rate-limiting enzyme for the biosynthesis of serotonin (5-HT). TPH converts tryptophan to 5-hydroxytryptophan. Two *tph* genes have been identified in mammal: *tph1* is expressed in the periphery and *tph2* in raphe nuclei.

TYROSINE HYDROXYLASE (TH): converts tyrosine to dihydroxyphenylalanine (DOPA). This reaction is the rate-limiting step in the biosynthesis of catecholamines (dopamine, norepinephrine, epinephrine).

VESICULAR ACETYLCHOLINE TRANSPORTER (VAChT): a synaptic vesicle protein mediating the accumulation of acetylcholine into secretory vesicles. VAChT use as driving force the proton gradient generated by the V-type H^+-ATPase.

VESICULAR INHIBITORY AMINO ACID TRANSPORTER (VIAAT, also named VGAT): a proton-dependent vesicular transporter that accumulates inhibitory transmitters GABA and glycine into synaptic vesicles.

VESICULAR MONOAMINE TRANSPORTER (VMAT1, VMAT2): synaptic vesicle proteins that translocate monoamines (dopamine, noradrenaline, 5-HT and histamine) from the cytoplasm into vesicles. The driving force is the proton gradient generated by the vacuolar type proton ATPase (V-type H^+-ATPase). Two isoforms have been cloned, *Vmat1* in the periphery and *Vmat2* in the CNS. VMATs belong to a large family of sugar transporters that also includes the vesicular acetylcholine transporter (VAChT).

ACKNOWLEDGEMENTS

Research in the El Mestikawy lab was supported by grants from Institut National de la Santé et de la Recherche Médicale (INSERM), Agence Nationale pour la Recherche (ANR), Centre National de la Recherche Scientifique (CNRS), Université Pierre et Marie Curie (UPMC Paris 6), Canadian Research chair (CRC), Douglas Mental Health University Institute, Canadian Foundation for Innovation (CFI), Canadian Institutes of Health Research (grant 977-ALZ-106889 CIHR). Research in the Mackenzie lab was supported by the Swedish Research Council, the Swedish Brain Foundation, the Åhlén and Wiberg Foundations, the National Board of Health and Welfare and Uppsala University. Research in the Descarries lab was supported by grant NRF-3544 from the Canadian Institutes of Health Research (CIHR). Research in the Trudeau lab was also supported by grants from the CIHR, the National Alliance for Research on Schizophrenia and Depression (NARSAD), Neuroscience Canada, and the Natural Sciences and Engineering Research Council (NSERC) of Canada. Trudeau and Mackenzie share a grant from The Swedish Foundation for International Cooperation in Research and Higher Education (STINT). Trudeau and Descarries also benefit from an infrastructure grant of the Fonds de la Recherche en Santé du Québec (FRSQ) to the Groupe de Recherche sur le Système Nerveux Central de l'Université de Montréal. The authors thank Dr. Bénédicte Amilhon for her help in the design of Figure 2, Noémie Bérubé-Carrière for her help in the preparation of Table 1 and Dr. Bruno Gastier for fruitful discussions.

FIGURE LEGENDS

Figure 1- Distribution of vesicular glutamate transporters in the brain

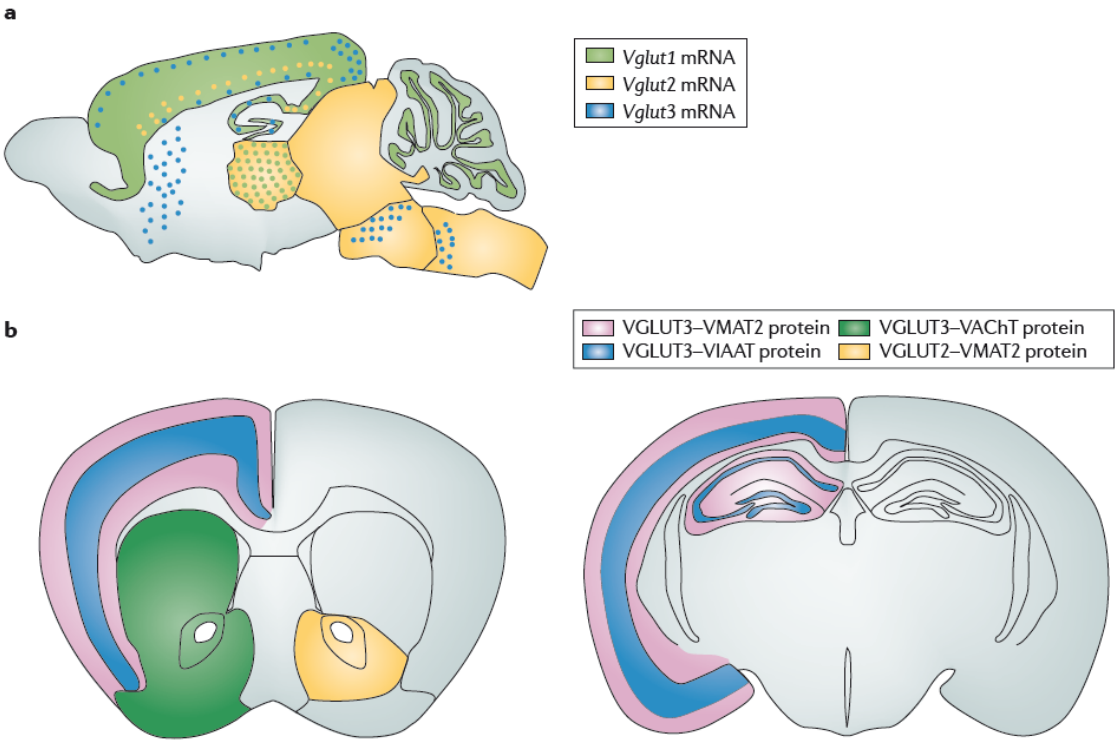

A. Schematic representation in a sagittal rat brain section of the anatomical distribution of mRNAs transcribed from the genes encoding the three VGLUTs. *Vglut1* (yellow) is found mostly in cerebral cortex and hippocampus, and *Vglut2* (orange) in subcortical structures including the thalamus and the brain stem. *Vglut3* (in blue) has a more restricted distribution in 5-HT neurons of the midbrain raphe nuclei, ACh neurons of the striatum and basal forebrain, and a subset of GABA neurons in cerebral cortex and hippocampus.

B. Schematic representation in coronal rat brain sections of the anatomical regions where VGLUT2 or VGLUT3 protein have been shown to be present in axon terminals containing DA (yellow), 5-HT (purple), ACh (green) or GABA (blue). Vesicular monoamine transporter 2 (VMAT2), vesicular ACh transporter (VAChT) and vesicular inhibitory amino acid transporter

(VIAAT) may also be used to visualize DA and 5-HT, ACh and GABA axon terminals, respectively. Vesicular synergy may theoretically occur in all brain regions indicated.

Figure 2- Heterogeneity of terminals co-expressing VGLUTs and other vesicular neurotransmitter carriers

Schematic representation of the possible modes of cotransmission in DA (A), 5-HT (B) and ACh neurons (C).

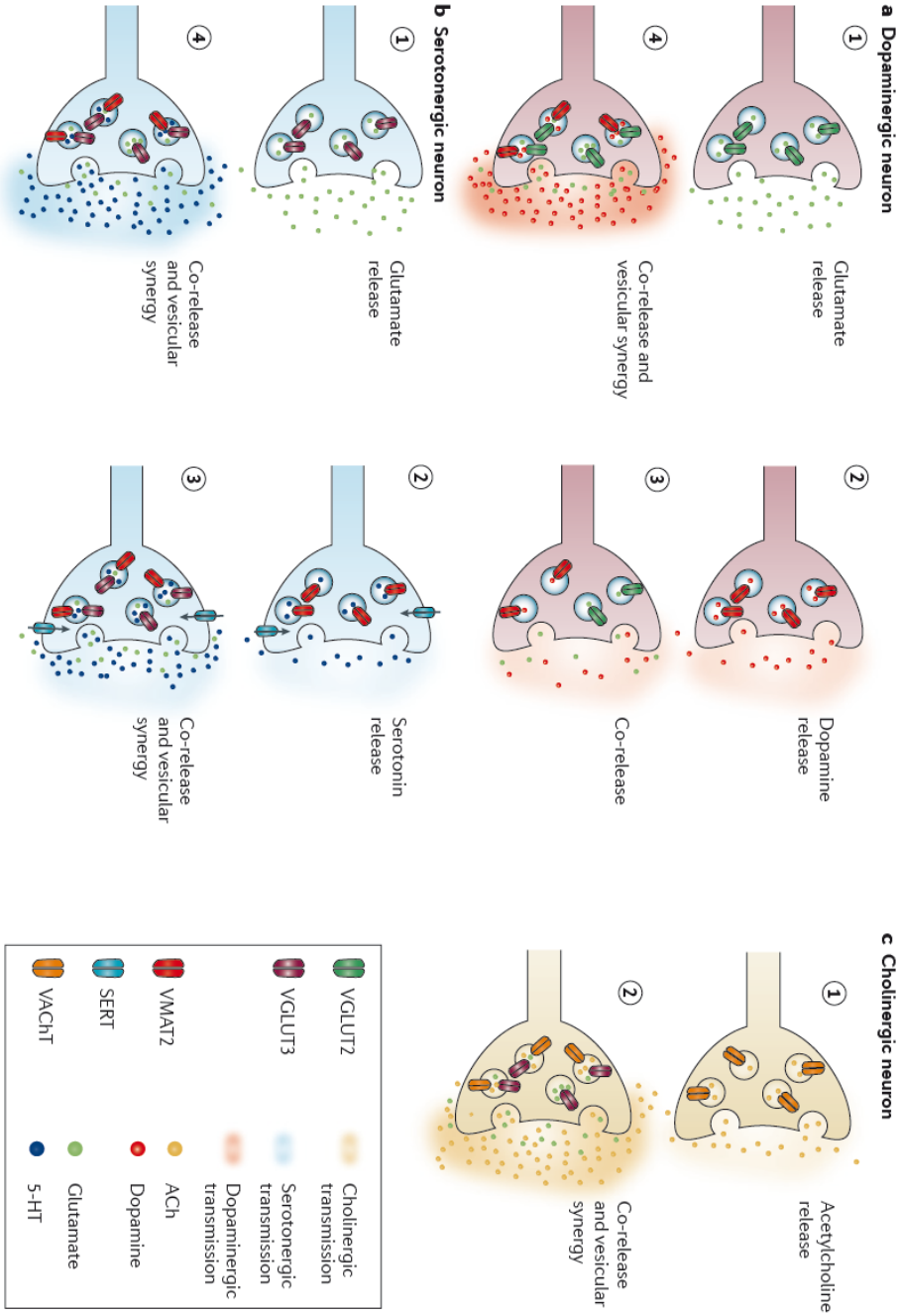

A. For DA neurons, [1] represents terminals that contain only VGLUT2 and that only release glutamate and; [2] represents terminals expressing VMAT2 alone; [3] represents terminals with both types of vesicular transporter, expressed in separate pools of synaptic vesicles; [4] represents terminals with synaptic vesicles that contain both VMAT2 and VGLUT2. We hypothesize that vesicular synergy only occurs at type 4 terminals, leading to enhanced extracellular accumulation of DA following its exocytotic release.

B. For 5-HT neurons, [1] represents terminals that contain only VGLUT3 and that only release glutamate; [2] represents terminals expressing VMAT2 and SERT; [3] represents terminals with synaptic vesicles that contain both VMAT2 and VGLUT3, in addition to the plasma membrane transporter SERT. Finally, [4] represents terminals with synaptic vesicles that contain both VMAT2 and VGLUT3, but without a plasma membrane transporter. We hypothesize that vesicular synergy only occurs at types 3 and 4, and that the absence of SERT leads to further enhancement of extracellular 5-HT following its exocytotic release**.**

C. For ACh neurons, [1] represents terminals expressing VAChT alone and [2] represents terminals with synaptic vesicles that contain both VAChT and VGLUT3. We hypothesize that vesicular synergy only occurs at type 2 terminals, leading to enhanced extracellular accumulation of ACh following its exocytotic release.

Thus, the various combinations of vesicular and plasma membrane transporters could determine the strength of DA, 5-HT and ACh neurotransmission.

Figure modified from Amilhon, B. et al., VGLUT3 (vesicular glutamate transporter type 3) contribution to the regulation of serotonergic transmission and anxiety. J Neurosci ***30*** *(6), 2198 (2010) (original figure 8).*

Table 1. Anatomical distribution of transmitter-defined neurons containing a VGLUT in CNS

Neuronal type	mRNA expression	Protein localization	
		Cell bodies	Terminals
Vglut1/VGLUT1			
Acetylcholine	Spinal cord motor neurons[45]		Nucleus interpeduncularis[49]
GABA		Retina[52]	Cerebral cortex[54], hippocampus[56], cerebellar cortex[35,56], retina[52]
Vglut2/VGLUT2			
Noradrenaline	Medulla A1, A2 cell groups[26], area prostrema[26]		
Adrenaline	Medulla C1 cell group[26,27], medulla C2, C3 cell group[26]		
Dopamine	Medulla A9, A10 cell groups[29–31,33,34], medulla A11 cell group[30]		Nucleus accumbens[33–35], neostriatum[33–35]
Acetylcholine	Spinal cord motor neurons[45,47]		Spinal cord[47]
GABA	AVPV[57]		rPOA[57], hippocampus[53,55,56]
Vglut3/VGLUT3			
Serotonin	DRN, MRN[18,36]	DRN[17,22,23,37,39,40], MRN[17,23,37,39,40]	Cerebral cortex[37,38,40], hippocampus[21,37,40,42], olfactory bulb[40] amygdala[40], VTA[43], supra-ependymal plexus[37], spinal cord (IML)[44]
Acetylcholine	Striatum[17,18], basal forebrain[50]	Striatum[16,51], basal forebrain[50]	Striatum[17,18,51], amygdala[50]
GABA	Hippocampus[45]	Cerebral cortex[38], hippocampus[16,21], Purkinje cells[58], nucleus of the trapezoid body[59]	Cerebral cortex[38], hippocampus[20,51], Purkinje cell layer[58], superior olive[59]

Data mostly from rat or mouse. Transmitter identity of CNS neurons defined by dual labeling of *Vglut* mRNA or VGLUT protein together with mRNA or protein for transmitter, biosynthetic enzyme, plasma membrane transporter or specific vesicular transporter. Abbreviations: AVPV, antero-ventral periventricular nucleus; DRN, dorsal raphe nucleus; IML, intermediolateral cell column; MRN, median raphe nucleus; rPOA, rostral preoptic area; VTA, ventral tegmental area.

REFERENCES

1. Ni, B., Rosteck, P.R., Jr., Nadi, N.S. & Paul, S.M. Cloning and expression of a cDNA encoding a brain-specific Na(+)-dependent inorganic phosphate cotransporter. *Proc Natl Acad Sci U S A* **91**, 5607-11 (1994).
2. Bellocchio, E.E., Reimer, R.J., Fremeau, R.T., Jr. & Edwards, R.H. Uptake of glutamate into synaptic vesicles by an inorganic phosphate transporter. *Science* **289**, 957-60 (2000).
3. Takamori, S., Rhee, J.S., Rosenmund, C. & Jahn, R. Identification of a vesicular glutamate transporter that defines a glutamatergic phenotype in neurons. *Nature* **407**, 189-94 (2000).
4. Disbrow, J.K., Gershten, M.J. & Ruth, J.A. Uptake of L-[3H] glutamic acid by crude and purified synaptic vesicles from rat brain. *Biochem Biophys Res Commun* **108**, 1221-7 (1982).
5. Naito, S. & Ueda, T. Characterization of glutamate uptake into synaptic vesicles. *J Neurochem* **44**, 99-109 (1985).
6. Ni, B., Wu, X., Yan, G.M., Wang, J. & Paul, S.M. Regional expression and cellular localization of the Na(+)-dependent inorganic phosphate cotransporter of rat brain. *J Neurosci* **15**, 5789-99. (1995).
7. Aihara, Y. et al. Molecular cloning of a novel brain-type Na(+)-dependent inorganic phosphate cotransporter. *J Neurochem* **74**, 2622-5. (2000).
8. Hisano, S. et al. Regional expression of a gene encoding a neuron-specific Na(+)-dependent inorganic phosphate cotransporter (DNPI) in the rat forebrain. *Brain Res Mol Brain Res* **83**, 34-43 (2000).
9. Bai, L., Xu, H., Collins, J.F. & Ghishan, F.K. Molecular and functional analysis of a novel neuronal vesicular glutamate transporter. *J Biol Chem* **276**, 36764-9 (2001).
10. Fremeau, R.T., Jr. et al. The expression of vesicular glutamate transporters defines two classes of excitatory synapse. *Neuron* **31**, 247-60 (2001).
11. Herzog, E. et al. The existence of a second vesicular glutamate transporter specifies subpopulations of glutamatergic neurons. *J Neurosci* **21**, RC181 (2001).

12. Takamori, S., Rhee, J.S., Rosenmund, C. & Jahn, R. Identification of differentiation-associated brain-specific phosphate transporter as a second vesicular glutamate transporter (VGLUT2). *J Neurosci* **21**, RC182 (2001).
13. Varoqui, H., Schafer, M.K., Zhu, H., Weihe, E. & Erickson, J.D. Identification of the differentiation-associated Na+/PI transporter as a novel vesicular glutamate transporter expressed in a distinct set of glutamatergic synapses. *J Neurosci* **22**, 142-55 (2002).
14. Bellocchio, E.E. et al. The localization of the brain-specific inorganic phosphate transporter suggests a specific presynaptic role in glutamatergic transmission. *J Neurosci* **18**, 8648-59. (1998).
15. Daniels, R.W. et al. A single vesicular glutamate transporter is sufficient to fill a synaptic vesicle. *Neuron* **49**, 11-6 (2006).
16. Fremeau, R.T., Jr. et al. The identification of vesicular glutamate transporter 3 suggests novel modes of signaling by glutamate. *Proc Natl Acad Sci U S A* **99**, 14488-93 (2002).
17. Gras, C. et al. A third vesicular glutamate transporter expressed by cholinergic and serotoninergic neurons. *J Neurosci* **22**, 5442-51 (2002).
18. Schafer, M.K., Varoqui, H., Defamie, N., Weihe, E. & Erickson, J.D. Molecular cloning and functional identification of mouse vesicular glutamate transporter 3 and its expression in subsets of novel excitatory neurons. *J Biol Chem* **277**, 50734-48 (2002).
19. Takamori, S., Malherbe, P., Broger, C. & Jahn, R. Molecular cloning and functional characterization of human vesicular glutamate transporter 3. *EMBO Rep* **3**, 798-803 (2002).
20. Herzog, E. et al. Localization of VGLUT3, the vesicular glutamate transporter type 3, in the rat brain. *Neuroscience* **123**, 983-1002. (2004).
21. Somogyi, J. et al. GABAergic basket cells expressing cholecystokinin contain vesicular glutamate transporter type 3 (VGLUT3) in their synaptic terminals in hippocampus and isocortex of the rat. *Eur J Neurosci* **19**, 552-69 (2004).
22. Commons, K.G. Locally collateralizing glutamate neurons in the dorsal raphe nucleus responsive to substance P contain vesicular glutamate transporter 3 (VGLUT3). *J Chem Neuroanat* **38**, 273-81 (2009).

23. Jackson, J., Bland, B.H. & Antle, M.C. Nonserotonergic projection neurons in the midbrain raphe nuclei contain the vesicular glutamate transporter VGLUT3. *Synapse* **63**, 31-41 (2009).
24. Ruel, J. et al. Impairment of SLC17A8 encoding vesicular glutamate transporter-3, VGLUT3, underlies nonsyndromic deafness DFNA25 and inner hair cell dysfunction in null mice. *Am J Hum Genet* **83**, 278-92 (2008).
25. Seal, R.P. et al. Sensorineural deafness and seizures in mice lacking vesicular glutamate transporter 3. *Neuron* **57**, 263-75 (2008).
26. Stornetta, R.L., Sevigny, C.P. & Guyenet, P.G. Vesicular glutamate transporter DNPI/VGLUT2 mRNA is present in C1 and several other groups of brainstem catecholaminergic neurons. *J Comp Neurol* **444**, 191-206 (2002).
27. Stornetta, R.L., Sevigny, C.P., Schreihofer, A.M., Rosin, D.L. & Guyenet, P.G. Vesicular glutamate transporter DNPI/VGLUT2 is expressed by both C1 adrenergic and nonaminergic presympathetic vasomotor neurons of the rat medulla. *J Comp Neurol* **444**, 207-20 (2002).
28. Dal Bo, G. et al. Dopamine neurons in culture express VGLUT2 explaining their capacity to release glutamate at synapses in addition to dopamine. *J Neurochem* **88**, 1398-405 (2004).
29. Mendez, J.A. et al. Developmental and target-dependent regulation of vesicular glutamate transporter expression by dopamine neurons. *J Neurosci* **28**, 6309-18 (2008).
30. Kawano, M. et al. Particular subpopulations of midbrain and hypothalamic dopamine neurons express vesicular glutamate transporter 2 in the rat brain. *J Comp Neurol* **498**, 581-92 (2006).
31. Yamaguchi, T., Sheen, W. & Morales, M. Glutamatergic neurons are present in the rat ventral tegmental area. *Eur J Neurosci* **25**, 106-18 (2007).
32. Yamaguchi, T. et al. Differential distribution of the two subtypes of glutamatergic neurons within the midbrain dopamine system *Neuroscience Meeting Planner, San Diego, CA, Society for Neuroscience* **Program #366.3**, Online (2010).
33. Dal Bo, G. et al. Enhanced glutamatergic phenotype of mesencephalic dopamine neurons after neonatal 6-hydroxydopamine lesion. *Neuroscience* **156**, 59-70 (2008).

34. Bérubé-Carrière, N. et al. The dual dopamine-glutamate phenotype of growing mesencephalic neurons regresses in mature rat brain. *J Comp Neurol* **517**, 873-91 (2009).
35. Descarries, L. et al. Glutamate in dopamine neurons: synaptic versus diffuse transmission. *Brain Res Rev* **58**, 290-302 (2008).
36. Hioki, H. et al. Vesicular glutamate transporter 3-expressing nonserotonergic projection neurons constitute a subregion in the rat midbrain raphe nuclei. *J Comp Neurol* **518**, 668-86 (2010).
37. Amilhon, B. et al. VGLUT3 (vesicular glutamate transporter type 3) contribution to the regulation of serotonergic transmission and anxiety. *J Neurosci* **30**, 2198-210 (2010).
38. Hioki, H. et al. Chemically specific circuit composed of vesicular glutamate transporter 3- and preprotachykinin B-producing interneurons in the rat neocortex. *Cereb Cortex* **14**, 1266-75 (2004).
39. Mintz, E.M. & Scott, T.J. Colocalization of serotonin and vesicular glutamate transporter 3-like immunoreactivity in the midbrain raphe of Syrian hamsters (Mesocricetus auratus). *Neurosci Lett* **394**, 97-100 (2006).
40. Shutoh, F., Ina, A., Yoshida, S., Konno, J. & Hisano, S. Two distinct subtypes of serotonergic fibers classified by co-expression with vesicular glutamate transporter 3 in rat forebrain. *Neurosci Lett* **432**, 132-6 (2008).
41. Hornung, J.P. The human raphe nuclei and the serotonergic system. *J Chem Neuroanat* **26**, 331-43 (2003).
42. Varga, V. et al. Fast synaptic subcortical control of hippocampal circuits. *Science* **326**, 449-53 (2009).
43. Zhang, S. & Morales, M. Serotonergic axons terminals with glutamatergic phenotype make synapses on both dopaminergic and nondopaminergic neurons in the ventral tegmental area. . *Neuroscience Meeting Planner, San Diego CA, Society for Neuroscience* **Program #448.6**, Online (2010).
44. Oliveira, A.L. et al. Cellular localization of three vesicular glutamate transporter mRNAs and proteins in rat spinal cord and dorsal root ganglia. *Synapse* **50**, 117-29 (2003).
45. Herzog, E. et al. Expression of vesicular glutamate transporters, VGLUT1 and VGLUT2, in cholinergic spinal motoneurons. *Eur J Neurosci* **20**, 1752-60 (2004).

46. Kraus, T., Neuhuber, W.L. & Raab, M. Vesicular glutamate transporter 1 immunoreactivity in motor endplates of striated esophageal but not skeletal muscles in the mouse. *Neurosci Lett* **360**, 53-6 (2004).
47. Nishimaru, H., Restrepo, C.E., Ryge, J., Yanagawa, Y. & Kiehn, O. Mammalian motor neurons corelease glutamate and acetylcholine at central synapses. *Proc Natl Acad Sci U S A* **102**, 5245-9 (2005).
48. Gezelius, H., Wallen-Mackenzie, A., Enjin, A., Lagerstrom, M. & Kullander, K. Role of glutamate in locomotor rhythm generating neuronal circuitry. *J Physiol Paris* **100**, 297-303 (2006).
49. Ren, J. et al. Habenula "cholinergic" neurons corelease glutamate and acetylcholine and activate postsynaptic neurons via distinct transmission modes. *Neuron* **69**, 445-452 (2011).
50. Nickerson Poulin, A., Guerci, A., El Mestikawy, S. & Semba, K. Vesicular glutamate transporter 3 immunoreactivity is present in cholinergic basal forebrain neurons projecting to the basolateral amygdala in rat. *J Comp Neurol* **498**, 690-711 (2006).
51. Boulland, J.L. et al. Expression of the vesicular glutamate transporters during development indicates the widespread corelease of multiple neurotransmitters. *J Comp Neurol* **480**, 264-80 (2004).
52. Kao, Y.H. et al. Evidence that certain retinal bipolar cells use both glutamate and GABA. *J Comp Neurol* **478**, 207-18 (2004).
53. Boulland, J.L. et al. Vesicular glutamate and GABA transporters sort to distinct sets of vesicles in a population of presynaptic terminals. *Cereb Cortex* **19**, 241-8 (2009).
54. Fattorini, G. et al. VGLUT1 and VGAT are sorted to the same population of synaptic vesicles in subsets of cortical axon terminals. *J Neurochem* **110**, 1538-46 (2009).
55. Soussi, R., Zhang, N., Tahtakran, S., Houser, C.R. & Esclapez, M. Heterogeneity of the supramammillary-hippocampal pathways: evidence for a unique GABAergic neurotransmitter phenotype and regional differences. *Eur J Neurosci* **32**, 771-785 (2010).
56. Zander, J.F. et al. Synaptic and vesicular coexistence of VGLUT and VGAT in selected excitatory and inhibitory synapses. *J Neurosci* **30**, 7634-45 (2010).

57. Ottem, E.N., Godwin, J.G., Krishnan, S. & Petersen, S.L. Dual-phenotype GABA/glutamate neurons in adult preoptic area: sexual dimorphism and function. *J Neurosci* **24**, 8097-105 (2004).

58. Gras, C. et al. Developmentally regulated expression of VGLUT3 during early post-natal life. *Neuropharmacology* **49**, 901-11 (2005).

59. Gillespie, D.C., Kim, G. & Kandler, K. Inhibitory synapses in the developing auditory system are glutamatergic. *Nat Neurosci* **8**, 332-8 (2005).

60. Sulzer, D. et al. Dopamine neurons make glutamatergic synapses in vitro. *J Neurosci* **18**, 4588-4602 (1998).

61. Bourque, M.J. & Trudeau, L.E. GDNF enhances the synaptic efficacy of dopaminergic neurons in culture. *Eur J Neurosci* **12**, 3172-80 (2000).

62. Descarries, L., Watkins, K.C., Garcia, S., Bosler, O. & Doucet, G. Dual character, asynaptic and synaptic, of the dopamine innervation in adult rat neostriatum: a quantitative autoradiographic and immunocytochemical analysis. *J Comp Neurol* **375**, 167-86 (1996).

63. Tecuapetla, F. et al. Glutamatergic signaling by mesolimbic dopamine neurons in the nucleus accumbens. *J Neurosci* **30**, 7105-10 (2010).

64. Stuber, G.D., Hnasko, T.S., Britt, J.P., Edwards, R.H. & Bonci, A. Dopaminergic terminals in the nucleus accumbens but not the dorsal striatum corelease glutamate. *J Neurosci* **30**, 8229-33 (2010).

65. Hattori, T., Takada, M., Moriizumi, T. & Van der Kooy, D. Single dopaminergic nigrostriatal neurons form two chemically distinct synaptic types: possible transmitter segregation within neurons. *J Comp Neurol* **309**, 391-401 (1991).

66. Forlano, P.M. & Woolley, C.S. Quantitative analysis of pre- and postsynaptic sex differences in the nucleus accumbens. *J Comp Neurol* **518**, 1330-48 (2010).

67. Tsudzuki, T. & Tsujita, M. Isoosmotic isolation of rat brain synaptic vesicles, some of which contain tyrosine hydroxylase. *J Biochem* **136**, 239-43 (2004).

68. Fortin, G., Mendez, J.A., Bourque, M.J. & Trudeau, L.E. Dopamine neurons establish heterogeneous subtypes of axon terminals only a subset of which contain VMAT2 and VGLUT2 *Neuroscience Meeting Planner, Chicago, IL, Society for Neuroscience* **Program #815.6**, Online (2009).

69. Johnson, M.D. Synaptic glutamate release by postnatal rat serotonergic neurons in microculture. *Neuron* **12**, 433-42 (1994).
70. Martin-Ibanez, R. et al. Vesicular glutamate transporter 3 (VGLUT3) identifies spatially segregated excitatory terminals in the rat substantia nigra. *Eur J Neurosci* **23**, 1063-70 (2006).
71. Huh, C.Y., Danik, M., Manseau, F., Trudeau, L.E. & Williams, S. Chronic exposure to nerve growth factor increases acetylcholine and glutamate release from cholinergic neurons of the rat medial septum and diagonal band of Broca via mechanisms mediated by p75NTR. *J Neurosci* **28**, 1404-9 (2008).
72. Sotty, F. et al. Distinct electrophysiological properties of glutamatergic, cholinergic and GABAergic rat septohippocampal neurons: novel implications for hippocampal rhythmicity. *J Physiol* **551**, 927-43 (2003).
73. Descarries, L., Gisiger, V. & Steriade, M. Diffuse transmission by acetylcholine in the CNS. *Prog Neurobiol* **53**, 603-25 (1997).
74. Mechawar, N., Watkins, K.C. & Descarries, L. Ultrastructural features of the acetylcholine innervation in the developing parietal cortex of rat. *J Comp Neurol* **443**, 250-8 (2002).
75. Gutierrez, R. et al. Plasticity of the GABAergic phenotype of the "glutamatergic" granule cells of the rat dentate gyrus. *J Neurosci* **23**, 5594-8 (2003).
76. Noh, J., Seal, R.P., Garver, J.A., Edwards, R.H. & Kandler, K. Glutamate co-release at GABA/glycinergic synapses is crucial for the refinement of an inhibitory map. *Nat Neurosci* **13**, 232-8 (2010).
77. Chery, N. & de Koninck, Y. Junctional versus extrajunctional glycine and GABA(A) receptor-mediated IPSCs in identified lamina I neurons of the adult rat spinal cord. *J Neurosci* **19**, 7342-55 (1999).
78. Herzog, E., Takamori, S., Jahn, R., Brose, N. & Wojcik, S.M. Synaptic and vesicular co-localization of the glutamate transporters VGLUT1 and VGLUT2 in the mouse hippocampus. *J Neurochem* **99**, 1011-8 (2006).
79. Gras, C. et al. The vesicular glutamate transporter VGLUT3 synergizes striatal acetylcholine tone. *Nat Neurosci* **11**, 292-300 (2008).

80. Hnasko, T.S. et al. Vesicular glutamate transport promotes dopamine storage and glutamate corelease in vivo. *Neuron* **65**, 643-656 (2010).
81. Santos, M.S., Li, H. & Voglmaier, S.M. Synaptic vesicle protein trafficking at the glutamate synapse. *Neuroscience* **158**, 189-203 (2009).
82. Fei, H., Grygoruk, A., Brooks, E.S., Chen, A. & Krantz, D.E. Trafficking of vesicular neurotransmitter transporters. *Traffic* **9**, 1425-36 (2008).
83. Grygoruk, A. et al. A tyrosine-based motif localizes a Drosophila vesicular transporter to synaptic vesicles in vivo. *J Biol Chem* **285**, 6867-78 (2010).
84. Voglmaier, S.M. & Edwards, R.H. Do different endocytic pathways make different synaptic vesicles? *Curr Opin Neurobiol* **17**, 374-80 (2007).
85. Mutch, S.A. et al. Protein quantification at the single vesicle level reveals that a subset of synaptic vesicle proteins are trafficked with high precision. *J Neurosci* **31**, 1461-70.
86. Ikemoto, S. Dopamine reward circuitry: two projection systems from the ventral midbrain to the nucleus accumbens-olfactory tubercle complex. *Brain Res Rev* **56**, 27-78 (2007).
87. Chuhma, N. et al. Dopamine neurons mediate a fast excitatory signal via their glutamatergic synapses. *J Neurosci* **24**, 972-81 (2004).
88. Birgner, C. et al. VGLUT2 in dopamine neurons is required for psychostimulant-induced behavioral activation. *Proc Natl Acad Sci U S A* **107**, 389-94 (2010).
89. Trudeau, L.E. & Gutierrez, R. On cotransmission & neurotransmitter phenotype plasticity. *Mol Interv* **7**, 138-46 (2007).
90. Moutsimilli, L. et al. Selective cortical VGLUT1 increase as a marker for antidepressant activity. *Neuropharmacology* **49**, 890-900 (2005).
91. Moutsimilli, L. et al. Antipsychotics increase vesicular glutamate transporter 2 (VGLUT2) expression in thalamolimbic pathways. *Neuropharmacology* **54**, 497-508 (2008).
92. Strata, P. & Harvey, R. Dale's principle. *Brain Res Bull* **50**, 349-50 (1999).
93. Eccles, J.C., Fatt, P. & Koketsu, K. Cholinergic and inhibitory synapses in a pathway from motor-axon collaterals to motoneurones. *J Physiol* **126**, 524-62 (1954).
94. Dale, H.H. Pharmacology and nerve endings. *Proc Roy Soc Med* **28**, 319-330 (1934).
95. Xie, X.S., Stone, D.K. & Racker, E. Determinants of clathrin-coated vesicle acidification. *J Biol Chem* **258**, 14834-8 (1983).

96. Hartinger, J. & Jahn, R. An anion binding site that regulates the glutamate transporter of synaptic vesicles. *J Biol Chem* **268**, 23122-7 (1993).
97. Juge, N. et al. Metabolic control of vesicular glutamate transport and release. *Neuron* **68**, 99-112 (2010).
98. Edwards, R.H. The neurotransmitter cycle and quantal size. *Neuron* **55**, 835-58 (2007).
99. Juge, N., Yoshida, Y., Yatsushiro, S., Omote, H. & Moriyama, Y. Vesicular glutamate transporter contains two independent transport machineries. *J Biol Chem* **281**, 39499-506 (2006).
100. Takamori, S. et al. Molecular anatomy of a trafficking organelle. *Cell* **127**, 831-46 (2006).
101. Schenck, S., Wojcik, S.M., Brose, N. & Takamori, S. A chloride conductance in VGLUT1 underlies maximal glutamate loading into synaptic vesicles. *Nat Neurosci* **12**, 156-62 (2009).
102. Almqvist, J., Huang, Y., Laaksonen, A., Wang, D.N. & Hovmoller, S. Docking and homology modeling explain inhibition of the human vesicular glutamate transporters. *Protein Sci* **16**, 1819-29 (2007).
103. Moriyama, Y. & Yamamoto, A. Glutamatergic chemical transmission: look! Here, there, and anywhere. *J Biochem* **135**, 155-63 (2004).
104. Maycox, P.R., Deckwerth, T., Hell, J.W. & Jahn, R. Glutamate uptake by brain synaptic vesicles. Energy dependence of transport and functional reconstitution in proteoliposomes. *J Biol Chem* **263**, 15423-8 (1988)

Chapitre 3 : Discussion

Le but de cette étude était de caractériser ainsi que d'étudier le rôle physiologique de la capacité des neurones dopaminergiques à libérer le glutamate comme co-transmetteur. Dans un premier temps, nous avons été en mesure d'élucider certains rôles physiologiques *in vitro* et *in vivo* de l'expression de VGLUT2 dans une sous-population de neurones dopaminergiques, identifiant notamment un rôle développemental. D'autre part, les résultats montrent qu'une interaction avec les neurones du striatum régule le co-phenotype glutamatergique et contribue à une ségrégation des sites de libération de la dopamine et du glutamate.

Rôles physiologiques de l'expression de VGLUT2 *in vitro*

La capacité d'une sous-population de neurones dopaminergiques de libérer du glutamate est une découverte relativement nouvelle et ainsi peu de travaux ont tenté d'élucider le rôle physiologique de ce phénomène. Toutefois, certaines hypothèses ont été proposées. Des études récentes ont par exemple suggéré que l'expression de VGLUT2 puisse avoir un rôle dans la croissance et la survie d'une sous-population de neurones dopaminergiques (Dal Bo et al., 2008; Mendez et al., 2008; Schmitz et al., 2009).

Afin de vérifier cette hypothèse, nous avons analysé l'expression de VGLUT2 dans les neurones dopaminergiques durant le développement chez la souris. En utilisant la technique de RT-CPR sur cellule unique à partir de cellules fraîchement dissociées du mésencéphale provenant de souris TH-GFP, nous avons quantifié le pourcentage de neurones exprimant l'ARNm de TH qui expriment aussi l'ARNm de VGLUT2. Nous avons ainsi observé qu'environ 50% des neurones TH expriment VGLUT2 durant la période embryonnaire. Cette expression diminue graduellement durant la période postnatale (14% à P14) et revient à un pourcentage plus élevé chez la souris adulte (50%). L'expression très précoce de VGLUT2 dans les neurones dopaminergiques et la variation de la proportion de neurones dopaminergiques exprimant l'ARNm de VGLUT2 suggère que le phénotype glutamatergique soit impliqué dans le

développement de ces neurones. Ces données confirment également des observations similaires chez le rat et la souris (Mendez et al., 2008; Bérubé-Carrière et al., 2009). Néanmoins, le pourcentage élevé de neurones dopaminergiques exprimant le transporteur VGLUT2 ne concorde pas avec des données récentes (15% à P45) chez la souris adulte (Mendez et al., 2008). Le fait que les populations cellulaires du CLi, RLi et IFN, structures où la majorité des neurones dopaminergiques expriment VGLUT2 (parfois jusqu'à 80%), n'ont pas été inclues dans la préparation de culture de l'étude de Mendez et collaborateurs pourrait potentiellement expliquer la différence (Kawano et al., 2006; Yamaguchi et al., 2011; Li et al., 2013).

De plus, il a été démontré que le pourcentage de neurones dopaminergiques au double phénotype augmente suite à une neurodégénérescence induite par une neurotoxine *in vivo*, suggérant la possibilité d'un rôle neuroprotecteur (Dal Bo et al., 2008). Puis, une autre étude a suggéré que l'application d'agonistes AMPA et NMDA sur une préparation cellulaire de neurones dopaminergiques *in vitro* module la croissance des dendrites et des axones des neurones dopaminergiques (Schmitz et al., 2009). Afin de confirmer l'hypothèse selon laquelle la co-libération de glutamate serait en mesure d'augmenter la croissance et la survie des neurones dopaminergiques en développement, nous avons généré une souris transgénique possédant une délétion constitutive embryonnaire spécifique de VGLUT2 dans les neurones dopaminergiques (cKO). Ainsi, à partir de jeunes cultures mésencéphaliques provenant de souris cKO, nous avons été en mesure de démontrer une diminution *in vitro* de la longueur axonale (20%), du diamètre du soma (10%) des neurones dopaminergiques ainsi que de la densité du nombre de neurones dopaminergiques (25%) confirmant notre hypothèse.

Ainsi, ces observations suggèrent que la libération de glutamate aux cônes axonaux des neurones en croissance accomplisse un rôle trophique. La maturation complète des neurones DAergiques dans notre système de culture est entre les jours 7-10 DIV. Ainsi, nous avons évalué si le blocage des différents récepteurs glutamatergiques des neurones DAergiques en croissance (moins de 7 DIV) ou mature (+ de 7 DIV) modulerait la survie. Nos données démontrant qu'un antagoniste des récepteurs NMDA diminue la survie de neurones dopaminergiques immatures (0-7 DIV) sans toutefois influencer la survie des neurones matures appuie l'hypothèse du rôle trophique de la libération du glutamate aux cônes de croissance. Ces données suggèrent également que l'activation du récepteur NMDA

puisse être impliquée dans l'effet trophique de la libération autocrine du glutamate aux cônes axonaux. Des études récentes démontrant que l'application d'un agoniste NMDA accélère la croissance de l'axone et que l'absence de la sous-unité NR1 du récepteur NMDA dans les neurones dopaminergiques diminue la libération de DA *in vivo* appuient également cette hypothèse (Schmitz et al., 2009). De plus, le rôle trophique du récepteur NMDA sur d'autres populations de neurones est également bien documenté depuis quelques années (Vernon et al., 2005; Hardingham and Bading, 2010). Afin de confirmer et d'observer la libération autocrine fonctionnelle du glutamate aux cônes axonaux des neurones dopaminergiques immatures, des expériences d'électrophysiologie en utilisant des cultures purifiées de neurones dopaminergiques et de «sniffer cells» (Allen, 1997) pourraient être en mesure de confirmer cette hypothèse. Finalement, afin de confirmer l'activité fonctionnelle des récepteurs NMDA aux cônes de croissance des neurones dopaminergiques, des expériences combinant l'imagerie calcique et l'application locale de glutamate répondraient également à cette question. De plus, des expériences de biologie moléculaire et de génomique *in vitro* seraient en mesure de déterminer si la délétion de VGLUT2 module certains facteurs de transcription importants pour la croissance et la survie des neurones dopaminergiques.

Il est également possible que cet effet trophique ou développemental du glutamate observé dans notre première étude soit expliqué par une action indirecte du glutamate sur la croissance et la survie des neurones dopaminergiques. Puisque nos cultures cellulaires sont tapissées d'une couche d'astrocytes, il est possible que le glutamate interagisse sur ces cellules afin de favoriser la production et la libération de facteurs neurotrophiques tels que le BDNF ou le GDNF. Il s'agit de facteurs qui sont bien documentés pour leurs rôles dans la croissance neuritique et la survie des neurones dopaminergiques (Lin et al., 1993; Bourque et Trudeau, 2000; Hartmann et al., 2001). De plus, puisque nous avons utilisé une préparation neuronale à faible densité préparée à partir du mésencéphale, une région du cerveau qui contient d'autre types de neurones, il est possible, bien que moins probable, que dans nos études, la diminution de croissance des neurones dopaminergiques observée chez les souris VGLUT2 KO ait été secondaire à une perturbation des neurones non-dopaminergiques de cette région du cerveau.

Rôles physiologiques de l'expression de VGLUT2 *in vivo*

Nos observations montrant une diminution du développement et du nombre de neurones dopaminergiques *in vitro* suggèrent une diminution du nombre de neurones dopaminergiques *in vivo* chez ces animaux préalablement à la culture cellulaire. Afin de vérifier cette hypothèse, nous avons réalisé un compte stéréologique de neurones dopaminergiques chez les souris cKO. Nous avons ainsi observé une diminution de 25% des neurones du VTA et de 20% des neurones de la SNpc. De plus, nous avons été en mesure de démontrer une baisse d'environ 30% de la densité des varicosités axonales dopaminergiques et glutamatergiques dans le striatum ventral grâce à la microscopie confocale. En somme, nos résultats suggèrent une altération du système dopaminergique *in vivo* et confirment les observations *in vitro*. Afin d'évaluer si la baisse du nombre de neurones et de l'innervation dopaminergique mène à une diminution de la libération fonctionnelle de DA, nous avons quantifié la concentration de DA extracellulaire par la technique de voltammétrie. Nous avons ainsi observé une diminution de 40% de libération de DA dans le sriatum ventral mais aucun changement dans le striatum dorsal. D'ailleurs, une autre étude a aussi confirmé ces résultats (Hnasko et al., 2010). Puisque nous n'avons pas été en mesure d'observer un changement dans la cinétique de la DA libérée et dans la quantité de DA libérée induite par un train de stimulation, il ne semble pas avoir de différence dans la recapture de la DA, la mobilisation des vésicules à l'intérieur des terminaisons ainsi que dans la régulation de l'autorécepteur D2 sur la libération de DA (Benoit-Marand et al., 2001).

Malgré une diminution du nombre de neurones dopaminergiques dans la SNpc observée lors de cette étude, la densité de l'innervation dopaminergique et la quantité de libération de DA dans le striatum dorsal ont cependant été inchangées. Ces observations pourraient potentiellement être expliquées par un mécanisme de bourgeonnement compensatoire des varicosités axonales du striatum dorsal établies par les neurones dopaminergiques de la SNpc. En effet, il est bien connu que chez les modèles animaux de la maladie de Parkinson, tels que ceux induits par une lésion au 6-OHDA, les neurones résiduels de la SNpc sont en mesure d'établir de nouvelles terminaisons dans le striatum dorsal dopaminergique (Rosenblad et al., 1997; Lee et al., 2008). Néanmoins, nos observations n'indiquent pas de changement radical dans l'organisation des fibres mésotriatales par immunohistochimie chez les souris cKO. Des études plus avancées à l'aide de

la microscopie confocale et une quantification de l'orientation des fibres axonales permettraient de répondre à cette hypothèse de bourgeonnement. Une étude récente a démontré une diminution de DA libérée induite par une dépolarisation au potassium dans le striatum dorsal chez des souris cKO pour VGLUT2 (Alsiö et al., 2011). Il est possible que cette contradiction apparente soit le résultat de la différence de technique utilisée pour stimuler les fibres axonales dopaminergique. Dans l'étude de Alsio et collaborateurs, la technique a fait appel à une dépolarisation massive et prolongée des axones et terminaisons, ainsi que des cellules striatales. Il s'agit d'une approche certainement moins physiologique que l'approche de stimulation extracellulaire locale utilisée dans notre étude. Néanmoins, le résultat obtenu par l'étude de Alsio et collaborateurs pourrait suggérer la possibilité d'une réserve de DA libérable plus faible dans les projections dopaminergiques nigro-striées chez ces souris KO, compatible avec un rôle développemental du glutamate dans ces neurones dopaminergiques. Il serait par ailleurs également possible que la perte des neurones dopaminergiques de la SNpc chez les souris cKO soit issue d'une sous-population de neurones innervant le striatum ventral (Lynd-Balta and Haber, 1994; Prensa and Parent, 2001), ce qui expliquerait l'absence de baisse de la libération de DA dans le striatum dorsal. L'observation d'une perte de 20% de la densité de neurones DAergiques dans la SNpc et l'absence de perte d'innervation DAergique dans le striatum dorsal pourrait également être expliqué par un bourgeonnement compensatoire par la sous-population de neurones DAergiques de la SNpc survivants. Finalement, les résultats obtenus en mesurant indirectement l'activité de la TH par une quantification de sa phosphorylation chez les cKO pourraient suggérer une autre explication. Nos observations d'une diminution de 40% de l'activité de l'enzyme dans la VTA mais aucun changement dans la SNpc pourraient être la cause d'une diminution spécifique de la quantité de DA libérée dans le striatum ventral. Toutefois, une étude récente n'a pas observée de différence dans l'activité de l'enzyme TH chez des souris cKO (Hnasko et al., 2010). De plus, nos résultats montrant une baisse de la densité des terminaisons dopaminergiques dans le striatum ventral restent l'explication la plus plausible de la baisse de libération de DA dans cette structure.

Nous avons également rapporté une diminution du nombre de terminaisons axonales exprimant VGLUT2 spécifiquement dans le striatum ventral. Ces résultats peuvent être expliqués par la diminution du nombre de terminaisons glutamatergiques établies par les neurones dopaminergiques du VTA projetant au striatum ventral. Des données récentes démontrant une

diminution de libération de glutamate induite par une dépolarisation au potassium du striatum ventral chez des souris cKO pour VGLUT2 est en accord avec cette hypothèse (Birgner et al., 2010). Cependant, il est également possible que ces observations reflètent une diminution de l'innervation glutamatergique provenant du thalamus, une région bien connue pour exprimer une grande densité de neurones glutamatergiques exprimant VGLUT2. Une analyse par qPCR de la quantité d'ARNm de VGLUT2 dans le thalamus des souris Ctrl et cKO permettrait de valider cette hypothèse.

D'autre part, l'analyse des fibres dopaminergiques et glutamatergiques du striatum ventral et dorsal nous a permis de démontrer que les différents marqueurs ne semblent pas être tous localisés au sein de la même population de terminaisons. En effet, nous avons remarqué une très faible co-localisation de TH et VGLUT2 chez les souris témoins. Ces observations de faible co-localisation ont également été rapportées dans d'autres études (Bérubé-Carrière et al., 2009; Forlano and Woolley, 2010). Ces données peuvent indiquer que les neurones dopaminergiques établissent des sites de libération distincts pour la DA et le glutamate *in vivo*. Une autre explication serait que les neurones dopaminergiques expriment faiblement la protéine VGLUT2 et qu'il soit ainsi difficile d'analyser une faible corrélation entre les deux marqueurs dans le striatum. En effet, une étude récente démontre que les neurones au double phénotype expriment entre cinq et dix fois moins de copies d'ARNm de VGLUT2 comparativement à TH, DAT et VMAT2 (Li et al., 2013). Il serait également possible que le niveau d'expression de TH dans certaines terminaisons soit faible, rendant difficile sa détection.

L'expression de VGLUT2 pourrait également être importante pour un autre processus physiologique des neurones dopaminergiques, le stockage vésiculaire de la DA. En effet, une étude a démontré que VGLUT2 serait en partie localisée sur certaines des mêmes vésicules exprimant VMAT2 dans le striatum du rat juvénile (Hnasko et al., 2010). La co-localisation de ces deux transporteurs permettrait d'augmenter le transport de la DA à l'intérieur de la vésicule par un processus appelé synergie vésiculaire (Gras et al., 2008; Hnasko et al., 2010). L'absence de ce processus de synergie pourrait représenter une autre explication possible de la diminution de DA libérée que nous avons observée chez les souris cKO. Cependant, une faiblesse de cette étude est le fait que les auteurs ont utilisé de la sérotonine au lieu de la DA afin de tester l'effet

du glutamate à promouvoir la synergie vésiculaire de VMAT2. De plus, des expériences démontrant l'absence de co-expression des transporteurs VMAT2 et VGLUT2 dans les vésicules purifiées de striatum d'animaux cKO tel que démontré précédemment pour VGLUT3 et VAChT manquent à cette étude (Gras et al., 2008). De plus, nos observations suggérant plutôt une complète absence de localisation de marqueurs dopaminergiques et glutamatergiques ne sont pas facilement réconciliables avec cette hypothèse. Il est peu probable que la diminution de la croissance et de survie observée dans notre étude soit le résultat d'une perte de synergie vésiculaire, puisque des données récentes suggèrent que la libération de DA par les neurones dopaminergiques n'améliore pas leur croissance et survie cellulaire (Fasano et al., 2010). Il serait également intéressant d'utiliser un KO inductible de VGLUT2 dans les neurones dopaminergiques adultes afin de distinguer entre les effets développementaux du glutamate et les effets chez le neurone adulte.

L'altération du système dopaminergique observée chez les souris cKO suggère la possibilité que les comportements qui sont sous le contrôle du système dopaminergique soient perturbés chez ces souris. Des études récentes ont suggéré en effet que la délétion de VGLUT2 dans les neurones dopaminergiques modifie l'activité locomotrice induite par l'amphétamine et la cocaïne (Birgner et al., 2010; Hnasko et al., 2010). Nos données supportent également une baisse d'activité locomotrice induite par l'amphétamine et la cocaïne chez ces souris. Néanmoins, l'effet locomoteur des deux autres doses d'amphétamine était moins prononcé chez les souris cKO. Des résultats démontrant une tendance similaire ont été rapportés dans une étude récente, bien que non significatifs Nous avons également observé que l'effet locomoteur de l'amphétamine était moins prononcé que l'effet locomoteur induit par la cocaïne. Ceci est dû principalement à la dose employée d'amphétamine (faible dose). Dans les doses plus élevées, l'augmentation de l'activité locomotrice est davantage évidente (Birgner et al., 2010). Des résultats démontrant une tendance similaire de l'effet de l'amphétamine ont été rapportés dans une étude récente De plus, nous avons observé une diminution de la coordination motrice chez les souris cKO à l'aide du test de rotarod. Cependant, une étude récente n'a pu être en mesure d'observer cette différence (Hnasko et al., 2010). Le sexe des animaux pourraient être en cause dans la variabilité des changements comportementaux observés chez ces souris, car seulement des femelles ont été utilisées dans l'étude de Hnasko et collaborateurs, alors que seulement les mâles ont été utilisés dans notre

étude. La diminution de la motricité observée chez les souris VGLUT2 cKO pourrait être le résultat de la perte d'une sous-population de neurones dopaminergiques de la SNpc. Cette possibilité est appuyée par des observations montrant que la relâche somato-dendritique de DA dans la SNpc contribuerait à la performance dans le test de rotarod (Andersson et al., 2006). L'altération de l'innervation glutamatergique du striatum doit également être considérée comme une cause potentielle de la performance diminuée des souris cKO dans le test du rotarod.

Puisque le système dopaminergique a été montré comme un facteur important impliqué dans la dépression, nous avons évalué le comportement dépressif des souris cKO à l'aide du test de nage forcée. Les souris cKO ont ainsi démontré une diminution de la performance dans ce test. L'observation d'une immobilisation plus rapide des souris cKO et aucune différence dans le temps total d'immobilisation pourrait être expliqué par une une diminution de la motivation chez les souris cKO considérant que l'expression de VGLUT2 dans les neurones dopaminergiques semble être cruciale pour les comportements motivationnels et le système de récompense (Alsiö et al., 2011). Le comportement dépressif de ces souris pourrait également être dû à une perturbation de l'interaction entre les neurones dopaminergiques et sérotoninergiques (Wong et al., 1995). Malgré les différents comportements évalués, l'étude comportementale de la délétion de VGLUT2 dans les neurones dopaminergiques chez ces souris dans notre étude reste incomplète. Il serait également intéressant d'évaluer le comportement anxieux, la mémoire spatiale et de reconnaissance de ces souris afin d'évaluer une perturbation potentielle de la voie mésocorticale (Hyman et al., 2006).

Hétérogénéité des neurones dopaminergiques

Considérant les rôles physiologiques importants du système dopaminergique, de nombreux travaux ont étudié et caractérisé les différentes populations de neurones dopaminergiques du mésencéphale. En effet, les neurones dopaminergiques de la SNpc et du VTA semblent posséder certaines propriétés biochimiques, morphologiques et électrophysiologiques distinctes associé à une grande hétérogénéité (Thompson et al., 2005; Björklund and Dunnett, 2007). Nous avons ainsi décidé dans un deuxième temps de caractériser

l'hétérogénéité des neurones dopaminergiques au double phénotype ainsi que les sites de libération du glutamate et de la dopamine.

Tout d'abord, à l'aide de la technique de RT-PCR sur cellule unique, nous avons démontré que la proportion de neurones qui expriment l'ARNm de TH et de VGLUT2 est élevée durant la période embryonnaire (47 % à E14), diminue graduellement durant le développement (33% à E16, 22% à P0, 14% à P14) et augmente par la suite vers l'âge adulte (30% à P35, et 47 % à P70). Par la suite, nous avons comparé la proportion de ces neurones entre le VTA et la SNpc. Nos résultats suggèrent que la proportion des neurones au double phénotype soit plus élevée dans le VTA que dans la SNpc, confirmant des observations similaires chez le rat (Yamaguchi et al., 2011). Ces données suggèrent donc que la plasticité phénotypique développementale des neurones dopaminergiques soit présente à la fois dans les neurones dopaminergiques de la SNpc et du VTA. Nos observations d'une plus grande proportion de neurones dopaminergiques exprimant VGLUT2 dans le VTA peuvent expliquer la baisse sélective de la libération de DA et de la densité des terminaisons VGLUT2-positives dans le striatum ventral, plutôt que dorsal, observée chez les souris cKO lors de notre première étude.

L'hypothèse que les neurones au double phénotype expriment un phénotype dopaminergique partiel et soient plutôt spécialisés dans la libération de glutamate a été par la suite explorée. Nous avons donc évalué les différentes populations de neurones exprimant l'ARNm de DAT et VMAT2 *in vivo*. Nos résultats démontrent que les neurones TH+VGLUT2- ont une tendance à une plus grande probabilité d'exprimer l'ARNm de DAT et VMAT2 en comparaison aux neurones TH+VGLUT2+ suggérant que les neurones au double phénotype ont un phénotype dopaminergique «partiel». De plus, nous avons noté la présence de 4 différentes classes de neurones TH+VGLUT2- et de neurones TH+VGLUT2+ : un premier groupe exprimant l'ARNm de DAT et VMAT2, un deuxième groupe exprimant seulement l'ARNm de DAT, un troisième groupe exprimant seulement l'ARNm de VMAT2 et finalement un quatrième group sans expression de ces marqueurs. Ces résultats confirment des observations similaires chez le rat (Li et al., 2013). En résumé, nos observations démontrent une grande hétérogénéité des neurones dopaminergiques *in vivo* et appuient l'hypothèse que les neurones dopaminergiques

au double phénotype expriment un phénotype dopaminergique partiel. Malgré que nous ayons observé des populations distinctes de neurones exprimant les différents marqueurs dopaminergiques et glutamatergiques, nous n'avons pas été en mesure d'évaluer le niveau d'expression de ces marqueurs. Ainsi, il serait envisageable d'évaluer le niveau moyen de copie d'ARNm de TH, DAT, VMAT2 et VGLUT2 dans ces différentes populations neuronales à l'aide de la technique de RT-qPCR sur cellule unique.

Étonnamment, nous avons observé que malgré que la majorité des neurones dopaminergiques dans le mésencéphale exprime VGLUT2, seule une très faible (3%) co-localisation des marqueurs TH et VGLUT2 est détectable dans le striatum *in vivo*. Ces données suggèrent ainsi une ségrégation des sites de libération pour le glutamate et la dopamine *in vivo*. À l'aide des souris cKO et la microscopie confocale, nous n'avons démontré aucune différence significative dans la co-localisation des marqueurs TH et VGLUT2 à l'intérieur des différentes sous-structures du striatum entre les animaux Ctrl et cKO. Une faible co-localisation a cependant été observée entre ces deux marqueurs chez les animaux témoins. Ceci pourrait être le résultat soit de l'existence d'une faible proportion aléatoire de terminaisons immunoréactives pour les deux protéines, soit un résultat artéfactuel dû aux limitations des techniques d'imagerie et de quantification utilisées. Afin de distinguer entre ces possibilités, nous avons par la suite utilisé la technique d'imagerie haute résolution SpIDA (Spatial Intensity Distribution Analysis) basée sur les marqueurs TH et VGLUT2. La distribution des nuages de points obtenus à partir de l'intensité relative des différents signaux détectés sur chaque pixel des images donne un indice direct de la présence de signaux qui co-localisent. Ainsi, nous avons observé une distribution aléatoire (moins de 0.5 % de co-localisation) des marqueurs TH et VGLUT2 dans le striatum ventral. Néanmoins, il serait également possible que les terminaisons glutamatergiques établient par les neurones dopaminergiques possèdent un phénotype dopaminergique partiel en exprimant seulement DAT. Cependant, l'absence de différence significative de la co-localisation des marqueurs DAT et VGLUT2 entre les animaux Ctrl et cKO ne supporte pas cette hypothèse.

Afin de tester l'hypothèse d'une ségrégation des sites de libération de la DA et du glutamate, nous avons utilisé des cultures de neurones dopaminergiques purifiées par la

cytométrie en flux à partir de souris TH-GFP. Nous avons ainsi démontré que la plupart des terminaisons glutamatergiques *in vitro* expriment TH ou DAT. Des observations similaires ont été rapportés en utilisant un système de micro-cultures (Dal Bo et al., 2004). Cependant, nous avons également observé une population de terminaisons glutamatergiques n'exprimant pas de marqueur dopaminergique, en accord avec l'hypothèse de ségrégation. En analysant la co-localisation des marqueurs GFP, TH et VGLUT2, nous avons observé que certaines de ces terminaisons glutamatergiques ségréguées semblent être localisées en alternance le long des mêmes branches axonales de neurones dopaminergiques individuels.

Dans une deuxième étape, nous avons documenté plus à fond l'hypothèse d'une ségrégation en examinant l'arborisation axonale de neurones dopaminergiques *in vivo* à l'aide d'une stratégie de surexpression virale. Nous avons injecté un virus permettant l'expression conditionnelle de la GFP dans les neurones dopaminergiques du VTA de souris DAT-Cre. Cette technique nous a permis de visualiser les terminaisons de ces neurones dans le striatum ventral et dorsal dopaminergique. Nous avons d'abord observé qu'une plus grande proportion de fibres GFP exprime la TH dans le striatum dorsal que dans le striatum ventral. Ceci pourrait s'expliquer les neurones dopaminergiques de la voie nigrostriée expriment plus de copies d'ARNm de TH, tel que démontré pour DAT (Björklund and Dunnett, 2007). Une autre explication serait que suite au contact des axones dopaminergiques avec les neurones du striatum ventral, une inhibition de l'expression de la TH ou un changement de sa distribution surviendrait. Une observation assez frappante de cette expérience a été la constatation que seulement la moitié des varicosités immunopositives pour la GFP innervant le striatum dorsal était immunopositive pour la TH. L'autre proportion des fibres GFP pourraient ainsi posséder la capacité de co-libérer le glutamate ou le GABA (Tritsch et al., 2012, 2014; Li et al., 2013). Nous avons par ailleurs démontré une augmentation significative du pourcentage de co-localisation des marqueurs GFP et VGLUT2 dans le striatum ventral comparativement au striatum dorsal. Le faible pourcentage obtenu dans le striatum dorsal (2%) est probablement une fausse co-localisation en se basant sur nos résultats obtenus à l'aide de la technique SpiDA. Des travaux démontrant la présence de libération de glutamate par les neurones dopaminergiques spécifiquement au niveau du striatum ventral par optogénétique confirment cette hypothèse (Stuber et al., 2010; Tecuapetla et al., 2010). Cependant, le pourcentage de varicosités dans lesquels la GFP co-localise avec VGLUT2

dans le striatum ventral demeure relativement faible (4%). Il se peut ainsi que les neurones dopaminergiques au double phénotype établissent un nombre relativement faible de terminaisons glutamatergiques. Des résultats démontrant que les neurones dopaminergiques expriment en moyenne pratiquement dix fois moins de copies d'ARNm de VGLUT2 que d'ARNm des autres marqueurs dopaminergiques sont en accord avec cette hypothèse (Li et al., 2013).

Une évaluation plus détaillée de certaines des varicosités axonales exprimant la GFP nous a permis d'observer des varicosités exprimant distinctivement TH et VGLUT2 le long d'une fibre axonale infectée. De façon similaire aux résultats obtenus en culture, nous avons été en mesure de distinguer différentes niveaux d'immunoréactivité anti-TH dans différentes varicosités axonales établissant ainsi des sites de libération dans lesquels le potentiel de synthèse de la DA serait donc élevé ou très faible. Nous avons observé que les varicosités immunopositives pour VGLUT2 étaient systématiquement faibles en immunoréactivité TH. Nos résultats suggèrent donc que les neurones dopaminergiques *in vivo* établissent des sites distincts pour la libération de la DA et du glutamate spécifiquement dans le striatum ventral.

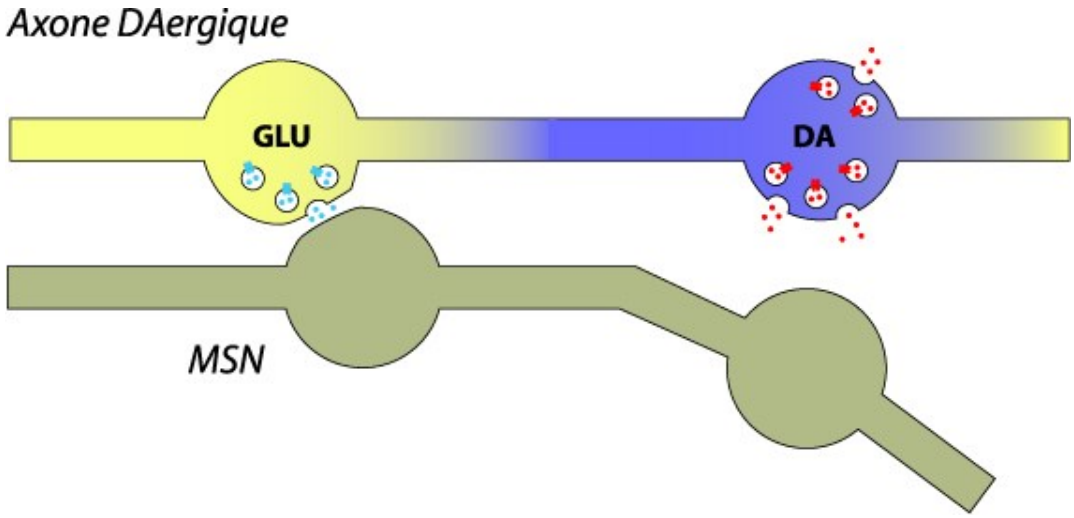

Figure 8. Établissement des sites de libération distincts de la dopamine et du glutamate provenant de la même fibre axonale dans le striatum.

Le mécanisme permettant l'établissement de sites distincts de libération du glutamate et de la dopamine reste encore inconnu. Un transport, adressage ou rétention sélective des marqueurs dopaminergiques et glutamatergiques au sein de différentes terminaisons serait une explication potentielle de nos observations *in vitro* et *in vivo*. Appuyant la plausibilité de cette hypothèse, il a été démontré que la TH semble être partiellement liée à la membrane (Fahn et al., 1969; Halskau et al., 2009; Cartier et al., 2010), ce qui pourrait limiter sa distribution le long des différents domaines du neurone dopaminergique.

Régulation du double phénotype des neurones dopaminergiques par les neurones striataux

La co-localisation partielle *in vitro* de TH et de VGLUT2 dans les terminaisons axonales établies par les neurones dopaminergiques et l'absence de co-localisation de TH et de VGLUT2 au niveau du striatum suggèrent une régulation de la ségrégation du phénotype *in vivo*. Une étude précédente a justement suggéré que le contact des neurones GABA modulerait le co-phénotype des neurones dopaminergiques (Mendez et al., 2008).

En utilisant un système de co-cultures de neurones dopaminergiques purifiées avec des neurones du striatum dorsal ou ventral, nous avons observé qu'une interaction avec les neurones du striatum ventral induit une ségrégation complète des marqueurs dopaminergiques et glutamatergiques. Cependant, le contact avec des neurones du striatum dorsal n'a pas pu induire cette ségrégation. Afin de vérifier si la ségrégation des terminaisons pourrait être expliquée par une régulation de l'expression des marqueurs dopaminergiques ou glutamatergiques, nous avons d'abord analysé la proportion des neurones au double phénotype en présence ou absence de neurones striataux. Nous n'avons pas observé de différence dans la proportion de neurones au double phénotype dans les différentes conditions de culture. Nous n'avons pas non plus observé de différence dans la proportion de neurones dopaminergiques exprimant le transporteur VMAT2. Cependant, la proportion de neurones dopaminergiques exprimant le transporteur DAT

a été plus faible dans les co-cultures de striatum ventral que dans les cultures purifiées. Ces données pourraient expliquer en partie la raison pour laquelle les neurones de la voie méso-limbique expriment généralement moins de DAT (Björklund and Dunnett, 2007).

Bien que la proportion des neurones au double phénotype n'ait pas été changée en présence des neurones du striatum, il est possible que le niveau moyen d'expression de TH ou de VGLUT2 ait été modifié. À l'aide de l'élaboration d'une nouvelle technique de RT-qPCR sur cellule unique, nous avons analysé quantitativement le niveau moyen d'ARNm de TH et de VGLUT2 dans des neurones dopaminergiques individuels en présence ou en absence de neurones du striatum. Bien que non significatif, nous avons observé une tendance à une diminution de l'expression de la TH et à une augmentation de l'expression de VGLUT2 (p=0.08) par les neurones dopaminergiques en présence des neurones du striatum ventral. Une augmentation de la quantité de l'expression de la protéine de VGLUT2 a malgré tout été observée dans ces cultures. Cependant, l'analyse électrophysiologique n'a pas été en mesure de rapporter une augmentation parallèle de la quantité de réponses synaptiques glutamatergiques, mesurées en présence des neurones du striatum. Une explication potentielle de ce paradoxe pourrait être que les protéines VGLUT2 nouvellement synthétisées se retrouvent dans des synapses non fonctionnelles ou silencieuses. De plus, la présence de terminaisons glutamatergiques exprimant VGLUT3 (provenant de neurones cholinergiques du striatum) pourrait potentiellement avoir masqué la détection d'une augmentation de la fréquence et de l'amplitude des réponses excitatrices provenant des terminaisons VGLUT2-positives dans nos expériences.

Ainsi, l'observation d'une diminution partielle du phénotype dopaminergique pourrait suggérer que le contact avec les neurones du striatum ventral diminue l'expression de certains marqueurs dopaminergiques dans les terminaisons au double phénotype et expliquerait la ségrégation induite par ces neurones. Une étude approfondie de l'expression de l'intensité relative de la GFP dans les varicosités axonales dopaminergiques à partir de co-cultures purifiées de neurones dopaminergiques et striataux d'animaux TH-GFP en utilisant l'imagerie en temps réel permettrait de répondre à cette hypothèse.

La raison pour laquelle seulement le contact avec les neurones du striatum ventral semble modifier le double phénotype des neurones dopaminergiques reste un mystère. Néanmoins, l'expression de certaines protéines et de certains types cellulaires semblent être différente entre les régions du striatum dorsal et ventral. En effet, il semble que les interneurones à parvalbumine sont localisés dans un gradient croissant du striatum ventral vers le striatum dorsal (Gerfen et al., 1985; Kita et al., 1990; Mura et al., 2000). De plus, il a été démontré que le striatum ventral est une région pauvre en expression de la calbindine mais élevée en transporteur de recapture de l'acétylcholine (Holt et al., 1997). De plus, il semble que les neurones épineux de taille moyenne expriment une densité plus élevée d'épine dendritique et d'embranchements dendritiques et axonaux (Meredith et al., 1993; Shirayama et al., 2006). Ainsi, il serait d'abord important d'élucider quel est le type cellulaire spécifique du striatum ventral capable d'initier la ségrégation. À l'aide de co-cultures de neurones du striataux trié par tri cellulaire provenant de souris D2-GFP ou VAchT-GFP, nous pourrions être en mesure de déterminer si c'est le contact avec les neurones GABA du striatum ventral qui initie la ségrégation ou alors le contact avec les neurones cholinergiques.

Le mécanisme moléculaire expliquant la ségrégation des sites de libération pour la dopamine et le glutamate suivant le contact avec les neurones du striatum ventral reste également inconnu. Puisque qu'il a été démontré que la protéine TH semble être partiellement liée à la membrane (Cartier et al., 2010; Fahn et al., 1969; Halskau et al., 2009), une rétention ou une exclusion de la protéine TH suite au contact des neurones du striatum ventral pourrait expliquer la ségrégation des sites de libération et la disparition partielle du phénotype DAergique. Le contact avec certaines molécules d'adhésion entre les neurones DAergiques et striataux pourraient réguler la localisation et le transport de la protéine TH. Par ailleurs, il été démontré que la molécule d'adhésion NCAM régule l'internalisation du récepteur D2 (Xiao et al., 2009). Considérant nos obervations d'une diminution partielle du phénotype DAergique suite au contact des neurones du striatum ventral, il est également envisageable que le contact avec des molécules d'adhésion soit en mesure de diminuer l'expression locale à la terminaison axonale de la tyrosine hydroxylase. Ceci pourrait également expliquer l'absence d'une diminution globale de l'expression de l'ARNm de la tyrosine hydroxylase et de la protéine provenant des co-cultures avec les neurones du striatum ventral.

Chapitre 4 : Perspectives

Ainsi, nos travaux suggèrent que VGLUT2 joue un rôle crucial dans le développement et la croissance d'une sous-population de neurones dopaminergiques. De plus, nous avons démontré qu'en absence du co-phénotype glutamatergique, de nombreux comportements tels que la réponse aux drogues d'abus, la motricité et la dépression sont altérés. Nous avons également démontré que les neurones dopaminergiques établissent des sites distincts de libération du glutamate et de la DA et que cette ségrégation est régulée par le contact avec les neurones cibles. Une analyse approfondie du rôle neurotrophique du phénotype glutamatergique des neurones dopaminergiques pourrait être effectuée afin de valider l'hypothèse proposée par nos travaux. La régulation et le rôle du co-phénotype dans des maladies et dans le contexte d'autres processus physiologiques impliquant le système dopaminergique pourraient également être des pistes intéressantes à évaluer.

Impacts physiologiques de la surexpression de VGLUT2

Les résultats de nos travaux démontrent que l'absence de la capacité de libérer le glutamate diminue le développement des neurones dopaminergiques. Ainsi, il serait possible que la surexpression de VGLUT2 augmente la croissance et la survie de ces neurones. Nous avons ainsi obtenu un vecteur lentiviral exprimant VGLUT2 afin de tester cette hypothèse. Après avoir exposé les cultures purifiées de neurones dopaminergiques au lentivirus pendant 7 jours et validé la surexpression de VGLUT2, nous avons observé une augmentation de la densité axonale ainsi que du nombre d'embranchements de ces neurones. Une plus grande complexité axonale, évalué par l'analyse sholl, a également été observée. Cependant, le vecteur viral n'a pas modifié la morphologie et la densité dendritique (voir annexe, Figure 9). Il se pourrait que le rôle de VGLUT2 soit strictement réservé à la croissance de l'axone et non dendritique considérant sa localisation spécifique au niveau des terminaisons axonales ou au cône de croissance axonal des neurones DAergiques. De plus, la libération locale de glutamate au cône de croissance pourrait

moduler la croissance spécifique de l'axone. En effet, l'activité des neurones en croissance et la libération spontanée de neurotransmetteurs semble promouvoir le développement et la guidance de l'axone, dans l'élongation et le branching (Catalano and Shatz, 1998; Uesaka et al., 2007 ; Mire et al., 2012).

Nous avons ensuite évalué l'hypothèse selon laquelle la surexpression de VGLUT2 augmente la survie des neurones dopaminergiques. Le vecteur viral n'a cependant pas augmenté de façon significative le nombre de neurones dopaminergiques *in vitro* (voir annexe, Figure 10). Afin de valider cette hypothèse, une étude approfondie en modifiant le titre viral ainsi que la durée d'exposition serait requise. Il serait par ailleurs intéressant d'évaluer si le récepteur NMDA est impliqué dans l'effet neurotrophique de la surexpression de VGLUT2. Il serait également intéressant d'évaluer si la vulnérabilité de ces neurones au MPP+ est modifiée.

Régulation de VGLUT2

Considérant le rôle de VGLUT2 dans la croissance et la survie des neurones dopaminergiques, il serait important d'évaluer la possibilité que l'expression de ce gène dans les neurones dopaminergique soit modifiée dans différents contextes physiologiques et pathologiques. Il serait par exemple possible que des facteurs neurotrophiques ou des neurotoxines modulent l'expression de VGLUT2. Le GDNF est un facteur neurotrophique bien établi des neurones dopaminergiques (Lin et al., 1993) qui pourrait potentiellement être en mesure de moduler l'expression de VGLUT2. De plus, il a été démontré que le GDNF augmente la libération de glutamate dans les cultures mésencéphaliques (Bourque and Trudeau, 2000). Dans des expériences préliminaires, nous avons effectué un traitement aigu de 3nM de GDNF sur des cultures mésencéphaliques, ce qui a augmenté la proportion de neurones dopaminergiques exprimant VGLUT2, tel que déterminé par la technique de RT-PCR sur cellule unique (voir annexe, Figure 11).

Puisqu'une lésion précoce des neurones dopaminergiques par la 6-OHDA semble moduler l'expression de VGLUT2 dans les neurones dopaminergiques survivants (Dal Bo. et al., 2008), l'étude de la régulation du double phénotype dans d'autres modèles animaux de la maladie de Parkinson pourrait être abordée. Nous avons commencé à tester cette hypothèse *in vitro* en étudiant l'influence du MPP+, un agent pharmacologique connu pour induire la neurodégénérescence des neurones dopaminergiques *in vitro*, à moduler l'expression de VGLUT2 dans les neurones dopaminergiques. Cependant, un traitement aigu de MPP+ 10nM n'a pas modifié la proportion des neurones au double phénotype (voir annexe, Figure 12). Nous avons par la suite testé cette hypothèse *in vivo* dans des modèles inductibles et génétiques de la maladie. Cependant, des données préliminaires obtenues ne suggèrent pas que la proportion des neurones au double phénotype soit modifiée dans le modèle de souris MPTP ou PARKIN-KO (voir annexe, Figure 13). Néanmoins, des résultats préliminaires suggèrent que la délétion du gène DJ-1 diminue la proportion des neurones dopaminergiques exprimant VGLUT2 (voir annexe, Figure 13). Néanmoins, l'analyse de l'expression moyenne de l'ARNm de VGLUT2 par neurone dopaminergique à l'aide de la technique de RT-qPCR sur cellule unique permettrait de valider cette hypothèse chez ces modèles. Il serait également intéressant d'évaluer la régulation du co-phénotype dans d'autres modèles d'animaux de la maladie de Parkinson tel que les souris surexprimant l'alpha-synucléine.

Il serait également pertinent d'étudier la régulation du co-phénotype par des agents pharmacologiques ciblant le système dopaminergique qui ne sont pas impliqués dans la maladie de Parkinson. Considérant qu'il a été démontré que les antipsychotiques modulent l'expression de VGLUT2 *in vivo* dans le striatum, cortex et thalamus (Moutsimilli et al., 2008), une étude de l'effet d'un traitement chronique avec ces agents sur le double phénotype des neurones dopaminergiques pourrait être envisagée.

Rôles de VGLUT2 dans la mémoire et la schizophrénie

Une étude récente a démontré que libération de DA dans l'hippocampe est cruciale pour plusieurs aspects de la mémoire (Rocchetti et al., 2014). De plus, il a été démontré que la

diminution de l'expression de VGLUT2 est corrélée avec l'induction de perte de déficits cognitifs important chez les patients atteints de la maladie d'Alzheimer (Kashani et al., 2008). Il est ainsi possible que l'expression de VGLUT2 dans les neurones dopaminergiques joue un rôle important dans certaines formes d'apprentissages. De plus, puisque le système dopaminergique est bien connu pour être impliqué dans la schizophrénie, il est également possible que le co-phénotype des neurones dopaminergiques ait un rôle dans cette maladie. Grâce à une collaboration avec le laboratoire du Dr Lalit Srivastava de l'Université McGill, nous avons commencé à tester ces hypothèses chez les souris cKO. Nous avons d'abord analysé le filtrage sensoriel des animaux cKO à l'aide du paradigme du prepulse inhibition, un test souvent utilisé chez les rongeurs pour évaluer des dysfonctions cérébrales analogues à celles retrouvées dans la schizophrénie. Ce test analyse la capacité de filtrage sensoriel des rongeurs en estimant la réponse à un sursaut sonore. Néanmoins, aucune modification de l'intensité du sursaut n'a été observée chez les souris cKO (voir annexe, Figure 13) suggérant que la délétion de VGLUT2 dans les neurones dopaminergiques n'induise pas des comportements liés à la schizophrénie. Il serait intéressant d'évaluer si l'expression de VGLUT2 module la potentialisation ou la dépression à long terme dans l'hippocampe ou certaines formes d'apprentissages qui dépendent de la dopamine, telle que la reconnaissance d'objet.

Chapitre 5 : Conclusions

Quatre-vingt ans après l'énoncé du fameux principe de sir Henry Dale, récipiendaire du prix Nobel, la capacité des neurones du système nerveux central à libérer plus d'un neurotransmetteur est un processus neurobiologique aujourd'hui largement soutenue par la communauté scientifique. Néanmoins, le rôle de ce phénomène dans le système nerveux central reste encore méconnu à ce jour. Les travaux de cette thèse ont ainsi permis d'élucider en partie la signification physiologique de la capacité des neurones dopaminergiques à libérer le glutamate. Ainsi, nos données suggèrent que l'expression de VGLUT2 dans les neurones dopaminergiques intervient dans le maintien de l'homéostasie du système dopaminergique et dans de nombreux processus physiologiques et comportementaux cruciaux. Il reste présentement à explorer si une perturbation de la cotransmission pourrait être en cause dans certaines maladies du cerveau.

Bibliographie

Acampora, D., Mazan, S., Lallemand, Y., Avantaggiato, V., Maury, M., Simeone, A., and Brûlet, P. (1995). Forebrain and midbrain regions are deleted in Otx2-/- mutants due to a defective anterior neuroectoderm specification during gastrulation. Dev. Camb. Engl. *121*, 3279–3290.

Allen, T.G.J. (1997). The `sniffer-patch' technique for detection of neurotransmitter release. Trends Neurosci. *20*, 192–197.

Alsiö, J., Nordenankar, K., Arvidsson, E., Birgner, C., Mahmoudi, S., Halbout, B., Smith, C., Fortin, G.M., Olson, L., Descarries, L., et al. (2011). Enhanced sucrose and cocaine self-administration and cue-induced drug seeking after loss of VGLUT2 in midbrain dopamine neurons in mice. J. Neurosci. *31*, 12593–12603.

Amilhon, B., Lepicard, E., Renoir, T., Mongeau, R., Popa, D., Poirel, O., Miot, S., Gras, C., Gardier, A.M., Gallego, J., et al. (2010). VGLUT3 (vesicular glutamate transporter type 3) contribution to the regulation of serotonergic transmission and anxiety. J. Neurosci. *30*, 2198–2210.

Andersson, D.R., Nissbrandt, H., and Bergquist, F. (2006). Partial depletion of dopamine in substantia nigra impairs motor performance without altering striatal dopamine neurotransmission. Eur. J. Neurosci. *24*, 617–624.

Banerjee, S.P., Zuck, L.G., Yablonsky-Alter, E., and Lidsky, T.I. (1995). Glutamate agonist activity: implications for antipsychotic drug action and schizophrenia. Neuroreport *6*, 2500–2504.

Beal, M.F. (1992). Mechanisms of excitotoxicity in neurologic diseases. FASEB J. Off. Publ. Fed. Am. Soc. Exp. Biol. *6*, 3338–3344.

Beaulieu, J.-M., Gainetdinov, R.R., and Caron, M.G. (2009). Akt/GSK3 signaling in the action of psychotropic drugs. Annu. Rev. Pharmacol. Toxicol. *49*, 327–347.

Bekris, L.M., Mata, I.F., and Zabetian, C.P. (2010). The Genetics of Parkinson Disease. J. Geriatr. Psychiatry Neurol. *23*, 228–242.

Bellocchio, E.E., Reimer, R.J., Fremeau, R.T., and Edwards, R.H. (2000). Uptake of Glutamate into Synaptic Vesicles by an Inorganic Phosphate Transporter. Science *289*, 957–960.

Benoit-Marand, M., Borrelli, E., and Gonon, F. (2001). Inhibition of Dopamine Release Via Presynaptic D2 Receptors: Time Course and Functional Characteristics In Vivo. J. Neurosci. *21*, 9134–9141.

BERTLER, A., and ROSENGREN, E. (1959). Occurrence and distribution of dopamine in brain and other tissues. Experientia *15*, 10–11.

Bérubé-Carrière, N., Riad, M., Dal Bo, G., Lévesque, D., Trudeau, L.-É., and Descarries, L. (2009b). The dual dopamine-glutamate phenotype of growing mesencephalic neurons regresses in mature rat brain. J. Comp. Neurol. *517*, 873–891.

Birgner, C., Nordenankar, K., Lundblad, M., Mendez, J.A., Smith, C., le Grevès, M., Galter, D., Olson, L., Fredriksson, A., Trudeau, L.-E., et al. (2010). VGLUT2 in dopamine neurons is required for psychostimulant-induced behavioral activation. Proc. Natl. Acad. Sci. *107*, 389–394.

Björklund, A., and Dunnett, S.B. (2007). Dopamine neuron systems in the brain: an update. Trends Neurosci. *30*, 194–202.

Blandini, F., and Armentero, M.-T. (2012). Animal models of Parkinson's disease. FEBS J. *279*, 1156–1166.

Blaschko, H. (1942). The activity of l (—)-dopa decarboxylase. J. Physiol. *101*, 337–349.

Dal Bo, G., St-Gelais, F., Danik, M., Williams, S., Cotton, M., and Trudeau, L.-E. (2004). Dopamine neurons in culture express VGLUT2 explaining their capacity to release glutamate at synapses in addition to dopamine. J. Neurochem. 1398–1405.

Dal Bo, G., Bérubé-Carrière, N., Mendez, J.A., Leo, D., Riad, M., Descarries, L., Lévesque, D., and Trudeau, L.-E. (2008). Enhanced glutamatergic phenotype of mesencephalic dopamine neurons after neonatal 6-hydroxydopamine lesion. Neuroscience *156*, 59–70.

Bolam, J.P., and Pissadaki, E.K. (2012). Living on the edge with too many mouths to feed: why dopamine neurons die. Mov. Disord. *27*, 1478–1483.

Bonifati, V., Rizzu, P., Baren, M.J. van, Schaap, O., Breedveld, G.J., Krieger, E., Dekker, M.C.J., Squitieri, F., Ibanez, P., Joosse, M., et al. (2003). Mutations in the DJ-1 Gene Associated with Autosomal Recessive Early-Onset Parkinsonism. Science *299*, 256–259.

Boulland, J.L. (2004). Expression of the vesicular glutamate transporters during development indicates the widespread corelease of multiple neurotransmitters. J Comp Neurol *480*, 264–280.

Boulland, J.L. (2009). Vesicular glutamate and GABA transporters sort to distinct sets of vesicles in a population of presynaptic terminals. Cereb Cortex *19*, 241–248.

Bourque, M.J., and Trudeau, L.E. (2000). GDNF enhances the synaptic efficacy of dopaminergic neurons in culture. Eur J Neurosci *12*, 3172–3180.

Carlsson, A., and Lindqvist, M. (1963). Effect of chlorpromazine or haloperidol on formation of 3methoxytyramine and normetanephrine in mouse brain. Acta Pharmacol. Toxicol. (Copenh.) *20*, 140–144.

Carlsson, A., Linqvist, M., Magnusson, T., and Waldeck, B. (1958). On the presence of 3-hydroxytyramine in brain. Science 127:471; 1958a. Science 471.

Carlsson, A., Falck, B., And Hillarp, N.A. (1962). Cellular localization of brain monoamines. Acta Physiol. Scand. Suppl. *56*, 1–28.

Cartier, E.A., Parra, L.A., Baust, T.B., Quiroz, M., Salazar, G., Faundez, V., Egaña, L., and Torres, G.E. (2010). A biochemical and functional protein complex involving dopamine synthesis and transport into synaptic vesicles. J. Biol. Chem. *285*, 1957–1966.

Castillo, S.O., Baffi, J.S., Palkovits, M., Goldstein, D.S., Kopin, I.J., Witta, J., Magnuson, M.A., and Nikodem, V.M. (1998). Dopamine biosynthesis is selectively abolished in substantia nigra/ventral tegmental area but not in hypothalamic neurons in mice with targeted disruption of the Nurr1 gene. Mol. Cell. Neurosci. *11*, 36–46.

Chapman, A.G., Smith, S.E., and Meldrum, B.S. (1991). The anticonvulsant effect of the non-NMDA antagonists, NBQX and GYKI 52466, in mice. Epilepsy Res. *9*, 92–96.

Di Chiara, G., Acquas, E., and Carboni, E. (1992). Drug motivation and abuse: a neurobiological perspective. Ann. N. Y. Acad. Sci. *654*, 207–219.

Chu, Y., Kompoliti, K., Cochran, E.J., Mufson, E.J., and Kordower, J.H. (2002). Age-related decreases in Nurr1 immunoreactivity in the human substantia nigra. J. Comp. Neurol. *450*, 203–214.

Chuhma, N., Zhang, H., Masson, J., Zhuang, X., Sulzer, D., Hen, R., and Rayport, S. (2004). Dopamine neurons mediate a fast excitatory signal via their glutamatergic synapses. J. Neurosci. Off. J. Soc. Neurosci. *24*, 972–981.

Curtis, D.R., and Watkins, J.C. (1960). The Excitation and Depression of Spinal Neurones by Structurally Related Amino Acids. J. Neurochem. *6*, 117–141.

Dahlstroem, A., And Fuxe, K. (1964). Evidence for the existence of monoamine-containing neurons in the central nervous system. i. demonstration of monoamines in the cell bodies of brain stem neurons. Acta Physiol. Scand. Suppl. SUPPL 232:1–55.

Deng, Q., Andersson, E., Hedlund, E., Alekseenko, Z., Coppola, E., Panman, L., Millonig, J.H., Brunet, J.-F., Ericson, J., and Perlmann, T. (2011). Specific and integrated roles of Lmx1a, Lmx1b and Phox2a in ventral midbrain development. Dev. Camb. Engl. *138*, 3399–3408.

Eiden, L.E., Schäfer, M.K.-H., Weihe, E., and Schütz, B. (2004). The vesicular amine transporter family (SLC18): amine/proton antiporters required for vesicular accumulation and regulated exocytotic secretion of monoamines and acetylcholine. Pflüg. Arch. Eur. J. Physiol. *447*, 636–640.

El Mestikawy, S., Wallén-Mackenzie, Å., Fortin, G.M., Descarries, L., and Trudeau, L.-E. (2011). From glutamate co-release to vesicular synergy: vesicular glutamate transporters. Nat Rev Neurosci *12*, 204–216.

Emborg, M.E., Ma, S.Y., Mufson, E.J., Levey, A.I., Taylor, M.D., Brown, W.D., Holden, J.E., and Kordower, J.H. (1998). Age-related declines in nigral neuronal function correlate with motor impairments in rhesus monkeys. J. Comp. Neurol. *401*, 253–265.

Enjalbert, A., and Bockaert, J. (1983). Pharmacological characterization of the D2 dopamine receptor negatively coupled with adenylate cyclase in rat anterior pituitary. Mol. Pharmacol. *23*, 576–584.

Erickson, J.D., and Eiden, L.E. (1993). Functional identification and molecular cloning of a human brain vesicle monoamine transporter. J. Neurochem. *61*, 2314–2317.

Fahn, S., Rodman, J.S., and Côté, L.J. (1969). Association of tyrosine hydroxylase with synaptic vesicles in bovine caudate nucleus. J. Neurochem. *16*, 1293–1300.

Felder, C.C., Jose, P.A., and Axelrod, J. (1989). The dopamine-1 agonist, SKF 82526, stimulates phospholipase-C activity independent of adenylate cyclase. J. Pharmacol. Exp. Ther. *248*, 171–175.

Ferri, A.L.M., Lin, W., Mavromatakis, Y.E., Wang, J.C., Sasaki, H., Whitsett, J.A., and Ang, S.-L. (2007). Foxa1 and Foxa2 regulate multiple phases of midbrain dopaminergic neuron development in a dosage-dependent manner. Development *134*, 2761–2769.

Forlano, P.M., and Woolley, C.S. (2010). Quantitative analysis of pre- and postsynaptic sex differences in the nucleus accumbens. J. Comp. Neurol. *518*, 1330–1348.

Fremeau, R.T. (2001). The expression of vesicular glutamate transporters defines two classes of excitatory synapse. Neuron *31*, 247–260.

Fremeau, R.T. (2002). The identification of vesicular glutamate transporter 3 suggests novel modes of signaling by glutamate. Proc Natl Acad Sci USA *99*, 14488–14493.

Funk, C. (1911). LXV.-Synthesis of dl-3 : 4-dihydroxyphenylalanine. J. Chem. Soc. Trans. *99*, 554–557.

Furshpan, E.J., MacLeish, P.R., O'Lague, P.H., and Potter, D.D. (1976). Chemical transmission between rat sympathetic neurons and cardiac myocytes developing in microcultures: evidence for cholinergic, adrenergic, and dual-function neurons. Proc. Natl. Acad. Sci. U. S. A. *73*, 4225–4229.

Gainetdinov, R.R., and Caron, M.G. (2003). Monoamine transporters: from genes to behavior. Annu. Rev. Pharmacol. Toxicol. *43*, 261–284.

George, S.R., Kern, A., Smith, R.G., and Franco, R. (2014). Dopamine receptor heteromeric complexes and their emerging functions. Prog. Brain Res. *211*, 183–200.

German, D.C., and Manaye, K.F. (1993). Midbrain dopaminergic neurons (nuclei A8, A9, and A10): three-dimensional reconstruction in the rat. J. Comp. Neurol. *331*, 297–309.

Gillespie, D.C., Kim, G., and Kandler, K. (2005). Inhibitory synapses in the developing auditory system are glutamatergic. Nat. Neurosci *8*, 332–338.

Giros, B., Jaber, M., Jones, S.R., Wightman, R.M., and Caron, M.G. (1996). Hyperlocomotion and indifference to cocaine and amphetamine in mice lacking the dopamine transporter. Nature *379*, 606–612.

Goff, D.C., and Wine, L. (1997). Glutamate in schizophrenia: clinical and research implications. Schizophr. Res. *27*, 157–168.

Gras, C. (2002). A third vesicular glutamate transporter expressed by cholinergic and serotoninergic neurons. J Neurosci *22*, 5442–5451.

Gras, C., Herzog, E., Bellenchi, G.C., Bernard, V., Ravassard, P., Pohl, M., Gasnier, B., Giros, B., and El Mestikawy, S. (2002). A Third Vesicular Glutamate Transporter Expressed by Cholinergic and Serotoninergic Neurons. J. Neurosci. *22*, 5442–5451.

Gras, C., Amilhon, B., Lepicard, E.M., Poirel, O., Vinatier, J., Herbin, M., Dumas, S., Tzavara, E.T., Wade, M.R., Nomikos, G.G., et al. (2008). The vesicular glutamate transporter VGLUT3 synergizes striatal acetylcholine tone. Nat. Neurosci. *11*, 292–300.

Guggenheim., M. (1913). Dioxyphenylalanin, eine neue Aminosäure aus Vicia faba. Hoppe-Seyler´s Z. Für Physiol. Chem. *88*, 276–284.

Gutiérrez, R. (2000). Seizures induce simultaneous GABAergic and glutamatergic transmission in the dentate gyrus-CA3 system. J. Neurophysiol. *84*, 3088–3090.

Hack, N., and Balázs, R. (1994). Selective stimulation of excitatory amino acid receptor subtypes and the survival of granule cells in culture: effect of quisqualate and AMPA. Neurochem. Int. *25*, 235–241.

Halskau, Ø., Ying, M., Baumann, A., Kleppe, R., Rodriguez-Larrea, D., Almås, B., Haavik, J., and Martinez, A. (2009). Three-way interaction between 14-3-3 proteins, the N-terminal region of tyrosine hydroxylase, and negatively charged membranes. J. Biol. Chem. *284*, 32758–32769.

Hardingham, G.E., and Bading, H. (2010). Synaptic versus extrasynaptic NMDA receptor signalling: implications for neurodegenerative disorders. Nat. Rev. Neurosci. *11*, 682–696.

Hartmann, M., Heumann, R., and Lessmann, V. (2001). Synaptic secretion of BDNF after high-frequency stimulation of glutamatergic synapses. EMBO J *20*, 5887–5897.

Hayashi, T. (1952). A physiological study of epileptic seizures following cortical stimulation in animals and its application to human clinics. Jpn. J. Physiol. *3*, 46–64.

Heal, D.J., Smith, S.L., Gosden, J., and Nutt, D.J. (2013). Amphetamine, past and present--a pharmacological and clinical perspective. J. Psychopharmacol. Oxf. Engl. *27*, 479–496.

Hegarty, S.V., Sullivan, A.M., and O'Keeffe, G.W. (2013). Midbrain dopaminergic neurons: a review of the molecular circuitry that regulates their development. Dev. Biol. *379*, 123–138.

Herzog, E. (2004). Localization of VGLUT3, the vesicular glutamate transporter type 3, in the rat brain. Neuroscience *123*, 983–1002.

Hnasko, T.S., Chuhma, N., Zhang, H., Goh, G.Y., Sulzer, D., Palmiter, R.D., Rayport, S., and Edwards, R.H. (2010). Vesicular Glutamate Transport Promotes Dopamine Storage and Glutamate Corelease In Vivo. Neuron *65*, 643–656.

Hökfelt, T., Björklund, A., and Dunnett, S.B. (1984). In Distributional of Tyrosine Hydroxylaseimmunoreactive Neurons in the Rat Brain, (Elsevier), pp. 277–379.

Hollmann, M., and Heinemann, S. (1994). Cloned glutamate receptors. Annu. Rev. Neurosci. *17*, 31–108.

Hollmann, M., O'Shea-Greenfield, A., Rogers, S.W., and Heinemann, S. (1989). Cloning by functional expression of a member of the glutamate receptor family. Nature *342*, 643–648.

Holtz, P. (1939). Dopadecarboxylase. Naturwissenschaften *27*, 724–725.

Holtz, P., Heise, R., and Lüdtke, K. (1938). Fermentativer Abbau von l-Dioxyphenylalanin (Dopa) durch Niere. Naunyn-Schmiedebergs Arch. Für Exp. Pathol. Pharmakol. *191*, 87–118.

Huh, C.Y., Danik, M., Manseau, F., Trudeau, L.E., and Williams, S. (2008). Chronic exposure to nerve growth factor increases acetylcholine and glutamate release from cholinergic neurons of the rat medial septum and diagonal band of Broca via mechanisms mediated by p75NTR. J Neurosci *28*, 1404–1409.

Hyman, S.E., Malenka, R.C., and Nestler, E.J. (2006). Neural mechanisms of addiction: the role of reward-related learning and memory. Annu. Rev. Neurosci. *29*, 565–598.

Ikonomidou, C., Bosch, F., Miksa, M., Bittigau, P., Vöckler, J., Dikranian, K., Tenkova, T.I., Stefovska, V., Turski, L., and Olney, J.W. (1999). Blockade of NMDA Receptors and Apoptotic Neurodegeneration in the Developing Brain. Science *283*, 70–74.

Johnson, M.D. (1994). Synaptic glutamate release by postnatal rat serotonergic neurons in microculture. Neuron *12*, 433–442.

Jonas, P., Bischofberger, J., and Sandkühler, J. (1998). Corelease of two fast neurotransmitters at a central synapse. Science *281*, 419–424.

Kao, Y.H. (2004). Evidence that certain retinal bipolar cells use both glutamate and GABA. J Comp Neurol *478*, 207–218.

Kashani, A., Lepicard, E., Poirel, O., Videau, C., David, J.P., Fallet-Bianco, C., Simon, A., Delacourte, A., Giros, B., Epelbaum, J., et al. (2008). Loss of VGLUT1 and VGLUT2 in the prefrontal cortex is correlated with cognitive decline in Alzheimer disease. Neurobiol. Aging *29*, 1619–1630.

Kawano, M. (2006). Particular subpopulations of midbrain and hypothalamic dopamine neurons express vesicular glutamate transporter 2 in the rat brain. J Comp Neurol *498*, 581–592.

Kebabian, J.W., and Calne, D.B. (1979). Multiple receptors for dopamine. Nature *277*, 93–96.

Kebabian, J.W., and Greengard, P. (1971). Dopamine-Sensitive Adenyl Cyclase: Possible Role in Synaptic Transmission. Science *174*, 1346–1349.

Kitada, T., Asakawa, S., Hattori, N., Matsumine, H., Yamamura, Y., Minoshima, S., Yokochi, M., Mizuno, Y., and Shimizu, N. (1998). Mutations in the parkin gene cause autosomal recessive juvenile parkinsonism. Nature *392*, 605–608.

Koob, G.F., and Volkow, N.D. (2010). Neurocircuitry of Addiction. Neuropsychopharmacology *35*, 217–238.

Kraus, T., Neuhuber, W.L., and Raab, M. (2004). Vesicular glutamate transporter 1 immunoreactivity in motor endplates of striated esophageal but not skeletal muscles in the mouse. Neurosci Lett *360*, 53–56.

Kuzhikandathil, E.V., Yu, W., and Oxford, G.S. (1998). Human dopamine D3 and D2L receptors couple to inward rectifier potassium channels in mammalian cell lines. Mol. Cell. Neurosci. *12*, 390–402.

Lacomblez, L., Bensimon, G., Leigh, P.N., Guillet, P., and Meininger, V. (1996). Dose-ranging study of riluzole in amyotrophic lateral sclerosis. Amyotrophic Lateral Sclerosis/Riluzole Study Group II. Lancet *347*, 1425–1431.

Lavin, A., Nogueira, L., Lapish, C.C., Wightman, R.M., Phillips, P.E.M., and Seamans, J.K. (2005). Mesocortical dopamine neurons operate in distinct temporal domains using multimodal signaling. J. Neurosci. Off. J. Soc. Neurosci. *25*, 5013–5023.

Lavine, N., Ethier, N., Oak, J.N., Pei, L., Liu, F., Trieu, P., Rebois, R.V., Bouvier, M., Hebert, T.E., and Van Tol, H.H.M. (2002). G protein-coupled receptors form stable complexes with inwardly rectifying potassium channels and adenylyl cyclase. J. Biol. Chem. *277*, 46010–46019.

Le, W., Sayana, P., and Jankovic, J. (2014). Animal models of Parkinson's disease: a gateway to therapeutics? Neurother. J. Am. Soc. Exp. Neurother. *11*, 92–110.

Lee, J., Zhu, W.-M., Stanic, D., Finkelstein, D.I., Horne, M.H., Henderson, J., Lawrence, A.J., O'Connor, L., Tomas, D., Drago, J., et al. (2008). Sprouting of dopamine terminals and altered dopamine release and uptake in Parkinsonian dyskinaesia. Brain *131*, 1574–1587.

Leigh, P.N., and Meldrum, B.S. (1996). Excitotoxicity in ALS. Neurology *47*, S221–S227.

Li, X., Qi, J., Yamaguchi, T., Wang, H.-L., and Morales, M. (2013a). Heterogeneous composition of dopamine neurons of the rat A10 region: molecular evidence for diverse signaling properties. Brain Struct. Funct. *218*, 1159–1176.

Li, X., Qi, J., Yamaguchi, T., Wang, H.-L., and Morales, M. (2013b). Heterogeneous composition of dopamine neurons of the rat A10 region: molecular evidence for diverse signaling properties. Brain Struct. Funct. *218*, 1159–1176.

Lin, L., Doherty, D., Lile, J., Bektesh, S., and Collins, F. (1993). GDNF: a glial cell line-derived neurotrophic factor for midbrain dopaminergic neurons. Science *260*, 1130–1132.

Lujan, R., Nusser, Z., Roberts, J.D., Shigemoto, R., and Somogyi, P. (1996). Perisynaptic location of metabotropic glutamate receptors mGluR1 and mGluR5 on dendrites and dendritic spines in the rat hippocampus. Eur. J. Neurosci. *8*, 1488–1500.

Luján, R., Roberts, J.D., Shigemoto, R., Ohishi, H., and Somogyi, P. (1997). Differential plasma membrane distribution of metabotropic glutamate receptors mGluR1 alpha, mGluR2 and mGluR5, relative to neurotransmitter release sites. J. Chem. Neuroanat. *13*, 219–241.

Lynd-Balta, E., and Haber, S.N. (1994). The organization of midbrain projections to the striatum in the primate: sensorimotor-related striatum versus ventral striatum. Neuroscience *59*, 625–640.

Martin-Ibanez, R. (2006). Vesicular glutamate transporter 3 (VGLUT3) identifies spatially segregated excitatory terminals in the rat substantia nigra. Eur J Neurosci *23*, 1063–1070.

McCormack, A.L., Di Monte, D.A., Delfani, K., Irwin, I., DeLanney, L.E., Langston, W.J., and Janson, A.M. (2004). Aging of the nigrostriatal system in the squirrel monkey. J. Comp. Neurol. *471*, 387–395.

Meldrum, B., and Garthwaite, J. (1990). Excitatory amino acid neurotoxicity and neurodegenerative disease. Trends Pharmacol. Sci. *11*, 379–387.

Mendez, J.A., Bourque, M.-J., Bo, G.D., Bourdeau, M.L., Danik, M., Williams, S., Lacaille, J.-C., and Trudeau, L.-E. (2008). Developmental and Target-Dependent Regulation of Vesicular Glutamate Transporter Expression by Dopamine Neurons. J. Neurosci. *28*, 6309–6318.

Moutsimilli, L. (2008). Antipsychotics increase vesicular glutamate transporter 2 (VGLUT2) expression in thalamolimbic pathways. Neuropharmacology *54*, 497–508.

Mukhin, A., Fan, L., and Faden, A.I. (1996). Activation of metabotropic glutamate receptor subtype mGluR1 contributes to post-traumatic neuronal injury. J. Neurosci. Off. J. Soc. Neurosci. *16*, 6012–6020.

Nabekura, J., Katsurabayashi, S., Kakazu, Y., Shibata, S., Matsubara, A., Jinno, S., Mizoguchi, Y., Sasaki, A., and Ishibashi, H. (2004). Developmental switch from GABA to glycine release in single central synaptic terminals. Nat. Neurosci. *7*, 17–23.

Nagatsu, T., Levitt, M., and Udenfriend, S. (1964). Conversion of L-tyrosine to 3,4-dihydroxyphenylalanine by cell-free preparations of brain and sympathetically innervated tissues. Biochem. Biophys. Res. Commun. *14*, 543–549.

Nakanishi, H., and Takeda, H. (1972). The possibility that adenosine triphosphate is an excitatory transmitter in guinea-pig seminal vesicle. Jpn. J. Pharmacol. *22*, 269–270.

Nakanishi, H., and Takeda, H. (1973). The possible role of adenosine triphosphate in chemical transmission between the hypogastric nerve terminal and seminal vesicle in the guinea-pig. Jpn. J. Pharmacol. *23*, 479–490.

Nelson, E.L., Liang, C.L., Sinton, C.M., and German, D.C. (1996). Midbrain dopaminergic neurons in the mouse: computer-assisted mapping. J. Comp. Neurol. *369*, 361–371.

Nishimaru, H., Restrepo, C.E., Ryge, J., Yanagawa, Y., and Kiehn, O. (2005). Mammalian motor neurons corelease glutamate and acetylcholine at central synapses. Proc Natl Acad Sci USA *102*, 5245–5249.

Noh, J., Seal, R.P., Garver, J.A., Edwards, R.H., and Kandler, K. (2010). Glutamate co-release at GABA/glycinergic synapses is crucial for the refinement of an inhibitory map. Nat. Neurosci *13*, 232–238.

Parent, M., and Parent, A. (2006). Relationship between axonal collateralization and neuronal degeneration in basal ganglia. J. Neural Transm. Suppl. 85–88.

Patterson, P.H., and Chun, L.L. (1974). The influence of non-neuronal cells on catecholamine and acetylcholine synthesis and accumulation in cultures of dissociated sympathetic neurons. Proc. Natl. Acad. Sci. U. S. A. *71*, 3607–3610.

Pickel, V.M., Nirenberg, M.J., and Milner, T.A. (1996). Ultrastructural view of central catecholaminergic transmission: immunocytochemical localization of synthesizing enzymes, transporters and receptors. J. Neurocytol. *25*, 843–856.

Prakash, N., Brodski, C., Naserke, T., Puelles, E., Gogoi, R., Hall, A., Panhuysen, M., Echevarria, D., Sussel, L., Weisenhorn, D.M.V., et al. (2006). A Wnt1-regulated genetic network controls the identity and fate of midbrain-dopaminergic progenitors in vivo. Dev. Camb. Engl. *133*, 89–98.

Prensa, L., and Parent, A. (2001). The Nigrostriatal Pathway in the Rat: A Single-Axon Study of the Relationship between Dorsal and Ventral Tier Nigral Neurons and the Striosome/Matrix Striatal Compartments. J. Neurosci. *21*, 7247–7260.

Ren, J. (2011). Habenula "cholinergic" neurons corelease glutamate and acetylcholine and activate postsynaptic neurons via distinct transmission modes. Neuron *69*, 445–452.

Ribeiro, D., Ellwanger, K., Glagow, D., Theofilopoulos, S., Corsini, N.S., Martin-Villalba, A., Niehrs, C., and Arenas, E. (2011). Dkk1 regulates ventral midbrain dopaminergic differentiation and morphogenesis. PloS One *6*, e15786.

Rocchetti, J., Isingrini, E., Dal Bo, G., Sagheby, S., Menegaux, A., Tronche, F., Levesque, D., Moquin, L., Gratton, A., Wong, T.P., et al. (2014). Presynaptic D2 Dopamine Receptors Control Long-Term Depression Expression and Memory Processes in the Temporal Hippocampus. Biol. Psychiatry.

Roe, D.L. (1999). The discovery of dopamine's physiological importance. Brain Res. Bull. *50*, 375–376.

Roeper, J. (2013). Dissecting the diversity of midbrain dopamine neurons. Trends Neurosci. *36*, 336–342.

Rosenblad, C., Martinez-Serrano, A., and Bjorklund, A. (1997). Intrastriatal glial cell line-derived neurotrophic factor promotes sprouting of spared nigrostriatal dopaminergic afferents and induces recovery of function in a rat model of Parkinson's disease. Neuroscience *82*, 129–137.

Rothman, R.B., and Baumann, M.H. (2003). Monoamine transporters and psychostimulant drugs. Eur. J. Pharmacol. *479*, 23–40.

Sacaan, A.I., and Schoepp, D.D. (1992). Activation of hippocampal metabotropic excitatory amino acid receptors leads to seizures and neuronal damage. Neurosci. Lett. *139*, 77–82.

Sahu, A., Tyeryar, K.R., Vongtau, H.O., Sibley, D.R., and Undieh, A.S. (2009). D5 dopamine receptors are required for dopaminergic activation of phospholipase C. Mol. Pharmacol. *75*, 447–453.

Sanchez, G., Varaschin, R.K., Büeler, H., Marcogliese, P.C., Park, D.S., and Trudeau, L.-E. (2014). Unaltered striatal dopamine release levels in young Parkin knockout, Pink1 knockout, DJ-1 knockout and LRRK2 R1441G transgenic mice. PloS One 9, e94826.

Sandler, R., and Smith, A.D. (1991). Coexistence of GABA and glutamate in mossy fiber terminals of the primate hippocampus: an ultrastructural study. J. Comp. Neurol. *303*, 177–192.

Sano, I., Gamo, T., Kakimoto, Y., Taniguchi, K., Takesada, M., And Nishinuma, K. (1959). Distribution of catechol compounds in human brain. Biochim. Biophys. Acta *32*, 586–587.

Schafer, M.K., Varoqui, H., Defamie, N., Weihe, E., and Erickson, J.D. (2002). Molecular cloning and functional identification of mouse vesicular glutamate transporter 3 and its expression in subsets of novel excitatory neurons. J Biol Chem *277*, 50734–50748.

Schmitz, Y., Luccarelli, J., Kim, M., Wang, M., and Sulzer, D. (2009). Glutamate Controls Growth Rate and Branching of Dopaminergic Axons. J. Neurosci. *29*, 11973–11981.

Seeman, P., Lee, T., Chau-Wong, M., and Wong, K. (1976). Antipsychotic drug doses and neuroleptic/dopamine receptors. Nature *261*, 717–719.

Shigemoto, R., Kinoshita, A., Wada, E., Nomura, S., Ohishi, H., Takada, M., Flor, P.J., Neki, A., Abe, T., Nakanishi, S., et al. (1997). Differential presynaptic localization of metabotropic glutamate receptor subtypes in the rat hippocampus. J. Neurosci. *17*, 7503–7522.

Silinsky, E.M. (1975). On the association between transmitter secretion and the release of adenine nucleotides from mammalian motor nerve terminals. J. Physiol. *247*, 145–162.

Smits, S.M., Ponnio, T., Conneely, O.M., Burbach, J.P.H., and Smidt, M.P. (2003). Involvement of Nurr1 in specifying the neurotransmitter identity of ventral midbrain dopaminergic neurons. Eur. J. Neurosci. *18*, 1731–1738.

Soussi, R., Zhang, N., Tahtakran, S., Houser, C.R., and Esclapez, M. (2010). Heterogeneity of the supramammillary-hippocampal pathways: evidence for a unique GABAergic neurotransmitter phenotype and regional differences. Eur J Neurosci *32*, 771–785.

Spano, P.F., and Trabucchi, M. (1978). Interaction of ergot alkaloids with dopaminergic receptors in the rat striatum and nucleus accumbens. Gerontology *24 Suppl 1*, 106–114.

Spano, P.F., Govoni, S., and Trabucchi, M. (1978). Studies on the pharmacological properties of dopamine receptors in various areas of the central nervous system. Adv. Biochem. Psychopharmacol. *19*, 155–165.

Stuber, G.D., Hnasko, T.S., Britt, J.P., Edwards, R.H., and Bonci, A. (2010). Dopaminergic Terminals in the Nucleus Accumbens But Not the Dorsal Striatum Corelease Glutamate. J. Neurosci. *30*, 8229–8233.

Sulzer, D. (1998). Dopamine neurons make glutamatergic synapses in vitro. J Neurosci *18*, 4588–4602.

Takamori, S., Rhee, J.S., Rosenmund, C., and Jahn, R. (2000). Identification of a vesicular glutamate transporter that defines a glutamatergic phenotype in neurons. Nature *407*, 189–194.

Tecuapetla, F., Patel, J.C., Xenias, H., English, D., Tadros, I., Shah, F., Berlin, J., Deisseroth, K., Rice, M.E., Tepper, J.M., et al. (2010). Glutamatergic Signaling by Mesolimbic Dopamine Neurons in the Nucleus Accumbens. J. Neurosci. *30*, 7105–7110.

Thompson, L., Barraud, P., Andersson, E., Kirik, D., and Björklund, A. (2005). Identification of dopaminergic neurons of nigral and ventral tegmental area subtypes in grafts of fetal ventral mesencephalon based on cell morphology, protein expression, and efferent projections. J. Neurosci. *25*, 6467–6477.

Tritsch, N.X., Ding, J.B., and Sabatini, B.L. (2012). Dopaminergic neurons inhibit striatal output through non-canonical release of GABA. Nature *490*, 262–266.

Tritsch, N.X., Oh, W.-J., Gu, C., and Sabatini, B.L. (2014). Midbrain dopamine neurons sustain inhibitory transmission using plasma membrane uptake of GABA, not synthesis. eLife *3*, e01936.

Tsudzuki, T., and Tsujita, M. (2004). Isoosmotic isolation of rat brain synaptic vesicles, some of which contain tyrosine hydroxylase. J Biochem *136*, 239–243.

Valente, E.M., Abou-Sleiman, P.M., Caputo, V., Muqit, M.M.K., Harvey, K., Gispert, S., Ali, Z., Turco, D.D., Bentivoglio, A.R., Healy, D.G., et al. (2004). Hereditary Early-Onset Parkinson's Disease Caused by Mutations in PINK1. Science *304*, 1158–1160.

Varga, V. (2009). Fast synaptic subcortical control of hippocampal circuits. Science *326*, 449–453.

Wallén, A., Zetterström, R.H., Solomin, L., Arvidsson, M., Olson, L., and Perlmann, T. (1999). Fate of mesencephalic AHD2-expressing dopamine progenitor cells in NURR1 mutant mice. Exp. Cell Res. *253*, 737–746.

Wong, P.T.-H., Feng, H., and Teo, W.L. (1995). Interaction of the dopaminergic and serotonergic systems in the rat striatum: effects of selective antagonists and uptake inhibitors. Neurosci. Res. *23*, 115–119.

Xu, B., Goldman, J.S., Rymar, V.V., Forget, C., Lo, P.S., Bull, S.J., Vereker, E., Barker, P.A., Trudeau, L.E., Sadikot, A.F., et al. (2010). Critical roles for the netrin receptor deleted in colorectal cancer in dopaminergic neuronal precursor migration, axon guidance, and axon arborization. Neuroscience *169*, 932–949.

Yamaguchi, T., Sheen, W., and Morales, M. (2007). Glutamatergic neurons are present in the rat ventral tegmental area. Eur. J. Neurosci. *25*, 106–118.

Yamaguchi, T., Wang, H.-L., Li, X., Ng, T.H., and Morales, M. (2011). Mesocorticolimbic Glutamatergic Pathway. J. Neurosci. *31*, 8476–8490.

Yan, C.H., Levesque, M., Claxton, S., Johnson, R.L., and Ang, S.-L. (2011). Lmx1a and lmx1b function cooperatively to regulate proliferation, specification, and differentiation of midbrain dopaminergic progenitors. J. Neurosci. *31*, 12413–12425.

Yan, Z., Song, W.J., and Surmeier, J. (1997). D2 dopamine receptors reduce N-type Ca2+ currents in rat neostriatal cholinergic interneurons through a membrane-delimited, protein-kinase-C-insensitive pathway. J. Neurophysiol. *77*, 1003–1015.

Yano, S., Tokumitsu, H., and Soderling, T.R. (1998). Calcium promotes cell survival through CaM-K kinase activation of the protein-kinase-B pathway. Nature *396*, 584–587.

Yin, M., Liu, S., Yin, Y., Li, S., Li, Z., Wu, X., Zhang, B., Ang, S.-L., Ding, Y., and Zhou, J. (2009). Ventral mesencephalon-enriched genes that regulate the development of dopaminergic neurons in vivo. J. Neurosci. *29*, 5170–5182.

Zander, J.F. (2010). Synaptic and vesicular coexistence of VGLUT and VGAT in selected excitatory and inhibitory synapses. J Neurosci *30*, 7634–7645.

Annexe

Résultats supplémentaires

Afin d'évaluer le rôle de la surexpression de VGLUT2 sur la croissance des neurones dopaminergiques, nous avons infecté des cultures purifiées de neurones dopaminergiques à l'aide d'un vecteur viral exprimant VGLUT2. Nous avons par la suite quantifié la complexité dendritique et axonale à l'aide de la technique d'immunocytochimie et la microscopie confocale.

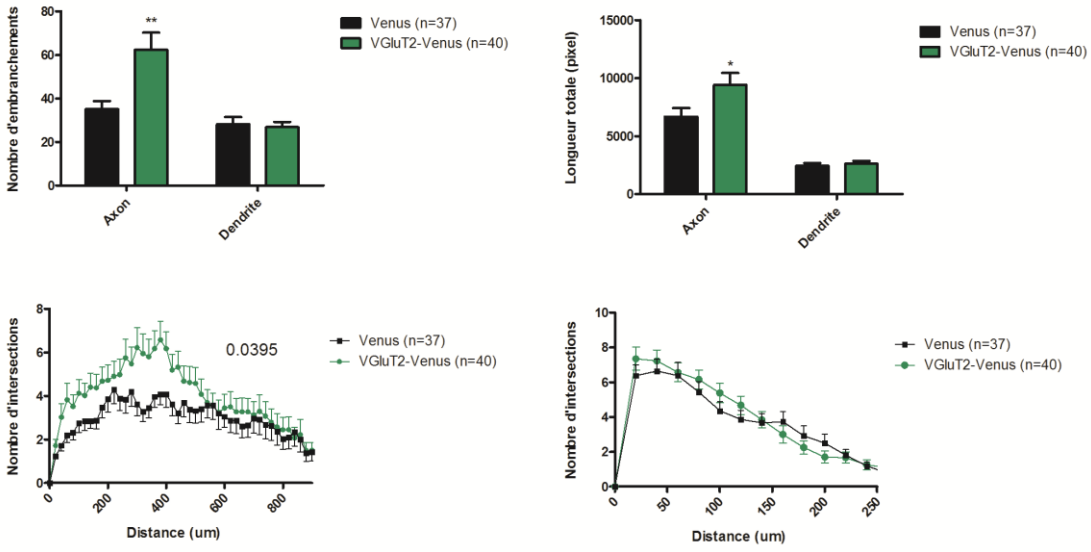

Figure 9. Effets de la surexpression de VGLUT2 sur la morphologie et la densité des axones et dendrites. Des cultures purifiées de neurones dopaminergiques à faible densité ont été infectées avec un lentivirus Venus ou Venus-VGLUT2 dès la mise en culture. À l'aide d'une immunocytochimie révélant la tyrosine hydroxylase et la microscopie confocale, des photos des neurones isolés ont été prises 7 jours plus tard. Une quantification de la densité et de la complexité neuritique a été réalisée sur les neurones reconstruits en utilisant le logiciel ImageJ. Le nombre entre parenthèses représente le nombre de neurones analysés sur un total de 3 cultures.

Afin d'évaluer le rôle de la surexpression de VGLUT2 sur la survie des neurones dopaminergiques, nous avons infecté des cultures purifiées de neurones dopaminergiques à l'aide d'un vecteur viral exprimant VGLUT2. Nous avons par la suite évalué la densité des neurones dopaminergiques à l'aide de la technique d'immunocytochimie.

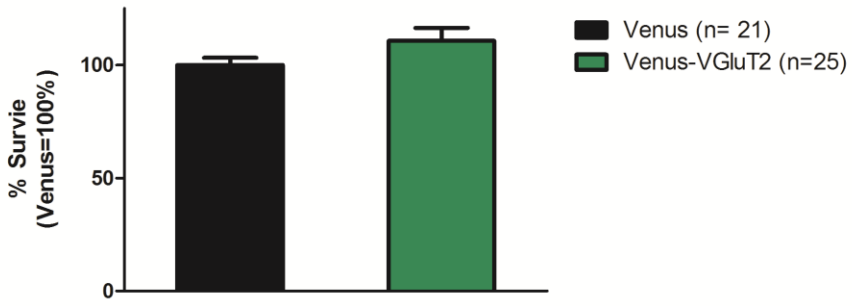

Figure 10. Effets de la surexpression de VGLUT2 sur la survie des neurones dopaminergiques. Des cultures purifiées de neurones dopaminergiques à faible densité ont été infectées avec un lentivirus Venus ou Venus-VGLUT2 dès la mise en culture. À l'aide d'une immunocytochimie révélant la tyrosine hydroxylase et la microscopie à épifluoresence, un compte du nombre de neurones dopaminergiques par lamelle a été réalisé. Le nombre entre parenthèses représente le nombre de lamelles analysées sur un total de 6 cultures. p=0.12

Afin d'évaluer la régulation de l'expression de VGLUT2 dans les neurones dopaminergiques par le facteur neurotrophique GDNF, nous avons exposé des cultures mésencéphaliques au GDNF durant trente minutes. Nous avons par la suite collecté individuellement des neurones et quantifié le nombre de neurones dopaminergiques exprimant VGLUT2 à l'aide de la technique de RT-PCR sur cellule unique.

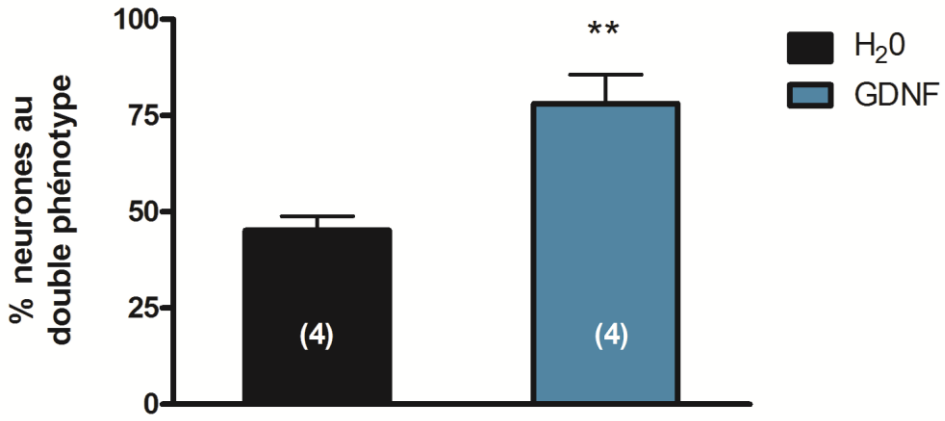

Figure 11. Régulation de l'expression de VGLUT2 dans les neurones dopaminergiques par le GDNF. Un traitement au GDNF (3nM) pendant 30 minutes a été effectué sur des cultures mésencéphaliques à 7 DIV. À la fin du traitement, les neurones dopaminergiques ont été collectés individuellement. À l'aide de la technique de RT-PCR sur cellule unique, nous avons quantifié la proportion de neurones exprimant l'ARNm de TH et VGLUT2. Le nombre entre parenthèses représente le nombre cultures analysées, et10 cellules ont été collectées pour chaque culture.

Afin d'évaluer la régulation de l'expression de VGLUT2 dans les neurones dopaminergiques par l'agent neurotoxique MPP+, nous avons exposé des cultures mésencéphaliques au MPP+ durant une ou deux heures. Nous avons par la suite collecté individuellement des neurones et quantifié le nombre de neurones dopaminergiques exprimant VGLUT2 à l'aide de la technique de RT-PCR sur cellule unique.

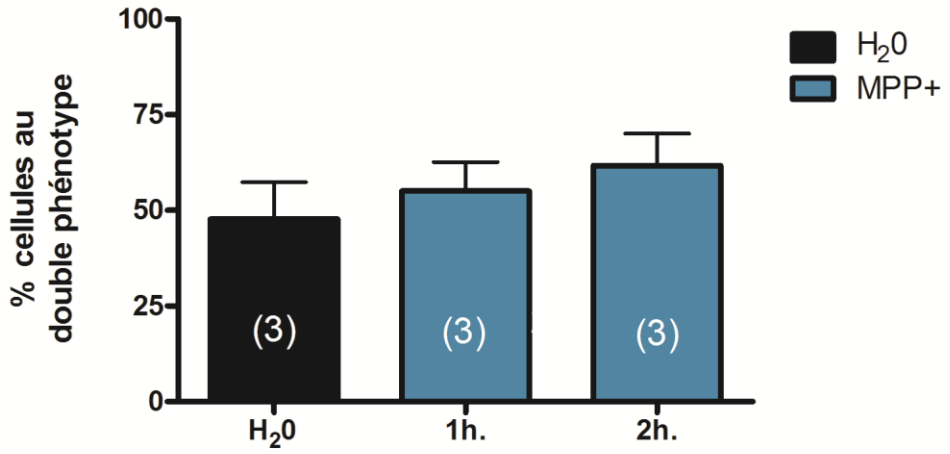

Figure 12. Régulation de l'expression de VGLUT2 dans les neurones dopaminergiques par le MPP+. Un traitement aigu de MPP+ 10µM a été effectué sur des cultures mésencéphaliques à 7 DIV. À la fin du traitement, des neurones dopaminergiques ont été collectés individuellement. À l'aide de la technique de RT-PCR sur cellule unique, nous avons quantifié le nombre de neurones exprimant l'ARNm de TH et VGLUT2. Le nombre entre parenthèses représente le nombre cultures analysées, et10 neurones ont été collectés pour chaque culture.

Afin d'évaluer la régulation de l'expression de VGLUT2 dans les neurones dopaminergiques par des modèles de la maladie de Parkinson *in vivo*, nous avons effectué des préparations de neurones mésencéphalique fraîchement dissociés provenant de souris Parkin KO, DJ-1 KO ou injectées au MPTP. Nous avons par la suite collecté individuellement des neurones et quantifié le nombre de neurones dopaminergiques exprimant VGLUT2 à l'aide de la technique de RT-PCR sur cellule unique.

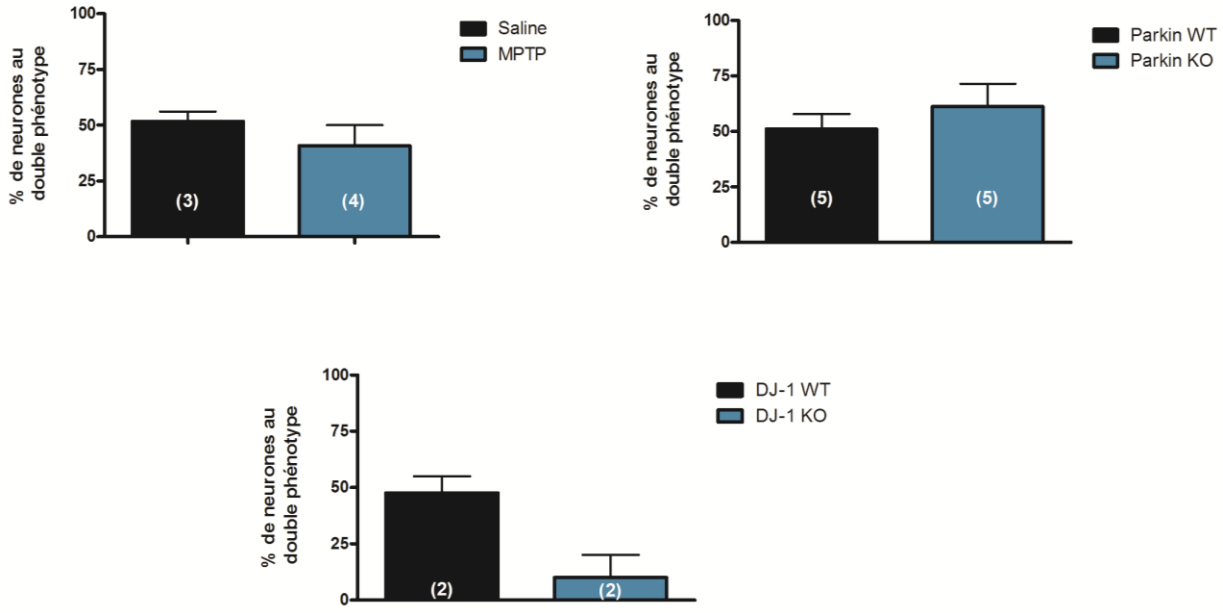

Figure 13. Régulation de l'expression de VGLUT2 dans les neurones dopaminergiques dans des modèles animaux de la maladie de Parkinson. À l'aide de la technique de RT-PCR sur cellule unique, nous avons quantifié le nombre de neurones exprimant l'ARNm de TH et VGLUT2 chez des souris traitées chroniquement au MPTP et chez des souris comportant une délétion du gène Parkin ou DJ-1. Le nombre entre parenthèses représente le nombre de souris et 10-20 neurones ont été collectés pour chaque animal.

Afin d'évaluer le rôle de l'expression de VGLUT2 dans les neurones dopaminergique sur la mémoire et la schizophrénie, nous avons effectué des tests comportementaux chez des souris VGLUT2 cKO.

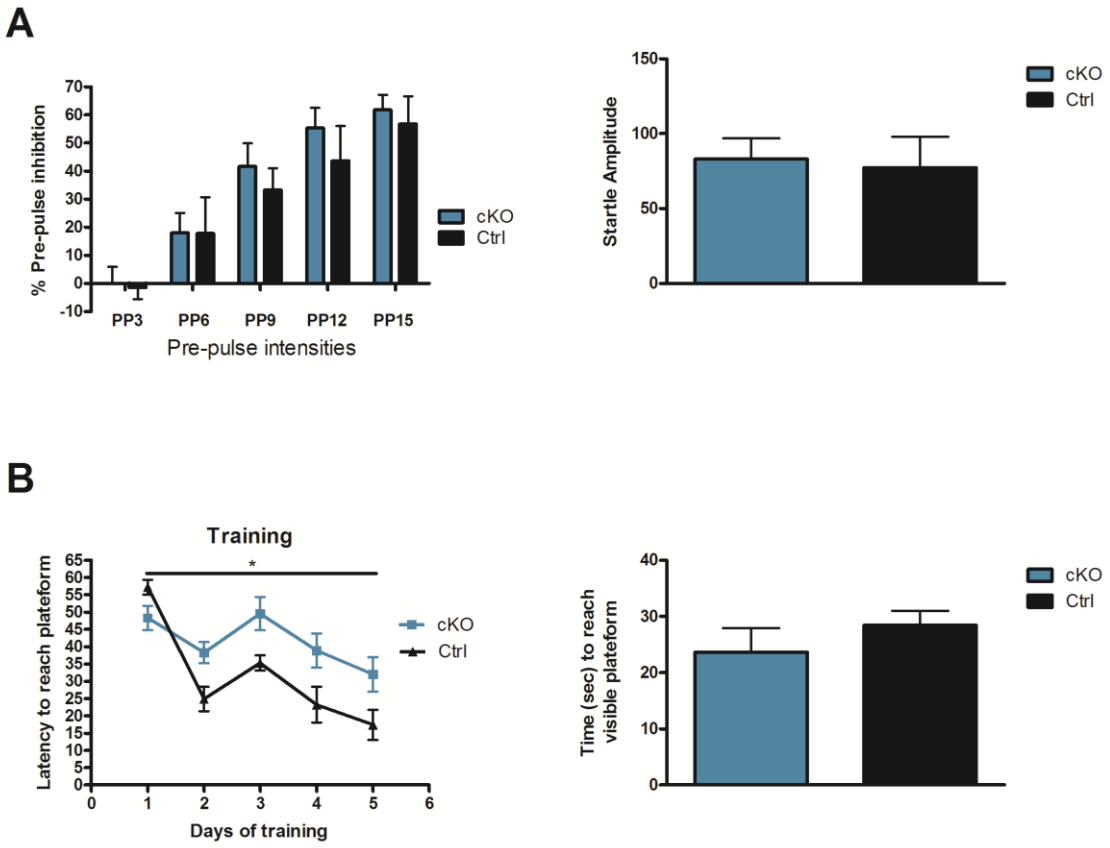

Figure 14. Analyse de l'immobilisation induite par un contexte de peur conditionnée et analyse de la mémoire spatiale chez les animaux VGLUT2 cKO. Le comportement des souris Ctrl ou cKo a été analysé à l'aide (A) du paradigme du prepulse inhibition (PPI) ou (B) de la piscine de Morris. 9 souris Ctrl et 13 souris cKO ont été testés.